THE UNIVERSITY
of EDINBURGH

Electrophysiological characterization of human stem cell-derived neurones and glia in models of neurodevelopmental and neurodegenerative diseases

by

Owain James, BSc, MSc

A thesis submitted for the degree of Doctor of Philosophy
at the University of Edinburgh
May 2016

College of Medicine and Veterinary Medicine
University of Edinburgh

Supervisor: Professor Peter C Kind
2nd Supervisor: Professor David J A Wyllie
3rd Supervisor: Dr. Matthew R Livesey

Abstract

Human pluripotent stem cell (hPSC)-derived neuronal and glial material presents a relatively new opportunity to model human neurophysiology in both health, and disease. Validation of regionally-defined hPSC-derived neurones and glia cultures thus represents the founding blocks of technology that aims to complement existing models. Principally, the relevance of *in vitro* hPSC-derived material is determined by how representative it is of native material, yet at present the physiology of these cells remains underexplored. Here, electrophysiology and pharmacology are used to functionally assess hPSC-derived excitatory cortical neurones (hECNs), motorneurones (MNs) and oligodendrocyte-lineage cells in the context of regional-specific properties and maturation. These properties are then examined in material derived from hPSCs generated from patients with neurological disorders.

This thesis examines of the properties of $GABA_A$Rs and strychnine-sensitive glycine receptors (GlyRs) in hECNs by assessing their subunit composition, and compares these with studies which have made comparable investigations of rodent tissue where maturation is associated with a shift in $GABA_A$ and GlyR compositions. Using pharmacology and RNAseq analysis, $GABA_A$R and GlyRs in hECNs were found to possess receptor populations typical of those reported in the immature cortex.

hECNs generated from patients harbouring a mutation to the Disrupted-in-schizophrenia-gene 1 (*DISC1*), a candidate schizophrenia gene, were then examined. Imbalances in the excitation/inhibition balance are suspected in schizophrenia and, in this regard, the intrinsic excitability properties alongside expression and composition of major neurotransmitter receptors and intracellular chloride concentration were assessed. No obvious differences in excitability or functional expression of AMPARs, $GABA_A$Rs or NMDARs were observed between case and control derived neurones. Receptor composition and intracellular chloride concentrations were found to be predominantly immature-like, however, AMPAR composition and intracellular chloride concentration were found to be like that of adult cortical neurones. These data are discussed in the context of modelling *DISC1*-associated pathologies.

Thirdly, MNs from hPSCs generated from ALS patients harbouring mutations on the *C9ORF72* gene were examined. The hypothesis that increased glutamate-mediated excitoxicity could, in part, be explained by increased expression of Ca^{2+}-permeable AMPARs was examined. The estimated mean single-channel conductance of AMPARs was found to be high in MNs derived from ALS patients, reminiscent of Ca^{2+}-permeable AMPARs and was reversed by gene-editing of the *C9ORF72* mutation.

Finally, oligodendrocytes generated from ALS patients harbouring *TARDBP* mutations were examined. Distinctive electrophysiological shifts in oligodendrocytes-lineage cell development are reported. A similar AMPAR phenotype of elevated Ca^{2+}-permeable AMPAR expression was observed in oligodendrocytes derived from two patient hPSC lines and was rescued in an isogenic, gene-edited line, raising the intriguing possibility of convergence in pathophysiologies in the nature of the overlap between cell-type, AMPAR pathology and excitotoxicity in ALS disease progression mechanisms.

Lay summary of thesis

The lay summary is a brief summary intended to facilitate knowledge transfer and enhance accessibility, therefore the language used should be non-technical and suitable for a general audience. (See the Degree Regulations and Programmes of Study, General Postgraduate Degree Programme Regulations. These regulations are available via: http://www.drps.ed.ac.uk/.)

Name of student:	Owain Thomas James	UUN	1165162
University email:	o.t.james@sms.ed.ac.uk		
Degree sought:	PhD	No. of words in the main text of thesis:	48986
Title of thesis:	Electrophysiological characterization of human stem cell-derived neurones and glia in models of neurodevelopmental and neurodegenerative diseases		

The human brain continuously sends, receives, and processes signals which control core aspects of our behaviour – from tasks such as breathing and walking to our ability to store and recall memories. Underlying this is a vastly complex network of interconnected brain cells with their own properties and behaviours. Human brain cells can now be grown in the laboratory from human stem cells – this provides a new way to investigate how brain cells function and how they are affected by disease. This thesis demonstrates that while this technology has limitations, laboratory-grown brain cells can be used to study human development, as well as conditions such as motor neurone disease. Initially this thesis confirms that these neurones are developing properly and can be used for drug testing on human brain tissue. From this, the thesis shows that while studying some conditions may require significant developments in the technology itself, highly promising results on the mechanisms of motor neurone disease are obtained from studying the behaviour of neurones grown from stem cells, taken from patients with the condition. This thesis concludes by suggesting that different types of mutations that cause motor neurone disease may all share a common mechanism, which can be reliably repeated large-scale in human tissue in the laboratory. Finally, this thesis shows that genetic engineering of mutant, diseased cells corrects the mechanisms which are thought to cause the disease. Thus, this thesis describes a single line of evidence as a prototype for advances in genetic engineering and drug development using laboratory-grown human brain cells – as well as outlining some of the clear limitations of the technology.

Related policies/regulations:
www.docs.sasg.ed.ac.uk/AcademicServices/Regulations/PGR_AssessmentRegulations.pdf

If you require this document in an alternative format please email Academic.Services@ed.ac.uk or telephone 0131 650 2138.	Date last reviewed: 15.05.15

K:\AAPS\D-AcademicAdministration\02-CodesOfPractice,Guidelines&Regulations\24-MainReferencesCopiesPolicies\01-Current\Assessment BOE SCC & Feedback\Forms\ThesisLaySummary

Declaration

I hereby declare that the majority of the following work is my own, with the contributions of others indicated where appropriate.

Owain Thomas James
Nov 2017

Table of contents

Chapter 1

Introduction

1.1 Introduction

The advent of stem cell technology derived from human sources presents an unprecedented opportunity to study human neural development *in vitro* in both health, and disease. This is highly relevant and useful in that the CNS is responsible for cognitive functioning, such as complex language, memory, executive function, and motor activity (see Tabar *et al*. 2014; Livesey *et al.* 2015; Defelipe. 2011). In order to perform these functions, the CNS possesses a highly sophisticated and specialised structure. This complexity is manifested anatomically, and physiologically by an array of variously interconnected cell types which are characterised by differing gene expression, morphology, and functional properties (see O'Leary *et al*. 2007; Stiles *et al*. 2010; Kiecker *et al*. 2010; Hamasaki *et al*. 2004). As such, any attempts to model either health, or disease must invariably reflect this complexity in providing a valid and reliable platform that is representative of human development *in utero*, which is comparable to the body of knowledge already obtained from other models of neurodevelopment in health, and disease, such as animal models.

Critically, there exist a number of highly relevant differences in brain development between humans and typical animal models, such as rodents. The human brain possesses an enlarged frontal cortex and is gyrencephalic, with many deep sulci, gyri, and fissures, and thus has a greater surface area for its volume than if it were smooth (Defelipe. 2011). It has been suggested that gyrencephalic features and the expansion in the human neocortex are the result of increased cell divisions in the outer sub-ventricular zone (OSVZ) during embryonic development, and a propensity for transit-amplifying cells to increase the speed of migration from the SVZ to the developing cortex (Lui *et al*. 2011). Additionally, it has been shown that white matter structure and cortical projections differ markedly between mouse and human (Chesselet *et al*. 2012), which has strong implications for animal models of demyelinating diseases such as ALS or FTD.

Presently, the capacity of human stem-cell derived systems to generate viable, functional neurones is well established (Bilican *et al*. 2014; Livesey *et al* 2014; (Hansen *et al*. 2011; van den Ameele *et al*. 2014), and includes experimentation on exogenous tissue implantation into host organisms up to, and including, primates (Kriks *et al*. 2011) as an attempted rescue of Parkinson's disease phenotypes in animal models. This technology has, more recently, been pursued in order to produce neuronal lineages corresponding to more precise regional specification, or cell type, such as cortical excitatory neurones, oligodendrocyte precursors which can be later differentiated into mature oligodendrocytes, and cortical motor neurones. Typically, these populations are defined by molecular markers as predicted by a combination of human, and animal, studies which are used to define an archetype against which functional data from the same cells can be tested.

This approach provides the foundation for examining pathophysiology in native human systems *in vitro*, in the form of iPSC-derived neuronal tissue taken from clinical patients in genetic diseases such as Rett's syndrome (Farra *et al*. 2012; Andoh-Noda *et al*. 2015), and Huntingdon's disease (Kirkeby *et al*. 2012). The pursuit of detailed knowledge of *in vitro* human systems derived from iPSCs and ESCs which allow more precise specification of tissues answers a particular need to assure the cellular identity of the tissue explants derived *in vitro* (see Tabar *et al*. 2014), and especially so in disease modelling (see Kriks *et al*. 2011). This is of great relevance when considering both the validity of the *in vitro* cultures, and the models to which they are transplanted in themselves, in how they represent the disease. This has had previous consideration in the study of Alzheimer's disease, where mouse and human models have been shown have both strong commonalities and strong differences in gene expression patterns (Miller *et al*. 2009). While this point may seem redundant in that it states the obvious, that a mouse is not a human, it invites a discussion of precisely what gene expression we ought to expect when engineering tissues *in vitro*, and what a deviation from any norm established in either species might indicate.

1.2 Development of the human central nervous system

While a vastly complex process, mediated by many factors both genetic and environmental, a brief overview of CNS development is necessary in order to establish context for any description of *in vitro* systems which aim to represent aspects of this process.

Shortly after fertilisation, the developing ball of cells (referred to as the blastula) undergoes gastrulation, ultimately yielding 3 layers of cells which are fate-mapped to a given lineage. Firstly, the endoderm stem cell layer, which gives rise to the gut and respiratory system; secondly, the mesoderm layer, which will give rise to structures such as the vascular system, muscle, cartilage, and bone; thirdly, the ectoderm, which produces both epidermal (skin, nails, and sweat glands) and neural lineages. This subdivision of the ectoderm, the neurectoderm (as opposed to the epidermal ectoderm), contains neural progenitor cells (NPCs) from which the CNS is derived. From the neurectoderm arises the neural tube, which occurs in humans between embryonic day 20 and 27 (see Stiles *et al*. 2010; Lui *et al*. 2011). This cylindrical structure has a central fluid filled vacuole which is lined with neural precursors (NPCs) known as the ventricular zone (VZ). The more caudal regions of the VZ give rise to the spinal cord, while the more rostral region becomes the telencephalon, and later, the brain, which in totality produces a vast array of cell types such as cortical excitatory neurones, interneurons, oligodendrocytes, and motor neurones.

1.2.1 Cortical development

Specification of cortical regions in the developing telencephalon is mediated by graded expression of transcription factors, proteins which bind to specific DNA sequences and regulate the transcription of DNA to mRNA. Various characteristic transcription factors are expressed by progenitor cells in the cortex, including Pax6, Gli3, Sp8, Emx2, and Coup-TF1 (O'Leary *et al*. 2007). Transcription factor expression in the developing cortex is predominantly regulated by three major telencephalic signalling centres that induce changes in transcription factor expression by secreting various chemical messengers: the ventral telencephalon that secretes sonic hedgehog (SHH), the anterior neural ridge that secretes fibroblast growth factor-8 FGF8, and the cortical hem that secretes WNT and bone morphogenetic protein (Marigo *et al.* 1995; Backman *et al.* 2005; Hebert *et al*. 2003). Gradients of these chemical messengers define cortical axes in this manner, whilst giving rise to regional specification. Subsequently, cortical progenitor cells differentiate to neurones and migrate radially out from the telencephalon in a time-dependent fashion (Noctor *et al*. 2004).

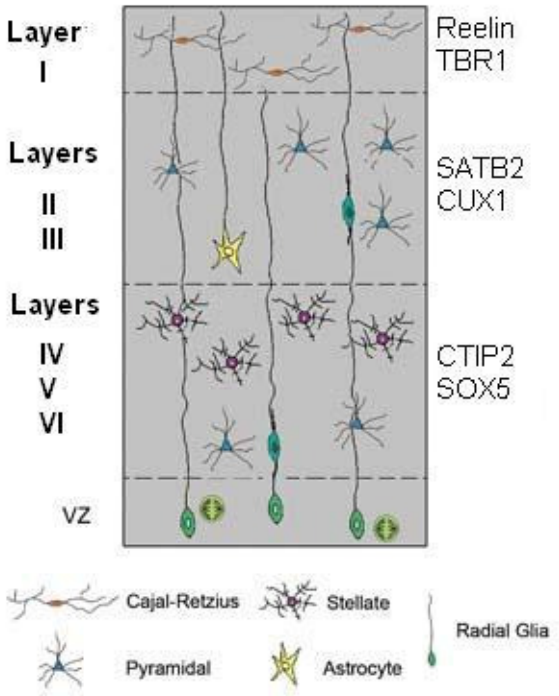

Figure 1.1, Schematic of cortical layers in developing human cortex. Shows subtypes of excitatory cortical neurones from upper (Layer I) to lower (Layer VI) cortical layers, and associated coritical markers Reelin, TBR1, SATB2, CUX1, CTIP2, and SOX5. Adapted from Gemaine *et al*. 2010.

This process results in cortical layers being formed 'inside out' - the deepest cortical layer VI forms first and the upper layer II last, in that layer I, containing reelin+ Cajal–Retzius cells, is exempted (Frotscher, 1998). The adult cortex has a structure made up of six defined layers (I–VI) of diverse excitatory cortical neuron types that can be identified by layer-specific markers, including Reelin (Layer I), CUX1 (layer II/III), ROR-β (layer IV), CTIP2 (layer V), SOX5 (layers V and VI) and TBR1 (layer VI) (Molyneaux *et al*. 2007). Additionally, interneurones also migrate to the cortical layers, however, they do so via a different migratory mechanism. While excitatory cortical neurones typically migrate radially from the VZ, interneurons are instead differentiated from NPCs in the ganglionic eminence (GE), a temporary structure that exists through embryonic and fetal development in humans. Interneurones differentiated here migrate tangentially into the cortex using

a multitude of local guidance cues (Marin and Rubenstein 2001; Huang 2009;Valiente and Marin 2010).

1.2.2 Spinal cord development

Similar processes of regional specification apply to the spinal cord. Cells are initially fated along the anterior–posterior axis by activation of Wingless-type MMTV integration site family members (WNTs), and fibroblast growth factors (FGFs), respectively. Mesodermal cells surrounding the spinal cord synthesize retinoic acid (RA) via the enzyme aldehyde dehydrogenase 1A2 (ALDH1A2). RA induces caudal neuronal cell types found in the hindbrain and spinal cord, e.g motor neurones, and oligodendrocyte precursors. Retinoic acid signalling decreases caudally down the spinal cord, as indicated by both decreased expression of ALDH1A2, and increased levels of FGF8, which is highly expressed in more caudal regions of the spinal cord. In addition to retinoic acid and FGFs, WNTs are also required for the induction of caudal hindbrain and spinal cord identities (Backman *et al.* 2005). Another key molecule is the signalling protein sonic hedgehog (SHH) a morphogen which here acts as a ventralising factor (see Marigo *et al.* 1995; also Hebert *et al*. 2003). Additionally, high SHH concentrations have been shown to induce NPC differentiation into ventral spinal lineages, and are critical for MN induction (see Qu *et al*. 2014). In rodents, oligodendrocyte precursors first arise in the ventral VZ at approximately E12, though slightly later in development at approximately E15, a dorsal VZ source of OPCs also develops. OPCs have been shown to migrate into the cortex from both sources, where they are tentatively considered equivalent (Richardson *et al*. 2006). Additionally, the specification of oligodendrocyte lineages has also been shown to be initiated by FGFs, SHH, BMP, and WNTs (see Richardson *et al*. 2006).

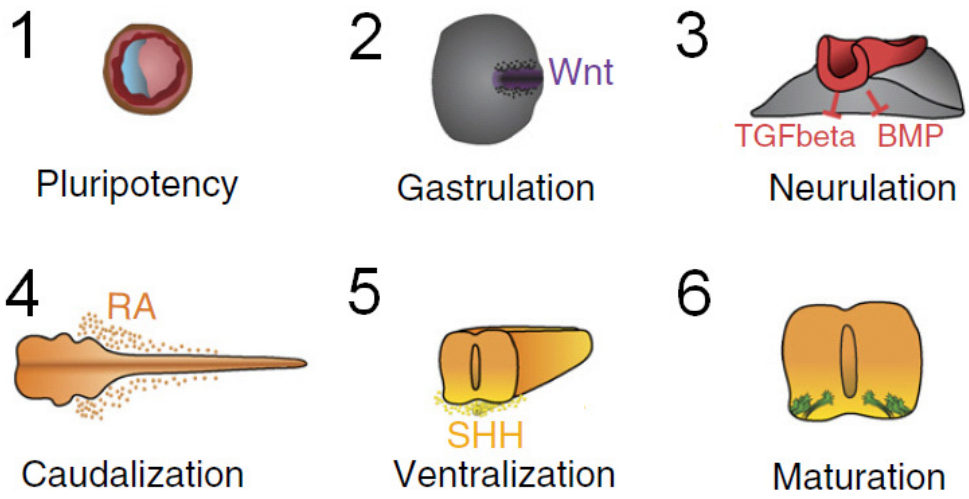

Figure 1.2, Schematic of developing mammalian spinal cord. Illustrates developmental stages from pluripotent blastula **(1)** to maturation **(6)**, and the role of various signalling molecules at each stage. The blastula **(1)** undergoes gastrulation, commencing with the archenteron induced by Wnt signalling **(2)**. Subdivision of layers lead to structures such as the neural tube **(3)** regulated by transcription factors such as TGF-β and BMP, among others. The neural tube is then caudalised by retinoic acid gradients **(4)** forming an anterior-posterior axis to the developing neural tube. Dorsal-ventral axis is then defined by sonic hedgehog signalling (**5**, SHH), resulting in a structure adequate to undergo later, more refined development **(6)**. Adapted from Sances *et al*. 2016.

1.3 Research on CNS patterning and transcription factors inform iPSC culture development

Previous research into CNS development has subsequently informed the generation of increasingly well-specified tissues *in vitro*. This thesis concerns itself with the functional outcomes of the generation of neuronal and oligodendrocytic lineages, and as such attempts to generate these various tissues are outlined with respect to cell type.

1.3.1 Cortical neurones

It has been previously shown that *in vitro*-derived cortical NPCs (from ESCs and iPSCs) spontaneously neuralise and differentiate into neurones (Bilican *et al.* 2014; Livesey *et al*. 2014; Mariani *et al*. 2012; Shi *et al*. 2012). Moreover, this process can be accelerated by using WNT, and BMP inhibitors, a process known as dual-SMAD inhibition (SMA and MAD-related protein inhibition; Chambers *et al*. 2009). SMADs represent a family of proteins that mediate cytokine signalling and are activated by an endogenous ligand, transforming growth factor-β (TGF-β), moreover, isoforms of SMADs also interact with each other in a complex manner. Interestingly, differentiation into interneurones can also be induced by SHH, and SHH agonists (Germain *et al*. 2010; Maroof *et al*. 2013), which is reflective of processes *in vivo* which involve the GE, the developmental source of interneurons in the cortex, which also produces SHH.

Excitatory cortical neurones produced by the 'default' approach (i.e withrawl of mitogens post-differentiation) have been shown to be broadly representative of their embryonic counterparts by genetic markers, and measures of functional maturity as described ion channel subunit expression (Bilican *et al.* 2014; Livesey *et al*. 2014; Mariani *et al*. 2012; Shi *et al*. 2012; James *et al*. 2014). Here, neurones can be differentiated and subsequently maintained for 5 weeks (35 DIV), during which a definite neuronal identity is maintained.

Additionally, hPSC-derived cortical progenitors typically acquire a caudal identity by default as shown by their pattern of projections when transplanted into

mouse brains (Espuny-Camacho *et al*. 2013), and can also be patterned to various cortical regions and respond to signalling cues when treated with morphogens (Eiraku *et al*. 2008; Espuny-Camacho *et al*. 2013; Kadoshima *et al*. 2013). Cortical layer formation is also somewhat reflected in previous study of hECNs, with relative expression of markers for each layer varying considerably between different culture protocols (see van den Ameele *et al*. 2014). This suggests that judgements about specific sub-populations outside of broadly specified cell type (cortical, excitatory) are difficult to make. Transcriptome analyses of in vitro hPSC-derived cultures reproduce gene expression profiles in hPSC-derived cortical neurone populations that seem equivalent to early native human embryonic cortical development (Stein *et al*. 2014; Pasca *et al*. 2015).

This thesis uses a protocol which generates highly pure (~90%) cortical neuronal cultures which can be maintained for 7 weeks *in vitro*, and display ion channel and gene expression patterns broadly typical of immature, embryonic cortical neurones, though with several exceptions (AMPARs, see Livesey *et al*. 2014; GlyRs, James *et al* 2015).

1.3.2 Lower motor neurones

Here, the 'default' protocol is supplemented with caudalising factors such as RA and SHH activators, yielding caudalised, spinal NPCs (see Chapter 2.2; Figure 2.1). Previous attempts to generate spinal motor neurones (lower motor neurones; LMNs) have met with a degree of success. Neural precursors derived from mouse ES cells exposed to retinoic acid and SHH in the presence of knockout serum, which is a proprietary, partial purification of albumin from bovine serum, have been specified to a motor neurone (MN) fate. This has been found to hold true in human ES derived neural precursors (Sances *et al*. 2016). Human ESCs can be differentiated to neural stem cells in the absence of morphogens, treated with RA and SHH to induce ventral spinal progenitors, before differentiation into MNs. Drawing from these discoveries, most differentiation protocols for human embryonic and iPSC-derived LMNs (hPSC-LMNs) share three fundamental steps in induction: neuralisation through dual-SMAD inhibition, caudalisation by RA exposure and ventralisation through SHH activation by recombinant SHH protein or small-molecule SHH activators (smSHHs). It has also been shown that WNT signalling plays a crucial role, with WNT activators inducing up to 80% Olig2 expression – a transcription factor, and marker for MN progenitors (Maury *et al*. 2015).

Currently, protocols which generate highly enriched cultures of MNs from iPSCs are available (Selveraj *et al*. 2016, manuscript in review). Neuronal cultures strongly express Islet-1 and choline acetyltransferase, markers of mature MNs (see Qu *et al*. 2014; Sances *et al*. 2016) at 5 weeks in culture, as well as other neuronal markers such as β3-tubulin.

1.3.3 OPCs and oligodendrocytes

Again, the 'default' protocol applied to ESCs/iPSCs is supplemented with caudalising factors such as RA, and SHH activators yielding caudalised, spinal NPCs (see Chapter 2.2; Figure 2.1) which are subsequently directed to an OPC fate by mitogens such as platelet derived growth factor-α, and SHH activator purmorphamine. As with MNs, has also been shown that WNT signalling plays a crucial role, with WNT activators inducing up to 80% Olig2 expression – a transcription factor, and marker for Oligodendrocyte precursors (Maury *et al*. 2015; see Sances *et al*. 2016; Livesey *et al*. 2015).

1.4 Introduction to ligand-gated ion channels

Ligand-gated ion channels (LGICs; also ionotropic receptors), are a group of transmembrane ion conducting protein assemblies, positioned at both synaptic, and extra-synaptic sites on neuronal membranes which act as gates, opening to allow ions such as Na^+, K^+, Ca^{2+}, and/or Cl^- to pass through the membrane in response to the binding of compounds (i.e. ligands) such as neurotransmitters (e.g glutamate). To re-iterate, a conformational change in the receptor assembly occurs which allows the free movement of ions across the cell membrane. Typically, activation of LGICs results in either a membrane depolarization, for an excitatory receptor response, or a hyperpolarization, for an inhibitory response, as determined by the ion species conducted by the ion channel and the resting membrane potential of the cell in question (here, neurones, oligodendrocytes).Typically, LGICs are grouped by amino acid sequence similarity, selectivity for certain ligands (e.g $GABA_A$ receptors), and physiological function – this will be explored in this thesis in the following sections, with relevance to these distinctions.

1.4.1 Introduction to ionotropic glutamate receptors

Glutamate is the principal excitatory neurotransmitter in the adult mammalian brain, and activates an array of pre- and post-synaptic receptors of two broad types; ionotropic, and metabotropic (see Traynelis *et al.* 2010). Ionotropic glutamate receptors consist of 3 subytpes named for their response to selective ligands; AMPA (α-amino-3-hydroxy-5-methyl-4-isoxazolepropionic acid) receptors, NMDA (N-methyl D-aspartate) receptors, and kainate (kainic acid) receptors. Altogether, these receptors mediate the vast majority of fast excitatory neurotransmission in the adult mammalian brain are typically selective for monovalent cations Na^+ and K^+. As a nerurones resting membrane potential is largely regulated by the active transport of Na^+ and K^+ ions across the membrane such that the inside of the cell has a potential difference of approximately -50 mV to -70 mV relative to the exterior of the cell. This potential difference is achieved by expending energy to force Na^+ and K^+ ions across the membrane against their electrical and chemical gradients, separating charges and thus generating an electrical potential difference. Thus, when an ion channel permeable to Na^+ and K^+ is opened, ions flow across the membrane causing the potential difference at the membrane to approach 0 mV, as there is now no separation of charge, causing neuronal depolarisation, and thus excitation of the membrane (for further explanation, see Hille, 2001).

Notably in terms of glutamate receptors, NMDA receptors, and certain configurations of AMPA receptors are also permeable to Ca^{2+} ions. This has been shown to contribute to the roles of these receptors in normal neurodevelopment, processes underlying learning and memory, and also in disease states. Metabotropic glutamate receptors (mGluRs) do not conduct ions, and instead influence a wide array of processes such as synaptic plasticity in the CNS by G-protein signalling cascades (see Trzaskowski *et al.* 2012; Overington *et al.* 2006) This thesis uses electrophysiological and pharmacological methods most amenable to the study of AMPA, and NMDA receptors, and as such these will be the focus amongst the known glutamate receptors.

1.4.2 AMPA receptor structure and physiological function

α-amino-3-hydroxy-5-methyl-4-isoxazolepropionic acid receptors (AMPARs) are ligand gated cation channels with a reversal potential of 0mV, which mediate the majority of fast excitatory synaptic transmission in the central nervous system (see Honore *et al*. 1982). AMPARs are tetrameric in structure, being composed of four subunits, designated GluA1 - GluA4. Most AMPARs are heterotetrameric, consisting of symmetric 'dimer of dimers' of GluA2 and either GluA1, GluA3 or GluA4 (Traynelis *et al*. 2010). Dimerisation occurs in the endoplasmic reticulum with the interaction of N-terminal domains, which "zips up" the two dimers from the ligand-binding domain into the ion pore. AMPARs also play a key role in synaptic plasticity, with AMPAR expression being linked to activation of other receptors involved in synaptic plasticity such as the NMDAR (Song & Huganir, 2002; Shi *et al*. 1999).

The AMPAR's ion selectivity is, in part, governed by the GluA2 subunit. If an AMPAR lacks a GluA2 subunit, then it will be permeable to Na^+, K^+, and Ca^{2+}. The presence of a GluA2 subunit will almost always render the channel impermeable to Ca^{2+}, but retain permeability to Na^+ and K^+ (see Kamboj *et al*. 1995). This is determined by post-transcriptional modification by RNA editing of the Q-to-R editing site of the GluA2 mRNA. Here, A→I editing alters the uncharged amino acid glutamine (Q) to the positively charged arginine (R) in the ion channel pore. The positively charged amino acid at this critical point makes it energetically unfavourable for Ca^{2+} to enter the cell through the pore, rendering the AMPAR impermeable to Ca^{2+} (Swanson *et al*. 1997).

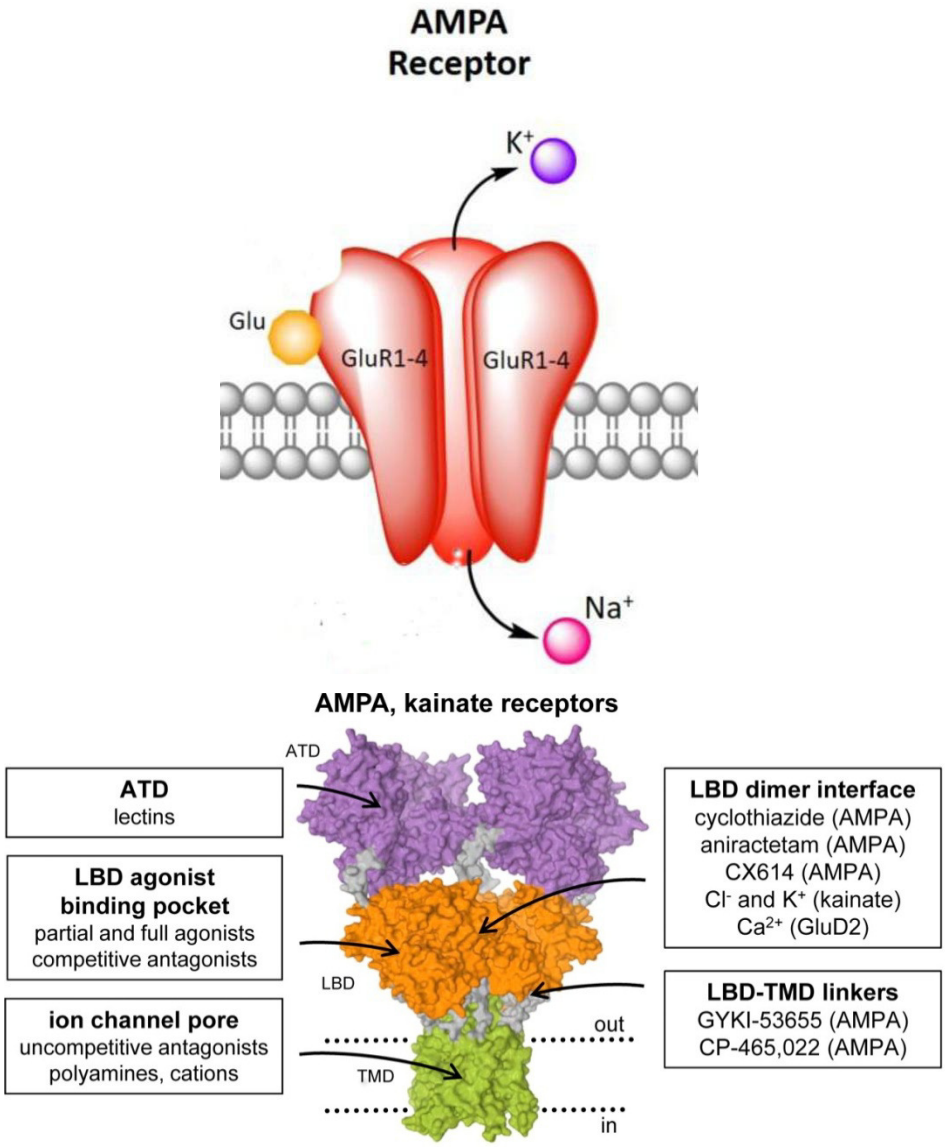

Figure 1.3. Schematic representation of AMPA and kainite receptor structure as found on the cell surface. *Above:* Schematic showing AMPA structure as a cross section around the central ion pore. *Below:* Structural representation of the AMPAR. Labels show approximate sites of action for commonly used receptor agonists (e.g AMPA), modulators (e.g. cyclothiazide), blockers (e.g polyamines, N-acetyl spermine), and antagonists (CNQX). Dotted lines indicate cell internal and external as indicated. Adapted from Barr & Burdette. (2017) and Traynelis *et al*. (2010).

AMPAR subunit composition is highly spatially and temporally regulated. In the embryonic cortex, AMPARs are typically GluA2 subunit-lacking, rendering them permeable to Ca^{2+}. In immature rodent, and human excitatory cortical neurons, GluA1/GluA4- containing AMPARs are predominantly expressed, whereas mature neurons predominantly express GluA1 and GluA2 subunits (Talos *et al*. 2006a, 2006b; Orlandi *et al*. 2011, see Traynelis *et al*. 2012). In normal development, the GluA2 subunit is predominantly RNA-edited (Q → R), with an edited GluA2 subunit being strongly suggestive of a postnatal phenotype. Inclusion of at least one (Q → R)- edited GluA2 subunit into the AMPAR tetramer confers specific biophysical properties such as lower single-channel conductance, insensitivity to channel-blocking spermines and Ca^{2+}-impermeability (Swanson *et al*. 1997; Traynelis *et al*.2010). Permeability to Ca^{2+}- has been shown to mediate processes relating to neuronal excitotoxicity, and, interestingly may relate to possible calcium dysregulation in schizophrenia, and negatively impact the development of excitatory networks (Berridge. 2012).

AMPAR subunits differ significantly at their C-terminal in their amino acid sequences. This region enables subunit interactions with many scaffolding proteins. While AMPARs all contain scaffolding protein binding domains, which PDZ domain they interact with is dependent on subunit composition. Interestingly, AMPARs do not directly bind to PSD-95 as they do not share common interaction domains. Both, however, interact with PSD-95 via stargazin, a member of the TARP family of AMPAR auxiliary subunits which regulate cell-surface AMPAR expression. Additionally, AMPAR phosphorylation can regulate channel conductance, and localisation. GluA1 has four known phosphorylation sites which are phosphorylated by protein kinase C, and from this has been shown to be necessary for long-term potentiation (LTP) by affecting delivery of the receptor complex to the synapse.

Developmental and activity-regulated changes in AMPAR expression (and composition) are thus instrumental in excitatory synapse formation, stabilization, and synaptic plasticity, and thus the development of functional networks. Additionally, defects in the processes that control AMPAR assembly, trafficking

and synaptic expression are intimately linked to psychiatric and neurological conditions, as well as to cognitive symptoms in neurodegenerative disorders.

1.4.3 AMPA receptor trafficking, expression, and links to disease

AMPARs are constructed as tetrameric complexes in the endoplasmic reticulum (ER), a subcellular structure responsible for protein synthesis, whereupon they are trafficked to the golgi apparatus and secreted in vesicles to be trafficked along the actin cytoskeleton as mediated by myosin, to synaptic and extrasynaptic sites (see Greger *et al*. 2002; Park *et al*. 2004; Wang *et al.* 2008). Dimerization of two subunits initially depends on interactions between N-terminal domains, followed by the second dimerization step mediated by associations at the ligand-binding and membrane domains. Typically, heterodimeric assemblies which preferentially incorporate GluA2 are highly typical in adulthood. However, there is considerable flexibility in the interface that allows the formation of GluA2-lacking AMPARs in both normal development, and also disease states.

Individual AMPAR subunits have either long or short intracellular C-terminal domains that bind to distinct sets of interacting proteins. The main splice isoforms of GluA1 and GluA4 have long tails, and GluA2 and GluA3 have short tails. Generally, the long-tailed GluA1 and GluA4 subunits dictate the trafficking properties of AMPARs when assembled in heteromers with short-tailed subunits and, as GluA4 is mainly expressed during early development, GluA1 is by far the most predominant long-tailed subunit in mature neurons.

GluA1 is not edited and, in the absence of GluA2, GluA1 assembles into CP-AMPARs that can be rapidly exported from the ER and trafficked to the membrane (Greger *et al* 2002). By contrast, edited GluA2 which accounts for more than 99% of all GluA2 in mature neurones is mostly unassembled and retained within the ER. Thus, in studies primarily using exogenous expression of GluA1 or GluA2, Q/R editing reduces the formation of GluA2 homotetramers and only allows GluA2 to exit from the ER when it is assembled with GluA1. AMPARs that contain both GluA1 and GluA2 follow GluA1 trafficking rules and override the ER retention of GluA2. Therefore, in addition to making GluA2-containing AMPARs Ca2+

impermeable, Q/R editing also promotes interaction with GluA1 to form heterotetrameric channels. This regulated ER exit limits the types and numbers of AMPARs that are available for synapses and, by disfavouring GluA2 homotetramer formation, maintainsa stable ER pool of edited GluA2, which is then expressed at the membrane later in development in the form of GluA2‐containing heteromeric AMPARs.

The TARP family, proteins considered AMPAR auxiliary subunits, also influence AMPAR assemblyand trafficking. TARPs act as chaperones that prevent the ER exit of incorrectly folded AMPAR proteins. Additionally, TARPs such as stargazin (Chen *et al.* 2000) are involved with ER export of correctly assembled receptor complexes. Interestingly, Ca^{2+}-permeable AMPARs (CI-AMPARs) and Ca^{2+}-impermeable AMPARs (CI‐AMPARs) may be differentially trafficked during synaptic plasticity. Synaptic retention of AMPARs also likely involves TARPs. Owing to incompatible PDZ-binding domains, AMPARs do not directly bind to PSD95. Instead, TARPs bind to MAGUKs to stabilize the AMPAR–TARP complex at synapses. Additionally, during LTP induction, CaMKII phosphorylates stargazin and increases its binding to PSD95.

Subunit-dependent and subunitindependentmodes of AMPAR trafficking are notnecessarily mutually exclusive. Currently, it is thought that receptors diffuse laterally at the membrane, and are captured at synapses during LTP. The extrasynaptic receptors themselves are replenished by newly assembled receptors. Interestingly, it takes longer for RNA-edited GluA2to actually incorporate into AMPARs than other AMPAR subunits (Greger *et al*. 2002).

The faster ER exit of unedited GluA2 facilitates faster forward-trafficking and membrane expression of CP‐AMPARs during synapse formation early in mammalian development. Later, CNS maturation is associated with RNA editing of GluA2, which hinders homodimerization and thus slows ER exit, which then increases incorporation of GluA2 into AMPAR heteromers. This is consistent with the switch from CP‐AMPARs to CI‐AMPARs during brain development. Interestingly,it has recently been shown that GluA2 forward trafficking is also regulated by intracellular Ca2+ release from stores, CaMKIIactivation and

interaction with protein interacting with C kinase 1 (PICK1) to facilitate ER exit, which may represent a form of synaptically-directed mechanism controlling AMPAR trafficking in neurones.

AMPARs are also suspected to play a role in the neurodegeneration and disease progression seen in amyotrophic lateral sclerosis (ALS). Evidence suggests that disease progression in ALS may be caused by glutamate-mediated excitotoxicity caused by aberrant expression of CP-AMPARs which takes effect over time as a progressive physiological stress (Rothstein & Cleveland, 2001.). Previous work has highlighted an intrinsic vulnerability of ALS MNs to glutamate excitotoxicity that is mediated by Ca^{2+}-permeable AMPARs (Donnelly *et al*. 2013; Rothstein *et al*. 1995). However, the literature has yet to directly link specific AMPAR structural properties that generate Ca^{2+}-permeability in ALS MNs to specific mechanisms or genetic abnormalities, though several specific genetic mutations are strongly linked to ALS (Duncan, 2009; Donnelly *et al*. 2013; Rothstein *et al*. 1995; see Cleveland and Rothstein. 2001). Crucially, the developmentally regulated AMPAR subunit compostion change is seen in stem-cell derived cortical neurones (Livesey *et al*. 2014), suggesting the potential for iPSC-derived systems to generate neurones from patients harbouring mutations associated with ALS. This, in turn, suggests the potential for studying normal AMPAR development and also in exploring potential mechanisms of disease progression. Thus, by studying the behaviour of the AMPARs expressed be iPSC-MNs with regard to Ca^{2+} permeability, it is possible that iPSC-MNs represent a viable platform to study mechanisms implicated in ALS.

1.4.4 Pharmacological agents which taget the AMPAR

There exist an array of compounds which behave variously as agonists, antagonists, and modulators at AMPARs. Worthy of note is the key determininant of an AMPA receptor – selective activation by AMPA, and conversely recetor inactivation by CNQX (see list of abbreviations for full compound names).

Agent	Effect at AMPAR	Reference(s)
AMPA	Agonist	Honore *et al.* (1982); Banke *et al*. (1997); Nakanshi *et* al. (1990); see Traynelis *et al*. (2010); Zhang *et al*. (2006).
CNQX	Antagonist (competetive)	Nakanshi *et* al. (1990); see Traynelis *et al*. (2010); Zhang *et al*. (2006).
NASPM	Channel blocker (voltage dependent)	Koike *et al*. (1997); Noh *et al*. (2005).

Table 1.1: Pharmacological agents used in this thesis which affect the AMPA receptor. This table describes the typical behaviour of agonists AMPA, CNQX, and NASPM. Note that typically subunit-selective drugs (indicated by a * prefix) is a brief description of the behaviour of a compound in terms of a broad electrophysiological response. Greater detail is supplied in later chapters where the compounds are used, and in discussion of results.

1.4.5 Introduction to NMDA receptors

The N-methyl-D-aspartate receptor (NMDAR) is an ionotropic glutamate receptor that is selectively activated by N-methyl-D-aspartate (NMDA) in the presence of a co-agonist, glycine. The NMDAR has a tetrameric structure potentially composed of subunits GluN1, GluN2A-D, and GluN3A-B (Traynelis *et al*. 2010). In the forebrain, most NMDARs are tetrameric formation of two GluN1 subunits and two GluN2 subunits, with the crystal structure of the NMDAR showing that GluN1 and GluN2 subunits are arranged alternately (i.e. 1, 2, 1, 2) in a circular fashion around a central ion pore (Lee et al. 2014). GluN1 houses the co-agonist glycine/d-serine binding site, and GluN2 contains the glutamate binding site, both of which are required to have their respective sites occupied by their agonists in order to activate the receptor. NMDARs are permeable to Na^+, K^+, and like the GluA2-lacking AMPAR, are also permeable to Ca^{2+}. NMDAR-mediated responses are typically voltage dependent, in that NMDARs are blocked by extracellular Mg^{2+} at typical neuronal resting membrane potentials (approx. -60 mV to -70 mV). This is due to NMDARs being impermeable to Mg^{2+}, which is drawn to the NMDAR pore by negative resting membrane potentials where it blocks the pore, occluding the vast majority of ion flow including Ca^{2+}. When the membrane local to the NMDAR is depolarised, the Mg^{2+} blockade of the NMDAR ceases. Under these circumstances, NMDAR activation causes Na^+, K^+, and Ca^{2+} to flow down their respective electrochemical gradients as is energetically favourable.

From this, at the synapse the NMDAR can be thought of as a molecular coincidence detector in line with the Hebbian principle of synchronised activity between a pre- and post-synaptic neurone strengthening the existing connection. When a presynaptic neurone depolarises and releases glutamate, the post-synaptic neurone is excited, and depolarises in response (typically *via* AMPARs). Under repeated, high-frequency firing, the post-synaptic membrane becomes sufficiently depolarised so as to release the Mg^{2+} blockade, causing a post-synaptic rise in intracellular Ca^{2+}. Many phenomena associated with the NMDAR are thought to form the basis for higher cognitive processes predicated on synaptic plasticity such as learning and memory of many types, and executive functioning. Indeed, the

NMDARs involvement and learning and memory is fairly well understood. In rodents NMDARs are known to play a prominent role in spatial learning, fear conditioning, place preference; behavioural tasks which are localised to the frontal cortex and hippocampus which depend on normal functioning in these areas.

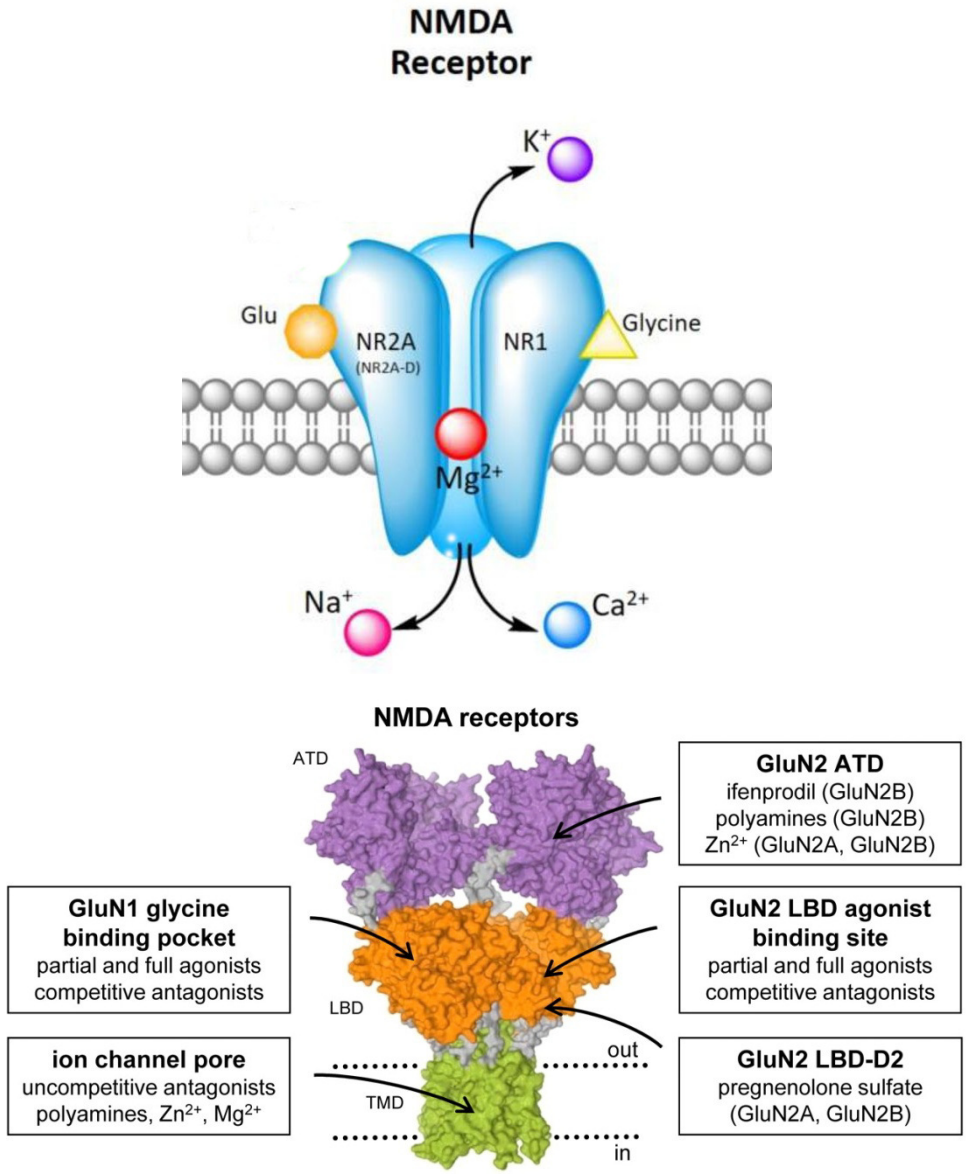

Figure 1.4. Schematic representation of NMDAR structure as expressed at the cell membrane. *Above:* Schematic showing NMDAR structure as a cross section around the central ion pore. *Below:* Structural representation of the NMDAR. Labels show approximate sites of action, and subunit selectivity (determined by presence of subunit noted e.g. ifenprodil is a GluN2B-selective inhibitor), for commonly used receptor modulators, blockers, and antagonists. Adapted from Adapted from Barr & Burdette. (2017) and Traynelis *et al*. (2010).

NMDAR subunit expression differs as a function of brain region and developmental age [Monyer *et al*. 1994; Watanabe *et al*. 1992; see Wyllie *et al*. 2013 Sans *et al*. 2000], and may determine subcellular localization, e.g., in adults, NR2A-containing receptors are predominantly expressed at synapses while extrasynaptic receptors are predominantly NR2B-containing .Additionally, it has been shown that multiple types of NR2 subunit in each complex exist (tri-heteromeric NR1/NR2X/NR2Y) Further to this, different NMDAR isoforms can be expressed at different synapses within the same neuron.

NMDAR subunit composition in the forebrain changes from a predominant GluN1/GluN2B population in immature neurones to a mixed GluN1/GluN2A/GluN2B population in the second week post-natally (Monyer *et al*. 1994; Watanabe *et al*. 1992; see Wyllie *et al*. 2013). The noncompetitive negative allosteric modulator ifenprodil (Williams, 1993) is a prime example of a wide range of compounds (Mony *et al*. 2009) that display a selectivity for GluN2B-containing NMDARs of around 100-fold over other diheteromeric NMDAR assemblies, binding at the interface of GluN1 and GluN2B subunit amino-terminal domains (Karakas *et al.* 2011; Williams, 1993; see Traynelis *et al*. 2010).

1.4.6 NMDA receptor trafficking, expression, and links to disease

Sequences which regulate trafficking of NMDARs to, and from, the cell membrane are found in the C-terminal region of NR1 subunits (e.g. RXR motif. PKC phosphorylation sites). Additionally, the HLFY motif on the C terminal of the NR2 subunit allows ER exit of NR2-containing NMDAR isoforms. Upon exiting the ER, NMDARs are then trafficked by microtubule proteins to the golgi apparatus, where they are packaged into mobile vesicles for transport to target sites. In immature cortical neurons, prior to synapse formation, NMDARs travel along dendrites and go through cycles of exocytosis to (dependent on SNARE protein SNAP-23) and endocytosis from dendrite surfaces. Export from the endoplasmic reticulum (ER) and synaptic delivery of NMDARs is also regulated by neuronal activity. Retention of GluN2B at synapses requires binding of the C terminus to membrane-associated guanylate kinases (MAGUKs; also known as PDZ

domaincontaining scaffold proteins). Several other kinases, including cyclin-dependent kinase 5 (CDK5), protein kinase A (PKA), protein kinase C (PKC) and SRC tyrosine kinases phosphorylate specific sites of GluN2 subunits, which may impact NMDAR assembly and trafficking. GluN2B–CaMKII interaction has major implications for synaptic plasticity. This interaction is also critical for proper synapse maturation and regulation of AMPAR content during brain development. The RAS-guanine-nucleotide-releasin factor 1 (RASGRF1 (REF. 78)) and the PSD95–neuronal nitric oxide synthase complex64 are other preferential binding partners of GluN2B's CTD. Their physical association with GluN2B couples NMDAR activation to the extracellular signalregulated kinase (ERK; also known as MAPK) pathway, and to cyclic AMP-responsive element-binding protein (CREB)-mediated signalling pathways.

Additionally, neuronal activity affects NMDAR synaptic targeting, incorporation, and retrieval, of receptors into the endosome–lysosome pathway for degradation, and lateral diffusion between synaptic and extrasynaptic sites. It has been shown that blocking neuronal activity promotes alternative RNA-splicing of the NR1 subunit and increases the rate of forward trafficking of NMDARs to the membrane. Conversely, chronic neural stimulation results in subunit-specific NMDAR internalization (as well as degradation) through the ubiquitin–proteasome system. Further to this, activity-dependent insertion and retrieval of NMDARs mediate some forms of LTP and LTD. Thus, they can regulate metaplasticity at central synapses, which is interesting in light of this thesis in that studies have implicated dysregulation of NMDAR trafficking in several neuropsychiatric disorders such as schizophrenia and Alzheimer's disease.

There is also a wide array of physiological, behavioural, and clinical literature concerning the effects of altered NMDA receptor function in humans, in the form of pharmacological blockade of NMDARs, and of extant NMDAR mutations found in humans which are associated with clinical pathology. Blockade of the NMDAR in humans can result in seizures, and often produces symptoms which approximate psychosis, including impaired cognitive ability, memory, and executive function, as well as hallucinations, and delusions. It is also known that various rare point mutations of the NMDAR can result in cognitive impairment. The NMDAR

antagonist ketamine is known to induce both the positive and negative symptoms of schizophrenia in humans (Krystal *et al*. 1994) while genetically reducing NMDAR expression in mice induces behaviours reminiscent of schizophrenia (Mohn *et al*. 1999).

Indeed, previous reports implicate the NMDA receptor (NMDAR) in schizophrenia, with NMDAR antagonists producing psychotic-like symptoms and NMDAR positive modulators ameliorating this to some degree (Coyle *et al*. 2012). NMDARs has been shown to vary post-mortem in the dorsolateral prefrontal cortex in humans with schizophrenia, with an unknown but suggested influence on NMDAR subunit stoichiometry (Weickert *et al*. 2013). NMDAR-mediated pathophysiology is also implicated in early developmental processes in Schizophrenia (see du Bois & Huang, 2007). The aetiology of schizophrenia is highly complex yet nevertheless, there is an overabundance of evidence which suggests a strong NMDAR hypofunction component. Currently, a great deal of research is aimed at treating NMDAR hypofunction by pharmacologically enhancing NMDA function via the glycine binding site (Chang *et al*. 2014). Importantly, NMDAR subunit composition in the forebrain changes from a predominant GluN1/GluN2B population in immature neurones to a mixed GluN1/GluN2A/GluN2B population in adults (Monyer *et al*. 1994; Watanabe *et al*. 1992; see Wyllie *et al*. 2013).

1.4.7 Pharmacological agents which taget the NMDAR

Agent	Effect at AMPAR	Reference(s)
NMDA	Agonist	See: Wyllie *et al*. (2013); McKay *et al*. (2013); Chen *et al*. (2008); Davies & Watkins (1982).
AP5	Antagonist (competetive)	See: Wyllie *et al*. (2013); McKay *et al*. (2013): Davies & Watkins (1982); Evans *et al*. (1982).
*Ifenprodil	Channel blocker	See: Wyllie *et al*. (2013); Williams (1993); McKay *et al*. (2013).

Table 1.2: Pharmacological agents used in this thesis which affect the NMDA receptor. This table describes the typical behaviour of agonists NMDA, AP5, and ifenprofil. Note that typically subunit-selective drugs (indicated by a * prefix) is a brief description of the behaviour of a compound in terms of a broad electrophysiological response. Greater detail is supplied in later chapters where the compounds are used, and in discussion of result

1.4.8 Introduction to GABA receptors

GABA (γ-amino butryate) receptors are a class of receptors found abundantly in the CNS, which principally bind GABA as an agonist, and are subdivided into two broad types, the ionotropic $GABA_A$ and $GABA_C$ receptors, and the metabotropic $GABA_BR$. Though both types of receptors are known to be heavily expressed in the developing cortex of rodents this thesis is concerned with ion channel physiology, and as such will focus on the $GABA_A$ receptor, as $GABA_C$ receptor expression is predominantly limited to the retina.

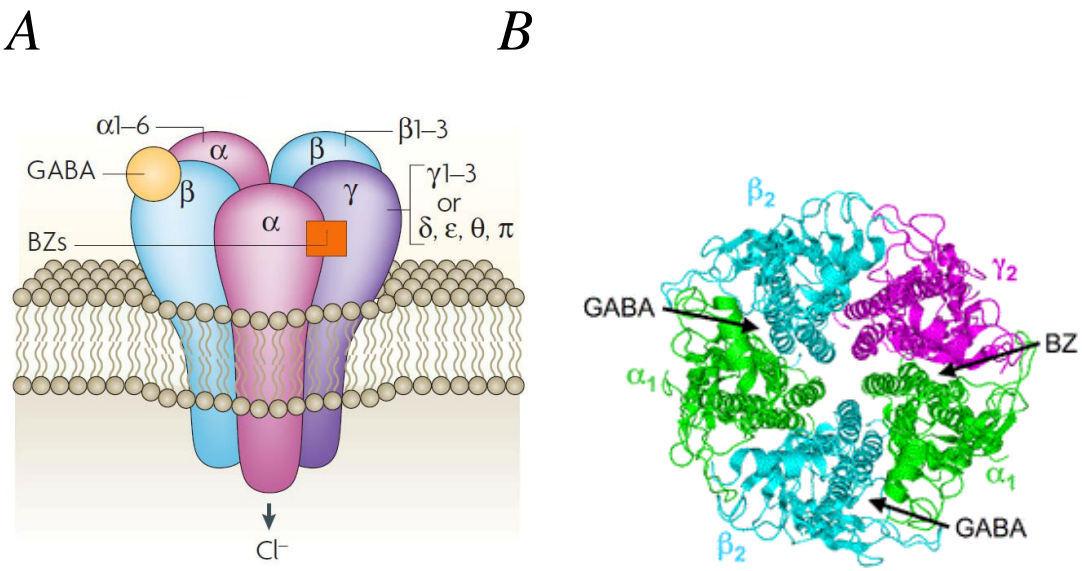

Figure 1.5. Schematic representation of $GABA_AR$ structure as found on the cell surface. ***A***: Schematic representation of GABAAR pentameric structure across the plasma membrane. Also shows GABA (α-β) and benzodiazepine (BZ, α-γ) binding sites as a product of the respective subunits. ***B***: Labels show potential variability of subunits with the subunit stoichiometry typically observed for the $GABA_AR$, with two α-subunits, two β-subunits, and a fifth additional subunit (typically γ though many others exist) around a central ion pore. Adapted from Jacob *et al.* (2008) and Clayton *et al.* (2007).

The $GABA_A$ receptors are members of the Cys loop ligand-gated ion channel superfamily which also includes the nicotinic acetylcholine receptors, the glycine receptors, and the ionotropic 5-HT_3 receptors. $GABA_A$Rs are ligand-gated anion channels that are assembled in a pentameric structure from 21 potential subunits (α_{1-6}, β_{1-4}, γ_{1-3}, δ, θ, ρ_{1-3}, ε, and π). $GABA_A$Rs are the principal mediators of fast inhibitory neurotransmission in the adult brain, and are important therapeutic targets in epilepsy, and anxiety disorder treatments, as well as being directly implicated in sedation, and anaesthesia (Reynolds *et al.* 2003). Subunit composition of $GABA_A$R confers characteristic pharmacological properties to the $GABA_A$R (Karim *et al.* 2013, Mortensen *et al.* 2011), and is tightly regulated across time and region (Laurie *et al.* 1992, Fritschy *et al.* 2005). Across development, $GABA_A$Rs are highly expressed on cortical neurones. During embryonic development the predominant isoform of $GABA_A$Rs expressed on cortical neurones is that of $\alpha_{2/3}\beta_{2/3}\gamma_2$, whereas postnatally, the most commonly expressed isoform is $\alpha_1\beta_{2/3}\gamma_2$.

$GABA_A$Rs have been shown to be instrumental in normal neuronal development, leading to the description of GABA as a 'pioneer' neurotransmitter (Ben-Ari *et al*. 2007). In embryonic development across a wide array of mammalian species, GABA-ergic transmission precedes glutamatergic transmission in early neuronal networks due to interneurone maturation which occurs at approximately E18 in rodents (Ben-Ari *et al*. 2004; Ben-Ari *et al*. 2007).

Interestingly, the initial activity of $GABA_A$Rs is depolarising, or shunting in nature, which later in development (postnatal day 5-7 in rodents) becomes excitatory (Ben-Ari *et al*. 2004). Cortical excitatory neurones exhibit a characteristic decrease in intracellular Cl- across development (see Kaila, *et al*. 2014). This shift in the action of GABA across development has also been confirmed in hECNs using an identical protocol to that used to produce hECNs used in this thesis. Intracellular Cl- activity (a measure dependent on intracellular [Cl-]) in hECNs falls from around 25 mM to <7 mM in hECNs (Livesey *et al*. 2014). This suggests a reliable platform for modelling neurodevelopmental conditions associated with impairments in Cl- co-transporter expression such as Rett syndrome (Tang *et al*. 2015; Chao *et al*. 2016), and psychotic disorders (Kalkman *et al*. 2011; Arion *et al*. 2011).

1.4.9 $GABA_A$receptor trafficking, expression, and links to disease

Like AMPARs, NMDARs, and GlyRs, $GABA_A$Rs are assembled from their component subunits in the endoplasmic reticulum (ER), whereupon they are trafficked to the golgi apparatus and secreted in vesicles to be trafficked along microtubules and the actin cytoskeleton to target sites. As with other receptors previously mentioned, this process plays a critical role in determining the diversity of receptor isoforms that are expressed on the membrane. In the case of $GABA_A$Rs exit from the ER is dependent upon proteins reaching "conformation maturity", with misfolded proteins being transferred for degradation in the proteasome. Many different subunit combinations are theoretically possible, however it has been shown that a limited number of these combinations actually leave the ER and are subsequently trafficked to the membrane. Most $GABA_A$Rs expressed on the surface of neurons are composed of 2α, 2β, and 1γ subunit (the γ subunit can be replaced by δ, ε or π depending on the neuron type and subcellular localization of the receptor), while most homomeric subunits, and αγ and βγ heteromers, are retained in the ER and degraded. This is mediated by mechanisms that involve classical ER-resident chaperones, such as heavy chain binding protein and calnexin, which facilitate the transport of selected subunit compositions. Exactly how this is achieved is not known, though it is thought that preferential subunit assembly in the ER occurs.

Studies on $GABA_A$R subunit-deficient mice demonstrate preferential assembly of subunits to form select $GABA_A$R isoforms in vivo. A loss of the δ subunit from cerebellar granule cells is seen in α6 knock-out mice. Similarly, there is a decrease in α4 subunit expression levels in the anterior cortex of δ subunit-deficient mice, whereas the levels of α1 subunits remain unchanged, showing that the δ subunit preferentially assembles with α4 and α6 subunits. Addiotionally, γ2 subunit expression also increases, perhaps as a compensatory mechanism, in δ subunit-deficient mice, additionally suggesting that γ2 willingly associates with the α4 subunit in the absence of the δ subunit. These findings overall suggest that subunits prefer certain oligomerization partners in the ER.

ER-associated degradation (ERAD) involves the process protein ubiquitination and degradation via the ubiquitin-proteasome system (UPS). $GABA_AR$ subunits are ubiquitinated in an activity-dependent manner. Long-term inhibition of neuronal activity can increase levels of $GABA_AR$ ubiquitination within the ER, resulting in decreased levels of expression at the plasma membrane, while increasing neuronal activity typically results in a decrease in $GABA_AR$ ubiquitination and thus an increase in cell surface expression. Additionally GABA receptor-associated protein (GABARAP) interacts with $GABA_ARs$ containing γ subunits and binds to microtubules as well as to N-ethylmaleimide-sensitive factor (NSF), which is implicated in vesicular fusion events. Another factor, GODZ is enriched in the trans-Golgi network, causing accumulation of γ2-containing $GABA_ARs$ at synapses. GODZ presumably acts to control $GABA_AR$ trafficking in the secretory pathway and the delivery of these receptors to the plasma membrane. Additionally, $GABA_AR$-interacting factor 1 (GRIF-1) interacts with the β2 subunit of $GABA_ARs$. It is a member of the TRAK family of coiled-coil domain proteins that have been implicated in the trafficking of intracellular vesicles by interacting with kinesin, a protein that is implicated in protein trafficking along neuronal processes.

$GABA_ARs$ are a key pharmacological target for the treatment of many illnesses such as epilepsy, stiff person syndrome, anxiety disorders, and schizophrenia. In the case of the latter, one candidate gene that is amenable to study in iPSC-derived neuronal material is the *DISC1 (1;11)(q42;q14.3)* mutation, a mutation in the DISC1 gene that is associated with psychotic disorders such as schizophrenia and bipolar disorder, as well as recurrent major depression. It is suspected that that DISC1 is involved in GABAergic neurotransmission by altering microtubule motor protein kinesin 1-mediated $GABA_AR$ trafficking in the cortex (Twelvetree *et al*. 2010; Yuen *et al*. 2012). Interestingly, knockdown of DISC1 results in a decrease in whole-cell $GABA_AR$ expression, as well as at the synapse, (Wei *et al*. 2015). As the *DISC1 (1;11)(q42;q14.3)* mutation has been associated with a lack of DISC1 protein product, it is thus highly possible that $GABA_AR$ expression in hECNs harbouring the *DISC1 (1;11)(q42;q14.3)* may be affected, and that this could be observed as a phenotype in iPSC-derived cortical neurones.

1.4.10 Pharmacological agents which taget the $GABA_AR$

Activity-dependent GABA, muscimol, bicuculline, picrotoxin, diazepam, gaboxadol, Zn^{2+}, propofol, etomidate, salycylidine salycylhydrazide, zolpidem

Agent	Effect at $GABA_AR$	Reference(s)
GABA	Agonist	See: Karim *et al*. (2013); (Mortensen *et al*. 2011).
Muscimol	Agonist	See: Karim *et al*. (2013); (Mortensen *et al*. 2011).
Bicuculline	Antagonist (competetive)	Von Blankenfeld & Kettenmann, (1991); Avoli (1992); Krishek *et al*. (1996).
Picrotoxin	Antagonist (channel blocker)	Newland & Cull-Candy (1992); Ten Bruggengate & Engberg (1971); Krishek *et al*. (1996).
*Diazepam	Potentiator	See: Riss *et al*. (2008); Hunt & Clements-Jewry (1981); Li *et al*. (2013).
*Gaboxadol	Agonist	Storustovu & Ebert (2006)
Propofol		Hill-Venning *et al.* (1997); Ruesch *et al.* (2012).
*Etomidate	Potentiator	Hill-Venning *et al.* (1997).
*SCS	Inhibitor	Thompson *et al*. (2004).
Zn^{2+}	Inhibitor	Draguhn *et al*. (1990).
*Zolpidem	Potentiator	Sanna *et al.* (2002).
*Furosemide	Inhibitor	Knoflach *et al.* (1996); Wafford *et al.* (1996).

Table 1.3: Pharmacological agents used in this thesis which affect the $GABA_A$ receptor. This table describes the typical behaviour of various agonists, antagonists, and modulators. Note that typically subunit-selective drugs (indicated by a * prefix) is a brief description of the behaviour of a compound in terms of a broad electrophysiological response. Greater detail is supplied in later chapters where the compounds are used, and in discussion of results.

1.4.11 Introduction to glycine receptors

The glycine receptor (GlyR) is a member of the pentameric Cys-loop ion channel receptor family, selectively activated by glycine and d-serine. These receptors mediate inhibitory neurotransmission in the spinal cord, brainstem and retina in mammalian species as a postsynaptic receptor, though they are also found presynaptically, where they modulate neurotransmitter release. GlyRs are pentameric ligand gated ion channels that are highly permeable to Cl^- ions, and are formed from a total of five subunits (α_1–α_4, β).

Subunit expression in the CNS also typically changes during development, with embryonic periods being defined by strong homomeric α_2 GlyR expression, which undergoes a transient postnatal shift to heteromeric $\alpha_2\beta$ before becoming a mix of mainly $\alpha_1\beta$ heteromers and smaller contributions of α_1, $\alpha 3$, and α_4 homomers in the cortex. While the precise function of different subunits remains unclear, β-subunit associates with gephyrin, and is classically known for mediating inhibitory synaptic transmission between interneurons and motor neurons in reflex circuits of the spinal cord. Even less is known about the general function of GlyRs in the human nervous system beyond their roles in adult neuronal inhibition, and by virtue of the

Early in development, GlyR predominantly have an α_2-homomeric configuration, with expression being predominantly in the spinal cord, though also in cortical areas. Postnatally, a switch occurs within the first 21 days which includes the β-subunit into the receptor complex, and coincides with the expression of α_1- and α_3-subunits at low levels in the brain, and again with typically higher levels in the spinal cord. Interestingly, α_2 mRNA has been detected in cortical layer VI in adult rats, as well as the β-subunit (Malosio *et al*. 1991). This is also reflected at the functional level by patch clamp data showing that Cajal-Retzius cells, a Layer I cortical neuronal subtype, express GlyRs shortly after birth.

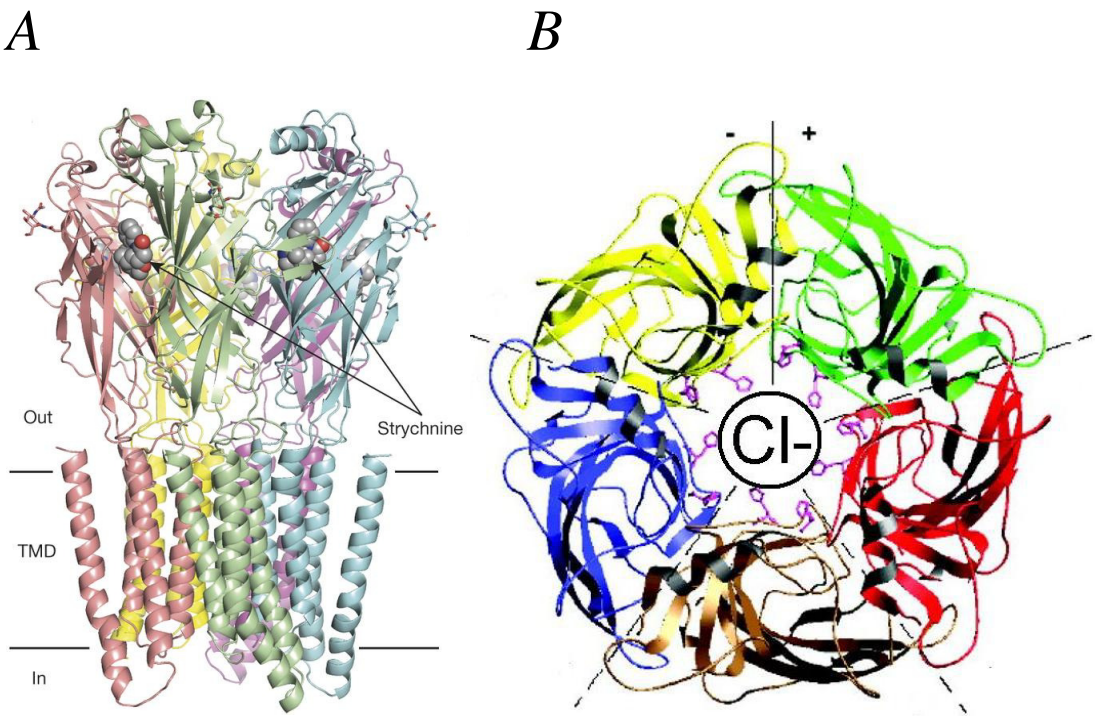

Figure 1.6. Schematic representation of GlyR crystal structure as expressed at the membrane. ***A*:** Labels show approximate sites of action for competitive antagonist strychnine. ***B*:** Crystal structure of α_3 homomeric GlyR, with ion pore indicated by Cl^- label. Adapted from Huang *et al*. (2015) and Lynch (2004).

Immunocytochemical and electrophysiological evidence also implicates $\alpha_3\beta$ GlyRs as critical mediators of glycinergic neurotransmission in nociceptive sensory neuronal circuits found in the spinal cord dorsal horn. At present, it is yet to be determined why multiple GlyR synaptic subtypes are differentially distributed in such a wide variety of tissues with specific expression patterns. The development of pharmacological agents that can discriminate strongly between GlyR isoforms is very much crucial to the advancement of this aspect of developmental study of GlyRs. A critical developmental role for GlyRs is also known, in the migration of interneurons in the developing cortex. Additionally, the $\alpha_1\beta$ GlyR is thought to be a principal mediator of both spinal pain reflexes, and neuropathic pain. As such, studying GlyR expression and subunit composition in ESCs/iPSCs is highly useful, as *in vitro* systems are highly amenable to drug screening and the assaying of

normal cortical neuronal development by implantation of exogenous tissues derived from ESCs/iPSCs.

Assembly of the GlyR complex is perdormed in the ER, whence they are trafficked to the golgi apparatus and secreted in vesicles to be trafficked along microtubules and the actin cytoskeleton to target sites. Most of the knowledge about GlyR signal processing comes from in vitro mutagenesis studies on structure-function relationships. Recently the structure of α3 and α1 were solved (Du *et al*. 2015; Huang *et al*. 2015). These structures provided deeper insights into the mechanisms of signal processing and gating. In GlyRs, the TM3–4 loops interact with the scaffold protein gephyrin important for synaptic anchoring or signal transduction processes. In addition, the TM3–4 loop is modified by posttranslational modifications and binds allosteric modulators that in turn influence functional ion channel properties (Ruiz-Gómez *et al*. 1991; Kirsch & Betz. 1995; Yevenes *et al*. 2008; Yevenes & Zeilhofer. 2011).

Subdomains of the GlyR TM3–4 loop have been demonstrated to be important for receptor trafficking to the cellular membrane and the nucleus (Sadtler *et al*. 2003; Melzer *et al*. 2010). Although different forms of plasticity at glycinergic synapses have been reported, the underlying mechanisms are unclear. For example, increases in postsynaptic Ca2+ concentration after high-frequency presynaptic activity are thought to affect the rates of insertion and retrieval of GlyRs into and from the plasma membrane. This allows modulation of the strength of glycinergic inhibition (overview in Legendre 2001). The number of GlyRs at synaptic sites is regulated by factors that control exocytotic receptor insertion into the postsynaptic membrane, anchoring of the receptors at synaptic sites by binding to the scaffolding protein gephyrin, and removal of the GlyR by endocytosis and subsequent proteolysis (overview in Moss and Smart 2001).

1.4.12 Pharmacological agents which taget the GlyR

Agent	Effect at GlyR	Reference(s)
Glycine	Agonist	Lynch (2009); Lynch (2004); De Sant-Jan *et al*. (2001); Vandenburg *et al*. (1992a)
Strychnine	Antagonist (competetive)	Ivic *et al*. (2003); Rajendra *et al*. (1991). Vandenburg *et al*. (1992b)
Picrotoxin	Antagonist (channel blocker)	Pribilla *et al*. (1992); Wang *et al*. (2006).

Table 1.4: Pharmacological agents used in this thesis which affect the glycine receptor (GlyR). This table describes the typical behaviour of agonists AMPA, CNQX, and NASPM. Note that typically subunit-selective drugs (indicated by a * prefix) is a brief description of the behaviour of a compound in terms of a broad electrophysiological response. Greater detail is supplied in later chapters where the compounds are used, and in discussion of results.

1.4.13 Introduction to Na^+-K^+-Cl^- co-transporters and Cl^- channels

Cortical excitatory neurones show a decrease in intracellular Cl^- across development, a process which is critical to normal development and maturation (see Kaila, *et al*. 2014; Ben-Ari *et al*. 2004). This is mediated by Cl^- transporter proteins, Na^+-K^+-Cl^- co-transporter 1 (NKCC1) and K^+-Cl^- co-transporter 2 (KCC2). These transporters utilise Na^+ and K^+ gradients across the cell membrane to drive Cl^- ions into the cell (NKCC1), or out of the cell (KCC2). In normal development, NKCC1 is the most strongly expressed Cl^- transporter in fetal cortical neurones, however, as postnatal development occurs, an isoform of KCC2 (KCC2b, Uvarov *et al*. 2006, Blaesse *et al*. 2009) Cl^- transporter comes to dominate. Thus there is a resultant hallmark developmental profile for neuronal tissue; when NKCC1 is dominant in early development, intracellular [Cl^-] is relatively high (approximately 25 mM), with the Cl^- reversal potential tending to be less negative than the neurones R.M.P. Thus, when a $GABA_AR$ (or indeed, a GlyR) is opened, the membrane potential depolarises to the reversal potential of chloride, occasionally resulting in excitation (Ben-Ari *et al*. 2007). As KCC2b expression increases dramatically leading to an increase in the relative expression of KCC2b with respect to NKCC1 leading to a net extrusion of Cl^- and a reduced intracellular [Cl^-] (usually <7 mM in adult excitatory neurones; Ben-Ari *et al*. 2004). The Cl^- reversal potential therefore becomes more negative and $GABA_AR$ (or GlyR) activation results in a net Cl^- influx and a hyperpolarising response (Blaesse *et al*. 2009).

Perturbed $GABA_AR$–mediated signalling has been implicated in diseases such as Rett syndrome (Chao *et al*. 2015). Previous studies using iPSC-derived neuronal material demonstrated an under-expression of KCC2 causing persistent GABA-ergic neuronal excitation, and showed a rescue to an unaffected phenotype (Tang *et al*. 2015). Intracellular chloride is also implicated in schizophrenia *via* dysregulation of intracellular chloride transporter activity that is hypothesised to disrupt normal development of neuronal networks by altering the overall balance between excitation and inhibition (see Kalkman *et al*. 2011; Arion *et al*. 2011). The previously observed phenotype in Schizophrenia is that NKCC1 expression is aberrantly increased in development, resulting in an increase in intracellular [Cl^-] in maturity.

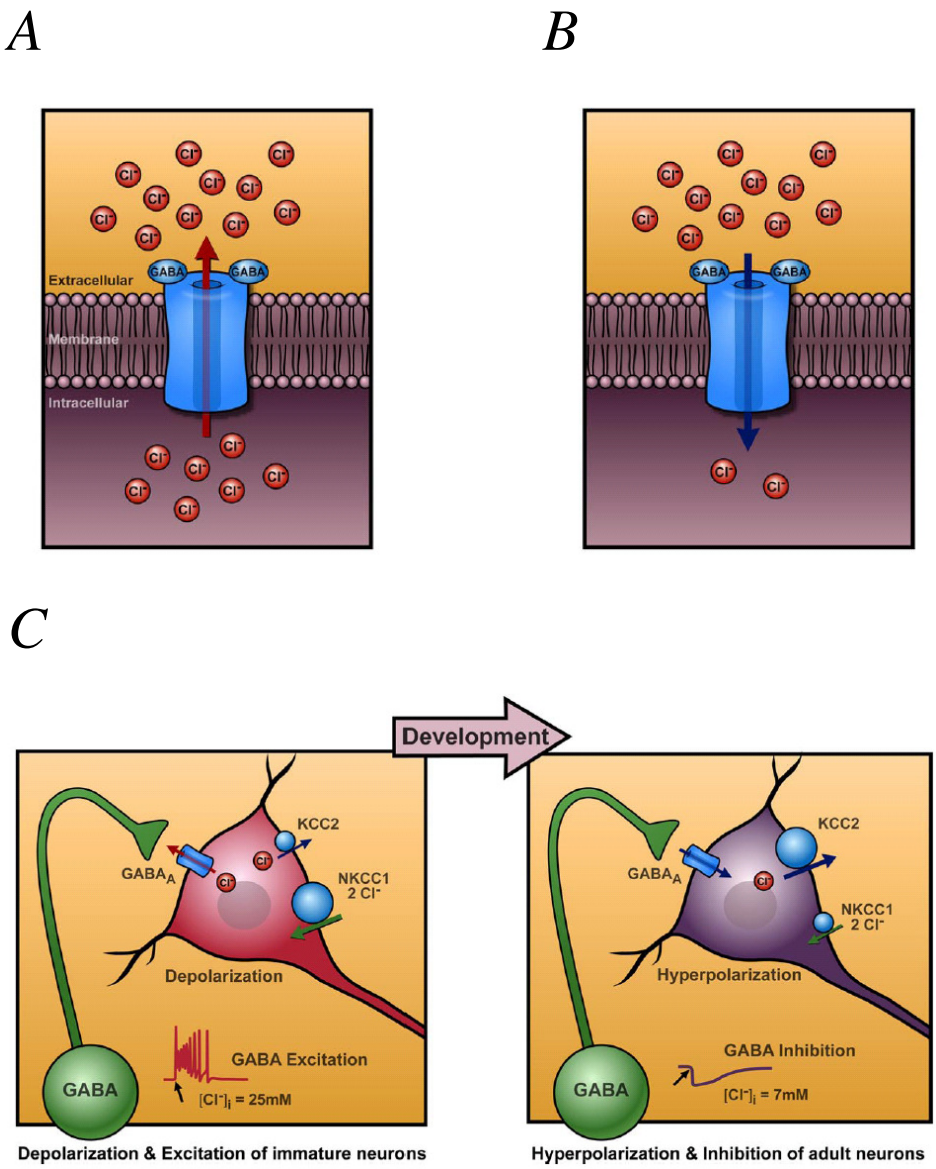

Figure 1.7. Schematic representing chloride transporter protein activity in cortical neurones across development. Adapted from Ben-Ari *et al*. (2004). ***A***: Schematic of net [Cl-] movement across the cell membrane (red arrow) upon $GABA_AR$ activation in embryonic neurones. ***B***: Schematic of net [Cl-] movement across cell membrane (red arrow) upon $GABA_AR$ activation in postnatal, and adult neurones. ***C***: Schematic illustrating net [Cl-] across development as influenced by transporter proteins KCC2 and NKCC1. Depiction of relative expression across development is determined by the size of the circles, and net ion flow as a result of transporter activity is shown by weight blue and green arrows. Resultant effect of [Cl-] on $GABA_AR$ activation (excitation, inhibition) is also shown as an example trace from image source. Note that "shunting" of inhibition is not shown.

1.5 Clinical presentation of mutations studied within this thesis, and potential indicators of ion-channel neuropathology

1.5.1 DISC1 (1;11)(q42;q14.3) translocation mutation and associated neuropsychiatric conditions

It is suggested that mutations in *DISC1* result in disrupted physiological and neuronal function leading to an imbalance in the excitation/inhibition state in the pre-frontal cortex that may underlie associated observed disease phenotypes (Bradshaw & Porteous. 2012; Lisman. 2012). Previous work has shown that *DISC1* mutations result in altered K^+-channel expression in rodent cortical neurones (Small conductance calcium-activated K^+ channels, El-Hassar *et al*. 2014; KCNQ5, Ozeki *et al*. 2003) and intrinsic neuronal excitability (Gamo *et al*. 2013) changes in neurotransmitter receptor expression and function (Akbarian *et al*. 1995; Callicot *et al*. 2013; Kim *et al*. 2012; Wright & Vissel 2012; see Hammond *et al*. 2010). Indeed, many basic functional properties of human cortical neurones harbouring the *DISC1* mutation remain to be described and iPSC technology offers a valuable opportunity to address this. Reports also suggest that epistatic interactions affecting genetic risk may occur between DISC1 and NDEL1/NDE1 (Hennah *et al*. 2007), with Ser704Cys status altering both risk of schizophrenia detected using the NDEL1/NDE1 SNPs, and NDEL1/ NDE1 binding to DISC1 (Burdick *et al*. 2008). An interaction between DISC1 3'UTR SNP rs1411771 and an intronic SNP in the gene encoding another DISC1 interactor, CIT, has also been shown to increase the risk of developing schizophrenia, and this was validated by fMRI (Nicodemus *et al*. 2010). Genetic interaction between DISC1 and PDE4B influences regional brain volume (Andreasen *et al*. 2011), while epistasis between Ser704Cys and FEZ1 is reported to act on the risk of developing schizophrenia, and synergistic effects of the two proteins on dendritic growth of newborn neurons in the adult mouse hippocampus are reported (Kang *et al*. 2011). Finally, SNPs within DISC1 and the gene encoding NKCC1 also interact (Kim *et al*. 2012). Altogether, these studies indicate that pathways involving DISC1 and these associated molecules may be of particular relevance to the aetiology of mental illness.

1.5.2 *TARDBP* mutations, and protein product TDP-43 in ALS

Amyotrophic lateral sclerosis (ALS) is the most common adult-onset motor neurone disease, and is characterized by the progressive loss of upper and lower motor neurons from the spinal cord and motor cortex which leads eventually to respiratory failure and subsequently, death. Approximately 7.5%of ALS cases are familial, with the remaining 90% being termed "sporadic" in origin. Interestingly, despite this, 97 % of patients display a common phenotype in disease-affected tissues. Deposits of TAR DNA binding protein (TDP)-43 - interestingly, TDP-43 is also the major feature of tau-negative frontotemporal dementia (FTD), which shows clinical overlap with ALS. This convergence of genetic and environmental risk factors in TDP-43 proteinopathy is hugely informative with regard to investigating general disease progression in ALS. Encoded by TARDBP, TDP-43 is a ubiquitously expressed DNA-/RNA-binding protein. TDP-43 predominantly resides in the nucleus, but is capable of moving into the cytoplams. In the nucleus, TDP-43 plays a critical role in regulating RNA splicing, as well as affecting mRNA synthesis and processing. TDP-43 also regulates the stability of its own mRNA, amounting to autoregulation of TDP-43 protein levels. TDP-43 regulates the expression of a great many other transcripts, suggesting TDP-43 influences perhaps a multitude of cellular and physiological processes. While mostly localised to the nucleus, approximately 25 % of TDP-43 protein can be found in the cytoplasm, with exit to the nucleus being regulated by both activity and stress. TDP-43 also plays a role in synaptic plasticity by modulating levels of local protein synthesis in dendrites. TDP-43 is also involved in a cytoplasmic stress response —the formation of granular protein complexes that scavenge un-needed mRNA molecules. Thus, TDP-43 function might be particularly important under conditions of physiological stress, such as excitotoxicity. Understanding the functions of endogenous TDP-43 is crucial to establishing whether loss of these functions might be key to disease pathogenesis, and to developing effective therapeutics.

TDP-43 protein was identified as a major component of the ubiquitinated neuronal cytoplasmic inclusions deposited in cortical neurones in FTD and in spinal motor neurons in ALS. TDP-43-positive inclusions have subsequently been shown to be common, if not near ubiquitous, being found in some 97 % of ALS cases

whether sporadic or familial. This transformation is evidenced by the deposition of full-length and fragmented TDP-43 protein as detergent-resistant,ubiquitinated and hyperphosphorylated aggregates in the cytoplasm, with associated clearing of TDP-43 from the nucleus. The regional spread of TDP-43 proteinopathy fromspinal and cortical motor neurons and glia to other corticalregions can be used to stage ALS progression , which suggests that some or all of the features of transformedTDP-43 protein are linked to pathogenesis.However, a key question in ALS research is which of thesefeatures of TDP-43 proteinopathy are required for the developmentof disease and thus represent therapeutic targets. Overexpression of wild-type TDP-43 recapitulatesTDP-43 proteinopathy and disease phenotypes in a range ofanimal models, supporting a role for gain of toxicfunction in disease. Initial studies testing a loss-of-functionhypothesis used knock-out of TDP-43 from mice, which resultedin embryonic lethality This demonstrated TDP-43 to play a vital role in early development without necessaril demonstrating that loss of function could be degenerative in adulthood. Interestingly, either overexpression or knockdown of TDP-43 selectively in glia or muscle also recapitulates ALS-like phenotypes [40, 41]. Previous work has highlighted an intrinsic vulnerability of ALS MNs to glutamate excitotoxicity that is mediated by Ca^{2+}-permeable AMPARs (Donnelly *et al*. 2013; Rothstein *et al*. 1995). However, the literature has yet to directly link specific AMPAR structural properties that generate Ca^{2+}-permeability in ALS MNs to genetic abnormalities (Duncan, 2009).

1.5.3 C9ORF72 (G4C2) nucleotide repeat expansion and ALS

A GGGGCC (G_4C_2) nucleotide repeat expansion (NRE) in the chromosome 9 open reading frame 72 (*C9ORF72*) gene is the most common genetic marker in familial amyotrophic lateral sclerosis (ALS) and in frontotemporal dementia (FTD)1,2. Additionally, this mutation has also been detected in approximately 12% of patients with sporadic ALS. The actual size of the NRE in terms of number of G_4C_2 repeats also varies between clinical patients with ALS and in patients with FTD carrying the mutation. While this NRE has been found to contain as many as hundreds or thousands of repeats, less than approximately 25 repeats is usually not associated with disease. At present, the size of the expansion does not appear to be related to disease severity, or age of onset. As this mutation is so commonly detected in both ALS and FTD, and also in both familial presentations, and apparent sporadic presentations of these disorders, understanding the underlying pathophysiology that it causes is possibly of use in both disease management and the development of future biomarkers for more representative or subtle physiological models for study, and the development of drug therapies.

C9ORF72 codes for a protein that can be expressed as 2 isoforms termed "long", and "short". Initially it was suspected that C9orf72 lacked structural homology with any known protein, however, recently it has been suggested that C9ORF72 protein contains a DENN domain (differentially expressed in normal and neoplastic cells), which may allow it to function as a Guanine nucleotide exchange factor (GEF). Experiments in animal systems have shown that C9ORF72 highly expressed in neurones. Additionally, it appears that the short isoform of C9ORF72 localizes to the nuclear membrane, whereas the long isoform is predominantly located in the cytoplasm. The significance of this distribution is unclear, particularly as the cellular function of C9ORF72 remains largely unknown.

The idea that aberrant C9ORF72 function imparts disease was explored in studies of patients with C9 ALS/FTD who exhibited a >50% reduction of C9ORF72 RNA levels but showed a phenotype similar to patients with C9 ALS/FTD who have higher C9ORF72 RNA levels44,45. However, recent work that used mouse models that expresses human C9ORF72 containing the (G_4C_2) NRE provided support for a possible C9ORF72 loss of function mechanism. In these studies, several gain of-function mechanisms and additional pathological features associated with disease were seen, however, the mice showed no neurodegenerative phenotypes, suggesting that gain-of-function mechanisms alone cannot explain disease pathogenesis. This suggests that loss of C9ORF72 contributes to neurodegeneration.

Crucially, there is strong evidence to show that disease progression in ALS is likely mediated, in part, by glutamate-mediated excitotoxicity (Rothstein & Cleveland, 2001.). Previous work has highlighted an intrinsic vulnerability of ALS MNs to glutamate excitotoxicity that is mediated by Ca^{2+}-permeable AMPARs (Donnelly *et al*. 2013; Rothstein *et al*. 1995). However, the literature has yet to directly link specific AMPAR structural properties that generate Ca^{2+}-permeability in ALS MNs to genetic abnormalities (Duncan, 2009).

1.6 Introduction to the patch-clamp technique

The patch-clamp technique pioneered by Sakmann and Neher (Neher & Sakmann, 1976) enabled a significant leap forward in electrophysiological study of ion channels. Previous methods such as sharp electrode intracellular recording (Ling & Gerard, 1949) were used to resolve macroscopic currents in intact neurones, however, a limitation of these approaches is an inherently high background noise and therefore were not suited to resolving the current passed by single ion channels. Thus, a technique was needed to reduce electrical noise in order to resolve activity at the level of the single ion channel.

Building on the work of Neher and Lux, Neher pressed an electrode tip against an isolated skeletal muscle fibre from frog endplate, electrically isolating the patch of membrane directly under the electrode (Neher and Lux, 1969). Given that background noise is associated with the area of membrane under study, this had the practical effect of reducing background noise closer to the pico-Ampere level, a more ideal set of conditions for recording microscopic currents.

In 1980, Sigworth & Neher established the use of high-resistance sealing of the electrode tip with the cell membrane, now commonly known as a Giga-seal (Sigworth and Neher, 1980). This had a dual effect which increased the potential quality of a recording. Firstly, the tight seal between membrane and a smooth glass electrode facilitates mechanically stable recordings, and also further electrically isolates the membrane from ion flux typical of lower resistance electrode-membrane seals (see Figure. 1.2.). The properties of mechanical stability and electrical isolation facilitated the study of ion channels through 3 key mechanisms. Firstly, the ability to record currents from the whole cell by breaking the seal such that the whole membrane is electrically continuous with the electrode ("whole-cell patch-clamp", see Figure. 1.2) enabled the examination of synaptic currents as well as bath-applied agonist-mediated ion channel activity and high-resolution recording of action potentials. Secondly, mechanical excision of the sealed patch of membrane in the "inside out" or "inside in" configurations (Figure. 1.2) enabled the study of single ion channels housed in the membrane patch. This was of great relevance as the mechanical membrane isolation methods described above enabled great advances in

structure-function studies, in that agonists and modulators could be applied to either the inside or outside of an excised membrane patch.

Thirdly, because of its high spatial and temporal resolution as a result of mechanical and electrical stability, the patch-clamp technique can be used to study the activity of transporters and metabotropic receptors on ionic balances using adaptations such as perforated patching. Here, a pore-forming antibiotic is added to the solution inside the electrode. Upon contact with the cell membrane, a Giga-seal is established. Slowly, the antibiotic polymerises into ring-like structures in the cell membrane, allowing ion conductivity with minimal dialysis of intracellular ions or proteins into the pipette solution (Kyrozis and Reichling, 1995).

1.7 Experimental aims

Thus far, it is argued that human ESC/iPSC-derived neuronal, and oligodendroglial material is sufficiently well developed as a technology to produce stable, replicable, and comparable platforms from which to study human development in both health, and disease. The scope of this thesis is to describe the extent to which iPSC technology can recapitulate certain aspects of development, and to observe any phenotypes imparted by mutations associated with neurological disease.

1.7.1 Characterising $GABA_A$Rs and GlyRs expressed on hECNs

As has been previously described, human embryonic cortical neurones derived from ESC/iPSC sources recapitulate many fundamental functional aspects of neurodevelopment as observed in animal models such as progressive lowering of intracellular [Cl^-], decreased AMPAR Ca^{2+} -permeability, and maturation of action potential parameters, little is known about the subunit composition of $GABA_A$Rs and GlyRs. Given the prominent role that GABA signalling plays in development, and recent suggestions that GlyRs may play a role in illness, such as inflammatory pain, and movement disorders, this thesis will address the question of which $GABA_A$R isoform(s) are expressed by hECNs. This represents an advance that may inform the utility of hECNs as a human *in vitro* model of $GABA_A$R, and GlyR development, particularly as a scaleable drug discovery system.

1.7.2 Investigating potential ion channel and Cl^- co-transporter function in hECNs harbouring the *DISC1* (1;11)(q42;q14.3) mutation

Thus far, it has been suggested that the *DISC1* (1;11)(q42;q14.3) mutation may result in ion channel pathologies which are highly amenable to electrophysiological study, in the form of altered AMPAR, NMDAR, and $GABA_AR$ expression, and composition. It has also been suggested that this mutation may affect Cl^- -transporter protein expression in hECNs, as has been observed in animal models. This may be relevant to the study of the inhibitory-excitatory balance during network formation in neurodevelopmental hypotheses of psychotic disorders associated with the DISC1 (1:11)(q42;114.3) mutation, such as schizophrenia.

Additionally, previous work suggests that the *DISC1* (1;11)(q42;q14.3) mutation may also produce subtle, yet general developmental deficits in maturation as described by ion channel expression.

1.7.3 General development, and possible AMPAR pathology in an iPSC-MN model of ALS

Crucially, there is strong evidence to show that disease progression in ALS is likely mediated, in part, by glutamate-mediated excitotoxicity (Rothstein & Cleveland, 2001.). Previous work has highlighted an intrinsic vulnerability of ALS MNs to glutamate excitotoxicity that is mediated by Ca^{2+}-permeable AMPARs (Donnelly *et al*. 2013; Rothstein *et al*. 1995). However, the literature has yet to directly link specific AMPAR structural properties that generate Ca^{2+}-permeability in ALS MNs

1.7.4 General development, and possible AMPAR pathology in an iPSC-OPC/OL model of ALS

Previous work has suggested an intrinsic vulnerability of OPCs and OLs to glutamate excitotoxicity that is mediated by Ca^{2+}-permeable AMPARs in a manner similar to that as described in MNs (see Donnelly *et al*. 2013; Rothstein *et al*. 1995). However, the literature has yet to directly link specific AMPAR structural properties that generate Ca^{2+}-permeability in OPC/OLs.

Chapter 2

Materials and Methods

2.1 Generation of induced pluripotent stem cells (iPSCs) and specification of cellular identities from iPSCs and embryonic stem cells (ESCs).

2.1.1 Sources of ESCs and iPSCs

ESCs were obtained from WiCell (Madison, WI) with full ethical/IRB approval of the University of Edinburgh. Hereafter, H9 ESC derived material will be described as '*ES*' in figures and text.

The technology of iPSC reprogramming is based on the use of Yamanaka factors, a set of transcription factors which are highly expressed in ESCs and which induce pluripotency in mouse and human somatic cells (Liu *et al*. 2008). Briefly, iPSCs were generated from grafted adult upper arm dermis by reprogramming fibroblasts to pluripotency using retroviral vectors expressing coding sequences of genes constituting Yamanaka factors *OCT4 and SOX2 ('core' factors)*, *c-MYC (upregulates metabolism)*, *KLF4 (enhances effects of core factors), and additional factors* hTERT and SV40 large T (see Liu *et al*. 2008). In the case of iPSCs, written informed consent was obtained from each individual participant. iPSC generation and derivation to regionally specific material was performed by the Chandran laboratory. iPSCs used in this Thesis:

2.1.2 Control iPSC lines

The iPSC control line was derived from fibroblasts taken from a 56-yr old normal male, hereafter designated as '*Control*.' For DISC1 experiments, control cell lines DR3 and GS8 not harbouring the (1;11)(q42;q14.3) translocation were derived from disease-unaffected relatives of diagnosed psychiatric patients. Hereafter, line DR3 and GS8 will be respectively described as '$DISC_{Control}$-*1*' and '$DISC_{Control}$-*2*'. Where data are pooled, lines will be referred to in graphs and text as 'Control', with 'N' denoting number of lines pooled.

2.1.3 Case iPSC lines

Two mutant lines were generated from MND patients harbouring the *C9ORF72* (G_4C_2) repeat expansion and will be referred to as "*C9-1*" and "*C9-2*" in the text. A third line derived from C9-2 which has the G_4C_2 repeats excised by Cas9/CRISPR is known as "*ΔC9-2*". Gene editing on line C9-2 was conducted by Dr. Bhuvaneish Selveraj using the CRISPR/Cas9 genome engineering system detailed in Ran & Hsu (2013). Briefly, hexanucleuotide repeats in *C9ORF72* mutant lines were excised using an RNA-guided nuclease (Cas9) targeted to the sequence of the hexanucleotide repeats.

Three separate lines expressing mutated forms of TDP-43 were also generated. Firstly, one derived from a patient harbouring the M337V mutation, referred to as "*TDP-1*", and two others harbouring the G298S mutation derived from two different patients, referred to in the text as "*TDP-2*", and "*TDP-3*". A third line, derived from *TDP-3*, with the G298S point mutation corrected using Cas9/CRISPR by Dr. Bhuvaneish Selveraj, is referred to as "*ΔTDP-3*".

Patient-derived DISC1 iPSC lines were taken from individuals with a diagnosed psychiatric disorder (MW and MR) who's genomes harbour the (1;11)(q42;q14.3) translocation mutation in the DISC1 gene, and are referred to in the text as '$DISC_{Case}$-*1*' (derived from MW) and '$DISC_{Case}$-*2*' (derived from MR). Where data are pooled, lines will be referred to in graphs and text as 'Case', with 'N' denoting number of lines pooled.

2.2 *In vitro* ESC/iPSC-derived material generation

2.2.1 Human excitatory cortical neurone (hECN) generation

The following protocol was employed previously in Bilican *et al*. (2014), Livesey *et al*. (2014) and is summarised in Figure. 2.1. ESCs/iPSCs were maintained on irradiated mouse CF-1 embryonic fibroblasts supplemented with Advanced DMEM/F12 (A-DMEM/F12), L-glutamine (1 mM), Knockout Serum Replacement (20%, PeproTech), FGF2 (10 ng/ml, Sigma), 2-mercaptoethanol (100 mM, Sigma) and 1% penicillin/streptomycin (P/S, 1%, Sigma). ESCs/iPSCs were neuralised in suspension in chemically defined medium as described in Stacpoole *et al*. (2011). The media was changed to Base media (A-DMEM/F12 (BD Biosciences), P/S (1%), Glutamax (1%, BD Biosciences), N2 (1%), B27 (0.4%), FGF-2 (2.5 ng/ml, Sigma) upon observation of radially oriented structures in neurospheres (10–21 days) and, after 7 days, plated on Laminin (Sigma) coated tissue culture plates (Nunc). Neural rosettes were mechanically isolated and subsequently dissociated with Accutase (Sigma). 20-40k cells were then plated onto one Laminin-coated well of a 96-well plate (Nunc) in proliferation media (Base media, B27 (0.1%), FGF2 (10 ng/ml), and EGF (10 ng/ml). Anterior neuronal precursors (aNPCs) were grown to high density before passaging 1:2 with Accutase (Sigma) on laminin (Sigma) coated plates until passage 5–6 and maintained on 1:100 Reduced-growth factor Matrigel (BD Biosciences) coated plates thereafter.

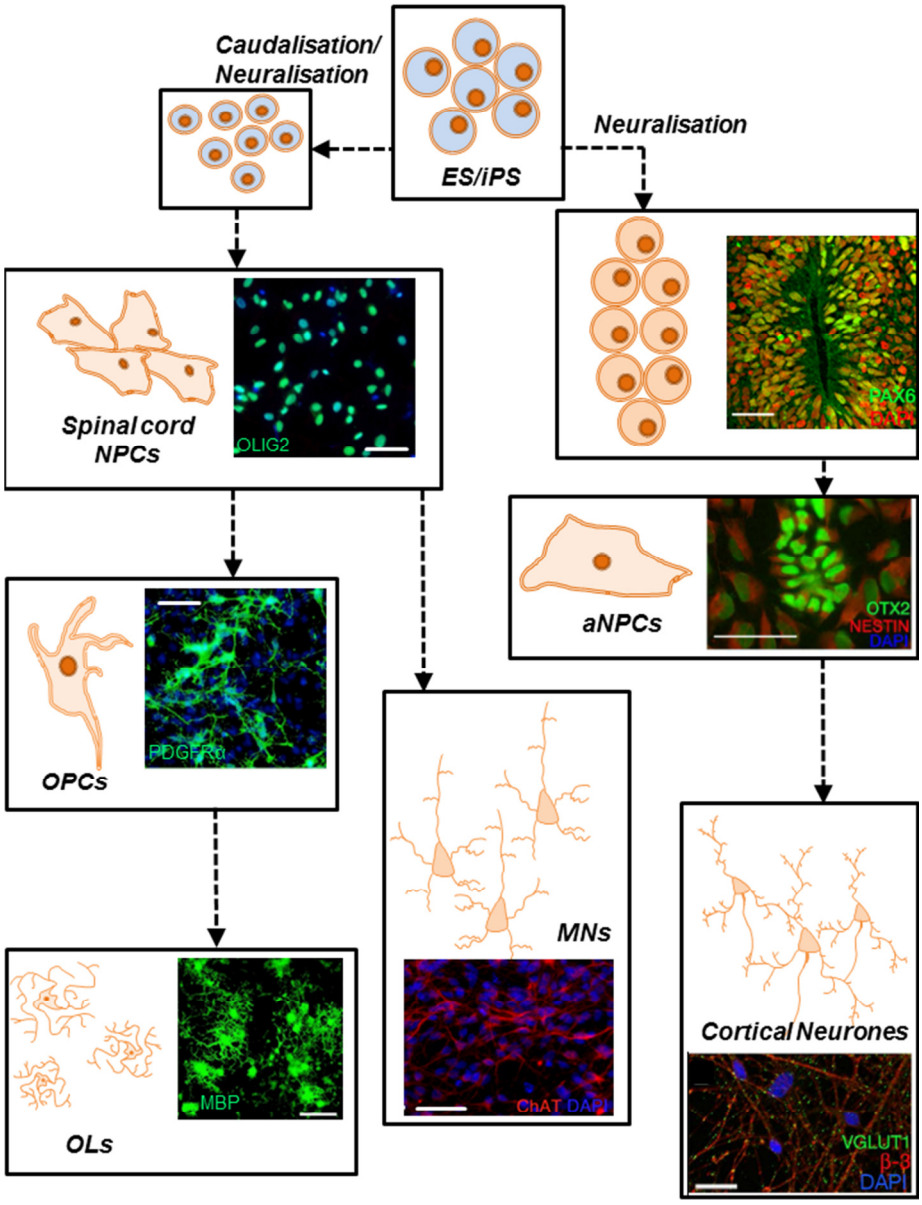

Figure. 2.1, Schematic describing generation of material. Cortical neurones were neuralised using the default method of neurogenesis involving minimal chemical conditioning. The NPCs generated stained for telencephaelic marker FOXG1. aNPCs were maintained in 3% O_2, plated down and FGF2 removed for differentiation. For both OLs and MNs, iPSC were neutralised using Dual SMAD inhibition and caudalised with RA to give spinal cord NPCs positive for OLIG2. For MNs, NPCs were induced by the addition of Purmorphamine and BDNF/GDNF. For OPCs/OLs, lineages were established by the addition of SAG, Purmorphamine, PDGFα, and T3. Terminal differentiation into OLs was achieved by mitogen withdrawl. Immunohistochemical stainings used with permission, taken from Bilican *et al.* (2012), Bilican *et al.* (2014), Livesey *et al.* (2014) and provided by D.Magnani. Scale bars = 20 μm.

For the generation of neuronal cultures, aNPCs (see Figure. 2.1) were plated at 20-25k (for ESC-derived aNPCs) or 100-120k (iPSC-derived aNPCs) in default media A-DMEM/F12, Invitrogen), containing P/S (1%, Sigma), Glutamax (0.5%, Sigma), N2 (0.5%, Sigma), B27 (0.2%), Heparin (2 µg/mL, Sigma) on poly-D-lysine (Sigma), laminin (Sigma), fibronectin (Sigma), coated coverslips for differentiation in 3% O_2, and fed twice weekly. For hECNs (see Figure. 1.1), default media was supplemented with forskolin (10 µM, Tocris) from DIV 14-21. From DIV 21 onwards forskolin was removed. Cells were stored in default media thereafter containing BDNF (20 ng/mlSigma) GDNF (20 ng/ml, Sigma) from DIV 21. For studies examining $[Cl^-]_i$, BDNF and GDNF were omitted and included IGF-1 (20 µg/ml, PeproTech) from week 4.

2.2.2 Human lower motor neurone generation

A summary of the protocol is given in Figure 1. For differentiation into motor neurons, iPSCs were initially neuralised to a caudal identity using proliferation media supplemented with with Retinoic Acid (RA, 0.3mM, Sigma), then plated down on poly-D-lysine (Sigma), laminin (Sigma)- and fibronectin (Sigma)-coated coverslips in Neurobasal, RA (0.1 mM), Purmorphamine (2 mM Calbiochem), N2 (1%), P/S (1%), Glutamax (1%), bFGF (5 ng/ml) for 7–10 days to promote generation of precursors. Motor neuron precursors were re-plated and media was switched to Neurobasal, N2 (0.5%, Sigma), B27 (0.2%, Sigma), P/S (1%, Sigma), Glutamax (0.5%, Invitrogen), BDNF (10 ng/ml, Sigma), GDNF (10 ng/ml, Sigma). The protocol follows a new protocol by Maury *et al*. (2015).

2.2.3 Human OPC/OL generation

A summary of the protocol is given in Figure 1. For the generation of oligodendrocytes and OPCs, derivation of spinal cord neural precursors (NPCs), was performed as described in Bilican *et al*. (2012). NPCs were cultured in suspension as neurospheres in Advanced DMEM/F12 (Invitrogen) supplemented with: GlutaMAX (0.5%, Invitrogen), FGF-2 (20 ng/ml PeproTech), N-2 (1%, Invitrogen), B27 (1%, Invitrogen), P/S (1%, Invitrogen), PDGFα (20 ng/ml, PeproTech), puromorphamine (1 μM,Calbiochem), SAG (1 μM, Calbiochem), T3 (60 ng/ml, Sigma), and IGF-1 (10 ng/ml, PeproTech), for 6-12 weeks. Neurospheres were dissociated with papain and plated Matrigel (BD Biosciences), Fibronectin (Sigma), Laminin (Sigma) coated coverslips. Terminal differentiation of oligodendrocytes was achieved by mitogen withdrawal (except for T3 and IGF-1).

2.3 Electrophysiology

2.3.1 Introduction to the patch-clamp technique

The patch clamp technique (Sigworth and Neher, 1980) is a high-resolution electrophysiological recording technique capable of observing minute current, or voltage changes, in the cell under recording. Because of its high spatial and temporal resolution as a result of mechanical and electrical stability, the patch-clamp technique can be used to study the activity of ion channels and the biophysical behaviour of cell membranes in a variety of configurations (see Figure. 1.2) as well as transporters and metabotropic receptors on ionic balances using adaptations such as perforated patching (Figure. 1.2). Here, a pore-forming antibiotic is added to the solution inside the electrode. Upon contact with the cell membrane, a Giga-seal is established. Slowly, the antibiotic polymerises into ring-like structures in the cell membrane, allowing ion conductivity with minimal dialysis of intracellular ions or proteins into the pipette solution (Kyrozis and Reichling, 1995). Recordings described in this thesis utilise either the whole-cell configuration, or the perforated patch recording method (where stated).

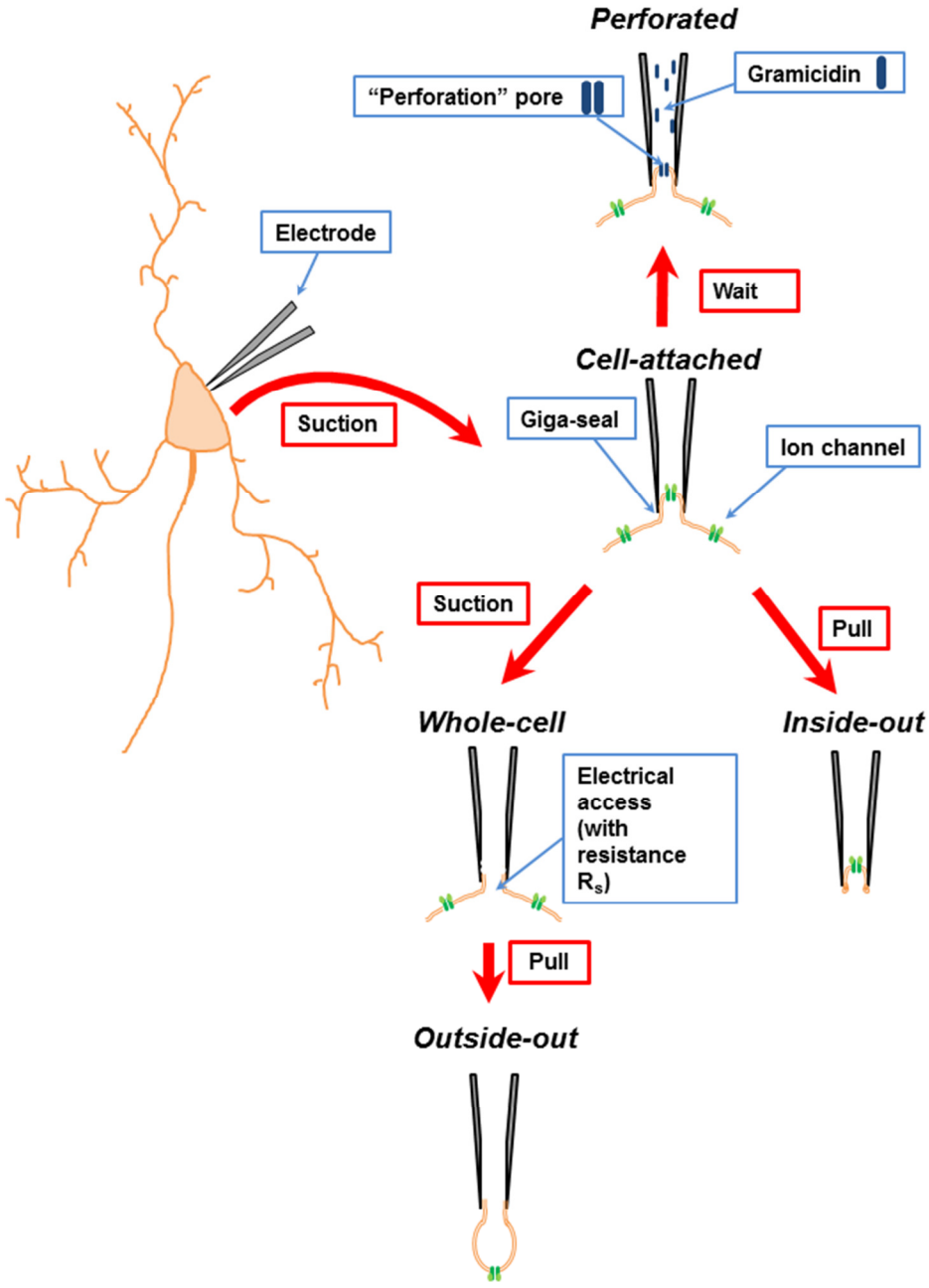

Figure 2.2, Patch-Clamp Configurations. Schematic showing the various methods of establishing different patch-clamp configurations. Initially, the "*Cell-attached*" configuration is achieved by application of negative pressure (mild suction) to produce a Giga-seal. In the presence of a perforation agent added to the patch pipette (here, Gramicidin), waiting results in the *perforated* configuration. Electrode withdrawal from the cell-attached configuration results in an *inside-out* patch, whereas an acute-application of sharp suction breaks the membrane isolated by the electrode tip resulting in a *whole-cell* patch.

Mechanical electrode withdrawal from the *whole-cell* configuration results in the *outside-out* configuration.

2.3.2 Patch electrodes

Electrodes were made from thick-walled borosilicate glass of 1.5 mm outer diameter and 0.86 mm inner diameter with filament (Harvard Apparatus). Electrodes were pulled on a Narishige PP-830 two-stage pipette puller (Narishige, Japan), and when were filled with an internal recording solution (see 2.3.3) had final resistances of 4 – 7 MΩ. .

2.3.3 Patch-clamp recording

The whole-cell patch-clamp technique was used to record currents from ESC/iPSC-derived material using an Axon Multiclamp 700B amplifier (Molecular Devices, Sunnyvale, CA). Patch electrodes were filled with internal recording solutions as described in the text, with the following compositions (amounts in mM):

Potassium Gluconate Internal Solution (K-Gluconate internal):
K-gluconate 155, $MgCl_2$ 2, Na-HEPES 10, Mg_2-ATP 2, Na-PiCreatine 10, and Na_3-GTP 0.3, pH 7.3 at 300 mOsm. The use of K-gluc asssocited with a liquid junction potential (LJP) of +14 mV (LJPcalc; Barry, 1994).), which was corrected *post hoc*. All reported voltage data is corrected for LJP.

Potassium Chloride Internal Solution (KCl internal):
KCl 145, $MgCl_2$ 1, $CaCl_2$ 0.1, EGTA 1, Na-HEPES 10, pH 7.3 at 300 mOsm. (LJP = +4.3 mV).

Caesium Chloride Internal Solution (CsCl internal):
CsCl 140, EGTA 1.1, $CaCl_2$ 0.1, $MgCl_2$ 1, Na-HEPES 10, Mg_2-ATP 2, pH 7.3 at 300 mOsm. (LJP = +1.3mV).

Glass coverslips containing ESC/iPSC-derived cultures were placed in the recording chamber and superfused with an external solution composed of (in mM) NaCl 152, KCl 2.8, glucose 10, $CaCl_2$ 2, HEPES 10, pH 7.3 (320–330 mOsm) using a gravity-fed perfusion system at room temperature (20-23°C), and, where indicated, a higher temperature of 30-33^{o}C, with a flow rate of approximately 4 ml.min^{-1} in all cases. Series resistance (R_s) was generally less than 25 MΩ in the case of whole-cell recordings, with an absolute cut off R_s of 30 MΩ. Recordings were discarded if change in R_s exceeded 10%.

In the case of perforated patch-clamp recording to examine $[Cl]_i$, a KCl internal solution was supplemented with gramicidin (75-100 μg mL^{-1}. Gramicidin is permeable to Na^+ and K^+ ions, but not Cl^- (Tajima *et al.* 1996). Therefore, the use of Gramicidin does not affect intracellular [Cl^-]. Perforation was monitored by the increase in size of capacitive transients which reflect R_s. Here, R_s was typically below 30 MΩ with an absolute cut off R_s of 40 MΩ. R_s was compensated to 80% in all cases, and recordings were discarded if R_s changed by greater than 15% during the recording.

2.3.4 Application of pharmacological agents

In the case of assessing agonist and antagonist potency, and current modulation (potentiation or inhibition), three applications of a given concentration of agonist that gave equivalent current amplitudes within 15% of the initial amplitude were obtained to establish a stable current response prior to the experimental pharmacological assay. Similarly, a control concentration of agonist was applied at the end of the assay to ensure recording stability. Recordings were only accepted as valid if the amplitude of the final control response was within 15% of the initial controls. Selective agonists, antagonists and allosteric modulators were purchased either from Tocris Bioscience (Bristol, UK) or Abcam (Cambridge, UK).

Pharmacological agents were applied using a bath-exchange system which utilised a gravity feed with multiple possible aCSF sources ("barrels") containing an appropriate concentration of experimental agents. These barrels are switched as required to deliver various agents, with the liquid aCSF contents of the bath being replaced within approximately 5 - 10 seconds of onset. With the exception of non-stationary fluctuation analysis experiments (which require slow onset of agonist as described in Chapter 2.4.2), onset time was minimised as much as possible with no recording with an onset time of greater than 5 seconds being considered for analysis.

2.4 Data analysis and statistics

Whole-cell patch-clamp, recordings were low-pass filtered at 2 kHz, digitized at 10 kHz via a BNC-2090A (National Instruments, Texas, USA) interface and recorded to computer using the WinEDR V2.7.6 Electrophysiology Data Recorder (J. Dempster, University of Strathclyde, UK (www.strath.ac.uk/departments/physpharm). Data are presented as mean ± standard error of the mean (s.e.m). The number of experimental replicates is denoted as 'n,' while 'N' represents number of de novo preparations of batches form which 'n' is obtained. Statistical analysis was conducted using Student's *t*-test as multiple comparisons across large data sets was not necessary. This form of *t*-test is considered standard format for peer review, including material contained Chapter 3, published as James *et al*. (2014), and Chapter 6, contributing to Livesey *et al*. (2015). Where results are described by asterisks (*), * indicates p=<0.05, ** indicates p=<0.01. *** indicates p=<0.001

The rationale for using individual cells as 'n', and number of experimental replicates as 'N' was to establish that so-called "batch to batch" variation did not underlie any putative cellular phenotype observed in stem-cell derived neuronal material grown *in vitro*, or rather, to account for this effect if noticed in order to interpret the effects of any experimental intervention. For example, if a cellular phenotype for a mutation which may impact general neuronal development was being studied, and one "batch" of hECNs typically displayed a slower maturational profile, then an artefactual phenotype would result. This effect is then presumed to be comparable between hECNs with and without the mutation when taking into account multiple derivations of either, and indeed, both.

2.4.1 Agonist and antagonist concentration response curves

Agonist concentration-response curves were fitted individually for each cell using the Hill equation:

$$I = \frac{I_{MAX}}{1 + \left(\frac{[EC_{50}]}{[A]}\right)nH}$$

where I is the current response to agonist concentration [A], n_H is the Hill coefficient, I_{max} is the maximum current and EC_{50} is the concentration of agonist that produces a half-maximal response. Each data point was normalized to the fitted maximum of the dose-response curve, then pooled, averaged and re-fitted again with the same equation with the maximum and minimum for each curve being constrained to asymptote to 1 and 0, respectively (Frizelle *et al.* 2006) .

Concentrations of antagonists required to inhibit agonist-evoked responses by 50% (IC_{50}) were determined by fitting inhibition curves with the equation:

$$I = \frac{I_{[B]0}}{1 + \left(\frac{[B]}{IC_{50}}\right)nH}$$

where n_H is the Hill coefficient, $I_{[B]0}$ is the predicted current in the absence of antagonist and [B] is the concentration of the antagonist. Data points were again normalized to the fitted maximum, before pooling, averaging and re-fitting as described above.

2.4.2 Non stationary fluctuation analysis

Non-stationary fluctuation analysis (Colquhoun, 1979; Dempster, 1993) was conducted on slow-rising whole-cell currents evoked by AMPA (10 μM) in the presence of cyclothiazide (10 μM) at a holding potential of –84 mV. Current recordings were split to generate AC- and DC- characteristics. To generate the AC-characteristic, currents were amplified 10 times to that of the DC current and low-pass filtered using a Butterworth filter (1 – 1200 Hz). The resultant variance in current evoked by AMPA was plotted against a simultaneously acquired DC component of the whole-cell current in order to yield a linear relationship. The resulting slope gave the estimated unitary single-channel current amplitude that was used to estimate AMPAR single-channel conductance (γ), which is given by the equation:

$$\gamma = \frac{i}{V_{hold} - E_{rev}}$$

Given the AMPAR is a non-selective cation channel (Jonas, 1993) and we established its E_{rev} to be close to 0 mV, then the AMPAR single-channel conductance equation was reduced to:

$$\gamma = \frac{\mathrm{i}}{\mathrm{V_{hold}}}$$

2.4.3 Rectification Indices

Ion channel rectification is the property of preferential movement of charge across the cell membrane at equal, but opposite driving forces. This is described in terms of "inward" and "outward" rectification or an Ohmic relationship where no rectification is present. A rectification index (RI) can be used to describe these properties and is given as the outward conductance divided by the inward conductance. Thus, with no rectification, the index is 1. When values are less than or greater than 1, this indicates inward and outward rectification, respectively. RIs were calculated from the following equation:

$$RI = \frac{I/(16 - E_{REV})}{I/(124 - E_{REV})}$$

where *I* is current amplitude, and, *Erev* indicates the reversal potential of currents under study.

2.4.4 The Nernst equation and estimation of $[Cl^-]_i$

The Nernst equation was used to estimate the $[Cl]_i$.

$$E_{GABA} = \frac{RT}{ZF} ln \frac{[Cl^-]_o}{[Cl^-]_i}$$

Where E_{GABA} represents the experimentally established $GABA_AR$-mediated reversal potentials (corrected for LJP *post hoc*), R is the universal gas constant, T is the temperature in Kelvin, *z* is the valence of the ion species in question (for chloride, -1), and F is the Faraday constant. $[Cl^-]_i$ is intracellular Cl^- activity. Cl^- activity was calculated using a thermodynamic activity co-efficient (0.76, Bormann *et al*. (1987).

2.5 Imaging and identification of cell types

Identification of oligodendrocyte precursors, and oligodendrocytes, was conducted *via* fluorescence microscopy on live iPSC-derived OPC/OL cultures *in vitro*, while simultaneously conducting electrophysiological experiments on said live tissue cultures. This process allows selective staining of cell types expressing PDGDFRα, a marker for OPCs, and O4, the canonical mature OL marker that strongly assiociates with myelin basic protein (MBP) expression – itself a marker of mature oligodendrocytes. A full characterisation of the protocol and methods used to establish the expression of these markers in iPSC- derived OPC/OLs can be found in Livesey *et al*. 2015. In experiments outlined within this thesis, the robust expression of this marker in these OPC/OL cultures facilitatesd quick and clear identification of these cell types.

2.5.1 Identification of iPSC-derived Oligodendrocytes and OPCs

In order to distinguish and identify OPCs and OLs, plated cultures were incubated in a 4-well culture plate (Nunc) with a PDGFRα primary antibody (Cell Signalling, 1:300), or in the case of oligodendrocytes, an O4 (R&D Systems, 1:1000) for 1h in default media. Cells were then washed by emptying 75% of media in each well, refilling each well with default media (500 μL) a total of 4 times. Cultures were subsequently incubated with a secondary antibody at 1:1000 dilution, conjugated to a fluorophore (Alexa Fluor 470, Molecular Probes Inc.) against anti-O4 primary Ab, Alexa Fluor 588, (Molecular Probes Inc) for anti-PDGFRα primary Ab) for 45 minutes after which each culture plate was washed with default media by replacement a further 5 times. Cells were then left to equilibrate in an incubator for a further hour and imaged live at the rig where electrophysiological experiments were conducted as described.

Live imaging was conducted using an Olympus IX51 Inverted microscope (Olympus, Shuinjuku, Japan) fitted with CoolLED pE100 (CoolLED, UK) fluorophore excitation light sources. Glass coverslips in the recording chamber were observed through a phase-contrast array and lit with an Olympus TL4 brightfield lighting system (Olympus, Japan) and a WAT902H CCD camera (Watec, USA).

2.5.2 Antibodies described in this thesis

Table 2.1

Antibody	Host	Company
BRN2	Goat polyclonal	Santa Cruz
CTIP2	Rat monoclonal	Abcam
CUX1	Mouse monoclonal	Abnova
EGFR1	Mouse monoclonal	BD biosciences
FOXG1	Rabbit polyclonal	Abcam
GAD65/67	Rabbit polyclonal	Millipore
HB9	Mouse monoclonal	DHSB
HOXB4	Mouse monoclonal	DHSB
MAP2	Mouse monoclonal	Sigma
NESTIN	Mouse monoclonal	Millipore
OLIG2	Rabbit polyclonal	Millipore
OTX2	Goat polyclonal	R&D Systems
PAX6	Mouse monoclonal	DHSB
PSD-95	Mouse monoclonal	Neuromab
PSD-95	Rabbit polyclonal	Cell Signaling
REELIN	Mouse monoclonal	Novus
SATB2	Mouse monoclonal	Abcam
Sox1	Rabbit polyclonal	Millipore
O4	Mouse monoclonal	R&D Systems
PDGFRα	Goat polyclonal	Cell Signalling
VGLUT1	Mouse monoclonal	Neuromab
β-3 Tub	Mouse monoclonal	Sigma

2.6 Full list of abbreviations used in this thesis

Table 2.2 For reference this list is presented in alphabetical order.

aCSF	Artificial cerebro-spinal fluid
AD	Alzheimer's disease
A-DMEM	Advanced Dulbecco's Modified Eagle's Medium
AHP	After-hyperpolarisation
ALDH1A2	Aldehyde dehydrogenase 1A2
ALS	Amyotrophic Lateral Sclerosis
AMPA	α-amino-3-hydroxy-5-methyl-4-isoxazolepropionic acid
aNPC	Anterior neural precursor cell
AP	Action potential
AP5	(2R)-amino-5-phosphonovaleric acid; (2R)-amino-5-phosphonopentanoate
Bic	Bicuculline
BMP	Bone morphogenic protein
BNC	Bayonet Neill–Concelman
C9ORF72	Chromosome 9, open reading frame 72
Ca2+	Calcium
CamKII	Calcium-calmodulin kinase 2
Cas9	CRISPR associated protein 9
CCD	Charge-coupled device
ChAT	Choline acetyltransferase
c-MYC	Myelocytomatosis viral oncogene c-variant
CNQX	6 -cyano-7-nitroquinoxaline-2,3-dione
CNS	Central nervous system
CRISPR	Clustered regularly interspaced short palindromic repeats
CSF	Cerebro-spinal fluid
CTIP2	Chicken ovalbumin upstream promoter transcription factor-interacting protein 2
CUX1	Cut-like homeobox-1

DISC1	Disrupted in schizophrenia-1 (gene product).
DISC1	Disrupted in schizophrenia-1 (gene).
DIV	Days *in vitro*
DMEM	Dulbecco's modified Eagle's medium
DNA	Deoxyribonucleic acid
DZ	Diazepam
EGTA	Ethylene glycol-bis(β-aminoethyl ether)-N,N,N',N'-tetraacetic acid
ESC	Embryonic stem cell
Etom	Etomidate
FEZ1	Fasciculation And Elongation Protein Zeta 1
FGF	Fibroblast growth factor
FGF-2	Fibroblast growth factor 2
FGF-8	Fibroblast growth factor 8
fMRI	Functional magnetic resonance imaging
FOXG1	Forkhead box G1
FTD	Fronto-temporal dementia
Furo	Furosemide
GABA	Gamma-amino butyric acid
GE	Ganglionic eminence
GEF	Guanine nucleotide exchange factor
GFAP	Glial fibrillary acidic protein
Gly	Glycine
GPCR	G-protein coupled receptors
HEPES	4-(2-hydroxyethyl)-1-piperazineethanesulfonic acid
HP	Holding potential
hPSC	Human pluripotent stem cell
hTERT	Human telomerase reverse transcriptase
K+	Potassium
KCC2	K+/Cl- co-transporter protein 2

LGE	Lateral ganglionic eminence
LGIC	Ligand-gated ion channel
LTD	Long-term depression
LTP	Long-term potentiation
Mg2+	Magnesium
MGE	Medial ganglionic eminence
MN	Motor neurone
MRI	Magnetic resonance imaging
mRNA	Messenger RNA
Mus	Muscimol
Na+	Sodium
NASPM	N-acetyl spermine
NDE1	NudE Neurodevelopment Protein 1
NDEL1	NudE Neurodevelopment Protein 1 Like 1
NKCC1	Na+/K+/Cl- co-transporter protein 1
NMDA	N-methyl D-aspartate
NPC	Neural precursor cell
NRE	Nuclear repeat expansion
O4	Oligodendrocyte marker 4
OCT4	Octamer-binding transcription factor 4
OL	Oligodendrocyte
Olig2	Oligodendrocyte transcription factor 2
OPC	Oligodendrocyte precursor cell
PDE4B	Phosphodiesterase 4B
PDGFRα	Platelet derived growth factor receptor alpha
PFC	Pre-frontal cortex
PKC	Protein kinase C
Prop	Propofol
PTX	Picrotoxin
RA	Retinoic acid

RI	Rectification index
RMP	Resting membrane potential
RNA	Ribonucleic acid
ROR-β	Retinoic acid-related orphan receptor beta
SATB2	Special amino terminal-rich sequence-binding protein 2
SC	Spinal cord
SCS	Salicylidine Salycylhydrazide
SHH	Sonic Hedgehog
SMAD	SMA and MAD-related protein
SNP	single nucleotide polymorphism
SOD-1	Superoxide dismutase 1
SOX2	Sex determining region Y box 2
SOX5	Sex determining region Y box 2
STX	Strychnine
SVZ	Sub-ventricular zone
TARDBP	TAR DNA-binding protein (gene).
TBR1	T-box brain 1
TDP-43	TAR DNA-binding protein 43 kDa.
TGF-β	Transforming growth factor beta
TTX	Tetrodotoxin
UTR	Untranslated region
Val	Valproic acid
VGLUT1	Vesicular glutamate transporter 1
VNa	Voltage-sensitive Na+ channel
VZ	Ventricular zone
WNT	Wingless-Int1 intracellular protein signalling pathway
Zn2+	Zinc
Zol	Zolpidem

Chapter 3

Characterisation of ionotropic GABA receptors expressed on hECNs

3.1 Motivation for study

Technological advances in the field of stem-cell biology have yielded the ability to generate human excitatory cortical neurones (hECNs) from pluripotent stemcells (hPSCs), giving the potential to study human-specific physiology and disease in vitro. Previous reports describe a protocol that generates cultures of predominantly hECNs by 4 weeks of differentiation from anterior neural precursors (which, incidentally can be derived from various stem cell lines; Bilican *et al*. 2014). The translational impact of this technology is ultimately determined by the ability of hECNs to display properties that reflect neurones in their native environment (Yang *et al*. 2011; Sandoe & Eggan, 2013). Indeed, we have previously identified that hECNs are a useful model to study the maturation of AMPAR composition and the reduction in intracellular Cl− concentration that is observed in native neuronal development (Livesey *et al*. 2014). The present study characterises the likely subunit composition of $GABA_AR$ and GlyRs expressed b hECNs and illustrates that their subunit composition are likely to be similar to those that have been described for inhibitory ionotropic receptors expressed in immature rodent cortex. Methods In vitro hECN preparation A detailed description of the derivation of hECNs can be found in Bilican *et al*. (2014). Briefly, hECNs were differentiated from anterior neural precursors that were derived from the H9 human embryonic stem cell line (WiCell), which was obtained under ethical approval of the University of Edinburgh. Experiments were carried out on cells that had been differentiated and maintained in culture for 28–42 days in vitro (DIV), or 49–56 DIV. At these time points, around 70% of cells were neuronal (β3-tubulin+), with little contamination from neural precursor cells (nestin+), astrocytes (GFAP+) or GABA-ergic (GAD65/67+) interneurons (Bilican *et al*. 2014; Livesey *et al*. 2014). Neurones were consistent with an excitatory (VGLUT1+) identity that also exhibited properties of neurones of the upper and lower layers of the cortex (see Bilican *et al*. 2014; Livesey *et al*. 2014).ve

3.1.1 Characterisation of hECNs

Previous work characterising hECNs derived from ESCs has shown hECN cultures at DIV 49-56 are 86.7% ± 3.6% β-3 Tubulin$^+$, and less than 10% GFAP$^+$, indicating cultures highly enriched for neurons with nominal presence (<10%) of astrocytes and interneurones (Bilican *et al*. 2014; Livesey *et al*. 2014). Neurites in hECNs were heavily enriched for VGLUT1, with nominal GAD-65/67 staining (3.5% ± 0.4%), indicating a predominant composition of excitatory neurones. Additionally, hECNs were shown to express cortical-layer markers CTIP2, BRN2, Reelin, CUX1, and SATB2 at 49-56 DIV (Figure. 3.1 *B-F).*

3.1.2 Motivation for studying $GABA_A$Rs and GlyRs in hECNs

$GABA_A$Rs are the principal mediators of fast inhibitory neurotransmission in the adult brain, and are important therapeutic targets in the treatment of epilepsy and anxiety disorders, as well as being directly implicated in anaesthesia and sedation (Reynolds *et al.* 2003). $GABA_A$Rs are pentameric, ligand-gated anion channels that are assembled from 21 potential subunits (α_{1-6}, β_{1-4}, γ_{1-3}, δ, θ, ρ_{1-3}, ε, and π). Subunit expression is tightly regulated both spatially and developmentally (Laurie *et al.* 1992, Fritschy *et al.* 2005), and further to this, $GABA_A$R subunit composition imparts distinctive pharmacological properties to the $GABA_A$R complex (Karim *et al.* 2013, Mortensen *et al.* 2011). Identification of the $GABA_A$R isoform/s expressed by hECNs would provide indications of the relative maturity of hECNs, and inform their potential to model normal development and disease. Additionally, this type of study may elucidate potential for hECNs to function as an *in vitro* drug discovery system. All material studied in this section (unless described otherwise) were cultured for 28-42 DIV.

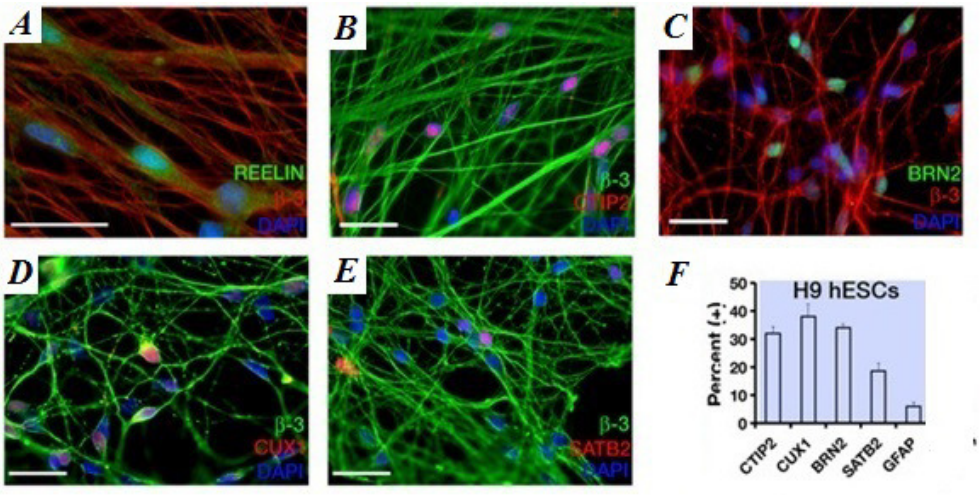

Figure 3.1. Initial immunohistochemical characterisation of hECNs by the Chandran Lab. *A:* Reelin stain (green) in Week 5 hECNs. ***B:*** β-3 Tubulin (green) and CTIP2 (red) stains. ***C:*** BRN2 stain (green). ***D:*** CUX1 stain (red). *E*: SATB2 stain (red). ***F***: Expression of cortical markers by %age of cells expressing a given marker. H9hESCs are referred to in this thesis as hECNs. Images taken with permission from Bilican *et al*. (2014) and Livesey *et al*. (2014).Panels A – E show images acquired using confocal fluorescence microscopy. All scale bars are 20 μm.

3.1.3 Determination of typical $GABA_AR$ agonist and antagonist potency

To initially examine the composition of $GABA_ARs$ expressed on hECNs (28-42 DIV), concentration-response experiments using GABA and the $GABA_AR$ agonist muscimol were conducted, given that the potency of agonists at $GABA_ARs$ has been shown to vary a great deal between isoforms (Mortensen *et al.* 2011; Karim *et al.* 2013). Previously, hECNs were found to robustly respond to GABA applications at this time point (Livesey *et al*. 2014). Upon establishing stable control responses to GABA (100 μM), or muscimol (300 μM), increasing concentrations of agonist were applied sequentially (see Figure. 3.2A) to generate dose-response curves. Mean EC_{50} values for GABA- and muscimol-activated currents were found to be 278 ± 11 μM (n = 12, N = 2) and 182 ± 10 μM (n = 6, N = 2), respectively (Figure. 3.2B, example traces shown in 4A), where coloured lines are graphical indications of EC_{50}. GABA (EC_{50})-evoked current responses were blocked by $GABA_AR$ antagonists bicuculline (100 nM to 30 μM, n = 5, N = 2) and picrotoxin (300 nM to 100 μM, n = 4, N = 2) in a dose-dependent manner giving respective IC_{50} values of 2.7 ± 0.2 μM and 5.1 ± 0.2 μM (Figure. 3.3B, with example traces in 3.3A).

The observed low potency of GABA was then confirmed not to be a consequence of the specific culture conditions that we employed. GABA potency was not influenced by the culture of hECNs in atmospheric O_2 concentrations 48 hours prior to recording (222 ± 13 μM, n = 3, N = 1), the absence of brain-derived neurotrophic factor and glial cell-derived neurotrophic factor media supplements (222 ± 36 μM, n = 5, N = 2), or maintaining hECNs for extended (49-56 DIV) culture periods (204 ± 17 μM, n = 5, N = 2).

It has been shown previously that relatively low GABA potency occurs at several receptor isoforms (Karim *et al.* (2013); Mortensen *et al.* (2011). In order to establish a more precise description of the subunit composition $GABA_ARs$ on hECNs, further pharmacological investigation was conducted.

A

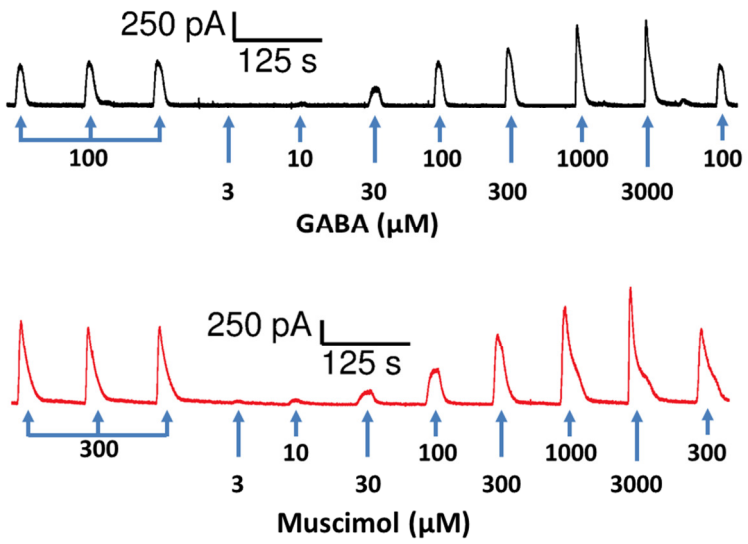

B

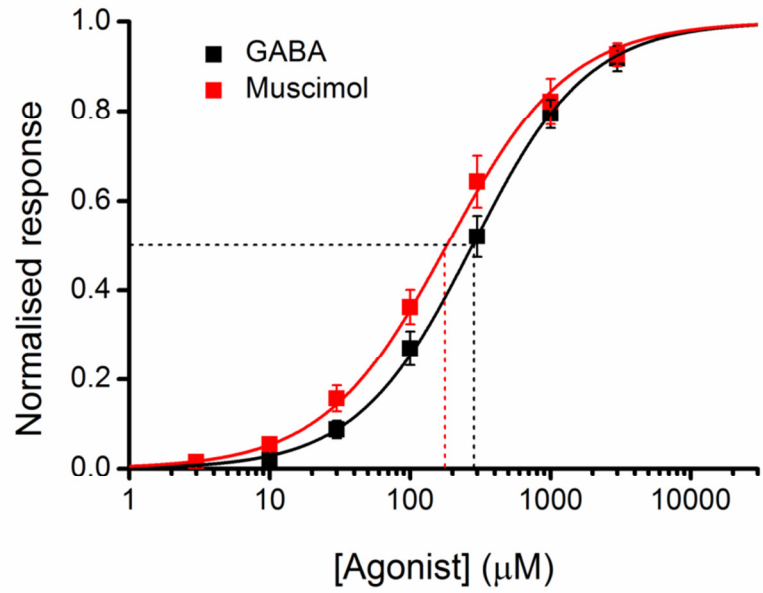

Figure 3.2. Assessment of agonist potency at $GABA_A$Rs expressed by hECNs. *A:* Example whole-cell voltage-clamp traces from data set in 4*B* showing 3 initial control amplitudes of agonist followed by sequentially applied experimental concentrations (as indicated), and final control application of agonist. ***B:*** Concentration-response curve for bath-applied agonists GABA and muscimol. Dashed lines indicate mean EC_{50} for GABA (278 ± 11 µM; n = 12, N = 2)- and muscimol (182 ± 10 µM; n = 6, N = 2).

A

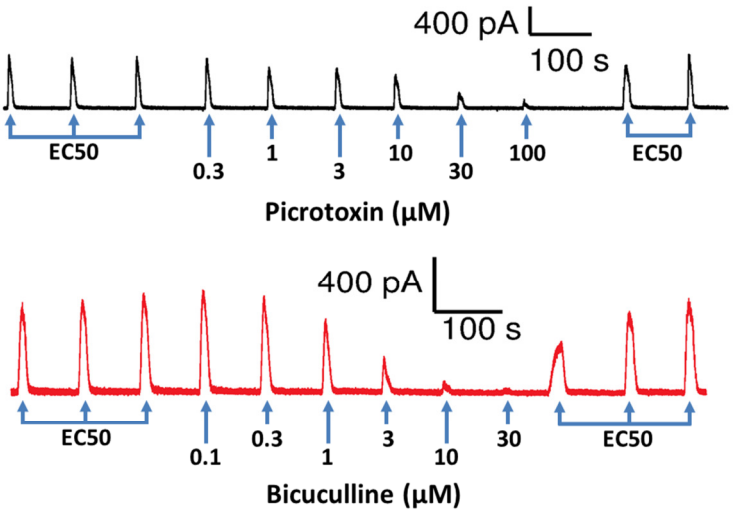

B

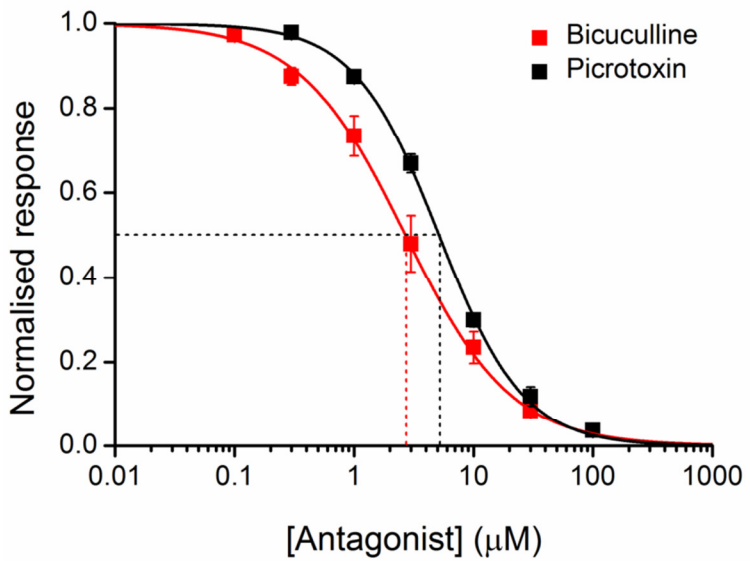

Figure 3.3. Assessment of antagonist potency at $GABA_A$Rs expressed on hECNs. *A:* Example whole-cell voltage-clamp traces from data set shown in 4*B* showing 3 initial control amplitudes of agonist followed by experimental concentrations (as indicated). Multiple end controls demonstrate wash-out of antagonist and thus return to uninhibited EC_{50} response. ***B:*** Concentration-response curve showing inhibition of responses (GABA EC_{50}) by antagonists bicuculline (IC_{50} 2.7 ± 0.2 µM; n = 5, N = 2) and picrotoxin (IC_{50} 5.1 ± 0.2 µM; n = 4, N = 2)

3.2 Subunit-selective pharmacological identification of $GABA_AR$ composition.

3.2.1 Assays for γ- and δ-subunit inclusion

A series of pharmacological assays to survey the presence of γ- and/or δ-subunit containing $GABA_ARs$ were performed. Applications of the γ-selective allosteric potentiator diazepam (30 nM and 3 μM, see Figure. 3.4A for traces) to GABA (EC_{10})-mediated currents potentiated the control GABA response by 10 ± 6 % (p = 0.1 vs. control) and 46 ± 10 % (p = 0.001 vs. control, Welch's t-test, n = 17, N = 3), respectively, showing inclusion of the γ-subunit (Figure. 3.4B). Further to this, the potent δ-containing $GABA_AR$-selective agonist gaboxadol (3 μM and 300 μM; (Storustovu & Ebert. 2006) elicited only nominal currents (6.0 ± 2.3% and 14.6 ± 3.7%, respectively) compared to the maximum response that could be elicited by GABA ($G_{MAX,}$ 3 mM; Figure. 3.4C, example traces in 6A) confirming the absence or nominal expression of a population of $GABA_ARs$ that contain δ subunits. Additionally, the currents elicited by gaboxadol (300 μM; 9.7 ± 4.1 %, n = 4, N = 1) upon 49-56 DIV hECNs were equivalent to the previous (p= 0.65, student's *t*-test) indicating the $GABA_AR$ population did not begin to express a δ-containing receptor population when maintained in culture to extended time periods.

Applications of Zn^{2+} (10 μM and 300 μM; n = 7, N = 2), which selectively inhibits $GABA_ARs$ composed of α- and β- subunits alone (Draguhn *et al*. 1990), did not significantly inhibit GABA (EC_{50})-evoked currents (Figure. 3.5B, traces in 3.5A). Thus the collective data obtained using diazepam, gaboxadol, and Zn^{2+} indicate the major presence of γ-subunit-containing $GABA_ARs$.

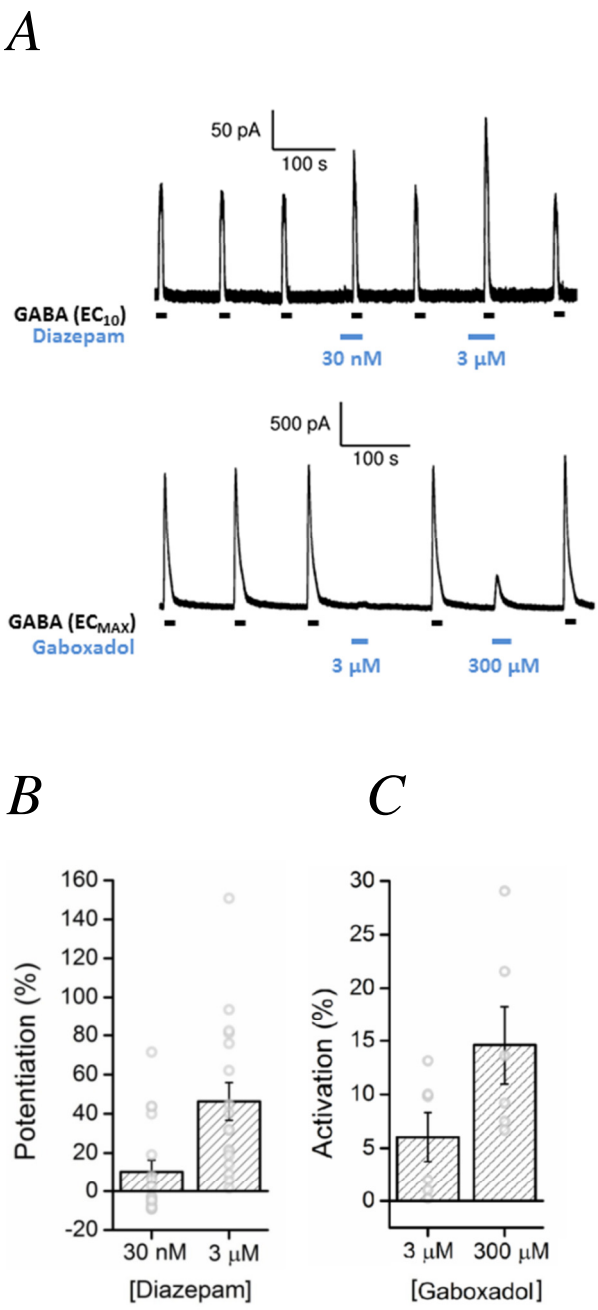

Figure 3.4. Modulatory effects of diazepam, and activation by gaboxadol of $GABA_A$Rs expressed on hECNs. ***A****:* Example whole-cell voltage-clamp traces detailing responses of γ-subunit selective positive allosteric modulator diazepam co-applied with GABA (*above)*, and direct activation by δ-subunit selective agonist gaboxadol (*below*). Coloured bars indicate application of pharmacological agents. ***B***: Mean potentiaton of $GABA_A$R responses by co application of diazepam and GABA (n = 17, N = 3). ***C***: Mean direct activation of $GABA_A$Rs by δ-selective gaboxadol (n = 6 - 7, N = 1) as a percentage of maximal GABA-mediated response.

A

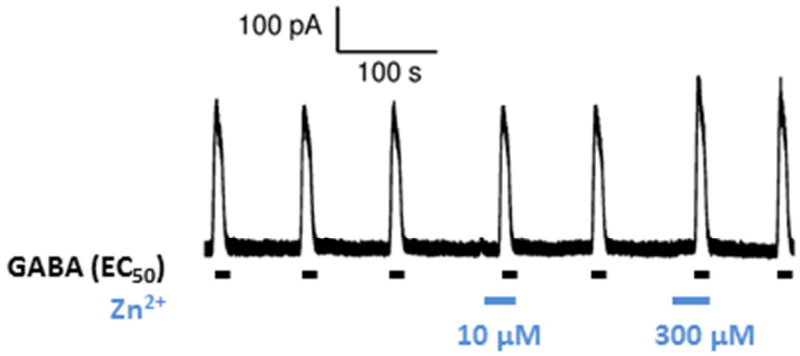

B

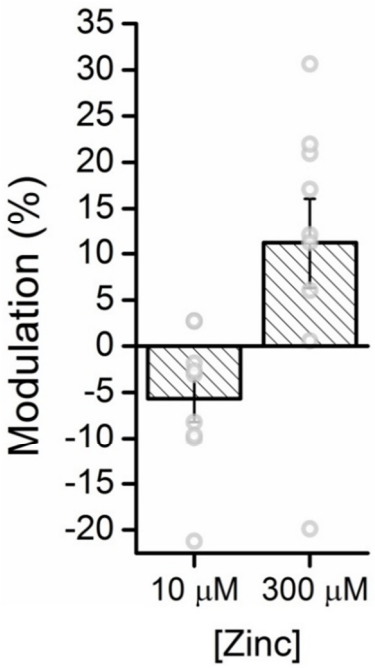

Figure 3.5. Modulation of $GABA_ARs$ by $Zn2^+$. ***A:*** Example whole-cell voltage-clamp trace showing control applications of GABA (EC_{50}), and responses to GABA (EC_{50}) co-applied with Zn^{2+} at concentrations and times indicated by coloured bars. ***B:*** Graph showing mean modulation of $GABA_ARs$ by Zn^{2+} as a percentage response vs control GABA applications (n = 9, N = 1; experiment illustrated by example trace in figure 3.5A).

3.2.2 Assaying β-subunit inclusion and identity

The presence of β-subunits in hECN $GABA_A$Rs was confirmed by potentiation of $GABA_A$R-elicited current by the intravenous anaesthetic propofol (n = 8, N = 3; 10 μM. Sanna *et al.* 1995; Hill-Venning *et al.* 1997) of GABA (EC_{30})-evoked currents which resulted in robust potentiation of the control current responses by 144 % ± 29 % (Figure. 3.6C, traces in 3.6A; p = 0.005 vs control, paired t-test. Furthermore, direct activation of $GABA_A$Rs was observed when propofol (100 μM) was applied on its own (n = 8, N = 3; 98 ± 21 % relative to control, Figure. 3.6B, traces in 3.6A). This behaviour is typical of native $GABA_A$Rs incorporaing a β-subunit (Hill-Venning *et al.* 1997, Ruesch *et al.* 2012).

Next, the β-subunit identity was examined, the $GABA_A$Rs being of known variants β_1, β_2, and β_3. The intravenous anaesthetic etomidate (3 μM) which is selective for $\beta_{2/3}$-subunit containing $GABA_A$Rs (Hill-Venning *et al.* 1997) also potentiated GABA (EC_{30})-evoked currents by 75 ± 20 % (n = 6, N = 2; Figure. 3.6B; p = 0.006 vs control, paired t-test) while application on its own and at a higher concentration (300 μM) directly activated $GABA_A$Rs (n = 6, N = 2; 116 ± 23 % relative to GABA (EC_{30})-evoked control; Figure. 3.6C,traces in 3.6A). Direct activation of $GABA_A$Rs containing a $\beta_{2/3}$-subunit by etomidate is a typical property of those $GABA_A$R isoforms (Ruesch *et al.* 2012; Hill-Venning *et al.* 1997). Altogether, these data indicate that $GABA_A$Rs expressed by hECNs are predominantly a $\beta_{2/3}$-containing isoform. Conversely, the absence of β_1-containing $GABA_A$Rs was demonstrated by the use of the selective inhibitor of β_1-containing $GABA_A$Rs, SCS (Salycylidine salycylhydrazide; Thompson *et al.* 2004). SCS failed to antagonise GABA (EC_{30})-evoked currents (n = 8, N = 3; Figure. 3.6C, traces in 3.6A; SCS vs control, p=0.3384), thus demonstrating the absence of β_1-subunits in hECN $GABA_A$Rs.

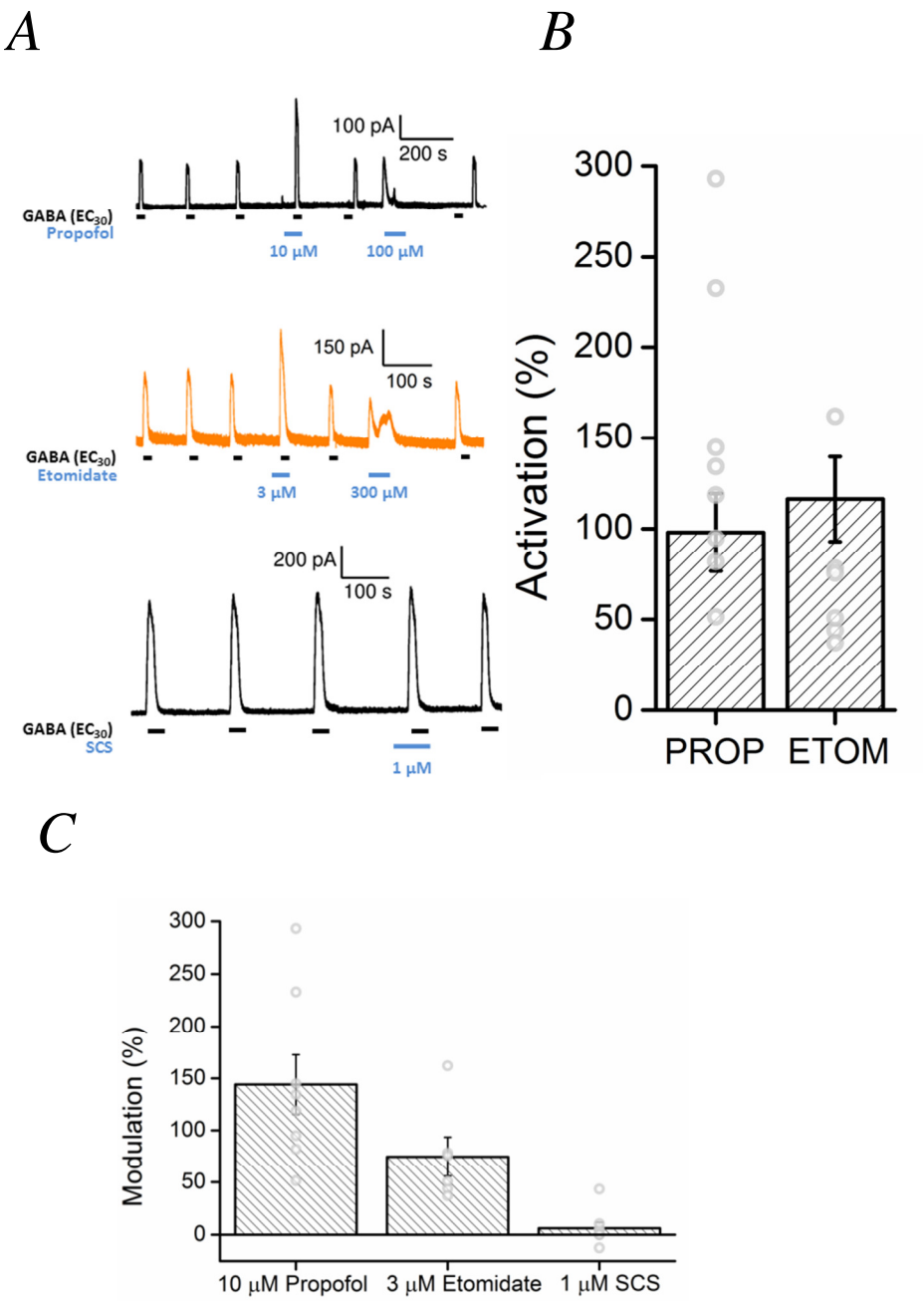

Figure 3.6, Modulation and activation of hECN $GABA_A$Rs by β-subunit selective agents. ***A***: Example whole-cell voltage-clamp traces showing control applications of GABA, and subsequent modulation by co-applied $GABA_A$R positive modulators: broadly β-selective propofol, $\beta_{2/3}$-selective etomidate, and β_1-selective negative modulator SCS. ***B:*** Direct $GABA_A$R activation (relative to controls shown in *8A*) by propofol (n = 8, N = 2), and etomidate (n = 6, N = 1). ***C:*** $GABA_A$R-mediated current is potentiated by propofol (n = 8, N = 2) and etomidate (n = 6, N = 1), and unaffected by SCS (n = 8, N = 3).

3.2.3 Assaying α-subunit identity

As illustrated above GABA-evoked currents are potentiated by diazepam which confirms the $GABA_AR$ population expressed by hECNs contain α_1-, α_2-, α_3-, or α_5-containing $GABA_ARs$ (Olsen & Sieghart. 2009), where a conserved histidine residue not present in α_4- and α_6-subunits confers insensitivity to benzodiazepines (Wafford *et al.* 2004). To rule out the possibility of the expression of α_4- and α_6-subunits, GABA (EC_{30})-elicited currents were shown to be insensitive to the α_4/α_6-subunit containing $GABA_AR$ inhibitor furosemide (100 μM; Figure. 3.7B, traces in 3.7A; (Knoflach *et al.* 1996; Wafford *et al.* 1996).

The observed low GABA and muscimol potencies (Figure. 3.2B) argues against the expression of α_4-, α_6-, and also, α_5-subunits, which typically display comparatively high GABA potency (Karim *et al.* 2013; Mortensen *et al.* 2011). To identfiy the α subunit subtype we then examined the actions of zolpidem (50 nM and 500 nM), which exhibits selectivity for α_1-containing $GABA_ARs$ with lesser potency at α_2- and α_3-containing $GABA_ARs$ and negligible activity at α_5-containing $GABA_ARs$ (Sanna *et al.* 2002). Co-application of zolpidem to GABA (EC_{10})-evoked currents resulted in only a mild potentiation of control currents (Figure. 3.7B, traces in 3.7A; 50 nM: 46 ± 10 %, $p = 0.003$ vs control; 500 nM: 70 ± 10 %, $p = 0.002$ vs control; paired *t*-tests) indicating the $GABA_AR$ population expressed by hECNs most likely contain α_2 and/or α_3 subunits.

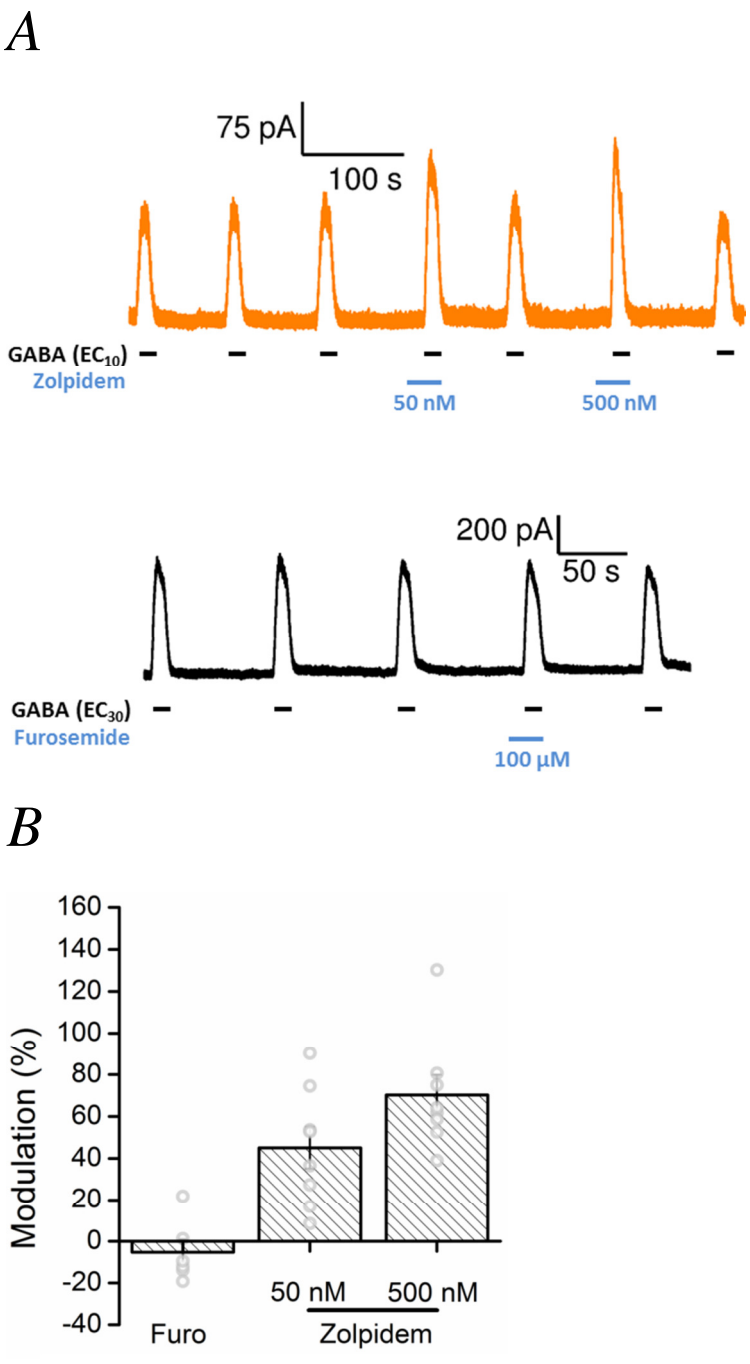

Figure 3.7. Modulation of $GABA_A$Rs by zolpidem, and furosemide. ***A:*** Example whole-cell voltage-clamp traces showing $GABA_A$R current elicited by control applications of GABA (at concentrations indicated), and the same concentration of GABA co-applied with a modulator at the concentrtations and times indicated. ***B:*** Mean percentage modulation of $GABA_A$R currents by the modulators furosemide (n = 6, N = 1; 100 µM), and zolpidem (n = 6-8; N = 2; 50 nM and 500 nM).

Further to the above measures, RNA sequencing and analysis on $GABA_AR$ subunits at 35 DIV was conducted by J. Qiu and O. Dando of the Hardingham, and Kind labs respectively. Figure. 3.8 shows the relative mRNA expression levels of $GABA_AR$ subunits (normalised to expression of the β_3 subunit). These sequencing data are in strong agreement with the established pharmacology of $GABA_ARs$ expressed by hECNs, giving a likely expressed $GABA_AR$ isoform of $\alpha_{2/3}\beta_3\gamma_2$.

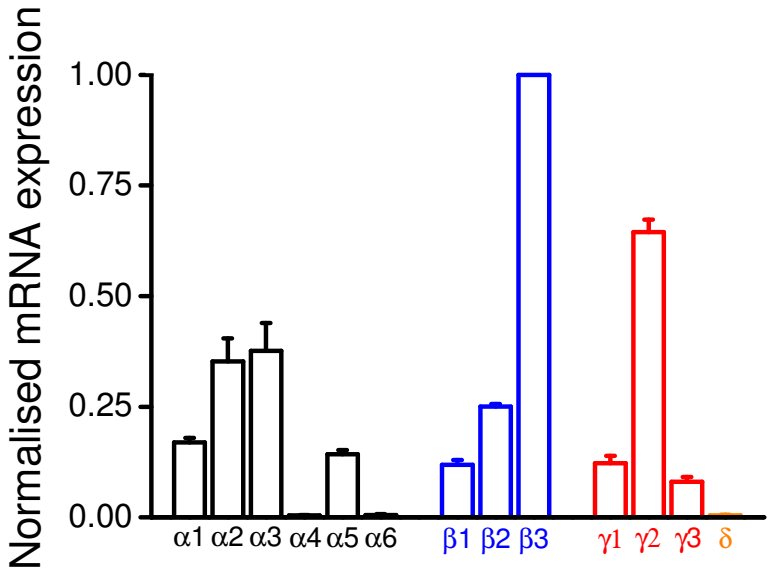

Figure 3.8. Graph showing RNA sequencing of hECNs for $GABA_AR$ subunit expression levels. Analysis conducted by O. Dando, using data supplied on hECNs by G. Hardingham. mRNA expression levels are normalised to β_3 expression.

3.3 Characterisation of ionotropic, strychnine-sensitive glycine receptors (GlyRs) expressed by hECNs

GlyRs are a pentameric ligand-gated ion channel assembled from 5 possible subunits (α_{1-4}, β), and are highly expressed in cortical development (Lynch *et al.* 2009). During embryonic development, the α_2 homomeric isoform dominates, with the $\alpha_1\beta$ isoform being expressed predominantly in adulthood. Recent discoveries concerning GlyRs in the CNS suggest their role in embryonic cortical development may be more extensive than previously understood, with indications they may play a role in neurodevelopmental disorders such as Schizophrenia and Autistic Spectrum Disorders, as well as some forms of temporal lobe epilepsy (Avila *et al*. 2013a).

3.3.1 Assessment of agonist potency at GlyRs expressed by hECNs

Similar to GABA, hECNs at DIV 35 exhibited robust responses to applications of glycine. The potency of glycine at hECN GlyRs was assessed by conducting concentration-response experiments similar to previous descriptions; initially, 3 control responses were elicited by glycine (300 μM), ascending concentrations of glycine were applied (3 μM – 3 mM), and a final control application of glycine to end the recording. Fitted curves to mean normalised responses to glycine yielded an EC_{50} of 167 ± 20 μM (Figure. 3.9B, traces shown in 3.9A).

Glycine-evoked (500 μM) currents were blocked fully by strychnine in a concentration-dependent manner with an IC_{50} of 630 ± 59 nM ($n = 5$, $N = 2$; Figure. 3.10B, traces in 3.10A). Note that an increased agonist concentration (EC_{85}), rather than the typical EC_{50}, was used to elicit suitable current responses to measure antagonist effects. The composition of the expressed GlyRs was probed using picrotoxin, which exhibits selectivity for homomeric over heteromeric GlyR forms, as the inclusion of the β subunit into the GlyR results in a reduction in sensitivity to picrotoxin (Pribilla *et al*. 1992; Wang *et al*. 2006; Lynch, 2009). Inhibition of GlyRs by picrotoxin (Figure. 3.10B, traces in 3.10A) gave an IC_{50} of 197 ± 22 μM ($n = 5$, $N = 2$), indicating the low potency of this antagonist at hECN GlyRs, and suggesting

that the majority of these receptors are heteromeric assemblies of α and β subunits. Interestingly, while the observed EC_{50} for glycine at the GlyR is roughly on the order of previous reports (approx. 100 μM – 300 μM; See De Sant-Jan *et al*. 2001), though the IC50 values for picrotoxin, and strychnine, were higher than expected. Typical values are on the order of 10 μM – 100 μM for picrotoxin (see Mangin *et al*. 2005), and strychnine (10 nM – 30 nM) and perhaps due to the use of an EC_{85} to elicit responses.

A

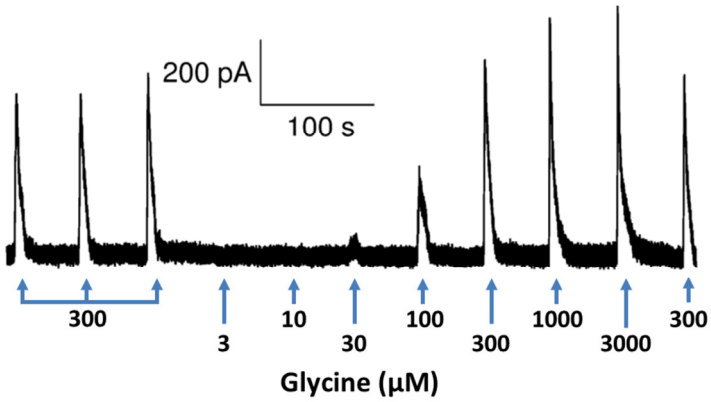

B

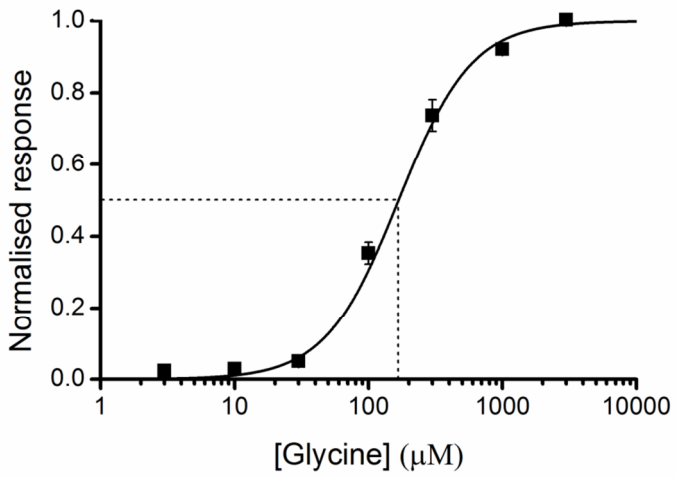

Figure 3.9. Assessment of agonist potency at GlyRs expressed on hECNs. ***A:*** Example whole-cell voltage-clamp traces showing 3 initial control amplitudes of agonist followed by experimental concentrations (at time and concentration shown) and final control application of agonist to indicate comparable access resistance to the start of the recording. ***B:*** Concentration-response curve for applied agonist glycine. Dashed lines indicate EC_{50} value (167 ± 20 µM; n = 7, N = 2), obtained by curve fit to normalised mean responses.

A

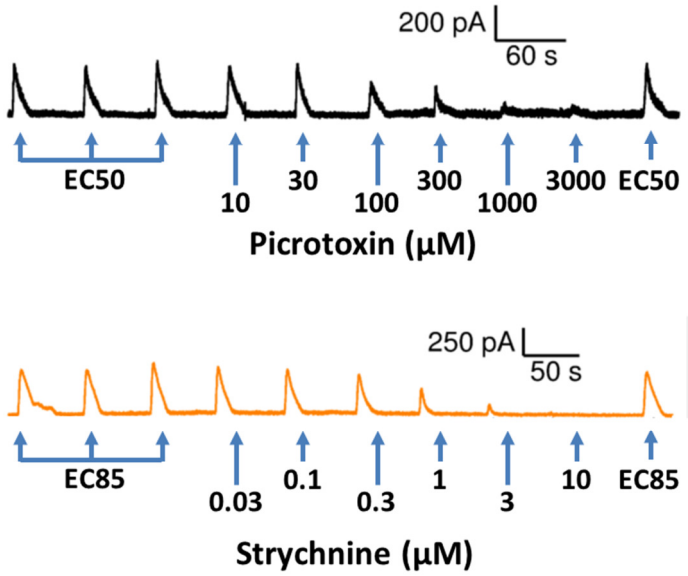

B

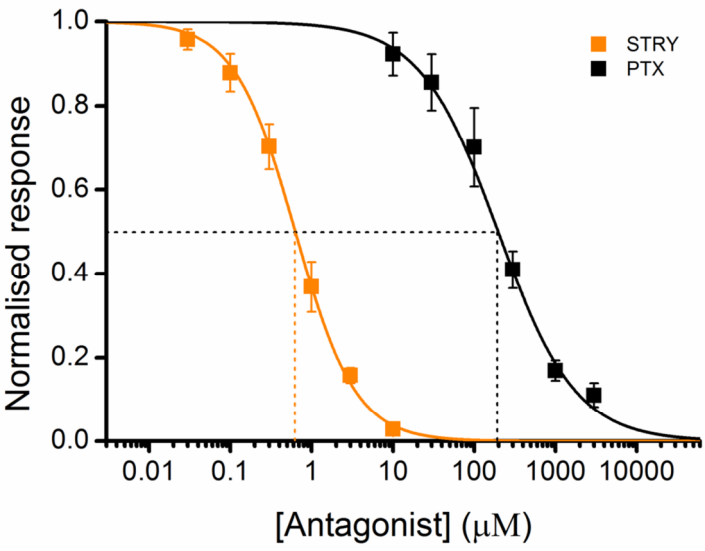

Figure 3.10. Assessment of antagonist potency at GlyRs expressed on hECNs. ***A***: Example whole-cell voltage-clamp traces showing 3 initial control amplitudes of agonist followed by experimental concentrations (at times and concentrations indicated). ***B***: mean inhibition curves (dashed lines) for GlyR antagonists picrotoxin (IC50 = 197 ± 22 µM; n = 5, N = 2) and strychnine (EC50 = 690 ± 59 nM; n = 5, N = 2).

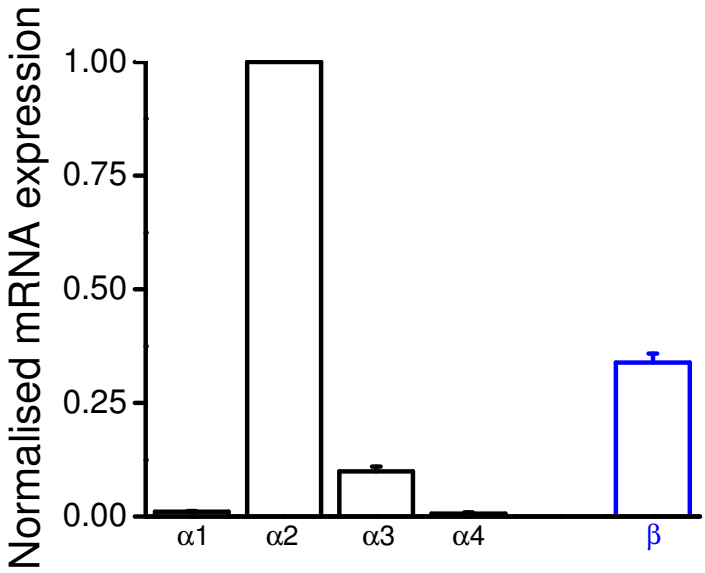

Figure 3.11. mRNA sequencing of hECNs for GlyR subunit expression levels. Analysis conducted by O. Dando, using data supplied on hECNs by G. Hardingham. mRNA expression levels are normalised to α_2 expression.

Additional GlyR characterisation was performed with RNA-seq analysis of GlyR subunit mRNA transcripts in hECNs at 35 DIV as described previously. Both α2 and β subunits were highly expressed at the mRNA level, whilst α1 and α3 subunits were nominally or weakly expressed, respectively, relative to α2 subunit expression (Figure. 3.11). α4 subunit mRNA was not detected as expected given its status as a pseudogene in humans (Lynch, 2009). Collectively, these data suggest a GlyR subunit composition of $\alpha_2\beta$.

3.4 Discussion on characterisation of $GABA_A$Rs and GlyRs in hECNs

Changes in $GABA_A$R subunit composition across development have been observed previously in other work, such that a characteristic isoform is expressed almost exclusively in cortical regions during embryonic development (Laurie *et al*. 1997, Fritschy *et al*. 2005). This isoform is composed of α2/3β3γ2 subunits, and has a typical response profile to pharmacological assay. Collectively, the above results demonstrate that this isoform predominates in $GABA_A$R populations on hECNs. In light of relative abundances for $GABA_A$R subunit mRNA expression in hECNs, a low potency for GABA suggests α2/3 expression, responses to diazepam indicate the presence of a γ2-subunit, and responses to etomidate indicate the expression of the β3 subunit. Notably, the use of agents which select for $GABA_A$R subunits atypical in embryonic development yielded nominal responses. These findings on responses are supported at the transcript level by an mRNA screen indicating low relative mRNA expression levels for these subunits (e.g δ-subunit or β1).

Interestingly, due to the method of drug delivery, by exchanging the bath aCSF to another aCSF source containing pharmacological agents, it is possible that some α_1 –subunit expression occurs and that the bath exchange time is sufficiently slow to activate and de-sensitise the α_1 –subunit containing $GABA_A$Rs, as α_1 –subunit containing $GABA_A$Rs typically show extremely rapid desensitisation (Bianchi & MacDonald. 2002). Under ideal conditions the extracellular fluid in the bath is encouraged to flow across the cellular material under study, providing as rapid an exchange time between extracellular fluid without a pharmacological agent present, and that of an extracellular fluid with an agent which produces the effect that the experiment aims to measure. Typically in whole-cell recordings from cell culture, this effect is produced using a rapid flow rate which hECNs do not tolerate well, often resulting in a lost recording.

As a result, flow rate was maximised and allowed an onset time of less than 5 seconds in all recordings. While RNA sequencing shows that the presence of α_1-subunits is likely to be relatively low, it cannot be discounted that a population of desensitised α_1 –subunit containing receptors may be present but unobserved. Given that zolpidem did potentiate responses somewhat more than expected, the possibility of α_1 at the $GABA_AR$ as a small sub-population of receptors seems more likely.

Assays of the GlyR isoform expressed on hECNs demonstrated robust GlyR responses with sensitivity to strychnine, a defining characteristic of GlyRs on cortical neurones. The observed potency of picrotoxin shows inclusion of the β-subunit into the GlyR complex, a finding more typical of maturity, however, relative mRNA expression levels for the typical counterpart of the β-subunit, the α1- subunit, were unexpectedly low. Instead, it is apparent that GlyRs expressed on hECNs are composed of α2β. Previous work (Okabe *et al*. 2014) has shown this isoform to be transiently expressed in cortical tissue during early postnatal development, however, which suggests a developmental identity for GlyRs expressed on hECNs, though little is known as to the precise role of α2β (Lynch. 2009).

Additionally, it is worthy of note that the methods used to apply pharmacological agents vary in terms of the speed at which an agent is delivered to the receptor. Crucial, however, in interpreting the results of these experiments is the idea that the "typical" adult $GABA_AR$ isoform of $\alpha_1\beta_{2/3}\gamma_2$ readily desensitises on a much shorter timescale than the typical onset time. Thus, the experimental results may not reflect the true complement of possible α_1- containing $GABA_ARs$, however, given the relative lack of potentiation by zolpidem at high concentrations, and relatively low mRNA transcript levels for α_1 $GABA_AR$ subunits, a significant complement of α_1- containing $GABA_ARs$ seems unlikely.

Also, RNA-sequencing, while undeniably a powerful tool for examining a plethora of physiological processes, also must be taken with some caveat in that the detection of an mRNA signal (termed "reads") is established by mapping the detected amino acid sequences of mRNA to known sequences from mapping to known sequences expressed by human cells. Thus, it does not measure the protein product, as proteins can be altered or degraded in a variety of ways before functional assembly into a protein isoform is performed. As such, RNA sequencing speaks to the potential for a predicted protein product to be formed (in this context $GABA_ARs$ and GlyRs). This being said, the RNA-sequencing data suggests high expression of receptor isoforms that are supported strongly by the attendant pharmacology.

3.4.1 Modelling the role of $GABA_ARs$ in development and disease using hECNs

$GABA_ARs$ have been shown to be instrumental in normal neuronal development, leading to the description of GABA as a 'pioneer' neurotransmitter (Ben-Ari *et al*. 2007). In embryonic development across a wide array of mammalian species, GABA-ergic transmission precedes glutamatergic transmission in early neuronal networks due to rapid interneurone maturation, occurring as early as E18 in rodents (Ben-Ari *et al*. 2004; Ben-Ari *et al*. 2007).

Interestingly, the initial activity of $GABA_ARs$ is depolarising, or shunting in nature, which later in development (postnatal day 5-7 in rodents) becomes excitatory (Ben-Ari *et al*. 2004). Cortical excitatory neurones exhibit a characteristic decrease in intracellular Cl- across development (see Kaila, *et al*. 2014). This is achieved by the activity of Cl- transporter proteins, Na+-K+-Cl- co-transporter 1 (NKCC1) and K+-Cl- co-transporter 2 (KCC2). These transporters utilise Na+ and K+ gradients across the cell membrane to drive Cl- ions into the cell (NKCC1), or out of the cell (KCC2). In normal development, NKCC1 is the dominant Cl- transporter in embryonic cortical neurones yet as postnatal maturation progresses, an isoform of KCC2 (KCC2b, Uvarov *et al*. 2006, Blaesse *et al*. 2009) Cl- transporter is

predominantly expressed. Post-natally, $GABA_AR$ activation causes a net influx of Cl- ions, leading to a more negative membrane potential, whereas in early development, the elevated intracellular [Cl-] causes the reversal potential of the $GABA_AR$ to shift to a value close to, or above that of the RMP (Ben-Ari *et al*. 2004).

This shift in the action of GABA across development has also been confirmed in hECNs using an identical protocol to that used to produce hECNs used in this thesis. Intracellular Cl- activity (a measure dependent on intracellular [Cl-]) in hECNs falls from around 25 mM to <7 mM in hECNs (Livesey *et al*. 2014). This suggests a reliable platform for modelling neurodevelopmental conditions associated with impairments in Cl- co-transporter expression such as Rett syndrome (Tang *et al*. 2015; Chao *et al*. 2016), and psychotic disorders (Kalkman *et al*. 2011; Arion *et al*. 2011).

Interestingly, hECNs do not show any change in receptor subunit expression. Typically, α2/3 expression in early development switches to a predominantly α1 – containing isoform post-natally (Laurie *et al*. 1992; Fritschy *et al*. 1994), which does not occur in hECNs in culture at 5 weeks, or for longer periods (7 weeks). Given that the intracellular [Cl-] at these later time-points describes a mature-like identity, the $GABA_AR$ subunit switch does not occur, indicating incomplete maturation of the GABA-ergic system in hECNs.

3.4.2 Modelling the role of GlyRs in development and disease using hECNs

The GlyR, like the $GABA_AR$, is an anion channel, conducting primarily Cl- ions. As a result, the previous description for Cl- -transporter proteins also applies (see above, Chapter 3.4.1). Typically in early development, GlyRs activation results in excitation or shunting which becomes an inhibitory action at P5-7.

The established GlyR isoform expressed on hECNs at 5 weeks in culture is that of α2β, an isoform that typically dominates, albeit transiently in the early postnatal period in rodents (Okabe *et al*. 2004). While it is suggested (Lynch, 2009) that the α2β receptor is not essential for neuronal functioning from studies in knockout mice, it remains to be seen as to the potential developmental function of this specific receptor isoform. It has been shown that the α2β GlyR co-localises with gephryin (Haverkamp *et al*. 2004), a synaptic protein that localises GlyRs and $GABA_ARs$ to synapses (Essrich *et al*. 1998; Giesemann *et al*. 2003). As such, this receptor isoform may serve a more subtle developmental function, though the tools to probe this effectively are lacking (Lynch. 2009).

Chapter 4

Characterisation of hECNs harbouring the *DISC1* (1;11)(q42;q14.3) mutation.

4.1 Motivations for study

A mutation in the Disrupted in schizophrenia 1 (*DISC1*) gene was originally identified from a Scottish family that co-segregated with schizophrenia, bipolar disorder and major depression (Millar *et al*. 2000; Millar *et al*. 2005). The mutation is a balanced translocation at the (1;11)(q42;q14.3) locus and yields a truncated DISC1 protein (A schematic of the truncated DISC1 protein is given in Figure. 4.1.). Other mutations are also known to be associated with psychiatric disorders and autism (Thomson *et al*. 2013). DISC1 is expressed widely in the adult and developing brain including the cortex and hippocampus, and in both excitatory and inhibitory neurones (Schurov *et al*. 2004). Furthermore, the DISC1 protein is widely intrinsically expressed within both inhibitory and excitatory neurones, particularly at or near the synapse, and participates in cellular proliferation, migration, neurite outgrowth and cell-to-cell adhesion, and other processes that regulate neural development *via* many potential signalling pathways (Bradshaw & Porteous. 2012). Much of this research has been performed upon rodent models and knowledge of DISC1 in normal human neuronal function and disease is lacking. Thus, following on from findings in animal models and elsewhere, hECNs derived from patients harbouring this mutation presents a unique opportunity to examine human tissue for previously observed pathophysiology associated with this DISC1 mutation.

Association studies have shown a link between genetic variations of DISC1 and specific endophenotypes that are commonly associated with schizophrenia, depression, and bipolar disorder (Brandon & Sawa. 2011; Callicott *et al*. 2005; Cannon *et al*. 2005; Carless *et al*. 2011; Prata *et al*. 2008). During early development, DISC1 affects cellular proliferation via glycogen synthase kinase 3-regulated WNT activity and post-differentiation neuronal migration by interacting with microtubules and the centrosome (Ishizuka *et al*. 2011; Kamiya *et al*. 2005; Mao *et al*. 2009). Additionally, inn the adult brain, DISC1 regulates neurogenesis (Duan *et al*. 2007; Kim *et al*. 2012).

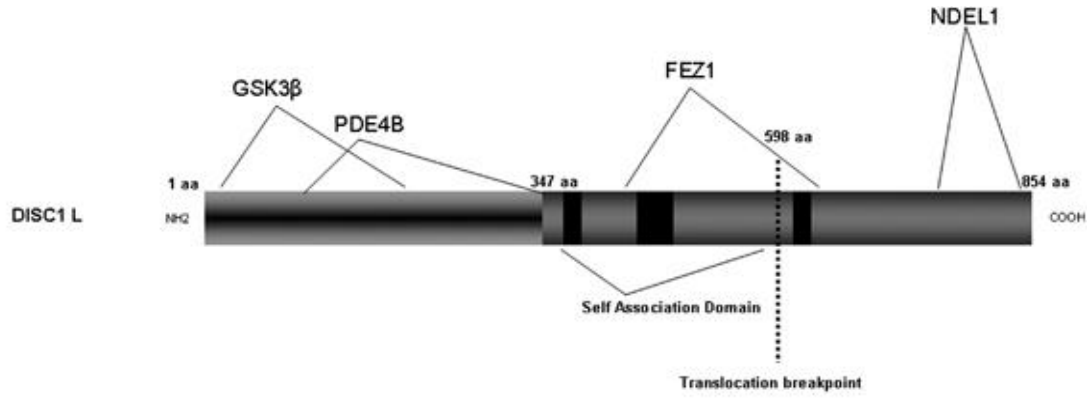

Figure. 4.1. Schematic representation of the DISC1 protein. Of note is the dotted line indicating the (1;11)(q42;q14.3) breakpoint at which the DISC1 protein is truncated. The schematic highlights the DISC1 interaction sites of selected proteins that are involved in neuronal physiological processes. In this regard, the DISC1 truncated protein loses interaction sites for NDEL1 and FEZ1 Splice variants are not included in this schematic. (adapted from Newburn *et al*. 2011).

It is hypothesised that mutations in *DISC1* result from a marked decrease of DISC1 protein product, and result in disrupted physiological neuronal function leading to an imbalance in the excitation/inhibition state in the pre-frontal cortex that may underlie the observed disease phenotypes (Bradshaw & Porteous. 2012; Lisman. 2012). Previous work has shown that *DISC1* mutations result in altered K^+-channel expression in rodent cortical neurones as mediated by PDE4, which binds to the PDEZ domain labelled in Fig. 4.1 (Small conductance calcium-activated K^+ channels, El-Hassar *et al*. 2014; KCNQ5, Ozeki *et al*. 2003) and intrinsic neuronal excitability (Gamo *et al*. 2013) changes in neurotransmitter receptor expression and function (Akbarian *et al*. 1995; Callicot *et al*. 2013; Kim *et al*. 2012; Wright & Vissel 2012; see Hammond *et al*. 2010). Note also the GSK3β interaction site, which has been shown to affect gene transcription and cell proliferation. If mis-folded or under-produced DISC1 protein were to impact this, it may also affect the broader maturation of neuronal processes such as changes in ion channel complement.

Additionally, the excitatory post-synaptic density is heavily enriched for DISC1 (Kirkpatrick *et al*. 2006), where it has been shown to regulate dendritic spine number and size. Additionally, it has been observed that DISC1 also mediates

AMPA receptor synaptic trafficking via the 7-Rac1-PAK pathway (see Hayashi-Kagaki *et al*. 2010). DISC1 also regulates the maintenance of synapses by interacting with NCK-interacting protein kinase (Wang *et al*. 2011) and exerts an important effect on NMDA receptor expression and function through a mechanism depending on the transcription factor cAMP response element binding protein (Wei *et al*. 2014).

Crucially, many basic functional properties of human cortical neurones harbouring the *DISC1* mutation remain to be described and iSPC technology offers a valuable opportunity to address this. Experiments in this chapter were conducted in order to explore the functional properties of two lines of hECNs each separately derived from iPSCs obtained from clinically-defined patients carrying the *DISC1* mutation (1;11)(q42;q14.3) with respect to two lines of equivalently derived hECNs from healthy (familial) patients. Work was carried out to confirm that these hECNs indeed harboured the mutation and minimally expressed the truncated or fully expressed a normal DISC1 protein, respectively (performed in the laboratories of Professor S .Chandran and Dr. K. Millar, both University of Edinburgh). Data sets for control- and mutant *DISC1*- case derived hECNs (hereafter referred to as 'Control' and 'Case', respectively), were pooled together as there was no statistical difference between data sets in Case or Control lines, for presentation of data (minimum p=0.15; Student's *t*-test).

4.2 Passive properties of DISC1 patient iPSC-derived hECNs.

Initial electrophysiological characterisation of hECNs derived from DISC1 iPSCs was conducted at 7, 21, and 35 DIV time points (Figure.4.1) in order to observe potential alterations in development in Case lines with respect to control lines. Typical patterns of maturation investigated in terms of the intrinsic properties of hECNs between DIV 7 and DIV 35 indicated that there was no notable difference between Case and Control hECNs. Input resistance measurements decreased (Figure. 4.1A), though not significantly (Student's *t*-test; Control p=0.56 and Case p=0.13). The mean resting membrane potential (RMP) in each line became more hyperpolarised with time (Figure. 4.1B), though again not significantly (Student's *t*-test; Control p=0.65 and Case p=0.22). From 7 DIV to 35 DIV, whole-cell capacitance significantly increased (Student's *t*-test; Control p=0.0002 and Case p=0.0002) in both Control and Case to similar levels (Figure. 4.1C). These data are consistent with a maturing neuronal profile, but no significant differences were found between Case and Control at any time point studied (Student's *t*-test, minimum p=0.15 for each parameter studied). Importantly, the mean values of passive properties obtained at all time points are not what are expected of adult cortical neurones (Moody & Bosma. 2005); input resistance measurements are 10-20–fold higher, whole-cell capacitance values are lower and RMP values are more hyperpolarised.

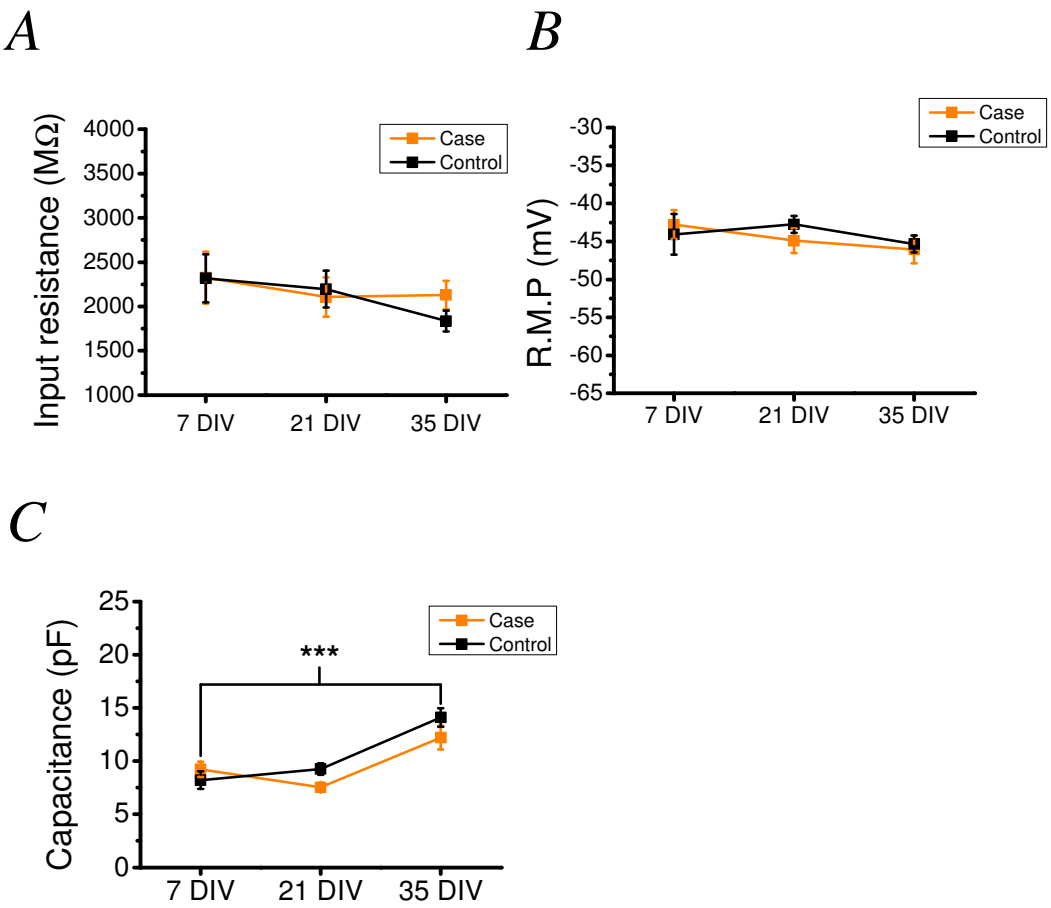

Figure. 4.2, Passive membrane properties of DISC1-iPSC-derived neurones at 7, 21 and 35 DIV as established using whole-cell patch-clamp. For all panels, Control; n= 14-21, N=2, Case; n= 10-20, N=2. ***A:*** Mean input resistances of Control and Case hECNs. Input resistance was established from the mean passive membrane current amplitude generated from thirteen sequential -50 mV pulses. ***B:*** Mean resting membrane potential (RMP) of Control and Case hECNs. ***C:*** Mean whole-cell capacitance of Control and Case hECNs. *** indicates p=<0.001; Student's *t*-test comparing 7 DIV and 35 DIV.

4.3 Firing properties of mutant *DISC1* Case and control iPSC-derived hECNs.

In order to examine the potential for more subtle, yet general, developmental pathology, both DISC1 Control and Case hECNs were examined with regard to their firing properties. Initial study in this area was focused on categorising the firing behaviour of neurones at 7, 21, and 35 DIV. Neurones were held at -70 mV (-84 mV) in the current-clamp configuration (see Methods) and depolarised by incremental current pulses of 10 pA of 500 ms duration. Responses were assigned to one of four categories describing action potentials (A.P.) detailed in Figure. 4.3A; "no response", "failed initialisation", "single" and "burst". "No response" indicates the lack of any response beyond the passive membrane response. "Failed initialisation" describes the mutual presence of two essential characteristics: a spike without a characteristic afterhyperpolarisation (A.H.P.), and of below 20 mV amplitude. A "single" A.P. categorisation was applied when a spike exceeded 20 mV and possessed an A.H.P. which undershot the plateau phase of the voltage response. Categorisation of a "Burst" was described as the firing of more than one A.P. in response to a rheobasic current injection. The results of this study are detailed in Figure. 4.3B.

A

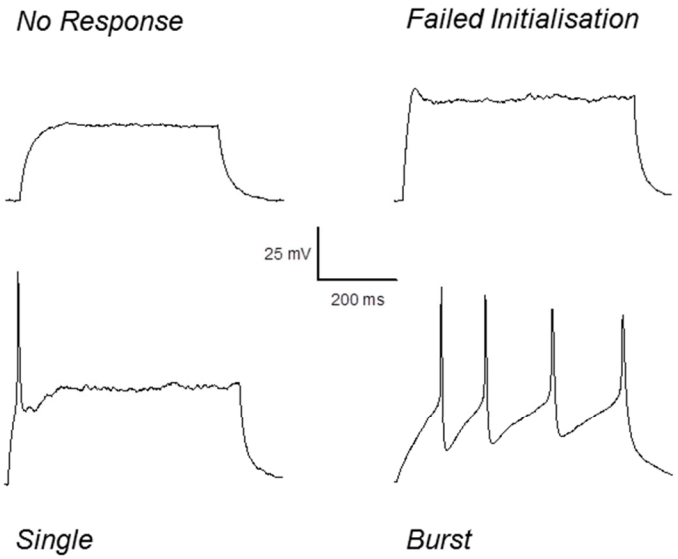

B

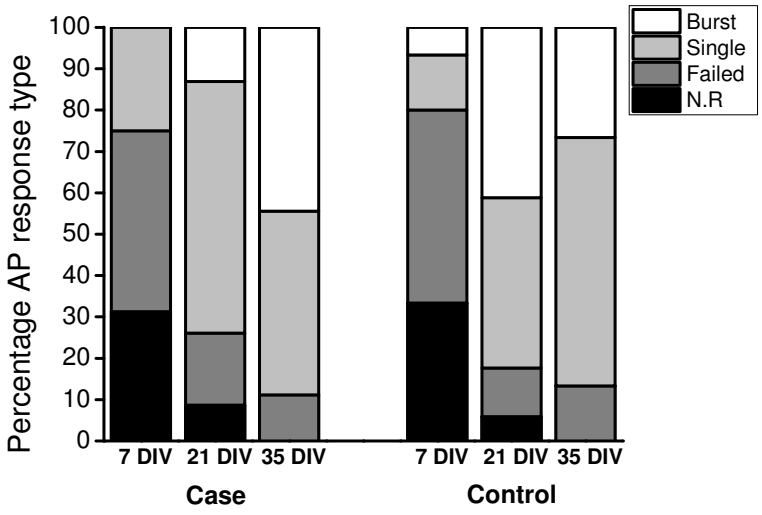

Figure. 4.3, Characterisation of firing properties in DISC1 iPSC-derived neurones using whoce-cell patch-clamp. ***A:*** Example traces illustrating action potential categories (signified by labels accordingly), which indicates functional development of action potentials in DISC1-hECNs. ***B:*** Graph showing development of DISC1-hECNs by proportional change in percentage responses of each AP category in Control (n= 15-17, N=1-2) and Case (n= 7-13, N=1-2) hECNs at 7, 21, and 35 DIV.

Resultant data gathered from Case and Control showed a progressive increase in the proportion of cells which fired at least 1 A.P. in response to a rheobase current injection, with almost all neurones firing at least 1 A.P at 35 DIV (Fig 4.3B); by 35 DIV, 87% of Control neurones (n=15, N=1) fired at least 1 A.P. while 89% of Case neurones did the same (n=9, N=1). No notable difference was observed across the general firing properties of the Case and Control hECNs. Theis observed pattern of results is similar to developmental timelines previously detailed in studies of hECNs derived from other human pluripotent stem cells (Bilican *et al.* 2014)..

Further to this, parameters of the A.P. were also measured, namely, amplitude (Figure. 4.4), threshold for A.P. generation (Figure. 4.5), half-width (Figure. 4.6; the width of an action potential at half of its peak amplitude, in ms), and size of after-hyperpolarisation (A.H.P; Figure. 4.7.). These measures were taken from either single A.P.s, or in the case of burst firing, the first A.P. of the barrage elicited by the rheobase. Collectively, these results show no statistical difference (minimum p=0.21) between Case and Control in any A.P. parameter observed. In terms of the development of neural properties *in vitro*, here between DIV 7 and DIV 35, A.P.s in both Case and Control became faster with a reduced half-width (Control, p=0.37; Case, p=0.06. Student's *t*-test), and an increase in amplitude (Control, p=0.05; Case, p=0.04; Students *t*-test). No significant development was observed for A.P. threshold (Control, p=0.30; Case, p=0.84. Students *t*-test) and A.H.P (Control, p=0.09; Case, p=0.84. Students *t*-test).

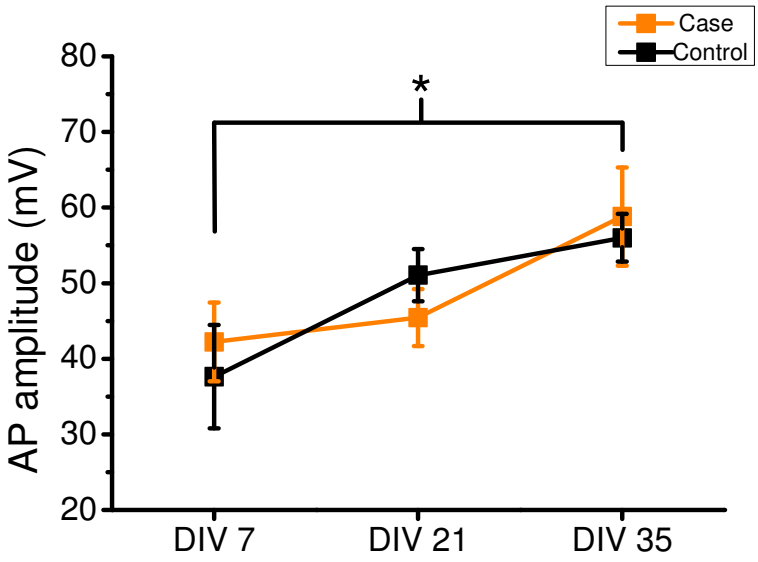

Figure. 4.4, Development of action potential amplitude in Case and Control hECNs across time in culture: Whole-cell current-clamp A.P amplitude was determined from the threshold potential to the maximum voltage deflection. From DIV 7 to DIV 35, mean amplitude of A.P.s increased progressively (Control, n= 7-19, N=1-2, p=0.05; Case, n= 3-13, N=1-2, p=0.04; Students *t*-test).

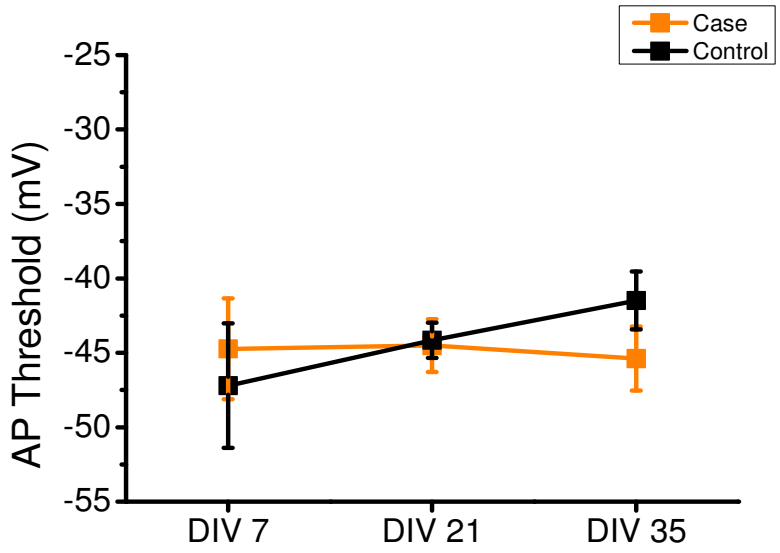

Figure. 4.5, Development of action potential threshold in Case and Control hECNs. Threshold was established in whole-cell current-clamp by pulsed rheobasic current input as described in Chapter 2: Methods & Materials. From DIV7 to DIV35, mean A.P. threshold did not change significantly (Control, n= 7-19, N=1-2, p=0.3; Case, n= 3-13, N=1-2, p=0.84; Students *t*-test).

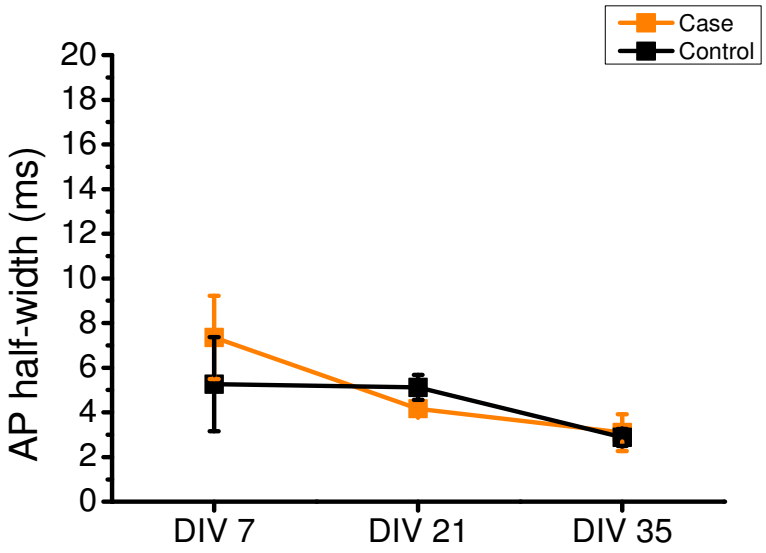

Figure. 4.6, Change in action Potential half-width across development in Case and Control DISC1-hECNs. Values established by whole-cell current-clamp using APs elicited by pulse rheobasic current injection as described in Chapter 2: Methods & Materials). From DIV7 to DIV35, mean A.P. half-width did not change significantly (Control, n= 7-19, N=1-2, p=0.3; Case, n= 3-13, N=1-2, p=0.06; Students *t*-test).

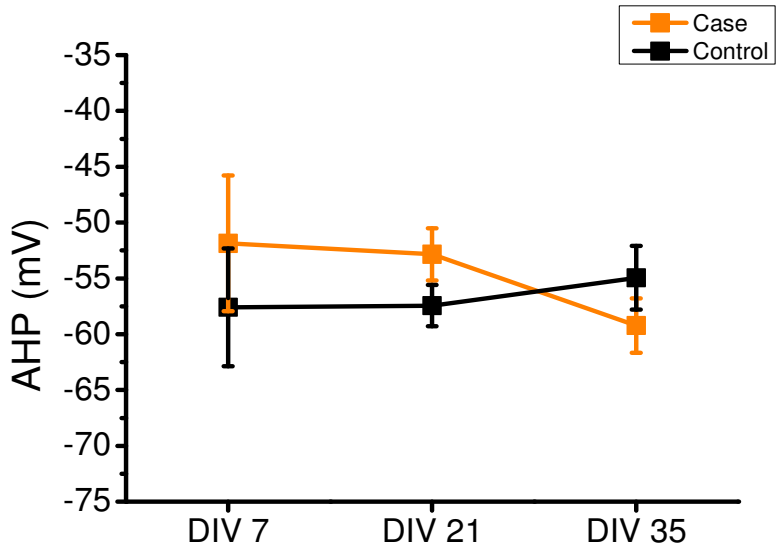

Figure. 4.7, Action potential after-hyperpolarisation (AHP) in Case and Control DISC1-hECNs: The after-hyperpolatisation (AHP) value was measured from the peak of the rising phase of the AP to its peak hyperpolarisation in whole-cell current-clamp (See Chapter 2: Methods & Materials). From DIV7 to DIV35, mean A.P. threshold did not change significantly (Control, n= 7-19, N=1-2, p=0.3; Case, n= 3-13, N=1-2, p=0.79, Students *t*-test).

4.4.1 Characterisation of neurotransmitter receptors expressed by Control and mutant *DISC1* Case hECNs

A key feature of cortical excitatory neurones' development is response to neurotransmitters such as GABA and glutamate, a property that has since been replicated in hECNs (Bilican *et al.* 2014). To that end, responses to GABA, AMPA, and NMDA were examined, along with a basic characterisation of $GABA_AR$, AMPAR, and NMDAR subunit composition. Collectively, these types of receptors are the primary mediators of neurotransmitter-mediated excitation and inhibition, with a balance between the two being suspected to be disrupted in schizophrenia (Gamo *et al*. 2013), which may have correspondent neuropathology reflected in the behaviour of these receptors.

4.4.2 Characterisation of $GABA_AR$-mediated responses, and $GABA_AR$ subunit composition.

Recently, DISC1 has been shown to be involved in the regulation of $GABA_AR$ trafficking in cortical pyramidal neurones (Wei *et al*. 2015). $GABA_ARs$ are assembled in the endoplasmic reticulum, and are then trafficked to the Golgi network. They are then transported along microtubules on dendrites and inserted into extra-synaptic sites, where they diffuse laterally into synapses (see Wei *et al*. 2015). It is suspected that that DISC1 exerts a critical effect on GABAergic inhibitory transmission by regulating microtubule motor protein kinesin 1-mediated $GABA_AR$ trafficking in the cortex (Twelvetree *et al*. 2010; Yuen *et al*. 2012). Crucially, knockdown of DISC1 results in a decrease in whole-cell $GABA_AR$ expression, as well as at the synapse, while overexpression results in an increase in whole-cell $GABA_AR$ expression, and also at the synapse (Wei *et al*. 2015). As the *DISC1 (1;11)(q42;q14.3)* mutation has been associated with a lack of DISC1 protein product, it is thus highly possible that $GABA_AR$ expression in hECNs harbouring the *DISC1 (1;11)(q42;q14.3)* may be affected.

Furthermore, previous studies demonstrate the involvement of the α_2 and α_3 $GABA_AR$ subunits in cognition in schizophrenia, with positive allosteric modulators selective for these subunits improving markers of cognition that are shown to be affected in schizophrenia (Lewis *et al.* 2005, also see Rudolph & Mohler. 2014). Given this and that previous work has indicated that hECNs show substantial $GABA_AR$ expression, which are likely composed of $\alpha_{2/3}\beta_{2/3}\gamma_2$ (see Chapter 3.2.1; James *et al.* 2014), initial experiments examined the current density of GABA (300 μM) responses at 35 DIV in Case and Control hECNs (Fig, 4.8 A,B). Responses to GABA, at a cell holding potential of 0 mV (-14 mV) were blocked by $GABA_AR$ antagonist, bicuculline (not shown). The current densities of $GABA_AR$-mediated responses did not significantly differ between Case and Control lines ($p=0.57$), with all cells responding to GABA.

A decreased level of γ_2 subunit mRNA has been observed in the frontal cortex in schizophrenia (Akbarian *et al*. 1995b; Huntsman *et al*. 1998), with little effect on γ_1- and γ_3- subunit expression (Ishikawa *et al*. 2004a). Potential alterations in expression of other subunits were examined by the effects of diazepam (γ-subunit selective) on GABA-mediated currents and responses to gaboxadol (δ-subunit selective). Diazepam (30 nM) mildly potentiated currents in both Control and Case hECNs, with strong potentiation achieved at a higher diazepam concentration (3 μM) in both Control and Case hECNs (no statistical difference observed, $p=0.62$, Student's *t*-test; Figure. 4.8C). Gaboxadol (3 μM) elicited nominal current relative to currents elicited by a saturating concentration of GABA (3 mM), while a higher concentration of gaboxadol (300 μM) showed little further activation in both Case and Control lines. No statistical difference was observed between Case and Contol ($p=0.51$, Student's *t*-test; Figure. 4.8D). Collectively, these data suggest that $GABA_ARs$ are not expressed differently in terms of total expression or composition between Case and Control hECNs.

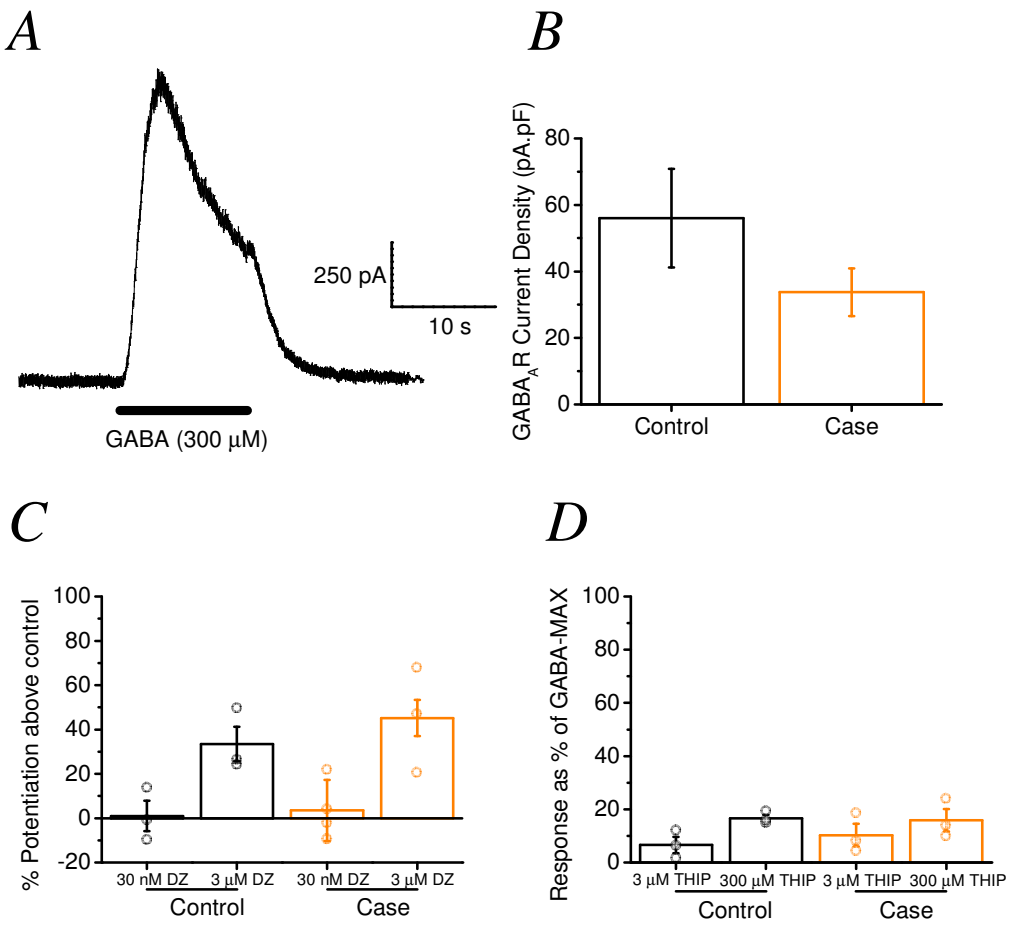

Figure. 4.8, GABA$_A$R mediated responses in Case and Control hECNs at 35 DIV. ***A:*** Trace showing a whole-cell voltage-clamp (0 mV; -14 mV LJP corrected) current response to bath applied GABA (300 µM). ***B:*** Mean whole-cell GABA$_A$R current densities (pA.pF) elicited by GABA (300 µM) are not significantly different between Case and Control hECNs (Control, n= 6-8, N=1-2; Case, n= 5-8, N=1-2). ***C:*** Mean potentiation of whole-cell GABA$_A$R-mediated responses by diazepam (30 nM and 3 µM) in Case and Control DISC1-hECNs (Control, n= 3, N=1; Case, n= 3, N=1). ***D:*** Mean responses to δ-subunit selective GABA$_A$R agonist THIP (gaboxadol) in Case and Control DISC-1 hECNs (Control, n= 3, N=1; Case, n= 3, N=1).

4.4.3 Examination of intracellular Chloride [Cl^-] concentration

Cortical excitatory neurones exhibit a typical decrease in intracellular Cl^- across development, a process which has been shown to be critical to normal development and maturation (see Kaila, *et al*. 2014). This is achieved by the use of Cl^- transporter proteins, Na^+-K^+-Cl^- co-transporter 1 (NKCC1) and K^+-Cl^- co-transporter 2 (KCC2). These transporters utilise Na^+ and K^+ gradients across the cell membrane to drive Cl^- ions into the cell (NKCC1), or out of the cell (KCC2). In normal development, NKCC1 is the dominant Cl^- transporter in fetal cortical neurones, however, as postnatal maturation progresses, an isoform of KCC2 (KCC2b, Uvarov *et al.* 2006, Blaesse *et al.* 2009) Cl^- transporter rapidly dominates. This results in a hallmark developmental profile for neuronal tissue; when NKCC1 is dominant in early development, intracellular [Cl^-] is known to be relatively high (approximately 25 mM), with the Cl^- reversal potential tending to be less negative than the neurones R.M.P. Thus, when a $GABA_AR$ is opened, the membrane potential depolarises to the reversal potential of chloride, sometimes resulting in excitation (Ben-Ari *et al*. 2007). With development KCC2b expression increases dramatically leading to an increase in the relative expression of KCC2b with respect to NKCC1 leading to a net extrusion of Cl^- and a reduced intracellular [Cl^-] (approximately 5-10 mM in adult excitatory neurones). The Cl^- reversal potential therefore becomes more negative and $GABA_AR$ (or GlyR) activation results in a net Cl^- influx and a hyperpolarising response (Blaesse *et al*. 2009).

Importantly, perturbed $GABA_AR$–mediated signalling has been implicated in diseases such as Rett syndrome. Previous studies using iPSC-derived neuronal material demonstrated an under-expression of KCC2 causing persistent GABA-ergic neuronal excitation, and showed a rescue to an unaffected phenotype (Tang *et al*. 2015). Intracellular chloride is also implicated in schizophrenia *via* dysregulation of intracellular chloride transporter activity that may disrupt normal development of neuronal networks by altering the overall balance between excitation and inhibition (Kalkman *et al.* 2011; Arion *et al.* 2011). The previously observed phenotype in Schizophrenia is that NKCC1 expression is aberrantly increased in development, resulting in an increase in intracellular [Cl^-] which pervades into adulthood. Given

previous findings about Cl^- transporters in hECNs (Livesey *et al*. 2014), showing that intracellular [Cl^-] decreases across development to a 'mature-like' state, it is thus plausible to examine the intracellular [Cl^-] in Case and Control hECNs for any Cl^- transporter-related pathophysiology. Notably, to obtain this reduction in intracellular [Cl^-] hECNs were maintained in media lacking neurotrophic factors (BDNF and GDNF), which are known to the influence intracellular [Cl^-], and required extended culture periods to 49DIV.

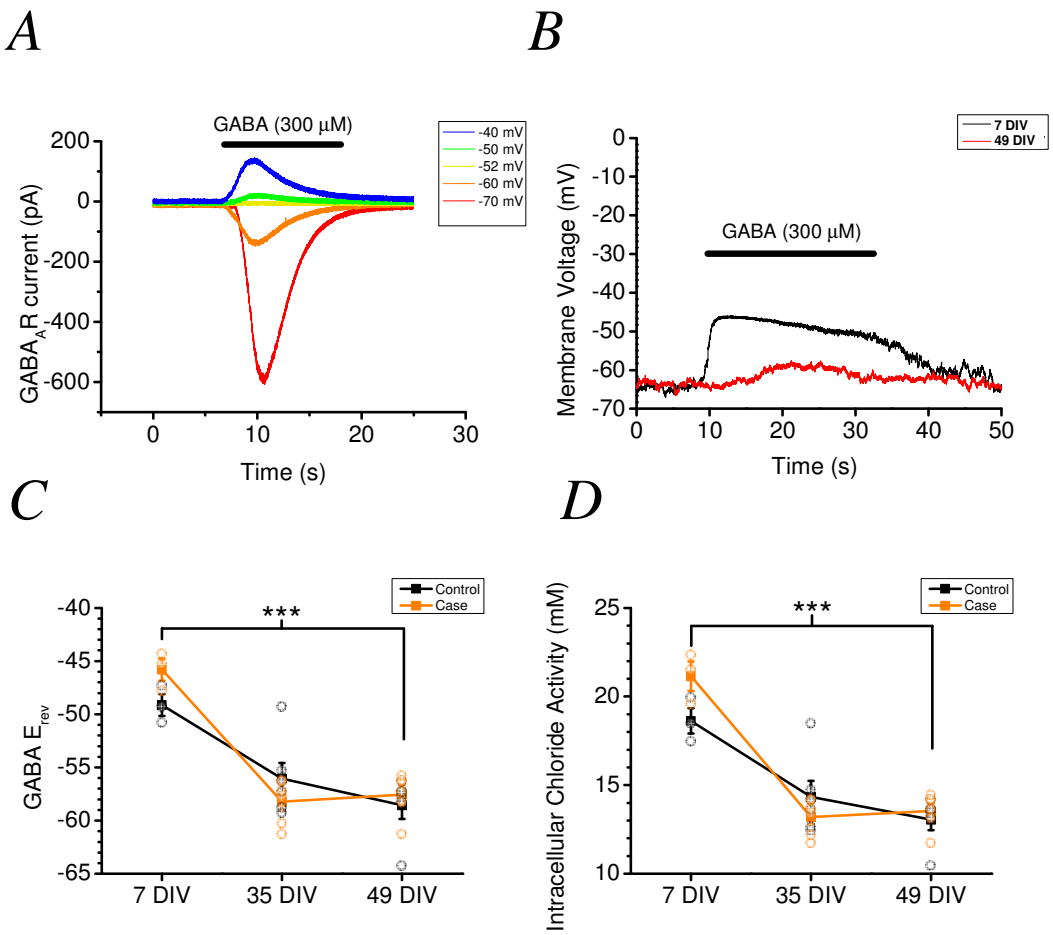

Figure. 4.9. Using perforated patch-clamp technique to elicit GABA$_A$R responses, and assaying intracellular [Cl-] activity in Case and Control DISC1-hECNs at 7, 35 and 49 DIV. Significance; *** indicates p=<0.001. ***A:*** The holding potential at which GABA application ceased to evoke a response was determined to be the reversal potential at the GABA$_A$R (GABA E_{rev}). GABA E_{rev} was then used to calculate intracellular [Cl^-] using the Goldman-Hodgkin-Katz equation, and subsequently to adjusted to give apparent thermodynamic activity. ***B:*** Trace showing current-clamp recordings of GABA responses from Case at 7 and 49 DIV..***C:*** Mean GABA reversal potentials (GABA E_{rev}) in Control and Case lines (Control, n= 3-6, N=1-2; Case, n= 3-6, N=1-2). ***D:*** Intracellular Cl^- activity (mM) in Control and Case lines (Control, n= 3-6, N=1-2; Case, n= 3-6, N=1-2). *** indicates p=<0.001.

Here, the perforated patch-clamp technique using gramicidin (75 – 100 μg.ml) in the patch pipette solution was used to measure intracellular [Cl^-] in hECNs (see Methods 2.3.3). Gramicidin has an ability to perforate the cell membrane and organise into ion channels that are permeable to cations (Na^+ and K^+) but not Cl^-, therefore this technique allows electrical access to the intracellular compartment of the cell whilst maintaining intracellular [Cl^-] (Owens *et al*. 1996). $GABA_AR$-mediated responses were elicited with applications of GABA (300 μM) and the holding potential was adjusted until no current was passed upon GABA application, indicating no net flow of Cl^- in or out of the cell and the reversal potential for Cl^- at the $GABA_AR$. Fig 4.9A shows GABA applications at varying holding potentials and the respective current response, while Figure. 4.9B shows current-clamp recordings from a Case hECN at 7 and 49 DIV showing the shift in the nature of membrane potential responses to GABA application over time.

Figure. 4.9C shows mean $GABA_AR$ reversal potentials in DISC1 Case and Control hECNs. In line with native excitatory cortical maturation, increasingly negative reversal potentials for the $GABA_AR$ was observed between 7 DIV and 49 DIV in Control (-49.1 mV ± 1 mV, n=3, N=1, to -58.6 mV ± 0.8 mV n=6, N=2; p=<0.0005) and Case (-49.2 mV ± 1 mV, n=3, N=1, to -57.6 mV ± 0.8 mV, n=6, N=2; p=<0.0003), in line with previously published work on hECNs (Livesey *et al*. 2014) and others concerning Cl^- transporter maturation (Uvarov *et al.* 2006, Blaesse *et al.* 2009), with no statistical differences being observed between Case and Control lines (minimum p=0.51, Student's *t*-test). These reversal potential values were entered into the Nernst equation to yield intracellular [Cl^-]. Note that Cl^- concentrations were then corrected for thermodynamic activity in line with the Guggenheim convention (Activity factor 0.77, Kielland, 1937).

Briefly, the Guggenheim convention describes the behaviour of ions in solution as thermodynamic activity as determined by concentration, as opposed to purely concentration alone. An intuitive description would be to say that as the concentration of ions in a solution increases, past a point those ions will begin to occlude each other, reducing their actual activity i.e. thermodynamic activity, which determines the physiological phenomenon being observed. This is useful because the behaviour of ions in intra- and extra-cellular fluids is thus subject to this process,

and when interpreting our assumed concentration, we must then apply the idea that the ionic concentration that is determined by the Nernst equation must be amended in terms of the thermodynamic activity of the ion species under consideration.

Figure. 4.9D shows intracellular Cl^- activity in mutant *DISC1* Case and Control hECNs. A typical reduction in intracellular Cl^- activity was observed between DIV 7 and DIV 49 in both Control (19 ± 0.7 mM, n = 3, N = 1, to 13 ± 0.6 mM, n = 6, N = 2; p=<0.0005, Students *t*-test) and Case (21 ± 0.8 mM, n = 3, N = 1, to 14 ± 0.5 mM, n = 6, N = 2; p=<0.0003, Students *t*-test). These results show no statistical difference in intracellular Cl^- activities between Control and Case at any time in culture (p=0.41; Student's *t*-test).

4.4.4 Characterisation of NMDA receptors.

Previous reports implicate the NMDA receptor (NMDAR) in schizophrenia, with NMDAR antagonists producing psychotic-like symptoms and NMDAR positive modulators ameliorating this to some degree (Coyle *et al*. 2012). Further to this, it has been shown that knock-down of DISC1 increased NMDAR-mediated currents in rodent cortical cultures (Wei *et al*. 2014). The expression of NMDARs was therefore intially examined in Case and Control hECNs. Whole-cell currents in 35 DIV hECNs were elicited using NMDA (100 μM; in the presence of glycine, 50 μM, Figure. 4.10A) and current densities calculated. Figure. 4.10B shows mean current densities at 35 DIV for both Case and Control hECNs and significant differences were observed in current density between Case and Control lines (p=0.86, Student's *t*-test). All cells responded to NMDA and were blocked by NMDAR antagonist APV (not shown).

NMDAR subunit mRNA for various NMDARs has been shown to vary post-mortem in the dorsolateral prefrontal cortex in humans with schizophrenia, with an unknown but suggested influence on NMDAR subunit stoichiometry (Weickert *et al*. 2013). NMDAR-mediated pathophysiology is also implicated in early developmental processes in Schizophrenia (see du Bois & Huang, 2007). Furthermore, Wei *et al*. (2014) determine that a DISC1 knock-out-mediated reduction in NMDAR expression in rodent cortical neurones is accompanied with an alteration in GluN2A subunit expression. Importantly, NMDAR subunit composition in the forebrain changes from a predominant GluN1/GluN2B population in immature neurones to a mixed GluN1/GluN2A/GluN2B population in adults (Monyer *et al*. 1994; Watanabe *et al*. 1992; see Wyllie *et al*. 2013). To establish the possibility of NMDAR subunit changes in Case and Control hECNs the GluN2B subunit-selective NMDAR antagonist ifenprodil (3 μM) was used. Ifenprodil (3 μM) strongly blocked NMDAR-mediated currents (Figure. 4.10C) in both Control and Case hECNs, respectively, to 76.1% ± 3.3%, (n = 3, N = 1), and 72.2%, (n = 3, N = 1; p=0.50, Student's *t*-test). This data is compatible with data from 'pure' recombinantly expressed GluN1/GluN2B NMDARs (Kew *et al*. 1996), indicating the predominant expression of GluN2B subunit-containing NMDARs on Case and Control hECNs.

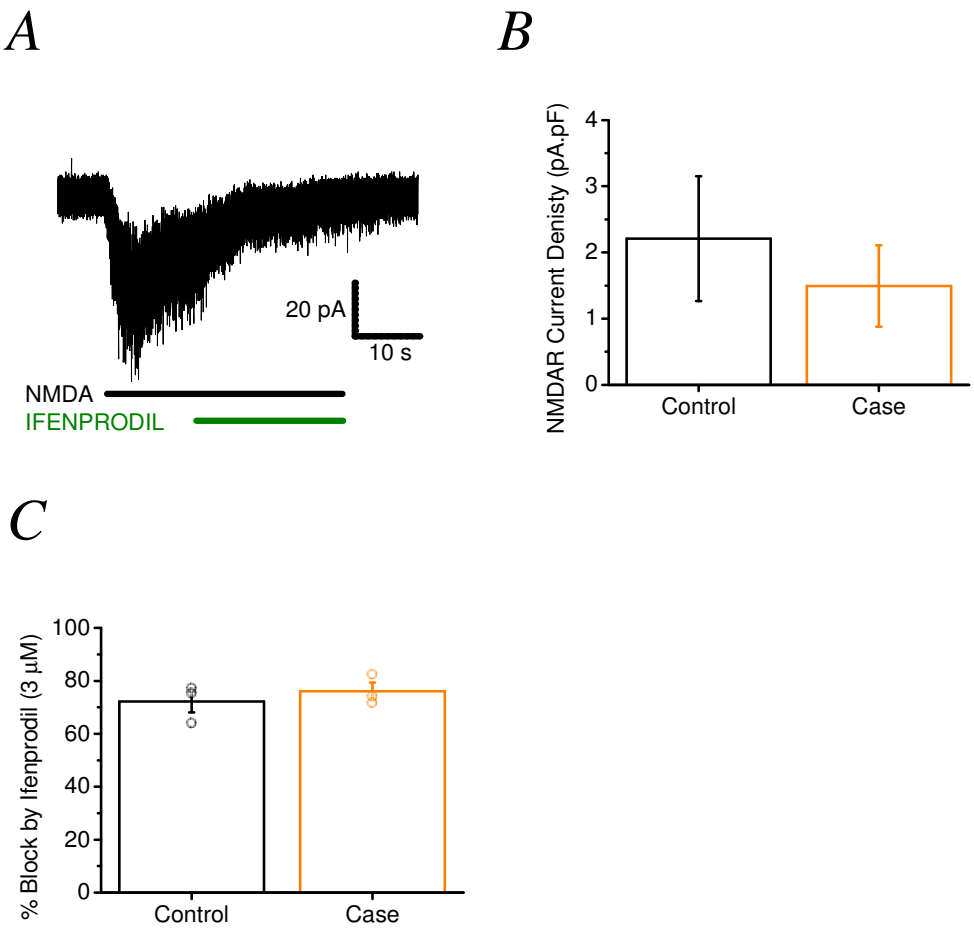

Figure. 4.10. NMDAR-mediated responses in Case and Control hECNs. ***A:*** Trace showing whole-cell voltage clamp response to NMDA (100 µM, in the presence of glycine, 50 uM) and block by ifenprodil (3 µM) as indicated by coloured bars. ***B:*** Mean NMDAR (100 µM) current density (pA.pF; n = 3, N = 1). ***C:*** Mean block of NMDAR- mediated responses by ifenprodil (3 µM; n = 3, N = 1).

4.4.5 Characterisation of AMPA receptors

Previous work has suggested possible AMPA receptor (AMPAR) pathophysiology in Schizophrenia in general, primarily through expression, mRNA editing, and trafficking of different AMPAR subunits (Akbarian *et al*. 1995; Wright & Vissel 2012; see Hammond *et al*. 2010) and DISC1 (Hayashi-Takagi *et al*. 2010) specifically, thus highlighting the potential for studying altered AMPAR expression and composition in mutant DISC1 Case hECNs with respect to Control hECNs.

Initially, to characterise the functional expression of AMPARs on 35 DIV Case and Control hECNs, whole-cell currents were elicited using AMPA (100 μM; Figure. 4.11A) and current densities were determined, using a whole-cell voltage-clamp holding potential of -60 mV (-74 mV). Figure. 4.11B shows the mean current densities at 35 DIV and no significant differences in current density were observed between Case and Control (Figure. 4.11B; p=0.54, Student's *t*-test) .with all cells responding to bath applications of AMPA and being blocked by CNQX (data not shown).

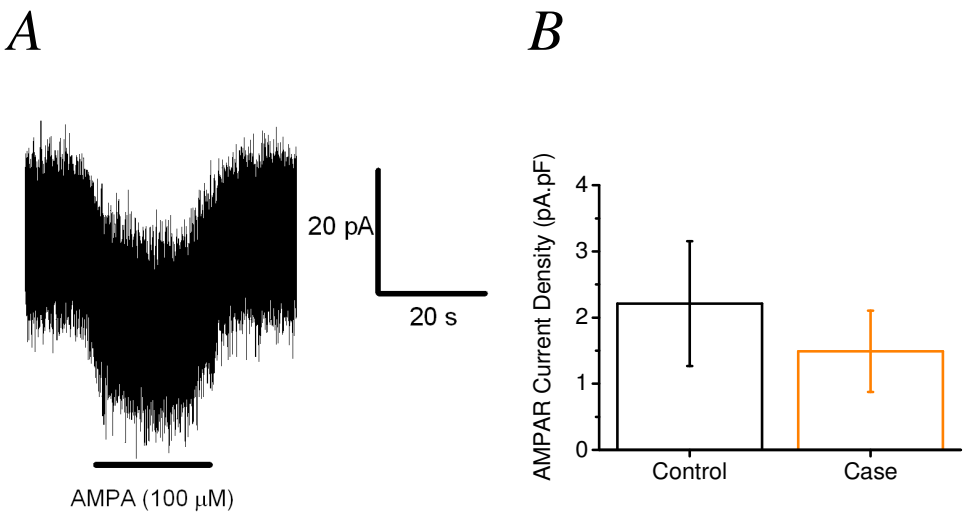

Figure. 4.11. AMPAR mediated responses in Control and Case hECNs. ***A:*** Trace showing whole-cell response to AMPA (100 μM) at a holding potential of -74 mV. ***B:*** No difference in the mean AMPAR current density (pA.pF). Control, n=8, N=2; Case, n=5, N=2;.

The composition of the AMPARs expressed upon Case and Control hECNs was then investigated. The AMPAR has a tetrameric structure, potentially composed of 4 subunits (GluA1-4), with developmentally regulated subunit composition. In immature rodent, and human excitatory cortical neurons, GluA1/GluA4- containing AMPARs predominate, whereas mature neurons have an increased expression of GluA1 and GluA2 subunits (Talos *et al*. 2006a, 2006b; Orlandi *et al*. 2011, see Traynelis *et al*. 2012). In normal development, the GluA2 subunit is predominantly RNA-edited (Q → R), with an edited GluA2 subunit being strongly suggestive of a postnatal phenotype (Brill & Huguenard. 2008). Inclusion of at least one edited GluA2 subunit into the AMPAR tetramer imparts distinct biophysical properties including a lower single-channel conductance, insensitivity to channel-blocking spermines and Ca^{2+}-impermeability (Swanson *et al*. 1997; Traynelis *et al*.2012). This has been shown to regulate Ca^{2+}-mediated processes relating to neuronal excitotoxicity, and, interestingly may relate to possible calcium dysregulation in schizophrenia, and may contribute to the aberrant development of excitatory networks (Berridge. 2012). Thus, an age-dependent phenotype may exist in mutant *DISC1* Case hECNS mediated by aberrant trafficking or regulation of different

AMPAR isoforms as evidenced by their AMPAR complement. Additional experiments were thus conducted to establish the likely AMPAR isoform expressed on Case and Control hECNs.

Alterations in AMPAR single-channel conductances are amenable to biophysical investigation using electrophysiological techniques. An estimate of the mean AMPAR single-channel conductance in hECNs at 35 DIV was made using non-stationary noise analysis. In the first, two simultaneous whole-cell voltage-clamp recordings were made in each experiment, where the described AMPAR-evoked responses in both Case and Control hECNs were made in AC and DC current formats (see Figure. 4.12A,B). For these experiments the extracellular recording solution was supplemented with cyclothiazide (20 μM), an AMPAR-selective positive modulator that prevents AMPAR desensitization (Cowen *et al.* 1998) to elicit larger responses. The resultant plot of AC-current variance against DC-current amplitude yielded a straight-line plot (example in 4.12C) from which the estimated AMPAR single-channel current amplitude was determined and single-channel conductance calculated (Shown in Figure. 14.3D). Mean estimated single-channel conductances for Case (2.3 ± 0.6 pS; n = 6, N = 1) and Control (2.3 ± 0.6 pS; n = 4, N = 1) hECNs were identical (p=0.97, Student's *t*-test). This data indicates Case and Control hECNs display low AMPAR conductances typical of AMPARs that are edited GluA2 subunit-containing (Figure. 4.12D; Swanson *et al.* 1997; Traynelis *et al.*2012).

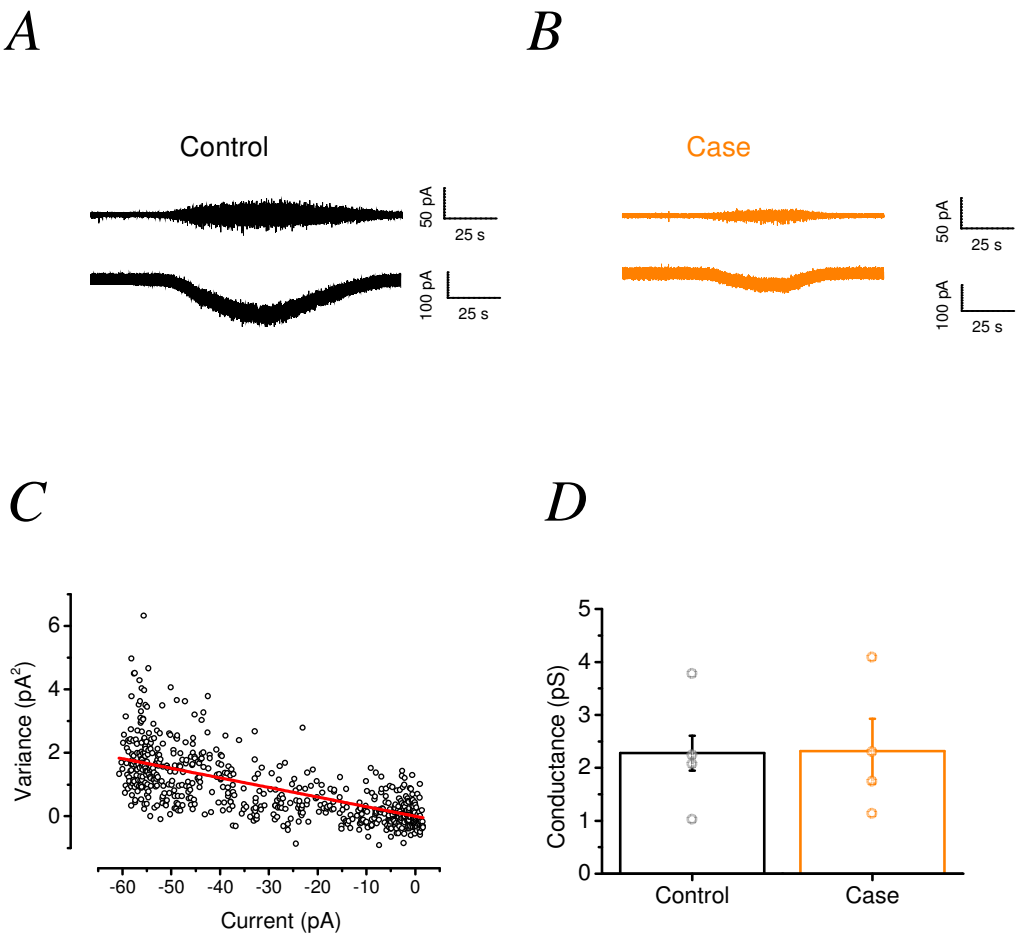

Figure. 4.12, Non-stationary noise analysis of AMPAR-mediated currents in Case and Control hECNs at 35 DIV. ***A:*** Traces from a Case hECN showing a slowly-rising and decaying whole-cell (-60 mv; -74 mV LJP corrected) response to AMPA (50 μM); the *upper* trace shows the AC current recording and the *lower* shows the DC current recording. ***B:*** As in '*A*' but for Case hECNs. ***C:*** Example current-variance plot. The relationship yields a linear relationship to which a straight line was fitted. The slope of the plot gave the estimated AMPAR single-channel current. ***D:*** Mean estimated AMPAR single-channel conductances of AMPARs expressed in Case and Control hECNs (n = 4; N = 2).

Next, in order to confirm the presence of edited GluA2 AMPAR subunits, experiments were conducted to assess the sensitivity of AMPAR-mediated currents to the channel blocker 1-naphthyl acetyl spermine (NASPM, 3 μM; Koike *et al*. 1997), which is selective for AMPARs that lack the edited GluA2 subunit. To examine NASPM block of AMPAR-mediated currents, I-V relationships in the presence and absence of extracellular applied NASPM were obtained (Figure. 4.13A and Figure. 4.13B). No receptor block was observed at negative or positive holding potentials in both Case and Control hECNs. This observed behaviour was quantified using 'rectification index' (RI; see Methods for details); a ratio of the conductances at a positive holding potential (+60 mV) and a negative holding potential (-100 mV). Rectification indices were calculated in the presence and absence of NASPM (Figure. 4.13C). Between Case (n = 3, N = 1) and Control (n = 3, N = 1), no significant differences were observed in the presence or absence of NASPM ($p>0.1$ in all cases; Student's *t*-test). These data confirm the predominant AMPAR composition contains the edited GluA2 subunit in both the Case and Control hECNs at 35 DIV.

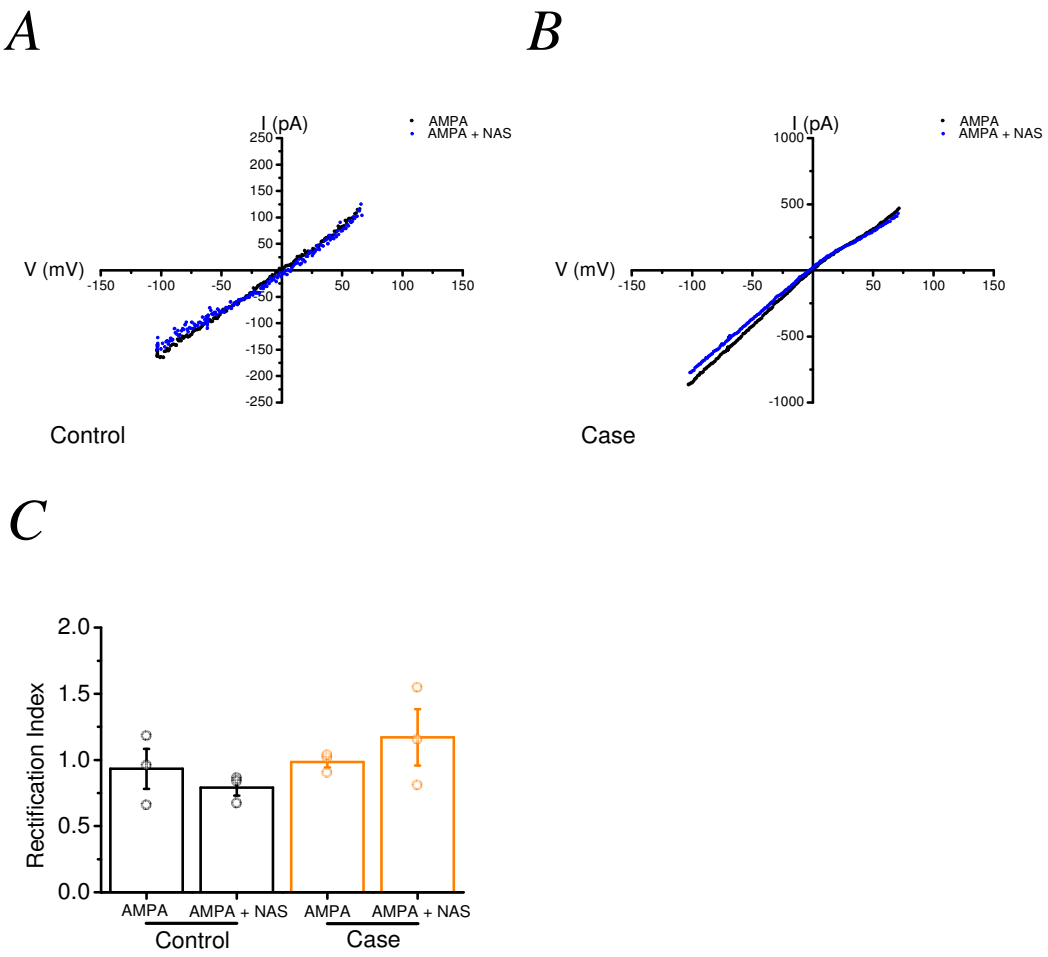

Figure. 4.13. NASPM sensitivity to AMPAR-mediated responses in Case and Control hECNs. ***A:*** Control hECN: leak subtracted I-V plot generated from an AMPAR-mediated steady-state response which was ramped from -100 mV to +60 mV for 1 s. ***B:*** As in '*A*', but for Case hECNs. ***C:*** Mean rectification indices for AMPAR-mediated I-V plots obtained from Control and Case hECNs (n = 3, N =1).

4.5 Discussion.

This study examines the functional properties of hECNs generated from patient-derived iPSCs harbouring a mutation to the *DISC1* gene (1;11)(q42;q14.3) that is strongly associated with psychiatric disorders including schizophrenia. Such disorders are associated with an imbalance in the relationship of cortical cellular excitation to inhibition that are thought to underpin some of the psychiatric phenotypes (Akbarian *et al*. 1995; Bradshaw & Porteous. 2012; Gamo *et al*. 2013; Lisman. 2012; Callicot *et al*. 2013; Kim *et al*. 2012; Schurov *et al*. 2004; Wright & Vissel 2012; see Hammond *et al*. 2010). In essence, the properties examined with this study did not reveal any mutant *DISC1*-associated phenotypes with respect to control.

4.5.1 Intrinsic excitability

Initially the intrinsic passive and firing properties of Case and Control hECNs were investigated across multiple time points in order to detect any potential developmental difference in excitability. The data in broad agreement with a developing neuronal phenotype (increasing whole-cell capacitance, increase in ability to fire and increase in amplitude and speed of action potentials) across all lines examined. The fact that no difference was found is consistent with a study where hippocampal CA1 neurones from a transgenic mouse expressing the equivalent truncated DISC1 protein also did not show any difference in the passive or intrinsic properties (Randall *et al*. 2014). Importantly, the properties of hECNs examined even at 35DIV are consistent with an immature neuronal profile; hyperpolarized RMP, high input resistance and low whole-cell capacitance, and are consistent with *in vitro* pluripotent stem cell derived neurones in general (see Kim *et al*. 2011; Pak *et al*. 2015; Scheglovitov *et al*. 2013). It maybe therefore plausible that *in vitro* hECNs may not have reached a sufficient level of maturity for excitability phenotypes to emerge. Moreover, hECN culture composition may not be sufficiently representative to the possibility that specific neurones of the cortex may exhibit subtle differences in intrinsic excitability. For example, hECN cultures only contain

nominal proportions of interneurones for which there is an important role in schizophrenia (Lewis *et al*. 2005).

4.5.2 Neurotransmitter receptor expression and composition

The properties of major neurotransmitter receptors, AMPARs, $GABA_A$Rs and NMDARs, were then investigated. The expression of $GABA_A$Rs upon Case and Control hECNs was found to be statistically equivalent indicating that mutant *DISC1* does not influence $GABA_A$R expression in hECNs. This is in agreement with a recent study examining mutant DISC1 protein in rodent cortical neurones which expressed equivalent levels of $GABA_A$Rs *versus* controls despite knock down and over expression of the full DISC1 protein having opposing effects upon $GABA_A$R expression (Wei *et al*. 2015). The previous results chapter determined that the composition of $GABA_A$Rs was representative of the major immature $GABA_A$R expressed in the immature cortex. Selected pharmacological analyses demonstrated that it is unlikely that $GABA_A$R composition in Case and Control hECNs was different. Similarly, the NMDAR receptor expression in Case hECNs was not different from Control hECNs and the composition was pharmacologically determined using ifenprodil to be representative of a predominantly immature NMDAR cortical profile, i.e., GluN1/GluN2B-containing. Recently, Wen *et al.* (2014) report a modest increase in the GluN2B mRNA level, but not GluN1 protein levels, in hECNs derived from mutant *DISC1* patients. Data presented here suggests that this disparity does not manifest at the functional level.

The finding that $GABA_A$R and NMDAR compositions are consistent with immature neuronal profiles clearly restricts conclusions to the subunits expressed. Mutant *DISC1* patients have a late juvenile/young adult symptomatic onset (Thomson *et al*. 2013) and maturation of cortical $GABA_A$R and NMDAR composition is expected to have taken place. For example, the findings that mutant *DISC1* affects GluN2A NMDAR subunit expression (Wei *et al*. 2013) and potentially reduces functional NMDAR expression to slow NMDAR maturation in the mouse barrel cortex (Greenhill *et al*. 2015) cannot be feasibly interrogated in this system. This highlights the value of thorough characterisation like that performed in

this study and that it is absolutely required if the field is to interpret findings from stem cell-derived neuron technology for disease-modelling studies.

AMPAR expression was observed to be equivalent between Case and Control hECNs at 35 DIV indicating that mutant *DISC1* has no apparent effect. AMPAR composition was then determined using non-stationary fluctuation analysis and the sensitivity of AMPAR-mediated currents to NASPM. This data was directly equivalent to that of rodent cortical neurones that had undergone a period of post natal development in which edited GluA2 is upregulated (Brill and Hugenuard. 2008) and also recombinantly expressed AMPARs containing edited GluA2 subunts. (Swanson *et al.* 1997). Both strategies clearly converged on the predominant AMPAR composition at 35 DIV as being edited GluA2-containing for both Case and Control hECNs. Contrary to the $GABA_AR$ and NMDAR, AMPAR expressed on hECNs have a composition that is expected of neurone that has undergone a period of maturation (Orlandi *et al*. 2011; Talos *et al.* 2006). A rapid upregulation of GluA2 AMPAR subunit transcripts has also been reported in other similar systems (Stein *et al*. 2014; van de Leemput *et al*. 2014). Wen *et al*. (2014) recently reported an increase in the mRNA level of GluA2 in hECNs generated from mutant *DISC1* patient-derived iPSCs over control and isogenic, gene-corrected mutant *DISC1* hECNs, though data obtained in this study indicates this transcriptional difference may not translate to a functional difference. It appears that the functional upregulation of the GluA2 subunit is much faster than expected from what is expected *in vivo* (Orlandi *et al*. 2011; Talos *et al.* 2006). Of note, Whitney *et al*. (2008) report that the GluA2 is rapidly edited and functionally upregulated within 4 weeks in *in vitro* neurones differentiated from human cortical progenitors. This suggests that the upregulation of the edited GluA2 subunit is a potential result of the *in vitro* environment.

4.5.3 Intracellular [Cl^-]

Previous studies of $GABA_AR$-mediated signalling has shown a developmental a change in the intracellular chloride concentration occurs as mediated by changes in expression levels of Cl^- transporter proteins NKCC1 and KCC2 (Blaesse *et al*. 2009). Here, the perforated patch-clamp technique was used to determine the reversal potential of the $GABA_AR$ in DISC1 iPSC-hECNs in light of the possibility of Cl^- transporter dysfunction or dysregulation as previously described for the *DISC1* (1;11)(q42;q14.3) mutation (Kalkman *et al.* 2011; Arion *et al.* 2011). Here, the data show an equivalent reduction in the $GABA_AR$ reversal potential and related intracellular Cl^- reported for other hECNs derived from other lines (Livesey *et al*. 2014), though no significant difference in the reduction in intracellular [Cl^-] between Case and Control hECNs,.It should be noted that the expression of Cl^- transporters and intracellular Cl^- are under complex homeostatic regulation (Blaesse *et al*. 2009). It is therefore quite possible that *in vitro* maintenance conditions may surmount any potential difference or signalling factor/s may not be present in the Case and Control hECN cultures.

It is particularly unusual that there is a reduction in intracellular [Cl^-] occurs over the period of 7 weeks as it is expected to mature in the human brain throughout the embryonic period and is reported to persist up to two years after birth in parts of the cortex (Bayatti *et al*. 2008; see Blaesse *et al*. 2009). It is therefore intriguing that a population of human sub-plate neurones (Pax-6^+) highly express KCC2 from 16 post-conception weeks and hECNs in this study are derived from Pax-6^+ neural progenitors (Bilican *et al*. 2014; see Methods and Chapter 2). Given that previous study of intracellular chloride in iPSC-derived material in other diseases (Rett syndrome, Tang *et al*. 2015) has demonstrated that the cultures can fundamentally replicate this pathology, and that a similar pattern of maturation is observed as elsewhere concerning intracellular [Cl^-] in normal, unaffected development (Livesey *et al*. 2014; Tang *et al*. 2015), it is concluded that DISC1-iPSCs demonstrate no effect of the *DISC1* mutation (1;11)(q42;q14.3) on intracellular [Cl^-] levels in development.

4.5.4 What about synaptic properties?

Very subtle phenotypic differences in some of the functional properties described above maybe resolved with extensive further experimentation, however together these data suggests that principle differences in neuronal dysfunction caused by the mutation in *DISC1* are to be found at the synaptic or circuit level.

DISC1 is particularly enriched in post-synaptic density fractions and in dendritic spines (Carlisle *et al*. 2011; Clapcote *et al*. 2007; Hayashi-Takagi *et al*. 2010; Kirkpatrick *et al*. 2006). Moreover, analysis of the DISC1 protein-protein interactions highlights that DISC1 interacts with a number proteins with known roles in synaptic function (Camargo *et al*. 2007). Studies examining mutant *DISC1* on synaptic properties in rodent models are not widespread and indicate alteration in the frequency in excitatory post-synaptic events compared to controls in cortical layer II/III pyramidal neurones due to an impairment in pre-synatptic glutamate release (Holley *et al*. 2013; Maher & LoTurco. 2012). Moreover, conditionally-induced mutant *DISC1*-associated deficits in synaptic plasticity in the mouse barrel cortex during a critical developmental window has prolonged effects on functional synaptic plasticity into adulthood (Greenhill *et al*.2015).

A major road block to studying synaptic properties in neurones derived from pluripotent stem cells is that the cultures do not commonly generate robust synaptic activity (Bardy *et al*. 2015). Indeed, cultures employed in this study were no exception to this. To circumvent this issue, numerous groups are now employing various strategies including co-culture of human stem cell-derived neurones with rodent astrocytes to promote functional synaptogenesis (Johnson *et al*. 2007; Kim *et al*. 2011; Pak *et al*. 2015; Shcheglovitov *et al*. 2013). Recently, Wen *et al*. (2014) employed this strategy to examine synaptic properties of hECNs generated from mutant *DISC1* patients and, also, isogenic-corrected mutant *DISC1* lines to similarly demonstrate a reduced post-synaptic synaptic event frequency due to impairments in neurotransmitter release. Additionally, Brennand *et al.* (2011), also showed a difference in frequency of spontaneous excitatory post-synaptic currents between *in vitro* neurones derived from clinically, but not genetically, defined schizophrenia

patients. It remains pertinent to note that potential synaptic plasticity deficits in human mutant *DISC1* neurones remain unreported.

In conclusion, this study highlights that mutant *DISC1* (1;11)(q42;q14.3) hECNs do not exhibit changes in intrinsic excitability, expression/composition of neurotransmitter receptors and maturation of intracellular [Cl^-] compared to healthy controls. Emerging evidence suggests that more definitive neuronal dysfunction associated with mutant DISC1 manifests at the synaptic level. A secondary, but nonetheless important, outcome of this study is the appropriateness of stem cell-derived neurones to model specific aspects of mutant *DISC1* pathophysiology and also other adult-onset neurological diseases. These data and other groups show that human pluritpotent stem cell technology requires to be further developed beyond 'standard' cultures in order to generate more relevant, native-like material.

Previous studies of $GABA_AR$-mediated signalling has shown a developmental a change in the intracellular chloride concentration occurs as mediated by changes in expression levels of Cl^- transporter proteins NKCC1 and KCC2 (Blaesse *et al*. 2009). Here, the perforated patch-clamp technique was used to determine the reversal potential of the $GABA_AR$ in DISC1 iPSC-hECNs in light of the possibility of Cl^- transporter dysfunction or dysregulation as previously described for the *DISC1* (1;11)(q42;q14.3) mutation (Kalkman *et al.* 2011; Arion *et al.* 2011). Here, the data show an equivalent reduction in the $GABA_AR$ reversal potential and related intracellular Cl^- reported for other hECNs derived from other lines (Livesey *et al*. 2014), though no significant difference in the reduction in intracellular [Cl^-] between Case and Control hECNs,.It should be noted that the expression of Cl^- transporters and intracellular Cl^- are under complex homeostatic regulation (Blaesse *et al*. 2009). It is therefore quite possible that *in vitro* maintenance conditions may surmount any potential difference or signalling factor/s may not be present in the Case and Control hECN cultures.

It is particularly unusual that there is a reduction in intracellular [Cl^-] occurs over the period of 7 weeks as it is expected to mature in the human brain throughout the embryonic period and is reported to persist up to two years after birth in parts of the cortex (Bayatti *et al*. 2008; see Blaesse *et al*. 2009). It is therefore intriguing that a population of human sub-plate neurones (Pax-6^+) highly express KCC2 from 16

post-conception weeks and hECNs in this study are derived from Pax-6^+ neural progenitors (Bilican *et al*. 2014; see Methods and Chapter 2). Given that previous study of intracellular chloride in iPSC-derived material in other diseases (Rett syndrome, Tang *et al*. 2015) has demonstrated that the cultures can fundamentally replicate this pathology, and that a similar pattern of maturation is observed as elsewhere concerning intracellular [Cl^-] in normal, unaffected development (Livesey *et al*. 2014; Tang *et al*. 2015), it is concluded that DISC1-iPSCs demonstrate no effect of the *DISC1* mutation (1;11)(q42;q14.3) on intracellular [Cl^-] levels in development.

Very subtle phenotypic differences in some of the functional properties described above maybe resolved with extensive further experimentation, however together these data suggests that principle differences in neuronal dysfunction caused by the mutation in *DISC1* are to be found at the synaptic or circuit level.

DISC1 is particularly enriched in post-synaptic density fractions and in dendritic spines (Carlisle *et al*. 2011; Clapcote *et al*. 2007; Hayashi-Takagi *et al*. 2010; Kirkpatrick *et al*. 2006). Moreover, analysis of the DISC1 protein-protein interactions highlights that DISC1 interacts with a number proteins with known roles in synaptic function (Camargo *et al*. 2007). Studies examining mutant *DISC1* on synaptic properties in rodent models are not widespread and indicate alteration in the frequency in excitatory post-synaptic events compared to controls in cortical layer II/III pyramidal neurones due to an impairment in pre-synatptic glutamate release (Holley *et al*. 2013; Maher & LoTurco. 2012). Moreover, conditionally-induced mutant *DISC1*-associated deficits in synaptic plasticity in the mouse barrel cortex during a critical developmental window has prolonged effects on functional synaptic plasticity into adulthood (Greenhill *et al*.2015).

A major road block to studying synaptic properties in neurones derived from pluripotent stem cells is that the cultures do not commonly generate robust synaptic activity (Bardy *et al*. 2015). Indeed, cultures employed in this study were no exception to this. To circumvent this issue, numerous groups are now employing various strategies including co-culture of human stem cell-derived neurones with rodent astrocytes to promote functional synaptogenesis (Johnson *et al*. 2007; Kim *et al*. 2011; Pak *et al*. 2015; Shcheglovitov *et al*. 2013). Recently, Wen *et al*. (2014)

employed this strategy to examine synaptic properties of hECNs generated from mutant *DISC1* patients and, also, isogenic-corrected mutant *DISC1* lines to similarly demonstrate a reduced post-synaptic synaptic event frequency due to impairments in neurotransmitter release. Additionally, Brennand *et al.* (2011), also showed a difference in frequency of spontaneous excitatory post-synaptic currents between *in vitro* neurones derived from clinically, but not genetically, defined schizophrenia patients. It remains pertinent to note that potential synaptic plasticity deficits in human mutant *DISC1* neurones remain unreported.

In conclusion, this study highlights that mutant *DISC1* (1;11)(q42;q14.3) hECNs do not exhibit changes in intrinsic excitability, expression/composition of neurotransmitter receptors and maturation of intracellular [Cl^-] compared to healthy controls. Emerging evidence suggests that more definitive neuronal dysfunction associated with mutant DISC1 manifests at the synaptic level. A secondary, but nonetheless important, outcome of this study is the appropriateness of stem cell-derived neurones to model specific aspects of mutant *DISC1* pathophysiology and also other adult-onset neurological diseases. These data and other groups show that human pluritpotent stem cell technology requires to be further developed beyond 'standard' cultures in order to generate more relevant, native-like material.

Chapter 5

Characterisation of motor neurones harbouring the *C9ORF72* hexanucleotide repeat expansion.

5.1 Motivations for study

Experiments in this chapter were conducted in order to explore the potential utility of lower motor neurones (LMNs) derived from iPSCs (iPSC-MNs) carrying the *C9ORF72* hexanucleotide repeat expansion mutation in modelling pathophysiology associated with amyotrophic lateral sclerosis (ALS). The *C9ORF72* gene is located on the short arm of chromosome 9 (open reading frame 72; see Mori *et al*. 2013). Normally, approximately 30 repeat expansions of GGGGCC (G_4C_2) are found, however, in the case of the hexanucleotide repeat expansion mutation, this number can be on the order of hundreds (Donnelly *et al*. 2013; DeJesus-Hernandez *et al*. 2011; see Figure. 5.1). As of 2012, the hexanucleotide repeat expansion mutation is the most common mutation in familial ALS (approx. 40% of cases; Zu *et al*. 2011), and is also associated with sporadic cases (approx. 8-10%; DeJesus-Hernandez *et al*. 2011), and interestingly, is linked to frontotemporal dementia (FTD), accounting for 10% of sporadic FTD cases (Khan *et al*. 2012; Majounie *et al*. 2012). It has been shown that significant overlap exists between these conditions, with as many as 50% of ALS patients displaying cognitive impairment, while approximately 50% of patients with FTD also suffer MN impairment (See Ferrari *et al*. 2011). Thus there is an imminent need to understand the role that the G_4C_2 repeat expansion plays in neurodegeneration in the hope that it may reveal mechanisms of disease progression.

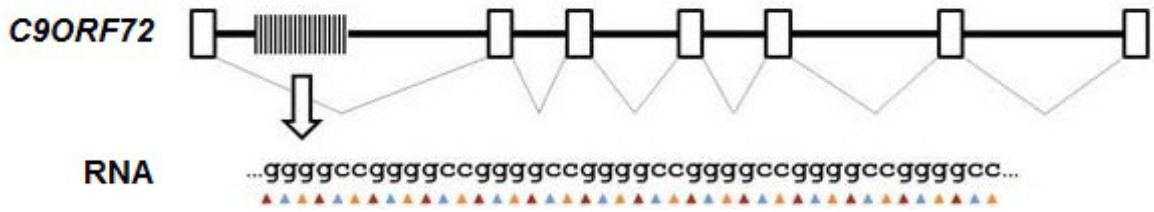

Figure. 5.1. Schematic of C9ORF72 including G4C2 repeat expansion. *Above*: *C9ORF72* gene schematic indicating region subject to repeat expansion of "ggggcc". *Below*: Resultant RNA containing G_4C_2 repeats. Adapted from Mori *et al.* (2013).

Crucially, there is strong evidence to show that disease progression in ALS is likely mediated, in part, by glutamate-mediated excitotoxicity (Rothstein & Cleveland, 2001.). Previous work has highlighted an intrinsic vulnerability of ALS MNs to glutamate excitotoxicity that is mediated by Ca^{2+}-permeable AMPARs (Donnelly *et al*. 2013; Rothstein *et al*. 1995). However, the literature has yet to directly link specific AMPAR structural properties that generate Ca^{2+}-permeability in ALS MNs to genetic abnormalities (Duncan, 2009).

To address this, MNs from patients harbouring the *C9ORF72* G_4C_2 repeat expansion, and unaffected controls were generated using a previously described protocol (Maury *et al*. 2015; Selvaraj *et al.* manuscript in review; see Methods). For all lines examined, cultures contained >95% cells that stained for neuronal marker, Tau^+, at week 3 (see Figure 5.2). These cells lines generated between 40-60% of neurones that stained for Islet1/2, a marker for MNs, at 1 week, with cultures also being heavily enriched for neuronal marker Tau, and displaying RNA foci, a key feature of ALS pathology *in vivo* that are enriched for G_4C_2 repeats (Figure 5.2). Figure contents taken with permission from authors.

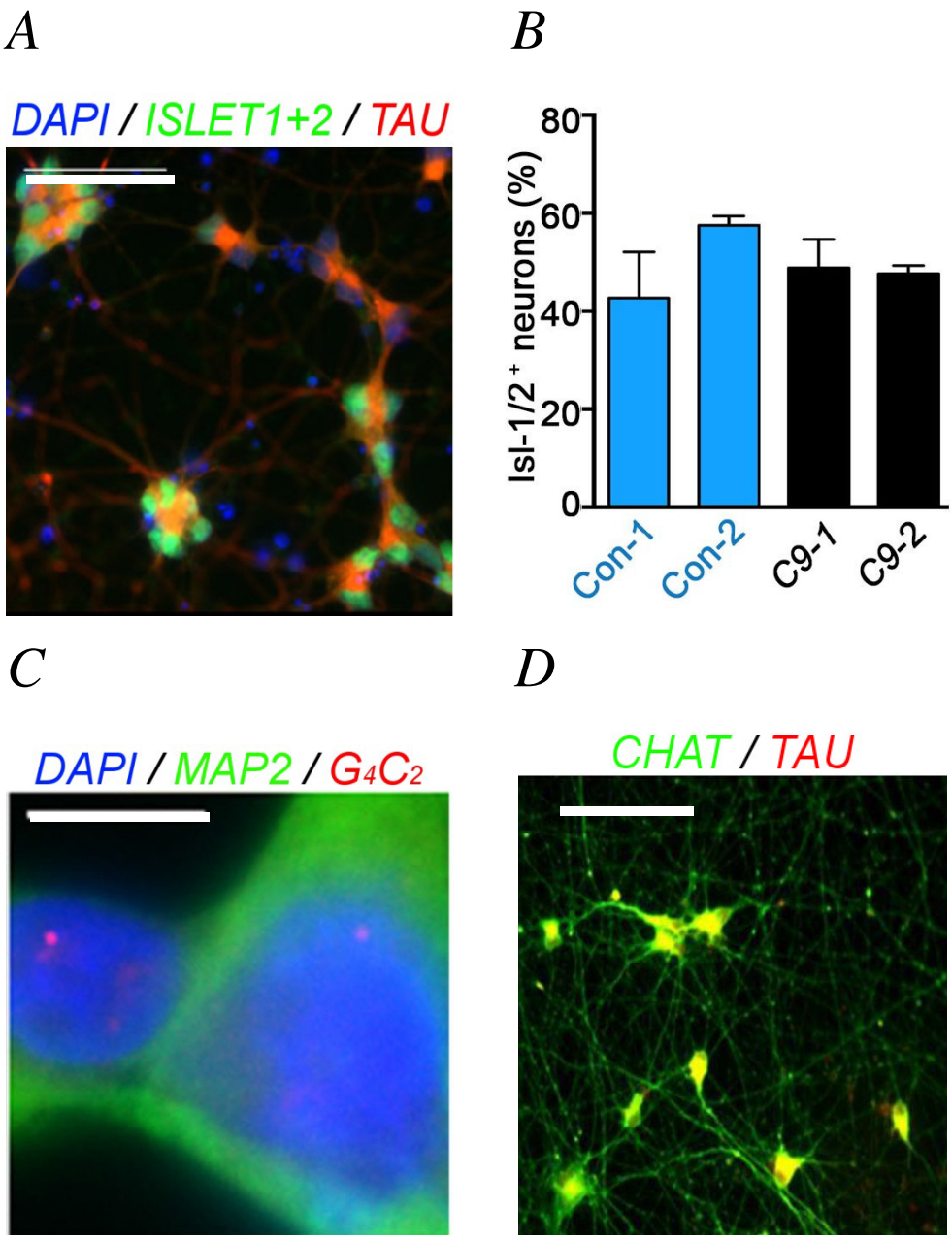

Figure. 5.2 Initial characterisation of MNs, and confirmation of RNA foci. Adapted with permission from Selveraj *et al*. (manuscript in review). All ***A:*** MN culture co-stained for DAPI, MN marker Islet 1/2, and neuronal marker Tau. Scale bar, 50 µm. ***B:*** Graph showing percentage of neurones in culture at week 3 which express Islet 1/2. ***C:*** Co-stain showing DAPI, Neuronal marker MAP2, and RNA foci containing G_4C_2 repeats. Scale bar, 5 µm. ***D:*** Co-stain of MN culture for MN marker CHAT, and neuronal marker Tau. Scale bar, 50 µm.

In this chapter, iPSC-MNs derived from a patient without the *C9ORF72* (G_4C_2) mutations will be referred to as "Control". Cell lines derived from two different patients, both harbouring the *C9ORF72* (G_4C_2) are referred to as C9-1, and C9-2, respectively (see Methods). iPSC-MNs derived from C9-2 with the *C9ORF72* (G_4C_2) hexanucleotide repeats excised using Cas9/CRISPR (see Ran *et al*. 2013) are referred to as ΔC9-2. This powerful approach allows the examination of 2 sets of material with an identical genetic background with the exception of the mutation that has been excised/corrected. In this regard, relative changes in the 'corrected line' to the paired patient line are therefore more likely to be as a result of the mutation rather than genetic variation that is associated with independently derived lines. In this case, this tool allows potential corrected phenotypes to be directly associated with the *C9ORF72* mutation.

5.2 Passive properties of iPSC-MNs.

Initial electrophysiological characterisation of iPSC-MNs was conducted at 1, 3, and 5 week time points (Figure.5.2) in order to observe potential alterations in development in C9-1, and C9-2 with respect to Control, and ΔC9-2. Typical patterns of maturation investigated in terms of the intrinsic properties of iPSC-MNs between week 1 and week 5 indicated that there was no notable difference between any iPSC-MN line at any specific time point.

From week 1 to week 5, mean input resistance measurements broadly decreased (Figure. 5.3A; all p=<0.05, Student's *t*-test). The mean resting membrane potential (RMP) in each line became more hyperpolarised with time (Figure. 5.3B; all p=<0.05, Student's *t*-test;). Additionally, whole-cell capacitance significantly increased (Student's *t*-test; all p=<0.05) in all lines to similar levels (Figure. 5.3C). These data are consistent with a maturing MN profile; importantly, the mean values of passive properties obtained at all time points are not what are expected of adult MNs (Oswald *et al*. 2013); input resistance measurements are somewhat higher, whole-cell capacitance values are slightly lower, and RMP values are more hyperpolarised.

While the maturation of some properties did not reach statistical significance between week 1 and week 5, general trends toward the same endpoint are as described, in that by week 5, all iPSC-MNs surveyed showed no statistical difference between one another.

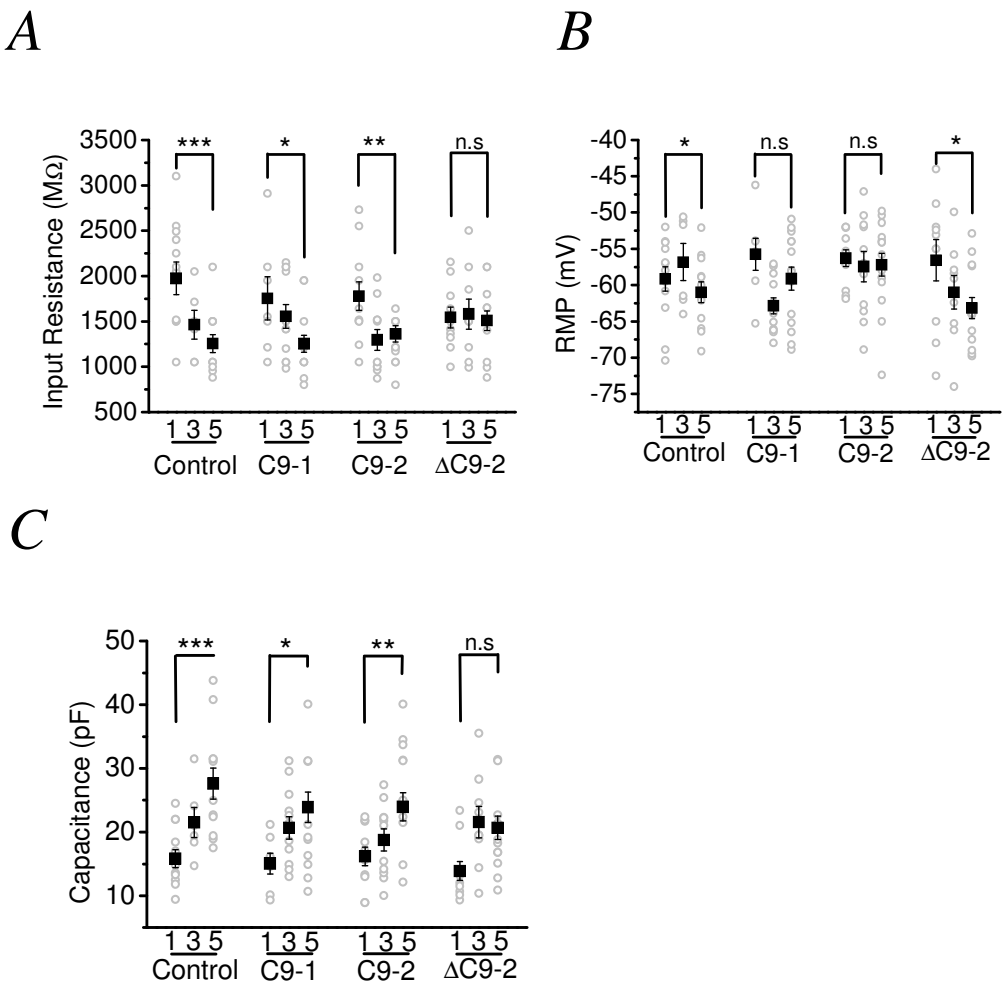

Figure. 5.3. Passive membrane properties of iPSC-MNs. For all panels, control iPSC-MN n = 6 - 14, N = 1-3, and *C9ORF72* (G_4C_2), n = 7 - 15, N = 1 - 3. X-axis labels denote weeks in culture. ***A:*** Mean input resistances of control, and *C9ORF72* (G_4C_2) iPSC-MNs. Input resistance was established from the mean passive membrane current amplitude generated from thirteen sequential -50 mV pulses. ***B:*** Mean resting membrane potential (RMP) of control, and *C9ORF72* (G_4C_2) iPSC-MNs. ***C:*** Mean whole-cell capacitance of control, and *C9ORF72* (G_4C_2) iPSC-MNs. * indicates p=<0.05; ** indicates p=<0.01; *** indicates p=<0.001.

5.3 Characterisation of the AMPAR on iPSC-MNs

Previous reports strongly implicate the AMPAR in ALS via a mechanism of "slow" excitotoxicity as mediated by Ca^{2+}-permeable AMPARs (Donnelly *et al*. 2013; Rothstein *et al*. 1995). Crucial to this hypothesis is the finding that MNs are inherently more susceptible to glutamate-mediated excitotoxicity. This is mediated by three key processes; a) a reduced ability to clear excess glutamate at the synapse, leading to increased AMPAR activation; b) Increased expression of Ca^{2+}-permeable AMPARs leading to increased/toxic Ca^{2+} entry into the cell; c) a reduced ability to buffer cytoplasmic Ca^{2+} levels.

Previous chapters have explored the utility of examining the AMPAR estimated mean single-channel conductance (γ) as a potential indicator of some broad developmental neuropathology in DISC1 iPSC-hECNs. Here, the AMPAR Ca^{2+} -permeability is of particular relevance with regard to the above concerning aberrant Ca^{2+} entry into the cell in ALS. Thus, it seems plausible that iPSC-MNs harbouring the *C9ORF72* (G_4C_2) repeat expansion mutation may show altered apparent Ca^{2+} -permeability at the AMPAR, using previously detailed methods of non-stationary noise analysis (See Methods; Chapter 3) and subunit selective pharmacology (See AMPAR characterisation in Chapter 3). To re-iterate, the AMPAR has a tetrameric structure, potentially composed of 4 subunits (GluA1-4), with developmentally regulated subunit composition. In early development, AMPARs are typically assembled without the RNA edited (Q → R) GluA2 subunit, and are typically Ca^{2+} -permeable. Inclusion of the edited form of GluA2 renders the AMPAR impermeable to Ca^{2+} (see Swanson *et al*. 1997), which is an isoform of the AMPAR associated with mature MNs, typically representing a postnatal phenotype (Talos *et al*. 2006a, 2006b; Orlandi *et al*. 2011, see Traynelis *et al*. 2012).

The estimated mean single-channel conductance (γ) at the AMPAR increases markedly with the property of Ca^{2+} -permeability (Swanson *et al.* 1997; see Traynelis *et al*. 2012). Thus pervasive expression of Ca^{2+} -permeable AMPARs by altered subunit composition or inefficient RNA editing is prospectively detectable in iPSC-MNs, and as a result may shed light on the viability of iPSC-MNs to model *C9ORF72* function, as well as ALS and related conditions (e.g FTD).

5.3.1 Establishing responses to AMPA in iPSC-MNs.

Initial experiments in characterising AMPARs expressed by iPSC-MNs confirmed reliable AMPAR expression, with all MNs studied responding to AMPA (Figure. 5.4A; n=20, N=4) Of note is the use of cyclothiazide (10 μM), an AMPAR-selective positive modulator that prevents AMPAR desensitization (Cowen *et al.* 1998), which reliably potentiated AMPAR-mediated currents by 531% - 808%, (n=20, N=4; Fig 4.2). Additionally this response was blocked by CNQX (20 μM, n=20, N=4).

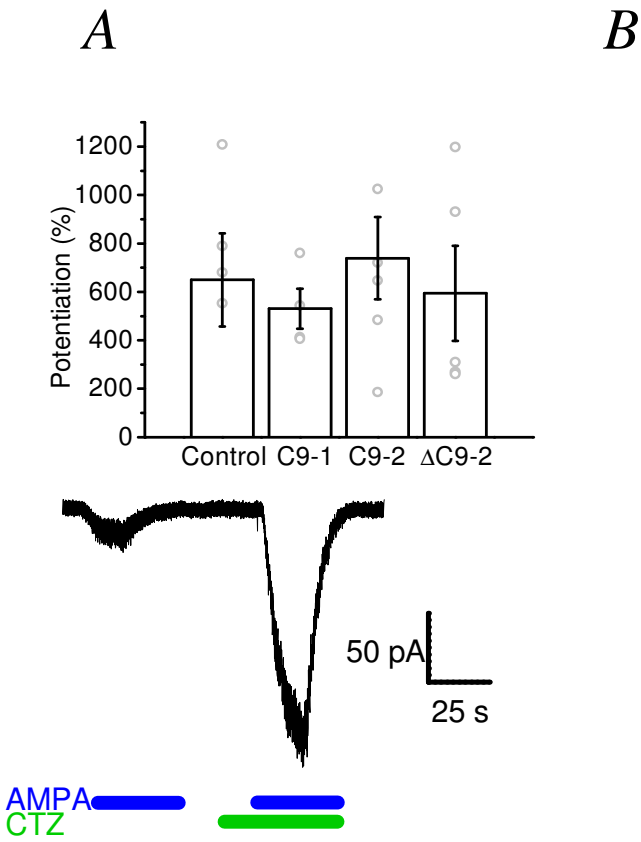

Figure. 5.4. Potentiation of AMPAR current by cyclothiazide. ***A:*** Mean potentiation of AMPA-mediated current by cyclothiazide (n=4-6, N=1). ***B:*** Example trace of recording from MN (Control) at -70 mV (-84 mV) showing application AMPA (blue bar), cyclothiazide (green bar), and CNQX (orange bar).

5.3.2 Characterising *C9ORF72* (G_4C_2) effects on AMPAR estimated mean single-channel conductance (γ).

As previously described (Materials and methods; see Chapter 4), non-stationary noise analysis was used to estimate the mean AMPAR single-channel conductance (γ) in iPSC-MNs from week 1 to week 5. As before, two simultaneous whole-cell voltage-clamp recordings were made in each experiment, where the described AMPAR-evoked responses were made in AC and DC current formats (see Figure. 5.4B). For these experiments the extracellular recording solution was supplemented with cyclothiazide (10 μM). The resultant plot of AC-current variance against DC-current amplitude yielded a straight-line plot (example in 5.4C) from which the estimated AMPAR single-channel current amplitude was determined and single-channel conductance calculated (Shown in Figure. 5.5D).

At 5 weeks, Control and isogenic control line ΔC9-2 showed markedly similar, low mean estimated channel single-channel AMPAR conductance (2.4 pS ± 0.5 pS; n = 6, N = 1, and 2.3 pS ± 0.2 pS; n = 12, N = 3; p=0.71 vs Control, Student's *t*-test, respectively), whereas in sharp contrast, both *C9ORF72* (G_4C_2) - harbouring lines, C9-1 and C9-2 showed pervasively elevated conductances (Figure 5.5D; 4.5 pS ± 0.5 pS; n=12, N=3; p=0.012 vs Control, Student's *t*-test, and 5.1 pS ± 0.7 pS; n = 12, N = 3; p=0.010 vs Control, Student's *t*-test, respectively), thus demonstrating that the *C9ORF72* (G_4C_2) mutation disrupts normal AMPAR development, maintaining an AMPAR conductance highly suggestive of Ca^{2+} - permeability, that of an AMPAR isoform relatively lacking the RNA edited (Q → R) GluA2 subunit.

Further to this, from week 1 – week 5, a significant reduction was observed in estimated mean AMPAR single channel conductance in both the Control line (5.4D; n = 6 - 11, N = 1 - 2; p=0.0074, Student's *t*-test) and the Cas9/CRISPR edited line ΔC9-2 (Figure. 5.4D; n = 8 - 17, N = 1 - 2; p=0.00039 Student's *t*-test), as would be expected of a typical AMPAR maturation profile (see Swanson *et al.* 1997; Traynelis *et al.* 2012). This maturation, the progressive lowering of AMPAR-γ between week 1 and week 5 did not occur in lines harbouring the *C9ORF72* (G_4C_2) repeat expansion mutation, namely C9-2 (Figure. 5.5A; n = 9 - 18, N = 2 - 4; p=0.0074, Student's *t*-test) and C9-1 (Figure. 5.5A; n = 7 - 12, N = 1 - 3; p=0.0074,

Student's *t*-test). These results again clearly demonstrate that the *C9ORF72* (G_4C_2) mutation perturbs AMPAR maturation in iPSC-MNs.

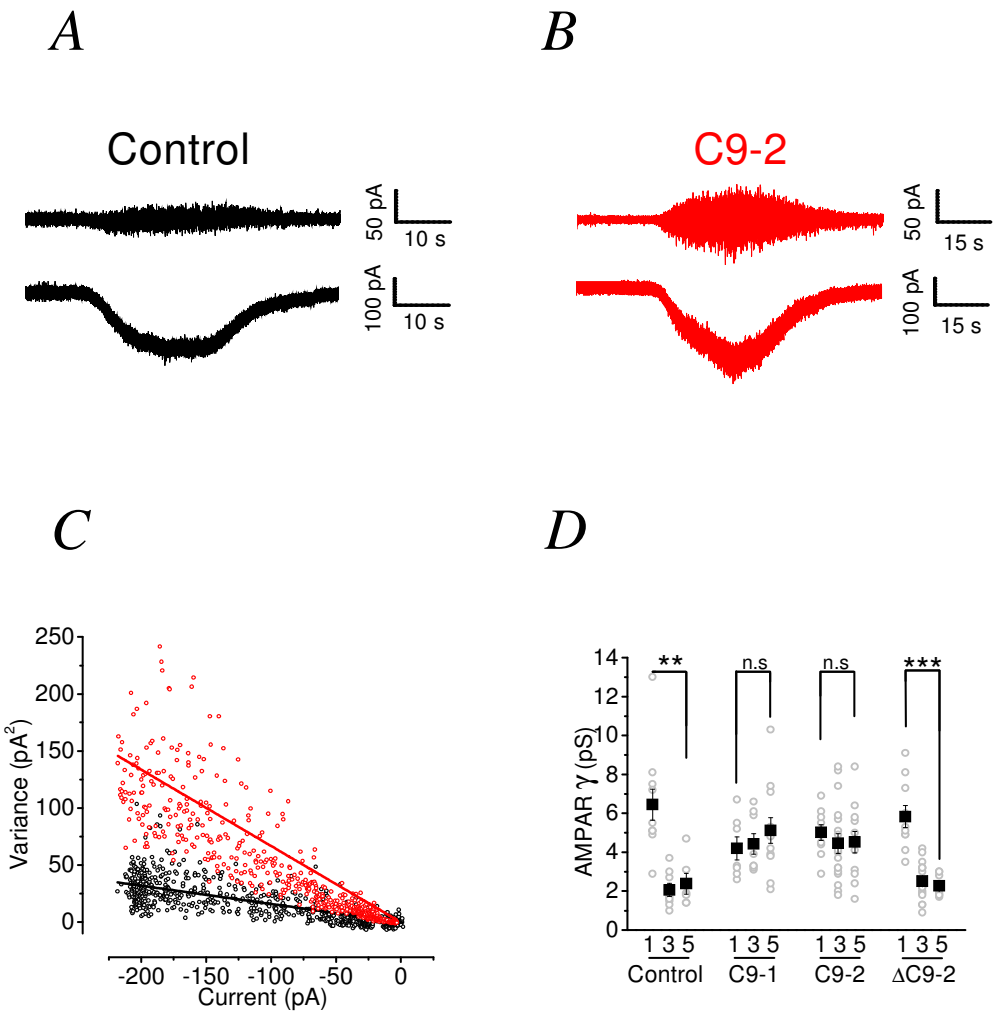

Figure. 5.5, Non-stationary noise analysis using whole-cell voltage-clamp, of AMPAR-mediated currents in C9ORF72 (G_4C_2), and control iPSC-MNs at week 5. ***A:*** Traces from a week 5, Control iPSC- MN showing a slowly-rising and decaying whole-cell response to AMPA (10 μM) at a membrane holding potential of -60 mV (-74 mV); the *upper* trace shows the AC current recording and the *lower* shows the DC current recording. *B*: As in '*A*' but for week 5, C9-2 iPSC-MN. ***C:*** Example current-variance plot from week 5, Control iPSC-MN (black) and C9-2 iPSC-MN (red). The relationship yields a linear relationship to which a straight line was fitted. The slope of the plot gave the estimated AMPAR single-channel current. ***D:*** Mean estimated AMPAR single-channel conductance of AMPARs expressed on iPSC-MNs (n = 9-18, N = 2-4).

5.3.3 Characterising the effect of the *C9ORF72* (G_4C_2) mutation on AMPAR blockade by NASPM.

Next, in order to confirm the observed persistent expression of Ca^{2+} -permeable AMPARs, experiments were conducted to assess the sensitivity of AMPAR-mediated currents to the channel blocker 1-naphthyl acetyl spermine (NASPM, 3 μM; Koike *et al*. 1997), which is selective for AMPARs that lack the Ca^{2+} -impermeable, RNA-edited GluA2 subunit (for traces, see Fig 5.6A, B).

At 5 weeks, Control, and isogenic control line ΔC9-2 showed low NASPM block (Fig 5.6C; 16.6% ± 2.2%; n=7, N=2, and 23.2% ± 2.1%; n=8, N=3, respectively; p=0.54 vs Control, Student's *t*-test), indicating predominant expression of the RNA edited (Q → R) GluA2 subunit, whereas in sharp contrast, both *C9ORF72* (G_4C_2) -harbouring lines, C9-2 and C9-1 showed consistently higher levels of NASPM blockade (Fig 5.5C; 38.6% ± 6.9%; n=9, N=3; p=0.0009 vs Control, Student's *t*-test, and 44.3% ± 4.1%; n=9, N=2; p=0.0004 vs Control, Student's *t*-test, respectively), thus demonstrating that the *C9ORF72* (G_4C_2) mutation disrupts normal AMPAR development, maintaining an AMPAR conductance highly suggestive of Ca^{2+} -permeability, an AMPAR isoform relatively lacking the RNA edited (Q → R) GluA2 subunit.

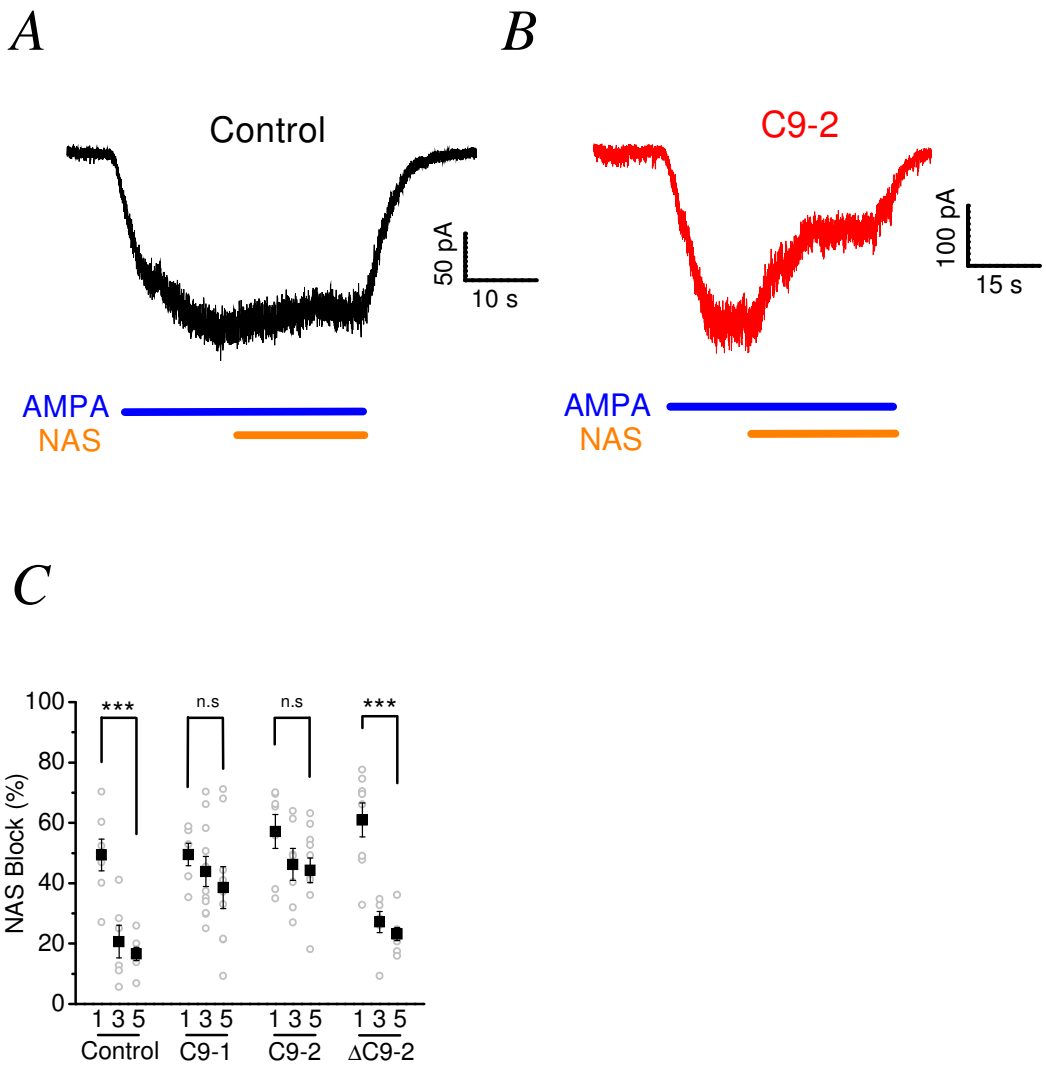

Figure. 5.6. Whole-cell voltage clamp NASPM blockade of AMPAR-mediated currents in iPSC-MNs. ***A:*** Traces from a week 5, Control iPSC-MN showing application of AMPA and NASPM (NAS) at a membrane holding potential of -60 mV (-74 mV). ***B:*** As in '*A*' but for C9-2 iPSC-MN. ***C:*** Graph showing NASPM block across all iPSC-MN lines from week 1 to week 5 (n = 9 -18, N = 2 - 4).

Further to this, from week 1 – week 5, a notable decrease was observed in mean NASPM block in both the Control line (Figure. 5.5C; n=6-7, N=1-2; p=0.0009, Student's *t*-test) and the Cas9/CRISPR edited line C9-2 (Figure. 5.5C; n=8-17, N=1-2; p=0.0004 Student's *t*-test), as would be expected of a typical AMPAR maturation profile (see Swanson *et al.* 1997; Traynelis *et al*. 2012). This progressive increase in AMPAR blockade by NASPM between week 1 and week 5 did not occur in lines harbouring the *C9ORF72* (G_4C_2) repeat expansion mutation, namely C9-2 (Figure. 5.5C; n=9-18, N=2-4; p=0.0074, Student's *t*-test) and C9-1 (Figure. 5.5C; n = 7 - 12, N = 1 - 3; p=0.0074, Student's *t*-test). These results again clearly demonstrate that the *C9ORF72* (G_4C_2) mutation perturbs AMPAR maturation in iPSC-MNs, causing a relatively increased expression Ca^{2+} -permeable, non- RNA edited (Q → R) GluA2 subunit -containing AMPARs.

5.4 Discussion

Here, the whole-cell patch-clamp technique was used in order to investigate the appealing prospect that iPSC-MNs may replicate previous findings in ALS research from other systems concerning increases in intracellular Ca^{2+}, and subsequent excitotoxicity mediated by aberrant, predominant expression of Ca^{2+}-permeable AMPARs (Donnelly *et al*. 2013; Rothstein *et al*. 1995; see Cleveland and Rothstein. 2001). Initial experiments surveying the development of passive membrane properties revealed no statistically significant effect of either the *C9ORF72* (G_4C_2) mutation or the use of CRISPR/Cas9 to excise the G_4C_2 repeats, demonstrating the validity of comparing a highly developmentally regulated system such as AMPAR Ca^{2+} -permeability between different lines and isogenic controls.
While occasional trends could arguably be observed in selected passive properties, no wide-ranging differences were seen, with all lines following highly similar developmental trajectories toward lower input resistances, increased capacitances, and more negative resting membrane potentials. Of particular note, the novelty and utility of a native human *in vitro* system for modelling ALS-related AMPAR pathology is manifold as detailed thusly:

5.4.1 Aberrant Ca2+ -permeable AMPAR expression

Here, findings using non-stationary noise analysis, and subunit-selective pharmacology show that multiple iPSC-MN lines harbouring the *C9ORF72* (G_4C_2) mutation do indeed show aberrant and persistent expression of Ca^{2+} -permeable AMPARs, a compelling finding that supports a large body of previous work (Donnelly *et al*. 2013; Rothstein *et al*. 1995), and invites further study of the iPSC-MNs capacity to model "slow" excitotoxicity in ALS as mediated by AMPARs (see Selvaraj *et al*. 2016, manuscript in review). Notably, the observed AMPAR conductance measurements for *C9ORF72* (G_4C_2) were in line with previously reported values in recombinant and animal systems which predominantly express Ca^{2+}-permeable AMPARs, typically in early development (Talos *et al.* 2006a, 2006b; Orlandi *et al.* 2011, see Traynelis *et al*. 2012). This is evidenced by the mean single-channel conductance (γ) established using non-stationary noise analysis. Early in development, Ca^{2+} -permeable AMPARs predominate, and are composed of receptor isoforms which do not contain an RNA-edited (Q → R) GluA2 subunit. Those AMPARs which do contain an RNA (Q → R) GluA2 subunit are typically expressed post-natally and are relatively Ca^{2+}-impermeable, while in ALS, this high Ca^{2+}-permeability persists and is, as described elsewhere (Donnelly *et al*. 2013; Rothstein *et al*. 1995), a compelling candidate for further examination as to the neuronal mechanisms affected in ALS in systems such as stem cell technologies, in that here it would appear that these systems are capable of modelling this phenomenon to refine targets for therapeutic intervention.

While it initially might seem plausible (if somewhat unlikely, given the stable nature of AMPAR responses) that other subunits might "fill in" an altogether-absent GluA2 in *C9ORF72* (G_4C_2), leading to another mechanism of sustained Ca^{2+}-permeability, the data does show that some AMPAR mean single channel conductance measurements are in the range expected of an edited GluA2 subunit. This interpretation, even at its most cautious, suggests at the least a problem with concerning a long-term reduction in expression of (Q → R) edited GluA2 subunits and thus increased Ca^{2+}-permeability as a phenotype. RNA sequencing or LICOR

quantitative expression by fluorescence might provide a definitive insight as to what is likely to be expressed at the membrane in light of the results in this thesis.

5.4.2 CRISPR/Cas9 and isogenic controls

Secondly, the amenability of iPSC-MNs to CRISPR/Cas9 gene editing was employed to produce isogenic controls also derived from patient lines and lacking a pathological number of G_4C_2 repeats. This was shown to rescue the observed persistent Ca^{2+} -permeable AMPAR expression found in the presence of *C9ORF72* (G_4C_2), which clearly implicates *C9ORF72* (G_4C_2) in ALS-related AMPAR pathology. Additionally, demonstrating the utility of gene-editing suites to directly remedy a disease phenotype is confluent with the goals of gene therapy; while not presently implemented large-scale, initial rigorous validation of genetically engineered iPSC-derived tissue in the modelling of disease represents robust groundwork in a promising emergent health technology.

5.4.3 What of other iPSC-MNs, and MNs in ALS in general?

A recent report also in iPSC-MNs (Selvaraj *et al*. 2016) demonstrates a direct link between aberrant Ca2+- permeable AMPAR expression in *C9ORF72* (G_4C_2) iPSC-MNs and MN vulnerability to excitotoxicity. Given additional previous reports of MN vulnerability to excitotoxicity via AMPAR pathology, it can be said that iPSC-MNs do represent an amenable system to the study of ALS, particularly in the case of *C9ORF72* (G_4C_2). Of particular note is the use of CRISPR/Cas 9 gene editing tools to generate an isogenic control line, which consistently displayed a control-like phenotype. Notably this resulted in AMPAR measurements being highly similar to control values (Selvaraj *et al*. 2016), again in agreement with the results presented in this chapter of this thesis. Such 'rescue' of the AMPAR phenotype clearly demonstrates the utility of the CRISPR/Cas 9 gene editing system in modelling disease using iPSC-MN cultures, and further compounds the findings comparing *C9ORF72* (G_4C_2) with non-isogenic control lines (i.e those who do not harbour excess G_4C_2 repeats in *C9ORF72* by default).

Chapter 6

Characterisation of OPCs and oligodendrocytes harbouring mutations in TDP-43.

6.1 Motivations for study

OLs and OPCs are highly relevant in the study of human brain development in general, in that they constitute approximately 5% of total cells in the adult human, and also rodent cortex (Ongur *et al*. 1998; Stark *et al*. 2004; for rodents see Irintchev *et al*. 2005; Jakovcevski *et al*. 2009) and are heavily implicated in a great number of crucial developmental processes involving the myelination of virtually all neurones in the CNS, a process in which a single OL enhances action potential conductance along the axons of multiple target neurones and is crucial for neuronal network function in mammals. Typically, a pool of self-regenerating OPCs is maintained in the sub-ventricular zone (SVZ) in both the developing, and adult human brain, however, in later development a population arising from the dorsal spinal cord also begins to myelinate the spinal cord, accounting for some 10-15% of the mature OL content there. It has been shown that across development and maturity, OPCs regenerate via a balance between proliferation, the replication of an OPC, and differentiation into mature OLs. This marks a process which leads from the predominant expression of OPC marker PDGFRα, to that of OL marker O4. Notably, no overlap in marker expression (PDGFRα/O4) within a single cell is typically observed in the maturation of OPCs to OLs, indicating a highly reliable marker for cell identity that can be used *in vitro* to identify a single cell.

A *B*

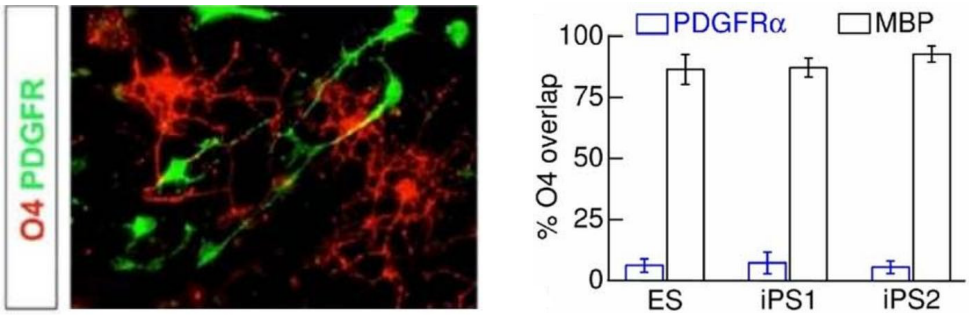

Figure. 6.1. iPSC-OPCs/OLs express key cell identity markers PDGFRα, and O4, respectively, with nominal overlapping expression. Aadapted with permission, from Livesey *et al*. (2015): ***A:*** Co-stain showing separate PDGFRα and O4 expression in OPCs and OLs. ***B:*** Graph showing co expression of OPC identity marker PDGFRα, and OL marker MBP, relative to their co-expression with O4, an OL marker.

The generation of functional, viable Oligodendrocytes (OLs) and Oligodendrocyte precursor cells (OPCs) from iPSCs, represents a stable platform to model normal human development in both health, and diseases implicating ion channel dysfunction, such as in ALS (Livesey *et al*. 2015). Importantly, ALS is characterised by excessive demyelination of axons by OLs, and neurodegeneration, with approximately 5-10% of cases being associated with a known mutation. One prominent mutation that has been studied in iPSC-derived neuronal material is the *TARDP* mutation TDP-43 (G298S). Mutations in the *TARDP* gene account for 2-6% of familial ALS cases, and presents hallmark ALS pathologies *in vitro* and *in vivo* in rodents and iPSC-derived material, of nuclear foci of mutant RNA, and susceptibility to neurodegeneration (Thomsen *et al*. 2014). Additionally, these typical pathologies have been replicated in iPSC-MN cultures, demonstrating their viability for more detailed study of any potential functional changes in ALS.

It has been shown that specific changes in ion channel expression, such as voltage sensitive Na^+-channels, K^+ channels, and ligand-gated ion channels such as the AMPAR are definitive of OPC maturation into OLs, a finding recently replicated in iPSC-OPC/OLs. This thesis has previously observed a tissue-specific maturational defect in MNs harbouring an ALS mutation which does not affect OPC/OLs, however, previous study has shown that OPC/OLs are affected in their own right, and that demyelination and neurodegeneration in ALS may be caused in part by OL-mediated effects. Thus, it may be the case that different ALS mutations cause tissue-specific impairments that converge on the known ALS phenotypes, and that these pathologies may be convergent on some common mechanism such as that suggested by slow excitotoxicity, or a more general maturational deficit.

Crucially, the AMPAR is heavily implicated in iPSC-derived models of ALS (see Chapter 4). To re-iterate, the AMPAR is heavily implicated in ALS via a mechanism of "slow" excitotoxicity brought about by Ca^{2+}-permeable AMPARs (Donnelly *et al*. 2013; Rothstein *et al*. 1995). Crucially, OLs may show similar responses to that of MNs, in that MNs are inherently more susceptible to glutamate-mediated excitotoxicity as mediated by three factors; 1) increased AMPAR activation due to a reduced ability to clear excess glutamate at the synapse; 2) Increased expression of Ca^{2+}-permeable AMPARs leading to increased/toxic levels of intracellular Ca^{2+}; 3) a reduction in ability to buffer cytoplasmic Ca^{2+} levels. This is of great relevance in light of seemingly conflicting findings in ALS, firstly that while iPSC-OLs harbouring the *C9ORF72* (G_4C_2) mutation do not show persistent aberrant AMPAR Ca^{2+} permeability, iPSC-MNs with this mutation do. Thus, it is possible that tissue type-specific changes associated with different mutations may be convergent toward a common pathology as mediated by "slow" excitotoxicity via the AMPAR as described, ultimately leading to demyelination and neuronal death.

In this chapter, OPCs and OLs derived from a patient without TDP-43 mutations will be referred to as "Control". Cells harbouring the TDP-43 M337V mutation will be referred to as "T-1", while those from two different patients harbouring the G298S mutation will be referred to as "T-2", and "T-3", respectively. iPSC-OPCs/OLs derived from Case-3 with the G298S mutation corrected by Cas9/CRISPR) are referred to as ΔT-3.

6.2 Passive properties of iPSC-OPC/OLs.

6.2.1 Input resistance, whole–cell capacitance, and resting membrane potential.

Initial electrophysiological characterisation of iPSC-OPC/OLs was conducted at 1 and 3 week time points (Figure.5.2) in order to observe potential alterations in development in lines harbouring ALS mutations (lines T1, T2, T-3) with respect to Control, and ΔT-3. Typical patterns of maturation investigated in terms of the intrinsic properties of iPSC-OPC/OLs between OPC at week 1, and mature OL at week 3 were observed. At any time point, lines harbouring TDP-43 mutations did not differ significantly from controls (typically p=>0.1), however, line T-2 showed a significantly decreased whole-cell capacitance (18.2 pF ± 1.7 pF, n = 5, N = 2; Control, 29.6 pF ± 3.7 pF, n = 12, N = 3; p=0.01398), as did line T-3 (19.2 pF ± 1.1 pF, n = 8, N = 3; Control, as above. p=0.03887).

Between OPCs at week 1, to OL at week 3, mean input resistance measurements broadly decreased (Figure 6.2A), except line T-1, which showed a trend of decreasing input resistance across time in culture, but failed to reach significance (p=0.12668). The mean resting membrane potential (RMP) typically became more hyperpolarised with time in the majority of lines, however, line T02 and line ΔT-3 showed a trend toward more hyperpolarised RMP which did not reach significance (Figure 6.2B; p=0.18836, and p=0.43945 respectively). Additionally, whole-cell capacitance significantly increased (Student's *t*-test; all p=<0.05) in all lines to similar levels (Figure. 5.2C). These data are generally consistent with the maturation of OPCs into OLs across development, showing trends where significance is not found; importantly, the mean values of passive properties obtained at all time points are not what are expected of adult OLs (Oswald *et al*. 2013); input resistance measurements are somewhat higher, whole-cell capacitance values are slightly lower, and RMP values are more hyperpolarised.

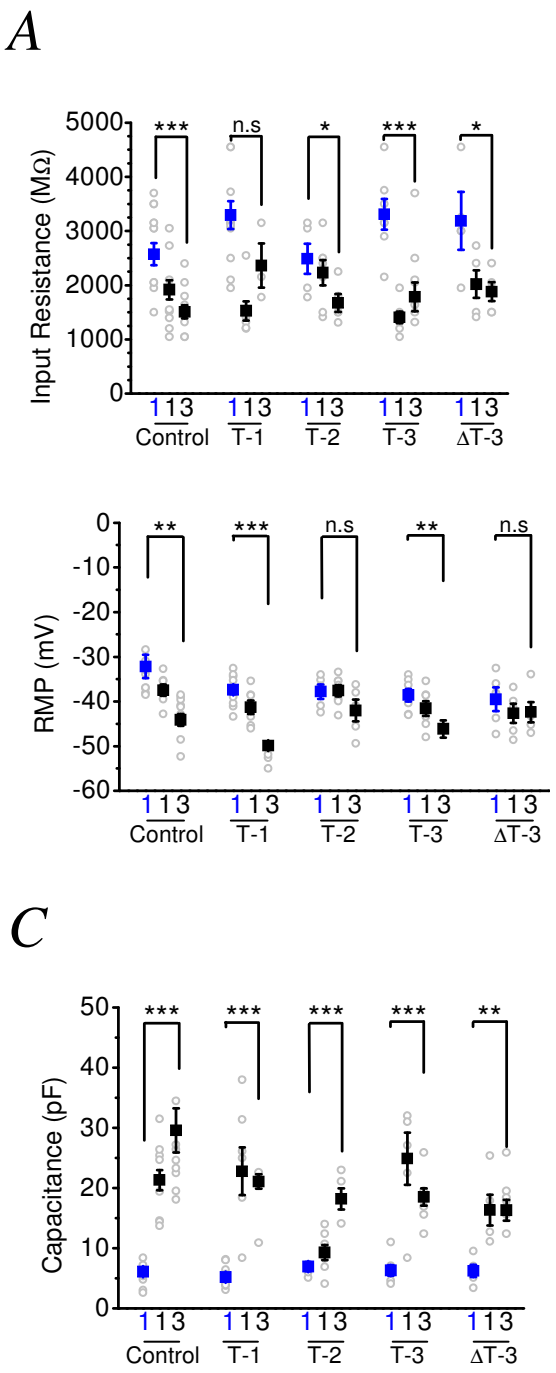

Figure. 6.2 Input resistance, resting membrane potential, and whole-cell capacitance of iPSC-OPCs/OLs. For all panels, n = 6 - 15, N = 1 - 3. Numbers on X axis indicate number of weeks in culture. Blue coloured symbols and text denotes OPCs, whereas black text and symbols indicate OLs at time in culture as labelled. ***A:*** Mean input resistances of iPSC-OPC/OLs. Input resistance was established from the mean passive membrane current amplitude generated from thirteen sequential -50 mV pulses. ***B:*** Mean resting membrane potential (RMP) of iPSC-OPC/OLs. ***C:*** Mean whole-cell capacitance of iPSC-OPC/OLs. * indicates p=<0.05; ** indicates p=<0.01; *** indicates p=<0.001.

6.2.2 Rectifying membrane conductances in iPSC-OPC/OLs

Typically, OPCs display outwardly rectifying membrane currents in response to applied voltages, passing a much greater amount of current at membrane potentials that are positive to the reversal potential of the channel, and relatively little current at potentials more negative. OPC differentiation to OLs results in a linearisation of this relationship, resulting in a lack of rectification and a linear I-V plot. These properties have been widely described in rodent oligodendroglial counterparts, *in vitro* mouse PSC-derived OPCs and integrated mouse PSC-derived glial restricted progenitor cells that contain a proportion of OPCs indicating that comparable changes in ion channel expression occur throughout human oligodendrogenesis *in vitro*.

Figure 5.3 shows a typical pattern as described in previous literature on iPSC-OPC/OLs. Similar to previous findings, membrane conductances in OPCs (see trace, Figure 6.3A) were highly non-linear, displaying strong outward rectification, whereas OLs typically displayed a more linear current response to applied voltage steps. Figure 6.3D shows an I-V plot normalised to the current passed at -64 mV, from an applied 20 mV step at a holding potential of -84 mV (See Chapter 2, Materials and methods), and displays a more linear I-V relationship in OLs than OPCs.

The rectification index, a measure used elsewhere in this thesis (See Materials and Methods, Chapter 2; Chapter 4), describes a ratio of the conductances at a positive holding potential (here, +16 mV) and a negative holding potential (here, -124 mV) as established by a sequential series of voltage steps of 20 mV (see figure

6.3A,B for example traces). Across all lines, OPCs displayed a higher rectification index, which typically significantly dropped upon differentiation and maturation into OLs (P=<0.05; Figure 6.3C), however, this did not reach statistical significance for line T-2. Notably, there were no statistical differences between lines at any point, with line T-2 showing a highly similar trajectory to other lines at week 3.

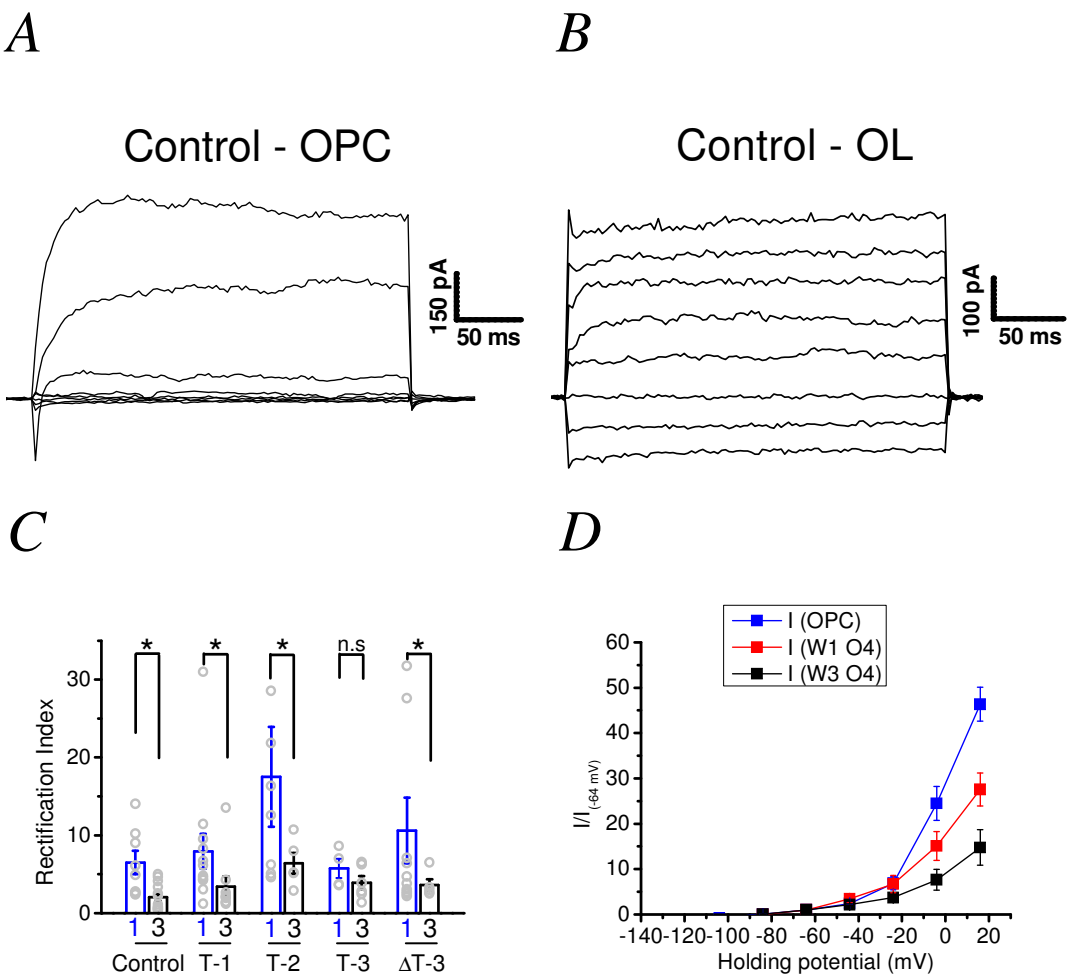

Figure. 6.3 Rectification of membrane conductances in iPSC-OPC/OLs. For all panels, n = 7 - 12, N = 1 - 3. * indicates p=<0.05; ** indicates p=<0.01; *** indicates p=<0.001. ***A:*** Example trace of membrane current responses to incremental 20 mV steps (shown *below*) at a holding potential of -84 mV in a control OPC at week 1 in culture. ***B:*** Example trace of current responses to incremental 20 mV steps (shown *below*) at a holding potential of -84 mV in a control OL at week 3 in culture. ***C:*** Rectification index of membrane current responses in iPSC-OPC/OLs. Numbers on X axis indicate number of weeks in culture. Blue

coloured symbols and text denotes OPCs, whereas black text and symbols indicate OLs at time in culture as labelled. ***D:*** Mean normalised current-voltage plots for OPCs, and OLs at 1, and 3, weeks in culture. Current amplitudes were measured 175 ms after the initiation of the voltage step and normalised to the current passed at -64 mV (See Chapter 2, Materials and Methods).

6.3 AMPAR subunit expression and Ca^{2+} -permeability in iPSC-OPC/OLs

6.3.1 Characterising the effects of TDP-43 mutations on AMPAR estimated mean single-channel conductance (γ).

It has been previously shown that iPSC-OPCs/OLs demonstrate a documented switch in AMPAR subunit expression that occurs upon the differentiation of OPCs into OLs. To re-iterate, the AMPAR has a tetrameric structure, potentially composed of 4 subunits (GluA1-4), with developmentally regulated subunit composition. In early development, AMPARs are typically assembled without the RNA edited (Q → R) GluA2 subunit, and are typically Ca^{2+} -permeable. Inclusion of the edited form of GluA2 renders the AMPAR impermeable to Ca^{2+} (see Swanson *et al*. 1997), which is an isoform of the AMPAR associated with mature OLs .This switch occurs in much the manner described for hECNs, DISC1 iPSC-hECNs, and control iPSC-MNs with regard to time in culture, and is estimated using non-stationary noise analysis to determine the estimated mean single-channel conductance of the AMPAR. As described in previous chapters, the estimated mean single-channel conductance (γ) at the AMPAR increases markedly with the property of Ca^{2+} -permeability (Swanson *et al.* 1997; see Traynelis *et al*. 2012). Thus pervasive expression of Ca^{2+} -permeable AMPARs by altered subunit composition or inefficient RNA editing is prospectively detectable in iPSC-OPCs/OLs, and as a result may shed light on the viability of iPSC-OPC/OLs to model disease progression mediated by the TDP-43 mutation in ALS in a tissue-specific manner, much as that seen for the *C9ORF72* (G_4C_2) mutation in iPSC-MNs.

Previous chapters have explored the utility of examining the AMPAR estimated mean single-channel conductance (γ) as an indicator of developmental pathology in DISC1 iPSC-hECNs (Chapter 3), and iPSC-MNs (Chapter 4). Similarly as with MNs harbouring the *C9ORF72* (G_4C_2) repeat expansion mutation, the AMPAR Ca^{2+} -permeability of iPSC-OLs is of particular relevance with regard to the above concerning the possibility of aberrant Ca^{2+} entry into the cell.

Thus, it seems plausible that iPSC-OLs harbouring the TDP-43 mutation may show altered apparent Ca^{2+} -permeability at the AMPAR, using previously detailed methods of non-stationary noise analysis (See Methods; Chapter 3; Chapter 4) and subunit selective pharmacology (See AMPAR characterisation, Chapter 3; Chapter 4).

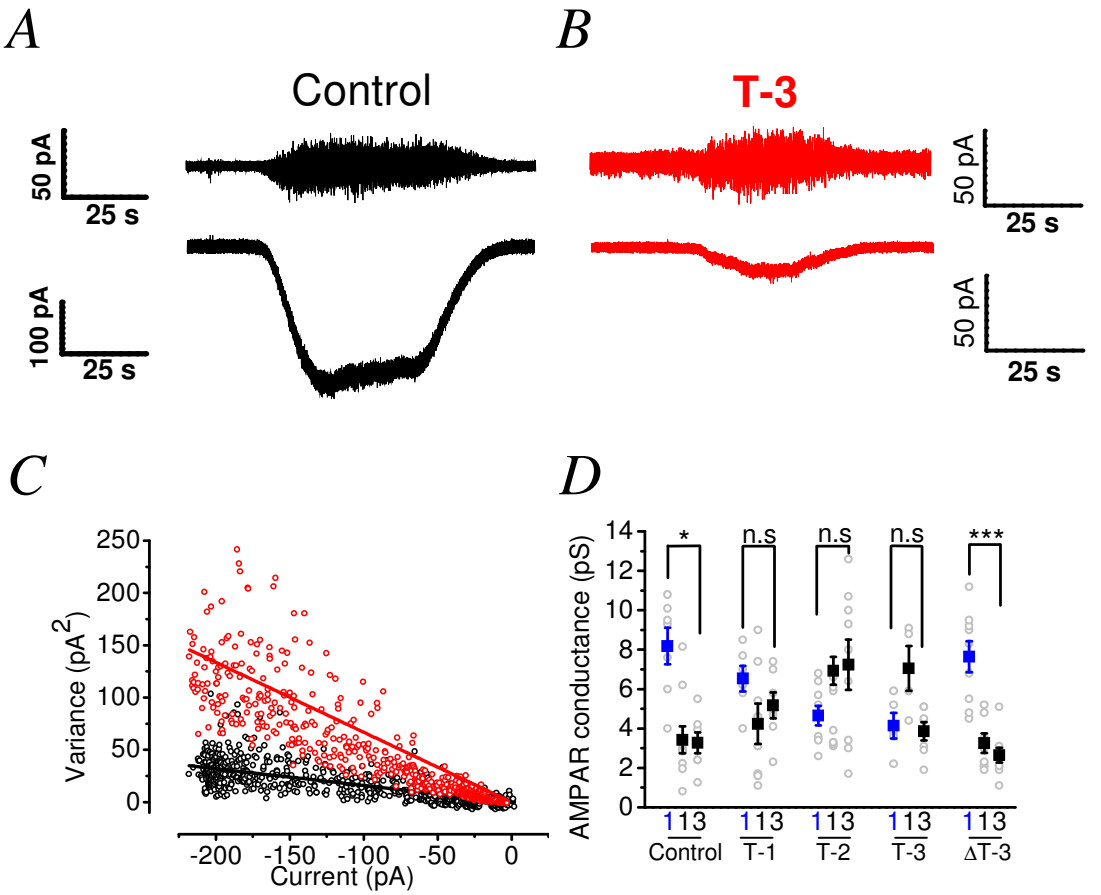

Figure. 6.4. Non-stationary noise analysis of AMPAR-mediated currents in iPSC-OPC/OLs in whole-cell voltage-clamp at -60 mV (-74 mV). ***A:*** Traces from a week 3, Control iPSC-OL showing a slowly-rising and decaying whole-cell response to AMPA (10 μM); the *upper* trace shows the AC current recording and the *lower* shows the DC current recording. ***B:*** As in '*A*' but for week 3, T-3, iPSC-OL. ***C:*** Example current-variance plot from week 3, Control iPSC-OL (black) and T3 iPSC-MN (red). The relationship yields a linear relationship to which a straight line was fitted. The slope of the plot gave the estimated AMPAR single-channel current. ***D:*** Mean estimated AMPAR single-channel conductance of AMPARs expressed on iPSC-OPC/OLs; n= 5 - 10, N = 1-3. Numbers on X axis indicate number of weeks in culture. Blue coloured symbols and text denotes OPCs, whereas black text and symbols indicate OLs at time in culture as labelled.

6.3.3 Characterising the effect of TDP-43 mutation on AMPAR blockade by NASPM.

Next, in order to confirm the observed persistent expression of Ca^{2+} -permeable AMPARs, experiments were conducted to assess the sensitivity of AMPAR-mediated currents to the channel blocker 1-naphthyl acetyl spermine (NASPM, 3 μM; Koike *et al*. 1997), which is selective for AMPARs that lack the Ca^{2+} -impermeable, RNA-edited GluA2 subunit (for traces, see Fig 5.5A, B).

At 5 weeks, Control, and isogenic control line ΔC9-2 showed low NASPM block (Fig 5.5C; 16.6% ± 2.2%; n=7, N=2, and 23.2% ± 2.1%; n=8, N=3, respectively; p=0.54 vs Control, Student's *t*-test), indicating predominant expression of the RNA edited (Q → R) GluA2 subunit, whereas in sharp contrast, both *C9ORF72* (G_4C_2) -harbouring lines, C9-2 and C9-1 showed consistently higher levels of NASPM blockade (Fig 5.5C; 38.6% ± 6.9%; n=9, N=3; p=0.0009 vs Control, Student's *t*-test, and 44.3% ± 4.1%; n=9, N=2; p=0.0004 vs Control, Student's *t*-test, respectively), thus demonstrating that the *C9ORF72* (G_4C_2) mutation disrupts normal AMPAR development, maintaining an AMPAR conductance highly suggestive of Ca^{2+} -permeability, an AMPAR isoform relatively lacking the RNA edited (Q → R) GluA2 subunit.

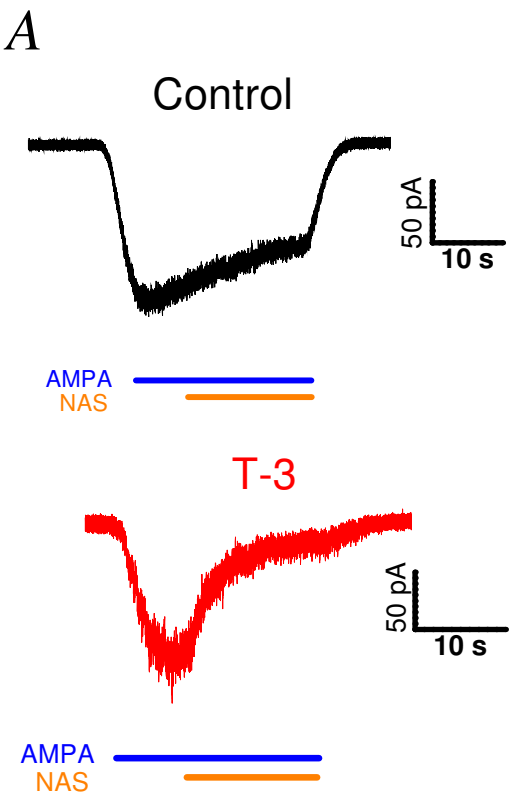

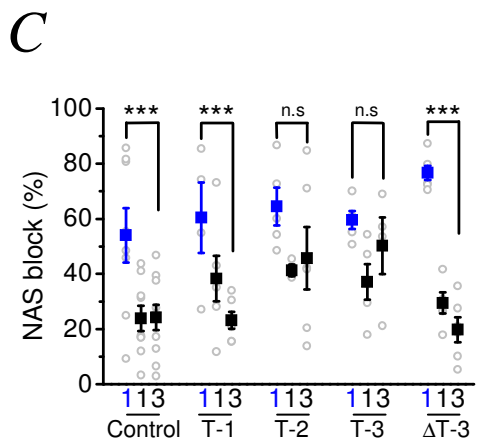

Figure. 6.5. NASPM blockade of AMPAR-mediated currents in iPSC-OPC/OLs. ***A:*** Traces from a week 3, Control iPSC-OL showing application of AMPA (blue bar) and NASPM (NAS; orange bar). ***B:*** As in '*A*' but for T-3 iPSC-OL. ***C:*** Graph showing NASPM block across all iPSC-OPC/OLs. N = 5 - 10, N = 1 - 3. Numbers on X axis indicate number of weeks in culture. Blue coloured symbols and text denotes OPCs, whereas black text and symbols indicate OLs at time in culture as labelled.

6.4 Discussion

Here, the whole-cell patch-clamp technique was applied in order to examine ion channel expression as a measure of developmental maturity in iPSC-OPC/OLs, and to identify possible phenotypes imparted by TDP-43 mutations M337V, and G298S on known ion-channel expression across development in ALS. Control iPSC-OPC/OLs used in this thesis have been studied elsewhere with highly similar results. iPSC-OPCs typically showed strong outward membrane conductances which linearised upon iPSC-OPC differentiation to OLs. Other passive properties such as whole-cell capacitance, RMP, and input resistance were also highly similar to previous work on iPSC-OPC/OLs (Livesey *et al*. 2015). This suggests that iPSC-OPC/OLs are a fundamentally viable model for the study of human development *in vitro*, and additionally demonstrates a reliable benchmark for results obtained from iPSC-OPC/OLs harbouring mutations associated with disease states which implicate OPCs and OLs.

6.4.1 General development in iPSC-OPC/OLs harbouring TDP-43 mutations

Initial experiments examining the development of passive membrane properties showed that OLs harbouring ALS mutations were smaller, perhaps indicating a general maturational defect. This has been previously observed in rodent models of ALS such as SOD1 (G93A), where reduced size and altered morphology of OLs is observed (Zawadzka *et al*. 2010), which here may be reflected in a reduced whole-cell capacitance. Additionally, previous reports in *SOD1* mutant mice indicate an increased level of OPC proliferation, and differentiation into OLs which precludes apparent disease onset, which again may be reflected in decreased cell size

and whole-cell capacitance. Mutations in ALS were not associated with changes to other passive properties and thus show normal ion channel development in this regard.

6.4.2 Ca2+ -permeable AMPAR expression in iPSC-OPC/OLs harbouring ALS mutations

Here, findings using subunit-selective pharmacology and non-stationary noise analysis show that multiple iPSC-OPC/OL lines harbouring TDP-43 mutations (G298S; M337V) do indeed exhibit persistent expression of Ca^{2+} -permeable AMPARs, a finding that is associated with ALS pathology and well supported by a large body of previous work (Donnelly *et al*. 2013; Rothstein *et al*. 1995; see Cleveland and Rothstein. 2001), inviting further study of iPSC-OPC/OLs capacity to model this described "slow" excitotoxicity in ALS as mediated by AMPARs (see Selvaraj *et al*. 2016, manuscript in review). Notably, and again, the observed AMPAR conductance measurements for iPSC-OPC/OLs with ALS mutations (G298S; M337V) were in line with previously reported values in recombinant and animal systems which predominantly express Ca^{2+}-permeable AMPARs, typical of early development (Talos *et al.* 2006a, 2006b; Orlandi *et al.* 2011, see Traynelis *et al*. 2012). Interestingly, previous findings from iPSC OPC/OLs harbouring an ALS-related mutation in *C9ORF72* show no effect on AMPAR Ca^{2+} -permeability (Livesey *et al*. 2015), while MNs harbouring this mutation do indeed show persistent expression of Ca^{2+} -permeable AMPARs, as shown in the previous chapter of this thesis (Chapter 5) which is corrected by CRISPR/Cas9. This chapter has demonstrated that certain ALS mutations do, in fact, show increased expression of Ca^{2+} -permeable AMPARs, a phenotype which is absent in isogenic controls, suggesting that different ALS mutations may impart tissue-specific pathologies which are convergent on the AMPAR. Thus, iPSC-OPCs and OLs are viable when studying the pathology of highly developmentally regulated systems such as AMPAR Ca^{2+} -permeability in ALS.

6.4.3 CRISPR/Cas9 and isogenic controls

The ability of iPSC-OLs to undergo CRISPR/Cas9 gene editing was employed to produce isogenic controls (ΔT-3) also derived from a patient line (T-3), with the point mutation G298S corrected. This was shown to rescue the observed persistent Ca^{2+} -permeable AMPAR expression found in the presence of TDP-43 (G298S), showing clear effects of TDP-43 mutations on Ca2+ -permeable AMPAR expression. As mentioned elsewhere, the utility of gene-editing platforms to alter gene sequences to rescue a disease phenotype is confluent with the goals of gene therapy; while not presently developed at a large-scale, validation of genetically engineered iPSC-derived tissue in the modelling of disease represents the solid foundations of a promising emergent health technology.

6.4.4 What of iPSC-OPC/OLs in general?

Despite controversy surrounding the developmental origin, and possible functional specification, of OPC/OLs, the derivation of functional OPCs and OLs sufficient to re-myelinate CNS structures has been achieved in culture (Livesey *et al* 2015, and implantation studies. Such validation of implanted ES-derived OPCs causing improvements in cognitive behavioural scores, and white matter structure is extremely promising given that cell identity is well established with expressed markers and functional properties. This suggests that iPSC-OPC/OLs represent a nascent technology with potential in CNS repair, as well as being representative of OPC/OLs *in vitro*. The latter provides a foundation for disease modelling, and the results detailed in this chapter thus argue that iPSC-OPC/OLs are a viable and

flexible model of human development and disease *in vitro* as suggested by study of iPSC-OPC/OLs elsewhere (Livesey *et al*. 2015).

Chapter 7

Discussion & Conclusion

7.1 Overview

The introduction of this thesis outlined several key research themes. Firstly, the over-arching research question concerns the validity of ESC and iPSC-derived neuronal, and oligodendrocyte, material in its recapitulation of development as recognised in animal models. This was conducted with the aim of establishing profiles of ion channel development which describe ESC/iPSC derived neurones, oligodendrocyte precursor cells, and oligodendrocytes in terms of particular hallmark profiles of receptor expression and their associated ion channel properties. Collectively, this thesis supports a broader effort in neurobiology and associated fields which is currently seeking rigorously defined and reproducible, viable tissues for a variety of purposes using well defined protocols. This process is arguably fundamental to progress in the development of more representative tissues, and possibly thus a reliable in vitro platform for the development of models which require that certain physiological processes particular to a disease state are replicated *in vitro*. Thus, initially this thesis supports ideas about "what one might expect" when interpreting results concerning the typical phenotypes observed elsewhere using similar stem-cell derived neuronal tissues.

The idea that human stem-cell cultures could become a useful companion of both rodent, and other systems such as recombinant expression systems, among many methods of exploring natural development, as well as examining disease pathology, is not a new one. Neither is the idea of seeking more specialised, or representative tissues with defined cellular lineages and phenotypes, or the potential utility of these systems in drug discovery. The emergent technology of CRISPR/Cas9 for gene editing is novel in general terms, and was implemented by other members of the lab to excise nuclear repeat expansions in cell lines derived from patients with mutations in disease-related genes. This being said, these things are not entirely novel in as much as they are experimentally verified. While cellular reprogramming and editing requires relatively painstaking and precise work even in terms of typically applied efforts, the successes in establishing Cas9/CRISPR indeed suggest work as is found in this thesis, namely utilising the technologies described to survey a reliable human in vitro platform in light of mechanisms described in other systems.

From this, the thesis then seeks to explore mechanisms of disease pathology using these established cellular phenotypes in terms of altered ion channel expression. Experiments in this thesis were broadly directed towards replicating previous electrophysiological findings which have used identical protocols to generate neuronal, and oligodendrocyte cultures. This initial step provides a reliability and replicability test for the basis of later questions concerning aberrant function. While it may seem to be stating the obvious, this is re-iterated in order to illustrate the broader effort, to relate this work directly what has been done previously in terms of making representative in vitro systems from human embryonic, and induced pluripotent stem cells that relaiably recapitulate the physiology of human development, and from this, the potential for mechanistic insights into disease states imparted by known mutations.

7.2 $GABA_A$Rs and GlyRs expressed by hECNs.

Initial experiments were conducted to establish the isoform(s) of $GABA_AR$ expressed on hECNs. Developmental regulation of the subunit composition of $GABA_A$Rs is a well noted hallmark of neuronal development, along with changes in transporter proteins which govern the relative intra- and extra- cellular concentrations of Cl^-, the primary ion species by which $GABA_A$Rs (and indeed, GlyRs) exert their effect. As has been previously noted in rodent, and human, systems, typical $GABA_AR$ subunit composition in pre-natal mammalian cortical neurones follows a typical expression pattern of $\alpha_{2/3}\beta_{2/3}\gamma$ (though occasionally also δ). Upon birth, this expression pattern in the cortex diversifies massively, incorporating a wide array of $GABA_AR$ subunits into the receptor complex, though still with a very large population of $\alpha_1\beta_2\gamma_2$, the often-described typical adult $GABA_AR$ isoform.

This thesis employs electrophysiology and pharmacology to identify the predominantly expressed subunit composition of $GABA_A$Rs on hECNs. Primarily, the data show that the $GABA_AR$ α subunits expressed by hECNs at 35 DIV in culture are α2 and/or α3 subunits, which is highly congruent with an expression profile

predominantly found in embryonic rodent cortical neurones (Laurie et al. 1992; Fritschy et al. 1994). Given that GABA-evoked currents were not noticeably affected by furosemide, hECN $GABA_A$Rs thus seemingly lack functional expression of α4 and α6 subunits. Additionally, the lower than perhaps expected action of zolpidem suggests the absence of the α1 subunit. This may be expected in that this subunit is associated with a more mature-like, post-natal neuronal phenotype (Laurie et al. 1992; Fritschy et al. 1994). RNA-seq (conducted by O. Dando) also demonstrates relatively low expression of the α1 subunit, and negligible expression of α4 and α6 subunits compared to abundantly expressed α2 and α3 subunit transcripts. Also, functional incorporation of the α5 subunit into $GABA_A$Rs, which is associated with very high agonist potency comparable to α1, was unlikely given the relatively low levels of mRNA detected and the low agonist potencies of GABA and muscimol. Indeed, low potency typically indicates $GABA_A$Rs that contain either α2 or α3 subunits (Mortensen et al. 2011; Karim et al. 2013). High expression of the $GABA_A$R β3 subunit has been associated with immature cortical neurones (Laurie et al. 1992), although the β2 subunit is often also reported to be heavily expressed in cortical neurones (Fritschy et al. 1994).

Potentiation of GABA-evoked currents by the use of low concentrations of etomidate and propofol, a lack of SCS inhibition and a high level of mRNA expression for the β3 subunit all collectively demonstrate that hECNs are likely to predominantly express β3 subunit-containing $GABA_A$Rs, although a contribution of β2 to $GABA_A$R assemblies cannot be solidly doubted. Generally, the vast majority of $GABA_A$Rs in the CNS contain a γ2 subunit. (Olsen & Sieghart, 2009). RNA-seq data supporting the pharmacology in this thesis suggests that hECNs predominantly express γ2 subunits, in agreement with pharmacological results that GABA-evoked currents were potentiated by the γ subunit-selective agent diazepam. On occasion, δ subunit-containing $GABA_A$Rs are selectively expressed by certain cortical adult neuronal phenotypes, and are typically described as being associated with $GABA_A$R-mediated tonic inhibition (Olsen & Sieghart, 2009). Here, the data show that hECNs lack δ subunit-containing $GABA_A$Rs, as gaboxadol elicited small current ampitudes compared to those seen with GABA. Further to this, the result that Zn2+ did not

inhibit GABA-evoked currents is also in agreement with the absence of $GABA_A$Rs composed of only α/β subunits.

This thesis thus demonstrates that RNA-seq analysis and $GABA_A$R pharmacology converge to indicate a predominant $GABA_A$R composition of α2/3β3γ2. Such isoforms are observed in recombinant expression systems to have low agonist potency relative to other isoforms and again this thesis argues that $GABA_A$R expressed upon hECNs exhibit relatively low agonist potency (Karim et al. 2013). This $GABA_A$R isoform is seemingly the most likely to be widely expressed in the immature rodent cortex (Laurie et al. 1992; Olsen & Sieghart, 2009).

Nevertheless, our data cannot exclude the possibility of other $GABA_A$R isoforms expressed at low levels. Additionally, Brainspan (Atlas of the Developing Human Brain http://www.brainspan.org/rnaseq/search) indicates that the levels of mRNA observed in the RNA-seq analysis of hECNs (Conducted by O. Dando) appear similar to those seen in human cortical neurones between 12 and 21 weeks post-conception, i.e mid-to-late embryonic human development. As a result, it can be concluded that hECNs represent a viable platform to investigate the properties of human $GABA_A$R pharmacology and $GABA_A$Rs in maturing cortical neurones (see Wang & Kriegstein, 2009).

Strong, yet transient GlyR expression is a typical feature of early neocortical development (see Avila *et al*. 2013). Indeed, hECNs cultured for 28–42 DIV give robust responses to glycine, which are blocked by GlyR antagonists such as picrotoxin and strychnine. Glycine concentration–response experiments give lower potency values than previously reported in other systems (Pribilla et al. 1992). Interestingly, glycine potency was observed to be higher than potencies typically observed in native cortical tissues (Okabe et al. 2004; Kilb et al. 2008). The reasons for these differences are essentially unknown, but may be due to differences in bath aCSF flow dynamics, where slower fluid exchange times are more likely to give shallower concentration–response curve observations. GlyRs expressed by rodent forebrain neurones have been described as progressing in development from an embryonic, homomeric to postnatal heteromeric (β subunit-containing) composition

(Lynch, 2009). Pharmacological tools to conclusively identify the exact stoichiometry in heteromers are lacking (see Han et al. 2004); however, RNA-seq analysis in this thesis shows α2 subunit mRNA is heavily expressed. Similarly to $GABA_AR$ subunit expression, levels of mRNA expression for GlyRs in our RNA-seq analysis are consistent with a developmental age in humans of between approximately 12–21 weeks post-conception (Atlas of the Developing Human Brain http://www.brainspan.org/rnaseq/search). Finally, it is known that there is a transient expression of heteromeric α2/β GlyRs in rodent Cajal–Retzius cells early in post-natal development (Okabe et al. 2004). This class of neurone is considered to form a significant population in hECN cultures (Bilican et al. 2014) and in this respect hECNs may well provide a useful human model of GlyR development.

As activating both GlyRs and $GABA_ARs$ typically gives anionic (typically Cl^- -based) currents, and that previous work in hECNs has shown intracellular $[Cl^-]$ to be approximate of human development as compared to other systems (Livesey et al. 2014), these findings on ion channel and Cl^- -transporter expression form a functionally representative, and replicable model of $GABA_AR$ and GlyR expression and function along with their underlying primary physiological processes.

Given previous exploration of other ion channels (e.g NMDAR, AMPAR development; Bilican et al 2014, Livesey et al 2014) in hECNs, this thesis contributes to, and is congruent with, an in vitro stem-cell derived model of human development which has been shown to be broadly representative of embryonic, and at most very early post-natal periods in human development. Given the arguable need for some kind of standardisation of comparability between protocols and systems, this work contributes to an ordered and rigorous view of stem cell protocol development, which suggests that the process can be scaled for a range of potential applications such as drug screening, or safety testing for compounds such as anaesthetics. Such a platform could be used to investigate the basic mechanisms of anaesthesia at the receptor level, and also may be useful for examining the safety of such compounds on immature human neurones found in vivo, i.e in a real child's head. This is desirable, as anaesthetics and $GABA_AR$-effective compounds are shown to in fact excite immature, embryonic or briefly postnatal neurones, and a

primary reason why drugs such as ketamine are used to anaesthatise neonatal humans.

Human embryonic cortical neurones displayed highly similar properties to those reported elsewhere, and represent a stable model human $GABA_AR$, and GlyR, and embryonic, and immediately postnatal periods, respectively. Interestingly, the DISC1 mutation studied did not show any suspected disease phenotypes in ion channel development, suggesting that the observed network pathologies in psychiatric disorders, particularly in terms of hypotheses describing balances between excitation and inhibition are not effected through a fundamental change in basic neuronal properties or basal ion channel expression/composition.

In rodents, transient functional GlyR expression is a key feature of early neocortical development (Flint et al. 1998; Avila et al. 2013a). Indeed, hECNS maintained for 28–42 DIV exhibited strong responses to glycine that were blocked by the GlyR antagonist strychnine. Glycine concentration–response experiments indicated glycine potency was lower than previously reported recombinant values (Pribilla et al. 1992) but is generally higher than glycine potencies observed in native cortical preparations (Flint et al. 1998; Okabe et al. 2004; Kilb et al. 2008; but see Avila et al. 2013b). The reasons for these differences are unknown, but may be related to systematic differences in the solution exchange times of these studies, where slower exchange times are more likely to give shallower observed concentration–response curves. In this regard, the ability to examine deactivation kinetics of GlyRs expressed by hECNs in isolated patches using fast agonist application may yield further details of GlyR identity (Mangin et al. 2003; Pitt et al. 2008; Krashia et al. 2011; Marabelli et al. 2013). GlyRs expressed by rodent forebrain neurones have been described as developing from an embryonic homomeric to postnatal heteromeric (β subunit-containing) composition (Lynch, 2009). To investigate the functional GlyR composition we used the antagonist picrotoxin, which inhibits homomeric over heteromeric GlyRs (Lynch, 2009). Given the observed low sensitivity of GlyRs to picrotoxin, our results suggest that the principal GlyR identity of hECNs is likely to a heteromeric α/β assembly. Pharmacological tools to identify unambiguously the nature of the α subunit within

the heteromer are lacking (but see Han et al. 2004); however, RNA seq analysis indicates that α2 subunit mRNA is the most abundantly expressed. As is the case for $GABA_AR$ subunit expression, levels of mRNA expression for GlyRs in our RNA-seq analysis are consistent with a development age of around 12–21 weeks post conception (Atlas of the Developing Human Brain http://www.brainspan.org/rnaseq/search). Finally, it is of interest to note that there is transient expression of heteromeric α2/β GlyRs by rodent Cajal–Retzius cells in early postnatal development (Okabe et al. 2004). This class of neurone is considered to form a significant population in our hECN cultures (Bilican et al. 2014) and in this respect hECNs may model this aspect of GlyR function in early postnatal human development

Native cortical maturation is associated with a change in expression from GluA2(R)-lacking to GluA2(R)-containing AMPARs. Importantly, the presence of one or more GluA2(R) subunit in an AMPAR complex results in reduced single-channel conductance, reduced sensitivity to channel-blocking polyamines and, crucially, reducedCa2+ permeability (Traynelis et al. 2010). Assessment ofthe functional AMPAR composition in hPSCC neuronesusing non-stationary fluctuation analysis to estimatemeanAMPAR single-channel conductance and their sensitivityto a GluA2(R)-lacking AMPAR channel blocker indicatesan activity-independent and native-like maturationfromGluA2(R)-lacking toGluA2(R)-containingAMPARswithin 5 weeks of in vitro differentiation (Livesey et al.2014). GluA2 transcript expression also increases withtime in culture (Chander &Weick, 2014; Stein et al. 2014;van de Leemput et al. 2014). Thus AMPAR expressionin hPSCC neurones appears to display properties that areobserved in native mature neuronal populations (Isaac et al. 2007). Both NMDARs and AMPARs are expectedto undergo maturational changes in composition in theearly postnatal weeks of cortical development in rodents(Traynelis et al. 2010) and in this regard the ontogeneticdevelopment of AMPARs in hPSCC neurones is muchmore rapid than expected. Interestingly, the GluA2 subunithas been shown to be rapidly edited and functionallyup-regulated 4 weeks after the in vitro differentiationof neurones from primary human cortical progenitors (Whitney *et al*. 2008) in contrast to the expected

longerin vivo developmental time scales (Talos et al. 2006).These data suggest the rapid maturation of theAMPAR complex is a potential product of the in vitroenvironment. Nonetheless, this feature provides anopportunity to examine numerous scenarios in which abnormal regulation of theGluA2 subunit is prevalent in adult human disease (Wright & Vissel,2012). The breadth of possible $GABA_AR$ composition results in considerable functional and pharmacological diversity across brain regions and even cellular locations (Olsen & Sieghart, 2009).

7.3 Surveying ion channels and neurodevelopment in hECNs with the *DISC1* (1;11)(q42;q14.3) mutation.

Human embryonic cortical neurones displayed highly similar properties to those reported elsewhere, and represent a stable model human $GABA_AR$, and GlyR, and embryonic, and immediately postnatal periods, respectively. Interestingly, the DISC1 mutation studied did not show any suspected disease phenotypes in ion channel development, suggesting that the observed network pathologies in psychiatric disorders, particularly in terms of hypotheses describing balances between excitation and inhibition are not effected through a fundamental change in basic neuronal properties or basal ion channel expression/composition.

Initially the intrinsic passive and firing properties of Case and Control hECNs were investigated across multiple time points in order to detect any potential developmental difference in excitability. The data in broad agreement with a developing neuronal phenotype (increasing whole-cell capacitance, increase in ability to fire and increase in amplitude and speed of action potentials) across all lines examined. The fact that no difference was found is consistent with a study where hippocampal CA1 neurones from a transgenic mouse expressing the equivalent truncated DISC1 protein also did not show any difference in the passive or intrinsic properties (Randall et al. 2014). Importantly, the properties of hECNs examined even at 35DIV are consistent with an immature neuronal profile; hyperpolarized RMP, high input resistance and low whole-cell capacitance, and are consistent with in vitro pluripotent stem cell derived neurones in general (see Kim et al. 2011; Pak et al. 2015; Scheglovitov et al. 2013). It maybe therefore plausible that in vitro hECNs may not have reached a sufficient level of maturity for excitability

phenotypes to emerge. Moreover, hECN culture composition may not be sufficiently representative to the possibility that specific neurones of the cortex may exhibit subtle differences in intrinsic excitability. For example, hECN cultures only contain nominal proportions of interneurones for which there is an important role in schizophrenia (Lewis et al. 2005).

The properties of major neurotransmitter receptors, AMPARs, $GABA_A$Rs and NMDARs, were then investigated. The expression of $GABA_A$Rs upon Case and Control hECNs was found to be statistically equivalent indicating that mutant DISC1 does not influence $GABA_A$R expression in hECNs. This is in agreement with a recent study examining mutant DISC1 protein in rodent cortical neurones which expressed equivalent levels of $GABA_A$Rs versus controls despite knock down and over expression of the full DISC1 protein having opposing effects upon $GABA_A$R expression (Wei et al. 2015). The previous results chapter determined that the composition of $GABA_A$Rs was representative of the major immature $GABA_A$R expressed in the immature cortex. Selected pharmacological analyses demonstrated that it is unlikely that $GABA_A$R composition in Case and Control hECNs was different. Similarly, the NMDAR receptor expression in Case hECNs was not different from Control hECNs and the composition was pharmacologically determined using ifenprodil to be representative of a predominantly immature NMDAR cortical profile, i.e., GluN1/GluN2B-containing. Recently, Wen et al. (2014) describe a small increase in the GluN2B mRNA level, but not GluN1 protein levels, in hECNs derived from mutant DISC1 patients. Data presented here suggests that this disparity does not manifest at the functional level.

The finding that $GABA_A$R and NMDAR compositions are consistent with immature neuronal profiles clearly restricts conclusions to the subunits expressed. Mutant DISC1 patients have a late juvenile/young adult symptomatic onset (Thomson et al. 2013) and maturation of cortical $GABA_A$R and NMDAR composition is expected to have taken place. For example, the findings that mutant DISC1 affects GluN2A NMDAR subunit expression (Wei et al. 2013) and potentially reduces functional NMDAR expression to slow NMDAR maturation in the mouse barrel cortex (Greenhill et al. 2015) cannot be feasibly interrogated in this

system. This highlights the value of thorough characterisation like that performed in this study and that it is absolutely required if the field is to interpret findings from stem cell-derived neurone technology for disease-modelling studies.

AMPAR expression was observed to be equivalent between Case and Control hECNs at 35 DIV indicating that mutant DISC1 has no apparent effect. AMPAR composition was then determined using non-stationary fluctuation analysis and the sensitivity of AMPAR-mediated currents to NASPM. This data was directly equivalent to that of rodent cortical neurones that had undergone a period of post natal development in which edited GluA2 is upregulated (Brill and Hugenuard. 2008) and also recombinantly expressed AMPARs containing edited GluA2 subunts. (Swanson et al. 1997). Both strategies clearly converged on the predominant AMPAR composition at 35 DIV as being edited GluA2-containing for both Case and Control hECNs. Contrary to the $GABA_AR$ and NMDAR, AMPAR expressed on hECNs have a composition that is expected of neurone that has undergone a period of maturation (Orlandi et al. 2011; Talos et al. 2006). A rapid upregulation of GluA2 AMPAR subunit transcripts has also been reported in other similar systems (Stein et al. 2014; van de Leemput et al. 2014). Wen et al. (2014) recently reported an increase in the mRNA level of GluA2 in hECNs generated from mutant DISC1 patient-derived iPSCs over control and isogenic, gene-corrected mutant DISC1 hECNs, though data obtained in this study indicates this transcriptional difference may not translate to a functional difference. It appears that the functional upregulation of the GluA2 subunit is much faster than expected from what is expected in vivo (Orlandi et al. 2011; Talos et al. 2006). Of note, Whitney et al. (2008) report that the GluA2 is rapidly edited and functionally upregulated within 4 weeks in in vitro neurones differentiated from human cortical progenitors.

7.4 Observing a possible mechanism of AMPAR pathology in MNs and OLs harbouring multiple ALS-related mutations.

The data presented in this thesis, alongside that which has been presented from elsewhere, collectively demonstrate that advances in protocols which aim to generate more homogenous, defined populations of neuronal and ologodendroglial celll lineages have led to a reliable, scaleable in vitro platform suitable for the modelling of basic, fundamental physiological processes in normal human development, and disease, with the limitations of such advances detailed previously. This is to say that thus far, the capacity to generate tissue "on-demand" which will have a defined identity (here, embryonic cortical neurones, OPCs, and oligodendrocytes) and a set of physiological properties not only representative of a moderately specific developmental period – that of reaching late pre-natal maturity after 35 DIV in culture in the case of hECNs, but also capable of demonstrating subtleties predicted by animal models, and indeed human findings in key disease theories of conditions such as ALS.

This thesis shows maturation-dependent changes in membrane conductances, occurring in human oligodendrocytes as they differentiate from OPCs which recapitulate many of the changes in ion channel expression previously observed in rodent-based systems. OPCs displayed outwardly rectifying membrane currents and differentiation to oligodendrocytes results in a linearization of the membrane currents. These properties have been widely described in rodent oligodendroglial counterparts, *in vitro* mouse PSC-derived OPCs and integrated mouse PSC-derived material. These data indicate that comparable shifts in ion channel expression are occurring throughout human oligodendrogenesis in vitro. Such data are in accordance with previously observed developmental shifts in IA and IK channel expression in rodent oligodendroglial cells and also prominent expression of these membrane conductances in *in vitro* mouse PSC-derived OPCs. Oligodendrocytes did not show any spiking activity, in agreement with reports from rodent oligodendroglial cells. It is important to highlight that numerous reports describe native OPCs being heterogeneous in their ability to display either spiking or non-spiking behaviours, which are likely to represent the differentiation/ maturation

status of the OPC rather than developmentally independent subclasses of OPC. The data in this thesis are consistent with numerous studies reporting an increase in functional expression of the GluA2(R) subunit in AMPARs expressed in rodent oligodendrocytes upon differentiation and maturation from OPCs in the case of control tissues, but not in one ALS model.

This developmental variability in AMPAR composition (and Ca^{2+}permeability) is disease-relevant and confers vulnerability of immature oligodendroglial cells to excitotoxic conditions. Taken together these findings show species conservation of the defining physiological properties of oligodendrocyte lineage cells, and crucially establish a platform to investigate possible disease-related changes. The precise function of the C9ORF72 protein itself remains largely unknown although accumulating evidence implicates a gain of function mediated toxicity in ALS.

In exploring the "slow excitotoxicity model" of ALS, the suggested mechanism of which being suggested is that aberrant Ca^{2+} - entry into cells is a cause of motor neurone degradation seen in ALS (*via* an increase in the relative expression of calcium-permeable CP-AMPARs which may pervade into adulthood). This thesis has demonstrated that in lower motor neurone tissue, the typical expression pattern of AMPAR expression, which terminates in a "mature-like" predominant expression of Ca2+ impermeable CI-AMPARs, is disrupted in cells harbouring the C9ORF72 (G4C2) NRE, which, unlike their "control" counterparts without said mutation, results in a relative increase in the expression of AMPARs permeable to calcium ions, CP-AMPARs.

This suspected mechanism of ALS progression, 'slow' excitotoxicity, as mediated by AMPARs was also observed in OPC/OLs harbouring known mutations strongly associated with ALS, though in the case of OPC/OLs in this thesis, it is TDP-43 mutation which is associated with increased relative CP-AMPAR expression. Interestingly, it has been shown that OPC/OLs harbouring the C9ORF72 mutation are not affected by this pervasive increase in relative CP-AMPAR expression (Livesey et al 2016).

Critically, the phenotype of aberrant Ca^{2+} -permeable AMPARs was replicated in a human system, a key finding in ALS research. This finding appears to be a

convergent on a phenotype across different tissue types, providing potentially valuable insights for further research. Motor neurone, and oligodendrocyte populations used in this thesis broadly recapitulated pathologies observed in animal models of heritable ALS imparted by mutations in novel candidate genes, and more classically studied mutations. Ultimately, this thesis argues that ESC and iPSC-derived neuronal cultures represent a stable and scaleable system for the modelling of disease, and also as potential drug screening and development platforms. Material produced in vitro often faithfully recapitulates ion channel development as described in rodent models and elsewhere, and is highly amenable to the study of ion-channel related diseases.

Synaptic events are often described in two general forms; phasic and tonic, and are both essential to the normal function of the CNS. Synaptic connectivity between cortical neurones is key to cortical network development and function (Spitzer,2006). It is therefore critical to the development of *in vitro* hPSCC-derived neurones to recapitulate native synaptic properties. The co-localization of pre- and post-synaptic membrane-associated scaffold proteins such as synaptophysin and PSD-95, however, it is largely accepted that many standard in vitro hPSC protocols do not generate cultures that exhibit robust synaptic activity (Bardy et al. 2015).

Many groups co-culture neurones with primary rodent astrocytes, which also promote synapse activity (Johnson et al. 2007; Kim et al. 2011;Shcheglovitov et al. 2013; Wen et al. 2014; Park et al .2015). Analysis of the field-evoked postsynaptic events in co-cultured neurones has shown that glutamate activates both fast AMPAR-mediated, and also slower GluN1/GluN2B-like NMDAR-mediated events in control neurones (Shcheglovitov et al. 2013). Pre-synaptic neurotransmitter-release related pathophysiology has been modelled in neurones derived from schizophrenia (DISC1; Wen et al. 2014) and autism (NRXN1;Pak et al. 2015) patients.

Also, inhibitory GABA-ergic interneurones are essential for maintaining the balanced activity of cortical neural circuits. GABA-ergic synaptic activity has been detected within hPSCC cultures in the form of spontaneous postsynaptic currents (Johnsonet al. 2007; Wu et al. 2007; Shcheglovitov et al. 2013).However, a recent report has observed synchronized excitatory neurotransmitter-driven network activity

that resembles that of early-stage cortical development and which occurs in cultures that contain a low percentageof interneurones and is insensitive to pharmacological blockade of $GABA_A$Rs (Kirwan et al. 2015). A key studyin the near future will therefore be the culture of defined mixtures of hPSCC neurones and defined populations of GABA-ergic interneurones. Notably, it has been demonstrated human pluripotent stem-cell-derived neurones can be integrated into neural networks in mice, (Weick et al.2011). Espuny-Camucho et al. (2013) successfully demonstrated differentiation and functional integration of stem-cell derived neurones into rodent cortex. Several months after transplantation into the developing cortex, neurones exhibited intrinsic membrane properties consistent with adult mature cortical neurones, in contrast to the more immature properties of *in vitro* differentiated pluripotent stem cell-derived neurones. While there is still much to learn in order to achieve fully developed functional integration, this thesis suggests that stem-cell derived tissues have the inherent potential to integrate into networks. In conclusion, a major challenge is to generate neuronal populations that exhibit maturation profiles thatmore closely reflect those seen in vivo. Co-culture with astrocytes and mixed neuronal populations, together with the maintenance of cells in media that promotes increased synaptic activity, indicates that such strategies are likely required to observe synaptic transmission.

7.5 Opportunities for further research

7.5.1 Developing networks *in vitro*

Here, the development of *in vitro* techniques which produce cells with a definitive neuronal or oligodendroglial identity is a double-edged sword. As the composition of hECNs is typically above 90% for cortical excitatory neurones, and that normal development of the nervous system is conducted by a vast network of interconnected molecular mechanisms which rely on interactions between the elements in order to produce the organism *in vivo*, it could be argued that the purity of the cultures allows the study of very specific neuronal phenotypes, though reaches its limit when examining whole networks as found *in vivo*. This presents a barrier in studying phenomena important for mechanisms thought to underlie learning and memory, as typically these phenomena are much easier to observe when anatomical organisation and stimulus pathways are known (e.g LTP in linear pathways in the hippocampus) in order to elicit a response that can be measured and altered by electrical or chemical stimulation. In the case of hECNs, these anatomically organised pathways are not a feature of the culture, nor ar predictable inputs and outputs between neurones. Additionally, there seems to be little basal synaptic activity in hECNs to begin with. Thus, before networks can be studied, they must be formed. One could study synaptic potentiation, and thus potentially the basic mechanisms of learning and memory in hECNs without this problem.

One immediate answer would be to use cultures of tissues which combine these elements to explore the possibility of the development of functional synapses. The initial problem of being unable, as yet, to produce truly functional, representative networks *in vitro* (a humongous task that no doubt will take much work), could be approached from the perspective of attempting to produce not only pure excitatory contrical neurones in culture, but to attempt to extend their lifespan, or trigger some increase in basal excitatory synaptic connectivity between neurones.

This initial suggestion is complemented by a divergent approach which is less concerned with the purity of cultures, and more focused on combining tissue types. While this type of experimentation typically involves a high failure rate, the possibility of producing a co-culture with excitatory and inhibitory cortical neurones, oligodendrocytes, and other glial cell types epitomises this idea in terms of combining specifically derived tissues, and grafting them in co-culture at various stages of neuronal development. Thus, by composition, events associated with the early stages of development of the nervous system such as early ripples of excitation spreading through the cortex, or the change in expression of chloride co-transporter proteins could be studied, along with the potential for examining network pathology within a more nuanced *in vitro* culture model that may accommodate such phenotypes as found in the study of complex neurobiological disorders. One example would be the study of *DISC1*, in this thesis the (1;11)(q42;q14.3). It is still highly possible that the properties which are sought of the disease model, such as some form of chloride transporter dysfunction, or alteration in excitability and ion channel function, are not produced until some developmental criteria is met that cannot be replicated in a pure culture in 35 DIV. From this, it seems immediately apparent that the first suggestion would be to attempt to introduce complex compositions from the starting point of purity of culture.

This stand in a similar perspective to previous work using human stem cell derived neuronal cultures which utilise mixed tissue types using more general protocols to generate neurones and glial cells of varying lineages. These cultures are then examined in light of disease-associated mutations such as those found in *DISC1* One potential pitfall of examining neuronal function in this way is that one cannot be sure of the exact nature of any cellular type within that culture – though it is an exceptional finding in itself that there may be phenotypes which indeed could be explored by more developed mixed culture populations. From this, an addition of the more specific approach, to the approach found in previous work of human stem-cell derived cultured neurones seems appropriate. Grafting populations of cells while maintaining their cellular identity along with integrating various cell types in this manner, is the technical limitation of this method that cannot be ignored, as ESC and

iPSC derived neuronal material is expensive and fragile. Conducting this type of experimentation then would likely involve taking "lifted" populations of cells and grafting them manually at certain times in development e.g by grafting 21 DIV hECNs onto a comparably mature layer of astrocytes. One could combine these in any fashion, though this in itself could be guided by attempting to "line up" findings with developmental periods, and attempting to transplant tissues accordingly to prepare for certain events such as the change in intracellular Cl^- concentration in neurodevelopment, or AMPAR/NMDAR subunit switching. Interneurones could also be amenable to this line of enquiry, in that DISC1 has been found to localise to inhibitory synapses and could be used to explore excitation-inhibition models, and cell-cycle exit theories in neuropsychiatric conditions associated with genetic mutations found to affect neuronal populations in some way in other models.

Another suggestion for the progression of the technology is to explore the potential of applying developmentally selected "cues" in the form of hormones which are active on neuronal tissues. As development is associated with changes in the levels of hormones at key developmental times, e.g birth, and that the pre- to post- natal period marks many changes in ion channel composition and function, it may be possible to approach the problem from a more artificial framework. This approach tackles the problem by attempting to replace some aspect of unsupplied external cue that is not found in more pure culture systems. In this way, it can be considered an extension of the development of protocol, with the caveat that it seeks to "trigger" some aspect of development which may yield the properties that are required for representative *in vitro* networks. This would take the form of introducing hormones that replace physiological events in line with the findings of reproductive biology. While currently a flight of fancy, this progresses to a very primitive model of an artificial womb in some senses. While this may initially seem grandiose, it is not intended to suggest that these experiments would engineer a revolution in reproductive technology, but merely that the attempt to replace external cues typically supplied by the organism at large to neurones *in vivo* in a culture model is akin to attempting to replicate, in some fashion, the operations of reproductive biology. As such, this indicates the potential for this type of intervention to yield not only insights into reproductive biology within the context of

neurobiological development, but also suggests a wider context that disease models could be studied within, again by attempting to replicate the influence of "the rest of the human" around neurones in stem cell derived culture.

7.5.2 Further work in disease modelling with stem cells

One key finding of this thesis, when taken in light of other work, is that there appears to be a neuronal phenotype of increased Calcium permeability, mediated by AMPARs, in motor neurones derived from iPSCs which harbour ALS mutations in *C9orf72*. This recapitulates aspects of the disease found elsewhere and in other models – moreover the AMPAR pathology is not found when the nuclear repeat expansion in *C9orf72* is excised by CRISPR/Cas9. Interestingly, oligodendroctyes which express nuclear repeat expansions in *C9orf72* do not show this phenotype, indicating the effect is tissue specific.

Of great interest, however, is the finding that mutations in other ALS-associated genes such as *TARDBP*, which are associated with disease markers in ALS and pathophysiology associated with expression of the misfolded protein product TDP-43, do not show this aberrant increase in AMPAR-mediated Calcium permeability in MNs. This demonstrates something perhaps of interest when examined in light of the finding that oligodendroglial lineages, themselves also suspected in ALS progression, aberrantly express calcium permeable AMPARs when derived from patients with mutations which are associated with TDP-43 production. Thus, mutations in *C9ofr72* seem to predominantly affect motor neurone AMPAR expression, while mutations which are associated with TDP-43 pathophysiology appear to predominantly affect oligodendroglial AMPAR expression. Indeed, both types of mutation are associated with a sustained permeability of AMPARs to Ca^{2+} ions

The next step is to directly test the prospect of calcium-mediated excitotoxicity, perhaps by linking excitotoxicity to mRNA expression which describes proteins associated with AMPAR editing and trafficking, along with assaying cell death or otherwise noticeable ALS-related neuropathology in cultured motor neurones as described in this thesis. At least in the short term, the mechanisms

which control AMPAR trafficking and disease are suggested as a core target for further research, perhaps by examining various protein interactions with AMPARs, as the commonalities between different mutations in different tissues suggest the potential for an up-stream intervention between direct receptor modulation, and gene editing which is nascent and not yet capable of intervening directly –though in future indeed it may in some form. Here, enzymes which control the RNA editing of GluA2, such as ADAR2, represent a possible link between observed neurophysiological phenotypes, the potential for observed excitotoxic cell death *in vitro*, and the observed mutations which link these processes to disease states *in vivo*. Indeed, other mutations have been studied in ALS in this manner with similar implications. The *ALS2* gene, which is involved in early-onset ALS and affects AMPAR trafficking by interfering with GRIP1, a glutamate receptor interacting protein necessary for AMPAR trafficking, shows alterations in AMPAR expression in line with observed findings in this thesis. It may also then be of interest to examine co-culture of tissues to explore how one particular mutation exerts an effect on the whole, e.g to co-culture oligodendrogilial and neuronal cells derived from cell lines which harbour certain mutations associated with ALS.

7.6 Concluding statement

This thesis has aimed to demonstrate the viability of stem-cell derived neuronal, and oligodendroglial cells, in generating a stable, scaleable, reliable platform to examine human physiology in normal development and disease *via* ion channel dysfunction as a potential mechanism. With the caveats supplied concerning limited capacity for network-focused study, and thus potentially the study of some disorders and mutations, stem-cell derived tissues of this nature do indeed replicate key, well defined hallmarks of normal development, and in some specific cases support models of disease states and their attendant neuropathological observations. Interestingly in the case of ALS, this thesis demonstrates the practical utility of stem-cell derived neuronal tissue and genetic modification techniques in studying disease pathology at the receptor level by elucidating potentially convergent mechanisms of disease phenotypes and progression.

7.7 Acknowledgements and thanks

The author would like to thank the donors of the cellular material required to generate the neurones and other tissues used in this thesis. Despite much consideration, the author can find no way of ordering a list of other people involved which adequately describes the contributions made, or the (great) extent of the thanks they are owed. Thus, in no particular order and in great amount the author thanks the following people (listed informally):

Matthew Livesey, Pete Kind, David Wyllie, Dario Magnani, Elaine Cleary, Navneet Vasistha, Bhuvaneish Selvaraj, Siddharthan Chandran, Karen Burr, David Story, Giles Hardingham, Ghazal Haghi, Rinku Rajan, Bilada Bilican, Owen Dando, Owen James (the genetics one, not the patch clamp one), Nora Markus, Jing Qiu, Marc-Andre Martel, Aleks Domanski, Roxy and Steve from Chancellor's Building café, Marcia Roy, Frances A. Edwards, Mike Cousin, Jeremy Lambert, Lindsay Mizen, Sean McKay, Steph Barnes, Adam Jackson, Laura Butterworth, and Jack Amiel.

The author would also like to thank Phil Badger, and Derek James for their wisdom.

References

Akbarian, S., Huntsman, M.S., Kim, J.J., Tafazzoli, A., Potkin, S.G., Bunney, W.E. & Jones, E.G. (1995b). $GABA_A$ receptor subunit expression in human prefrontal cortex: comparison of schizophrenics and controls. Cerebral Cortex, 5: 550-560.

Akbarian, S., Smith, M.A. & Jones, E. G. (1995a). Editing for an AMPA receptor subunit RNA in prefrontal cortex and striatum in Alzheimer's disease, Huntington's disease and schizophrenia. Brain Res. 699(2):297-304.

Alexander S. P. H., Peters J. A., Kelly E., Marrion N., Benson H. E., Faccenda E., et al. . (2015). The concise guide to PHARMACOLOGY 2015/16: ligand-gated ion channels. Br. J. Pharmacol. 172, 5870–5903.

Andoh-Noda, T., Akamatsu, W., Miyake, K., Matsumoto, T., Yamaguchi, R., Sanosaka, T., Okada, Y., Kobayashi, T., Ohyama, M., Nakashima, K., Kurosawa, H. Takeo Kubota, T. & Okano, H. (2015). Differentiation of multipotent neural stem cells derived from Rett syndrome patients is biased toward the astrocytic lineage. Molecular Brain 8:31

Arion, D. & Lewis, D.A. (2011). Altered expression of regulators of the cortical chloride transporters NKCC1 and KCC2 in schizophrenia. Arch Gen Psychiatry. 68(1):21-31.

Avou, M. (1992). Synaptic activation of $GABA_A$ receptors causes a depolarizing poteatial under physiological conditions in rat hippocampal pyramidal cells. Ear. J. Neurosci. 4: 16-26.

Backman, M., Machon, O., Mygland, L., Van Den Bout, C. J., Zhong, W., Taketo, M. M., & Krauss, S. (2005). Effects of canonical Wnt signaling on dorso-ventral specification of the mouse telencephalon. Developmental Biology, 279(1), 155-168.

Banke, T.G., Schousboe, A., & Pickering, D.S. (1997) Comparison of the agonist binding site of homomeric, heteromeric, and chimeric GluR1(o) and GluR3(o) AMPA receptors. J Neurosci Res 49:176–185

Barr, C.A. & Burdette, S.C. (2017). The zinc paradigm for metalloneurochemistry. Essays In Biochemistry 61(2) 225-235.

Ben-Ari, Y., Gaiarsa, J.L., Tyzio, R. & Khazipov, R. (2007). GABA: a pioneer transmitter that excites immature neurons and generates primitive oscillations. Physiol Rev. 87(4):1215-1284.

Berridge, M.J. (2013). Dysregulation of neural calcium signaling in Alzheimer disease, bipolar disorder and schizophrenia. Prion. 7(1):2-13.

Bilican, B., Livesey, M.R., Haghi, G., Qiu, J., Burr, K., Siller, R., Hardingham, G.E., Wyllie, D.J. & Chandran, S. (2014). Physiological oxygen levels and EGF withdrawal are required for scalable generation of functional cortical neurones from human pluripotent stem cells. Plos One 9, e85932.

Blaesse, P., Airaksinen, M.S., Rivera, C. & Kaila, K. (2009). Cation-chloride cotransporters and neuronal function. Neuron 61: 820-838.
Bonnert, T.P., Whiting, P.J. & Brandon, N.J. (2007). Disrupted in Schizophrenia 1 Interactome: evidence for the close connectivity of risk genes and a potential synaptic basis for schizophrenia. Mol Psychiatry. 12(1):74-86.

Bormann, J., Hamill, O. P. & Sakmann, B. (1987). Mechanism of anion permeation through channels gated by glycine and gamma-aminobutyric acid in mouse cultured spinal neurones. J physiol 385 (1), 243-286.

Bradshaw NJ, Porteous DJ (Mar 2012). "DISC1-binding proteins in neural development, signalling and schizophrenia". Neuropharmacology 62 (3): 1230.

Brandon, N. J., and Sawa, A. (2011) Linking neurodevelopmental and synaptic theories of mental illness through DISC1. Nat. Rev. Neurosci. 12, 707–722

Brennand, K.J., Simone, A., Jou, J., Gelboin-Burkhart, C., Tran, N., Sangar, S., Li, Y., Mu, Y., Chen G., Yu, D., McCarthy, S., Sebat, J. & Gage, F.H. (2011). Modelling schizophrenia using human induced pluripotent stem cells. Nature. 473(7346):221-5.

Brill, J. & Huguenard, J.R. (2008). Sequential changes in AMPA receptor targeting in the developing neocortical excitatory circuit. J Neurosci. 28:13918–13928.

Callicott, J. H., Straub, R. E., Pezawas, L., Egan, M. F., Mattay, V. S., Hariri, A. R., Verchinski, B. A., Meyer-Lindenberg, A., Balkissoon, R., Kolachana, B., Goldberg, T. E., and Weinberger, D. R. (2005) Variation in DISC1 affects hippocampal structure and function and increases risk for schizophrenia. Proc. Natl. Acad. Sci. U.S.A. 102, 8627–8632

Callicott, J.H., Feighery, E.L., Mattay, V.S., White, M.G., Chen, Q., Baranger, D.A., Berman, K.F., Lu, B., Song, H., Ming, G.L. & Weinberger, D.R. (2013). DISC1 and SLC12A2 interaction affects human hippocampal function and connectivity. J Clin Invest. 123(7):2961-2964.

Camargo, L.M., Collura, V., Rain, J.C., Mizuguchi, K., Hermjakob, H., Kerrien, S., Cannon, T. D., Hennah, W., van Erp, T. G., Thompson, P. M., Lonnqvist, J., Huttunen, M., Gasperoni, T., Tuulio-Henriksson, A., Pirkola, T., Toga, A. W., Kaprio, J., Mazziotta, J., and Peltonen, L. (2005) Association of DISC1/TRAX haplotypes with schizophrenia, reduced prefrontal gray matter, and impaired short- and long-term memory.Arch. Gen. Psychiatry 62, 1205–1213

Cantanelli, P., Sperduti, S., Ciavardelli, D., Stuppia, L., Gatta, V. & Sensi1, S.L. (2014). Age-Dependent Modifications of AMPA Receptor Subunit Expression Levels and Related Cognitive Effects in 3xTg-AD Mice. Front Aging Neurosci. 6: 200.

Carless, M. A., Glahn, D. C., Johnson, M. P., Curran, J. E., Bozaoglu, K., Dyer, T. D., Winkler, A. M., Cole, S. A., Almasy, L., MacCluer, J. W., Duggirala, R., Moses, E. K., Göring, H. H., and Blangero, J. (2011) Impact of DISC1 variation on neuroanatomical and neurocognitive phenotypes. Mol. Psychiatry 16, 1096–1104, 1063

Carlisle, H.J., Luong, T.N., Medina-Marino, A., Schenker, L., Khorosheva, E., Indersmitten, T., Gunapala, K.M., Steele, A.D., O'Dell, T.J., Patterson, P.H. & Kennedy, M.B. (2011). Deletion of densin-180 results in abnormal behaviors associated with mental illness and reduces mGluR5 and DISC1 in the postsynaptic density fraction. J Neurosci. 31(45):16194-207.

Chen, L., Chetkovich, D.M., Petralia, R.S., Sweeney, N.T., Kawasaki, Y., Wenthold, R.J., Bredt, D.S. & Nicoll, R.A. (2000). Stargazin regulates synaptic targeting of AMPA receptors by two distinct mechanisms. Nature. 408 (6815): 936–43.

Chabwine, J.N., Talavera, K., Van den Bosch, L. & Callewaert, G. (2015). NKCC1 downregulation induces hyperpolarizing shift of GABA responsiveness at near term fetal stages in rat cultured dorsal root ganglion neurons. BMC Neurosci. 16: 41.

Clapcote, S.J., Lipina, T.V., Millar, J.K., Mackie, S., Christie, S., Ogawa, F., Lerch, J.P., Trimble, K., Uchiyama, M., Sakuraba, Y., Kaneda, H., Shiroishi, T., Houslay, M.D., Henkelman, R.M., Sled, J.G., Gondo, Y., Porteous, D.J.& Roder, J.C. (2007). Behavioral phenotypes of Disc1 missense mutations in mice. Neuron. 54(3):387-402.

Clayton, T., Chen, J.L., Ernst, M., Richter, L., Cromer, B.A., Morton, C.J., Ng, H., Kaczorowski C.C., Helmstetter, F.J., Furtmüller, R., Ecker, G., Parker, M.W., Sieghart, W. & Cook, J.M. (2007). An updated unified pharmacophore model of the benzodiazepine binding site on gamma-aminobutyric acid(a) receptors: correlation with comparative models. Curr. Med. Chem. 14 (26): 2755–75.

Cleveland, D.W., & Rothstein, J.D. (2001). From Charcot to Lou Gehrig: deciphering selective motor neuron death in ALS. Nat Rev Neurosci 2, 806-819.

Colquhoun, D., Dreyer, F. & Sheridan, R.E. (1979). The actions of tubocurarine at the frog neuromuscular junction. J Physiol 293:247-284.

Cowen, M.S. & Beart, P.M. (1998). Cyclothiazide and AMPA receptor desensitization: analyses from studies of AMPA-induced release of [3H]-noradrenaline from hippocampal slices. Br J Pharmacol.123(3):473-80.

Coyle, J.T (2012). NMDA receptor and schizophrenia: a brief history. Schizophr Bull 38(5):920-926.

Defelipe, J. (2011). The evolution of the brain, the human nature of cortical circuits, and intellectual creativity. Front Neuroanat 5, 29.

DeJesus-Hernandez, M., Mackenzie, I.R., Boeve, B.F., Boxer, A.L., Baker, M., Rutherford, N.J., Nicholson, A.M., Finch, N.A., Flynn, H., Adamson, J., Kouri, N., Wojtas, A., Sengdy, P., Hsiung, G.Y., Karydas, A., Seeley, W.W., Josephs, K.A., Coppola, G., Geschwind, D.H., Wszolek, Z.K., Feldman, H., Knopman, D.S., Petersen, R.C., Miller, B.L., Dickson, D.W., Boylan, K.B., Graff-Radford, N.R. & Rademakers, R. (2011). Expanded GGGGCC hexanucleotide repeat in noncoding region of C9ORF72 causes chromosome 9p-linked FTD and ALS. Neuron 72, 245-256.

Dempster J. Computer Analysis of Electrophysiological Signals. London: Academic Press; 1993.

Dolmetsch, R.E. (2013). SHANK3 and IGF1 restore synaptic deficits in neurons from 22q13 deletion syndrome patients. Nature 503, 267–271.

Donnelly, C.J., Zhang, P.W., Pham, J.T., Haeusler, A.R., Mistry, N.A., Vidensky, S., Daley, E.L., Poth, E.M., Hoover, B., Fines, D.M., Maragakis, N., Tienari, P.J., Petrucelli, L., Traynor, B.J., Wang, J., Rigo, F., Bennett, C.F., Blackshaw, S., Sattler, R. & Rothstein, J.D. (2013). RNA toxicity from the ALS/FTD C9ORF72 expansion is mitigated by antisense intervention. Neuron 80, 415-428.

Draguhn, A., Verdorn, T.A., Ewert, M., Seeburg, P.H. & Sakmann, B.(1990). Functional and molecular distinction between recombinant rat $GABA_A$ receptor subtypes by Zn2+. Neuron 5, 781–788.

Du Bois, T.M. & Huang, X.F. (2007).Early brain development disruption from NMDA receptor hypofunction: relevance to schizophrenia. Brain Res Rev. 53(2):260-70.

Duan, X., Chang, J. H., Ge, S., Faulkner, R. L., Kim, J. Y., Kitabatake, Y., Liu, X. B., Yang, C. H., Jordan, J. D., Ma, D. K., Liu, C. Y., Ganesan, S., Cheng, H. J., Ming, G. L., Lu, B., and Song, H. (2007) Disrupted-in-schizophrenia 1 regulates integration of newly generated neurons in the adult brain. Cell 130, 1146–1158

Duncan, K. (2009). The role of AMPA receptor-mediated excitotoxicity in ALS:
Is deficient RNA editing to blame? Current Anaesthesia & Critical Care 20 227–235.

Eiraku, M.,Watanabe, K., Matsuo-Takasaki, M., Kawada, M., Yonemura, S., Matsumura, M.,Wataya, T., Nishiyama, A., Muguruma, K. & Sasai, Y. (2008). Self-organized formation of polarized cortical tissues from ESCs and its active manipulation by extrinsic signals. Cell Stem Cell 3, 519–532.

El-Hassar, L., Simen, A.A., Duque, A., Patel, K.D., Kaczmarek, L.K., Arnsten, A.F. & Yeckel M.F. (2014). Disrupted in schizophrenia 1 modulates medial prefrontal cortex pyramidal neuron activity through cAMP regulation of transient receptor potential C and small-conductance K+ channels. Biol Psychiatry. 76(6):476-485.

Espuny-Camacho, I., Michelsen, K.A., Gall, D., Linaro, D., Hasche, A., Bonnefont, J., Bali, C., Orduz, D., Bilheu, A., Herpoel, A., Lambert, N., Gaspard, N., Peron, S., Schiffmann, S.N., Giugliano, M., Gaillard, A. & Vanderhaeghen, P. (2013). Pyramidal neurons derived from human pluripotent stem cells integrate efficiently into mouse brain circuits in vivo. Neuron 77, 440–456.

Essrich, C., Lorez, M., Benson, J.A., Fritschy, J.M. & and Lüscher, B. (1998). Postsynaptic clustering of major $GABA_A$ receptor subtypes requires the γ2 subunit and gephyrin. Nature Neuroscience 1 (7): 563-571.

Farra, N., Zhang, W-B., Pasceri1, P., Eubanks, J.H. MW Salter, M.W. & Ellis, J. (2012). Rett syndrome induced pluripotent stem cell-derived neurons reveal novel neurophysiological alterations. Molecular Psychiatry 17, 1261–127.

Fatemi, S.H., King, D.P., Reutiman, T.J., Folsom, T.D., Laurence, J.A., Lee, S. et al. (2008). PDE4B polymorphisms and decreased PDE4B expression are associated with schizophrenia. Schizophrenia Res 101:36–49.

Fritschy, J.M., Paysan, J., Enna, A. & Mohler, H. (1994). Switch in the expression of rat $GABA_A$-receptor subtypes during postnatal development: an immunohistochemical study. J Neurosci 14, 5302–5324.

Frizelle, P.A., Chen, P.E. & Wyllie, D.J. (2006). Equilibrium constants for (R)-[(S)-1-(4-bromo-phenyl)-ethylamino]-(2,3-dioxo-1,2,3,4-tetrahydroquinoxalin-5-yl)-methyl]-phosphonic acid (NVP-AAM077) acting at recombinant NR1/NR2A and NR1/NR2B N-methyl-d-aspartate receptors: Implications for studies of synaptic transmission. Mol Pharmacol 70, 1022–1032.

Gamo, N.J., Duque, A., Paspalas, C.D., Kata, A., Fine, R., Boven, L., Bryan, C., Lo, T., Anighoro, K., Bermudez, L., Peng, K., Annor, A., Raja, A., Mansson, E., Taylor, S.R., Patel, K., Simen, A.A. & Arnsten, A.F.T. (2013). Role of disrupted in schizophrenia 1 (DISC1) in stress-induced prefrontal cognitive dysfunction. Translational Psychiatry 3, e328.

Gemaine, N., Banda, E. & Grabel, L. (2010). Embryonic stem cell neurogenesisand neural specification Cell Biochem. 111(3):535-542

Greger, I.H., Khatri, L. & Ziff, E.B. (2002). RNA editing at arg607 controls AMPA receptor exit from the endoplasmic reticulum. Neuron. 34 (5): 759–72.

Greenhill, S.D., Juczewski, K., de Haan, A.M., Seaton, G., Fox, K. & Hardingham, N.R. (2015). NEURODEVELOPMENT. Adult cortical plasticity depends on an early postnatal critical period. Science. 349(6246):424-427.

Hammond, J.C., McCullumsmith, R.E., Funk, A.J., Haroutunian, V. & Meador-Woodruff, J. H. (2010). Evidence for Abnormal Forward Trafficking of AMPA Receptors in Frontal Cortex of Elderly Patients with Schizophrenia. Neuropsychopharmacology. 10: 2110–2119.

Haverkamp, S., Muller, U., Zeilhofer, H.U., Harvey, R.J., Wassle, H., 2004. Diversity of glycine receptors in the mouse retina: localization of the alpha2 subunit. J. Comp. Neurol. 477, 399–411.

Shi, S.H., Hayashi, Y., Petralia, R.S., et al. (1999). Rapid spine delivery and redistribution of AMPA receptors after synaptic NMDA receptor activation. Science. 284 (5421): 1811–6.

Hayashi-Takagi, A., Takaki,M., Graziane, N., Seshadri, S.,Murdoch, H., Dunlop, A. J., Makino, Y., Seshadri, A. J., Ishizuka, K., Srivastava, D. P., Xie, Z., Baraban, J. M., Houslay, M. D., Tomoda, T., Brandon, N. J., Kamiya, A., Yan, Z., Penzes, P., and Sawa, A. (2010) Disrupted-in-Schizophrenia 1 (DISC1) regulates spines of the glutamate synapse via Rac1. Nat. Neurosci. 13, 327–332

Hébert, J. M., Hayhurst, M., Marks, M. E., Kulessa, H., Hogan, B. L. M., & McConnell, S. K. (2003). BMP ligands act redundantly to pattern the dorsal telencephalic midline. Genesis, 35(4), 214-219.

Hideyama, T. & Kwak, S. (2011). When Does ALS Start? ADAR2–GluA2 Hypothesis for the Etiology of Sporadic ALS. Front Mol Neurosci 4: 33-42.

Hille, B. (2001). Ion Channels of Excitable Membranes (3rd ed). (Sinauer: Sunderland, MA), p. 151.
Hill-Venning, C., Belelli, D., Peters, J.A. & Lambert, J.J. (1997). Subunit-dependent interaction of the general anaesthetic etomidate with the gamma-aminobutyric acid type A receptor. Br J Pharmacol 120, 749–756.

Hinton, T. & Johnstone, G.A.R. (2008). The Role of $GABA_A$ Receptors in Schizophrenia, Cellscience Rev, 5, 180-194.

Holley, S.M., Wang, E.A., Cepeda, C., Jentsch, J.D., Ross, C.A., Pletnikov, M.V. & Levine, M.S. (2013). Frontal cortical synaptic communication is abnormal in Disc1 genetic mouse models of schizophrenia. Schizophr Res.146(1-3):264-72.

Hollmann M., Hartley M., Heine-mann S. (1991). Ca2+ permeability of KA-AMPA – gated glutamate receptor channels depends on sub-unit composition. Science 252 851–853.

Honore, T., Lauridsen, J. & Krogsgaard-Larsen, P. (1982). "The binding of [3H]AMPA, a structural analogue of glutamic acid, to rat brain membranes". Journal of Neurochemistry. 38 (1): 173–178.

Hunt, P. & Clements-Jewery, S. (1981). A steroid derivative, R 5135, antagonizes the GABA/benzodiazepine receptor interaction. Neuropharmacology 20: 357–361.

Huntsman, M.M., Tran, B.V., Potkin, S.G., Bunney, W.E. & Jones, E.G. (1998). Altered ratios of alternatively spliced long and short γ2 subunit mRNAs of the γ-amino butyrate type A receptor in prefrontal cortex of schizophrenics. PNAS, 95: 15066-15071.

Ishikawa, M., Mizukami, K., Iwakiri, M., Hidaka, S. & Asada, T. (2004b). Immunohistochemical and immunoblot study of $GABA_A$ α1 and β2/3 subunits in the prefrontal cortex of subjects with schizophrenia and bipolar disorder. Neurosci. Res. 50: 77-84.

Ishizuka, K., Kamiya, A., Oh, E. C., Kanki, H., Seshadri, S., Robinson, J. F., Murdoch, H., Dunlop, A. J., Kubo, K., Furukori, K., Huang, B., Zeledon, M., Hayashi-Takagi, A., Okano, H., Nakajima, K., Houslay, M. D., Katsanis, N., and Sawa, A. (2011) DISC1-dependent switch from progenitor proliferation to migration in the developing cortex. Nature 473, 92–96

Ivic, L., Sands, T.T., Fishkin, N., Nakanishi, K., Kriegstein, A.R., & Stromgaard, K. (2003). Terpene trilactones from Ginkgo biloba are antagonists of cortical glycine and $GABA_A$ receptors. J Biol Chem 278: 49279–49285.

Jacob, T.C., Moss,S.J. & Jurd, R. (2008). $GABA_A$ receptor trafficking and its role in the dynamic modulation of neuronal inhibition. Nat Rev Neurosci. 9(5): 331–343.

James O.T., Livesey, M.R., Qiu, J., Dando, O., Bilican, B., Haghi, G., Rajan, R., Burr, K., Hardingham, G.E., Chandran, S., Kind, P.C & Wyllie, D.J. (2014). Ionotropic GABA and glycine receptor subunit composition in human pluripotent stem cell-derived excitatory cortical neurones. J Physiol 592, 4353–4363.

Johnson, M.A., Weick, J.P., Pearce, R.A. & Zhang, S.C. (2007). Functional neural development from human embryonic stem cells: accelerated synaptic activity via astrocyte coculture. J Neurosci 27, 3069–3077.

Jonas, P. (1993). AMPA-type glutamate receptors--nonselective cation channels mediating fast excitatory transmission in the CNS. Laurie D.J.,Wisden,W.& Seeburg, P.H. (1992). The distribution of thirteen $GABA_A$ receptor subunit mRNAs in the rat brain. Embryonic and postnatal development. J Neurosci 12, 4151–4172.

Kadoshima, T., Sakaguchi, H., Nakano, T., Soen, M., Ando, S., Eiraku, M. & Sasai, Y. (2013). Self-organization of axial polarity, inside-out layer pattern, and species-specific progenitor dynamics in human ES cell-derived neocortex. Proc Natl Acad Sci USA 110, 20284–20289.

Kaila, K., Price, T.J., Payne, J.A., Puskarjov, M. & Voipio, J. (2014. Cation-chloride cotransporters in neuronal development, plasticity and disease. Nat. Rev. Neurosci. 15, 637–654.

Kalkman H.O. (2011). Alterations in the expression of neuronal chloride transporters may contribute to schizophrenia. Prog Neuropsychopharmacol Biol Psychiatry. 35(2):410-4.

Kamboj, S.K., Swanson, G.T. & Cull-Candy, S.G. (1995). Intracellular spermine confers rectification on rat calcium-permeable AMPA and kainate receptors. J Physiol. 486(2): 297–303.

Kamiya, A., Kubo, K., Tomoda, T., Takaki, M., Youn, R., Ozeki, Y., Sawamura, N., Park, U., Kudo, C., Okawa, M., Ross, C. A., Hatten, M. E., Nakajima, K., and Sawa, A. (2005) A schizophrenia-associated mutation of DISC1 perturbs cerebral cortex development. Nat. Cell Biol. 7, 1167–1178

Karim, N., Wellendorph, P., Absalom, N., Johnston, G.A., Hanrahan, J.R. & Chebib, M. (2013). Potency of GABA at human recombinant $GABA_A$ receptors expressed in Xenopus oocytes: a mini review. Amino Acids 44, 1139–1149.

Kew, J.N, Trube, G. & Kemp, J.A. (1996). A novel mechanism of activity-dependent NMDA receptor antagonism describes the effect of ifenprodil in rat cultured cortical neurones. J Physiol. 497(Pt 3): 761–772.

Khan, B.K., Yokoyama, J.S., Takada, L.T., Sha, S.J., Rutherford, N.J., Fong, J.C., Karydas, A.M., Wu, T., Ketelle, R.S., Baker, M.C., Hernandez, M.D., Coppola, G., Geschwind, D.H., Rademakers, R., Lee, S.E., Rosen, H.J., Rabinovici, G.D., Seeley, W.W., Rankin, KP., Boxer, A.L. & Miller, B.L. (2012). Atypical, slowly progressive behavioural variant frontotemporal dementia associated with C9ORF72 hexanucleotide expansion. J Neurol Neurosurg Psychiatry. 83:358–364.

Kim, J. Y., Liu, C. Y., Zhang, F., Duan, X., Wen, Z., Song, J., Feighery, E., Lu, B., Rujescu, D., St Clair, D., Christian, K., Callicott, J. H.,Weinberger, D. R., Song, H., and Ming, G. L. (2012) Interplay between DISC1 and GABA Signaling regulates neurogenesis in mice and risk for schizophrenia. Cell 148, 1051–1064

Kim, J.E., O'Sullivan, M.L., Sanchez, C.A., Hwang, M., Israel, M.A., Brennand, K., Deerinck, T.J., Goldstein, L.S., Gage, F.H., Ellisman, M.H. & Ghosh, A. (2011).

Investigating synapse formation and function using human pluripotent stem cell-derived neurons. Proc Natl Acad Sci USA 108, 3005–3010.

Kim, Y.J., Liu, C.Y., Zhang, F., Duan, X., Wen, Z., Song, J., Feighery, E., Lu, B., Rujescu, D, StClair, D., Christian, K., Callicott, J.H., Weinburger, D.R., Song, H. & Ming, G. (2012). Interplay between DISC1 and GABA Signaling Regulates Neurogenesis in Mice and Risk for Schizophrenia. Cell. 148(5): 1051–1064.

Kirkeby, A. et al. (2012). Generation of regionally specified neural progenitors and functional neurons from human embryonic stem cells under defined conditions. Cell Rep. 1, 703–714.

Kirkpatrick, B., Xu, L., Cascella, N., Ozeki, Y., Sawa, A. & Roberts, R.C. (2006) DISC1 immunoreactivity at the light and ultrastructural level in the human neocortex. J Comp Neurol. 497(3):436-50.

Koike, M., Iino, M. & Ozawa, S. (1997). Blocking effect of 1-naphthyl acetyl spermine on Ca(2+)-permeable AMPA receptors in cultured rat hippocampal neurons. Neurosci Res. 29(1):27-36.

Kozlovsky, N., Weickert, C.S., Crook, E.T., Kleinman, J.E., Belmaker, R.H. & Agam, G. (2004). Reduced GSK-3β mRNA levels in postmortem dorsolateral prefrontal cortex of schizophrenia patients. J Neural Transm 111: 1583–1592.

Krystal, J.H., Anand, A. & Moghaddam, B. (2002) Effects of NMDA receptor antagonists: implications for the pathophysiology of schizophrenia. Arch Gen Psychiatry. 59:663–664.

Kumar, S.S., Bacci, A., Kharazia, V. & Huguenard, J. (2002). A Developmental Switch of AMPA Receptor Subunits in Neocortical Pyramidal Neurons. J Neurosci. 22(8):3005–3015.

Kyrozis, A. & Reichling, D.B. (1995). Perforated-patch recording with gramicidin avoids artefactual changes in intracellular chloride concentration. J Neurosci Methods 57:27–35.

Lai, C., Xie, C., McCormack, S. G., Chiang, H.-C., Michalak, M. K., Lin, X., Chandran, J., Shim, H., Shimoji, M., Cookson, M. R., Huganir, R. L., Rothstein, J. D., Price, D. L., Wong, P. C., Martin, L. J., Zhu, J. J., and Cai, H. (2006) Amyotrophic lateral sclerosis 2-deficiency leads to neuronal de- generation in amyotrophic lateral sclerosis through altered AMPA receptor trafficking. J. Neurosci. 26, 11798–11806.

Lewis, D.A., Hashimoto, T. & Volk, D.W. (2005). Cortical inhibitory neurons and schizophrenia. Nat Rev Neurosci. 6(4):312-24.

Li, P., Eaton, M.M., Steinbach, J.H. & Akk, G. (2013). The benzodiazepine diazepam potentiates responses of α1β2γ2 γ-aminobutyric acid type A receptors activated by either γ-aminobutyric acid or allosteric agonists Anesthesiology 118(6): 1417–1425.

Li, X.J. et al. (2005). Specification of motoneurons from human embryonic stem cells. Nat. Biotechnol. 23, 215–221.

Ling. G. & Gerard (1949). The normal membrane potential of frog sartorius fibers. Journal of Cellular and Comparative Physiology 34 (3), 393-396.

Lipska, B.K., Peters, T., Hyde, T.M., Halim, N., Horowitz, C. Mitkus S et al. (2006). Expression of DISC1 binding partners is reduced in schizophrenia and associated with DISC1 SNPs. Human Mol Gen 15: 1245–1258.

Liu, X., Huang, J., Chen, T., Wang, Y., Xin, S., Li, J., Pei, G. & Kang, J. (2008). Yamanaka factors critically regulate the developmental signalling network in mouse embryonic stem cells. Cell Research 18:1177–1189.

Liu, X.B., Murray, K.D. & Jones, E.G. (2004). Switching of NMDA receptor 2A and 2B subunits at thalamic and cortical synapses during early postnatal development. J Neurosci. 24(40):8885-95.

Livesey, M.R., Bilican, B., Qiu, J., Rzechorzek, N.M., Haghi, G, Burr, K, Hardingham, G.E., Chandran, S. & Wyllie, D.J. (2014). Maturation of AMPAR Composition and the $GABA_AR$ Reversal Potential in hPSC-Derived Cortical Neurons. J Neurosci 34, 4070-4075.
Lynch, J.W. (2009). Native glycine receptor subtypes and their physiological roles. Neuropharmacology 56, 303–309.

Maher, B.J. & LoTurco, J.J. (2012) Disrupted-in-Schizophrenia (DISC1) Functions Presynaptically at Glutamatergic Synapses. PLoS ONE 7(3): e34053. doi:10.1371/journal.pone.0034053.

Majounie, E., Renton, A.E., Mok, K., Dopper, E.G.., Waite, A., Rollinson, S., et al. (2012). Frequency of the C9orf72 hexanucleotide repeat expansion in patients with amyotrophic lateral sclerosis and frontotemporal dementia: A cross-sectional study. Lancet Neurol. 11:323–30.

Mali, P., Yang, L., Esvelt, K.M., Aach, J., Guell, M., DiCarlo, J.E., Norville, J.E., & Church, G.M. (2013). RNA-guided human genome engineering via Cas9. Science 339, 823-826.

Malosio, M.L., Marqueze-Pouey, B., Kuhse1, J. & Betz, H. (1991).Widespread expression of glycine receptor subunit mRNAs in the adult and developing rat brain. EMBO 10 (9):2401-2409.

Mangin, J.M., Nguyen, L., Gougnard, C., Hans, G., Rogister, B., Belachew, S., Moonen, G., Legendre, P. & Rigo, J.M. (2005). Developmental Regulation of β-Carboline-Induced Inhibition of Glycine-Evoked Responses Depends on Glycine Receptor β Subunit Expression. Molecular Pharmacology 67 (5) 1783-1796.

Mao, Y., Ge, X., Frank, C. L., Madison, J. M., Koehler, A. N., Doud, M. K., Tassa, C., Berry, E. M., Soda, T., Singh, K. K., Biechele, T., Petryshen, T. L., Moon, R. T., Haggarty, S. J., and Tsai, L. H. (2009) Disrupted in schizophrenia 1 regulates neuronal progenitor proliferation via modulation of GSK3/-catenin signaling. Cell 136, 1017–1031

Mariani, J., Simonini, M.V., Palejev, D., Tomasini, L., Coppola, G., Szekely, A.M., Horvath, T.L. & Vaccarino, F.M. (2012). Modeling human cortical development in vitro using induced pluripotent stem cells. Proc Natl Acad Sci USA 109: 12770–12775

Marigo, V., Roberts, D.J., Lee, S.M., Tsukurov, O., Levi, T., Gastier, J.M., Epstein, D.J., Gilbert, D.J., Copeland, N.G. & Seidman, C.E. (1995). Cloning, expression, and chromosomal location of SHH and IHH: two human homologues of the Drosophila segment polarity gene hedgehog. Genomics. 28 (1): 44–51.

Maroof, A.M., Keros, S., Tyson, J.A., Ying, S.W., Ganat, Y.M., Merkle, F.T., Liu, B., Goulburn, A., Stanley, E.G., Elefanty, A.G.,Widmer, H.R., Eggan, K., Goldstein, P.A., Anderson, S.A. & Studer, L. (2013). Directed differentiation and functional maturation of cortical interneurons from human embryonic stem cells. Cell Stem Cell 12: 559–572.

Maury, Y., Côme, J., Piskorowski, R.A., Salah-Mohellibi, N., Chevaleyre, V., Peschanski, M., Martinat C. & Nedelec, S. (2015). Combinatorial analysis of developmental cues efficiently converts human pluripotent stem cells into multiple neuronal subtypes. Nat Biotechnol. 33:89-96.

Millar, J.K., James, R., Brandon, N.J. & Thomson, P.A. (2005). DISC1 and DISC2: discovering and dissecting molecular mechanisms underlying psychiatric illness. Annals of Medicine. 36 (5): 367–78.

Millar, J.K., Wilson-Annan, J.C., Anderson, S., Christie, S., Taylor, M.S., Semple, C.A., Devon, R.S., St Clair, D.M., Muir, W.J., Blackwood, D.H. & Porteous ,D.J. (2000). Disruption of two novel genes by a translocation co-segregating with schizophrenia. Hum Mol Genet. 9(9):1415-23.

Monyer, H., Burnashev, N., Laurie, D.J., Sakmann, B., Seeburg, P.H., 1994. Developmental and regional expression in the rat brain and functional properties of four NMDA receptors. Neuron 12, 529e540.

Moody, W.J. & Bosma MM. (2005). Ion channel development, spontaneous activity, and activity-dependent development in nerve and muscle cells. Physiol Rev. 85(3):883-941.

Mori, K., Weng, S.M., Arzberger, T., May, S., Rentzsch, K., Kremmer, E, Schmid, B., Kretzschmar, H.A., Cruts, M., Van Broeckhoven, C., Haass, C. & Edbauer, D. (2013). The C9orf72 GGGGCC repeat is translated into aggregating dipeptide-repeat proteins in FTLD/ALS. Science 339(6125), 1335–1338.

Mortensen, M., Patel, B. & Smart, T.G. (2011). GABA Potency at $GABA_A$ receptors found in synaptic and extrasynaptic zones. Front Cell Neurosci 6, 1.

Nakanishi, N., Shneider, N.A. & Axel, R. (1990) A family of glutamate receptor genes: evidence for the formation of heteromultimeric receptors with distinct channel properties. Neuron 5:569–581.

Neher, E. & Sakmann, B. (1976). Single-channel currents recorded from membrane of denervated frog muscle fibres. Nature 260, 799 – 802.

Newburn, E.N., Hyde, T.M., Ye, T., Morita, Y., Weinberger, D.R., Kleinman, J.E. & Lipska, B.K. (2011). Interactions of human truncated DISC1 proteins: implications for schizophrenia. Translational Psychiatry 1, e30.

Newland, C. & Cull-Candy, S.G. (1992) On the mechanism of action of picrotoxin on GABA receptor channels in dissociated sympathetic neurones of the rat. J Physiol 447, pp. 191-213.

Noctor, S.C., Martínez-Cerdeño, V., Ivic, L. & Kriegstein, A.R. (2004).Cortical neurons arise in symmetric and asymmetric division zones and migrate through specific phases. Nature Neuroscience 7, 136 – 144.

Noh, K., Yokota, H., Mashiko, T., Castillo. P.E., Zukin, R.S. & Bennett, M. V. L. (Blockade of calcium-permeable AMPA receptors protects hippocampal neurons against global ischemia-induced death. PNAS 102(34): 12230-12235.

Okabe, A., Kilb, W., Shimizu-Okabe, C., Hanganu, I.L., Fukuda, A. & Luhmann, H.J. (2004). Homogenous glycine receptor expression in cortical plate neurons and Cajal–Retzius cells of neonatal rat cerebral cortex. Neuroscience 123, 715–724.
Orlandi C., La Via L., Bonini D., Mora C., Russo I., Barbon A. and Barlati S. (2011). AMPA receptor regulation at the mRNA and protein level in rat primary cortical cultures. PLoS ONE 6, e25350

Oswald, M.J., Tantirigama, M.L.S., Sonntag, I., Hughes, S.M., Empson, R.M. (2013). Diversity of layer 5 projection neurons in the mouse motor cortex. Frontiers in Cellular Neuroscience. 7:74-82.

Overington, J.P., Al-Lazikani, B. & Hopkins, A.L. (2006). How many drug targets are there?. Nature Reviews Drug Discovery. 5 (12): 993–6.

Owens, D.F., Boyce, L.H., Davis, M.B. & Kriegstein, A.R. (1996). Excitatory GABA responses in embryonic and neonatal cortical slices demonstrated by gramicidin perforated-patch recordings and calcium imaging. J Neurosci. 1996 Oct 15;16(20):6414-23

Ozeki, Y., Tomoda, T., Kleiderlein, J., Kamiya, A., Bord, L., Fuiji, K., Okawa,., Yamada, N., Hatten, M.E., Snyder, S.H., Ross, C.A. & Sawa, A. (2002). Disrupted-in-Schizophrenia-1 (DISC-1): Mutant truncation prevents binding to NudE-like (NUDEL) and inhibits neurite outgrowth. PNAS. 100(1): 289–294.

Pak, C., Danko, T., Zhang, Y., Aoto, J., Anderson, G., Maxeiner, S., Yi, F., Wernig, M. & Südhof, T.C. (2015). Human neuropsychiatric disease modeling using conditional deletion reveals synaptic transmission defects caused by heterozygous mutations in NRXN1. Cell Stem Cell 17, 316–328.

Park, M., Penick, E.C., Edwards, J.G., Kauer, J.A. & Ehlers, M.D. (September 2004). Recycling endosomes supply AMPA receptors for LTP. Science. 305 (5692): 1972–1975.

Park, I.H., Zhao, R., West, J.A., Yabuuchi, A., Huo, H., Ince, T.A., Lerou, P.H., Lensch, M.W. & Daley, G.Q. (2008). Reprogramming of human somatic cells to pluripotency with defined factors. Nature 451, 141-146.

Philips, T., Bento-Abreu, A., Nonnerman, A., Haeck, W., Staats, K., Geelen, V., Hersmus, N., Ku, B., Van den Bosch, L., Van Damme, P., Richardson, W.D. & Robberecht, W. (2013). Oligodendrocyte dysfunction in the pathogenesis of amyotrophic lateral sclerosis. Brain. 136: 471-482.

Prata, D. P., Mechelli, A., Fu, C. H., Picchioni, M., Kane, F., Kalidindi, S., McDonald, C., Kravariti, E., Toulopoulou, T.,Miorelli, A.,Murray, R., Collier, D. A., and McGuire, P. K. (2008) Effect of disrupted-in-schizophrenia-1 on pre-frontal cortical function. Mol. Psychiatry 13, 915–917, 909

Pribilla, I., Takagi, T., Langosch, D., Bormann, J. & Betz, H. (1992). The atypical M2 segment of the beta subunit confers picrotoxinin resistance to inhibitory glycine receptor channels. EMBO J 11, 4305–4311.

Rajendra, S., Vandenberg, R.J., Pierce, K.D., Cunningham, A.M., French, P.W., Barry, P.H., & Schofield, P.R. (1995). The unique extracellular disulfide loop of the glycine receptor is a principal ligand binding element. EMBO J 14: 2987–2998.

Ran, F.A., Hsu, P.D., Wright, J., Agarwala, V., Scott, D.A., and Zhang, F. (2013).Genome engineering using the CRISPR-Cas9 system. Nat Protoc 8, 2281-2308.

Reynolds, D.S., Rosahl, T.W., Cirone, J., O'Meara, G.F., Haythornthwaite, A., Newman, R.J., Myers, J., Sur, C., Howell, O., Rutter, A.R., Atack, J., Macaulay, A.J., Hadingham, K.L., Hutson, P.H., Belelli, D., Lambert, J.J., Dawson, G.R.,

McKernan, R., Whiting, P.J. & Wafford, K.A. (2003). Sedation and anesthesia mediated by distinct GABA(A) receptor isoforms. J Neurosci 23(24):8608-8617.

Richardson, W.D., Kessaris, N. & Pringle, N. (2006). Oligodendrocyte wars. Nat Rev Neurosci. 7:11-18.

Riss, J., Cloyd, J., Gates, J. & Collins, S. (2008). Benzodiazepines in epilepsy: pharmacology and pharmacokinetics. Acta Neurologica Scandinavica. 118 (2): 69–86.

Rothstein, J.D., Van Kammen, M., Levey, A.I., Martin, L.J., and Kuncl, R.W. (1995). Selective loss of glial glutamate transporter GLT-1 in amyotrophic lateral sclerosis. Ann Neurol 38, 73-84.
Ruesch, D., Neumann, E., Wulf, H. & Forman, S.A. (2012). An allosteric coagonist model for propofol effects on α1β2γ2L γ-aminobutyric acid type A receptors. Anesthesiology 116(1):47-55.

Sances, S., Bruijn, L.I., Chandran, S., Eggan, K., Ho, R., Klim, J.R., Livesey, M.R., Lowry, E., Macklis, J.D., Rushton, D., Sadegh, C., Sareen, D., Wichterle, H., Zhang, S-C & Svendsen, C. (2016). Modeling ALS with motor neurons derived from human induced pluripotent stem cells. Nature Neuroscience 19(4): 542-553.

Sanna, E., Mascia, M.P., Klein, R.L., Whiting, P.J., Biggio, G. & Harris, R.A. (1995). Actions of the general anesthetic propofol on recombinant human $GABA_A$ receptors: influence of receptor subunits. J Pharmacol Exp Ther 274, 353–360.

Schurov, I. L., Handford, E. J., Brandon, N. J. & Whiting, P. J. (2004) Expression of disrupted in schizophrenia 1 (DISC1) protein in the adult and developing mouse brain indicates its role in neurodevelopment. Mol. Psychiatry 9, 1100 – 1110.

Shcheglovitov, A., Shcheglovitova, O., Yazawa, M., Portmann, T., Shu, R., Sebastiano, V., Krawisz, A., Froehlich, W., Bernstein, J.A., Hallmayer, J. & Dolmetsch, R.E. (2013). Shank3 and IGF1 restore synaptic deficits in neurons from 22q13 deletion syndrome patients. Nature 503(7475): 267–71

Shepherd, J.D. & Huganir, R.L. (2007). The cell biology of synaptic plasticity: AMPA receptor trafficking. Annu. Rev. Cell Dev. Biol. 23: 613–43.

Shi Y, Kirwan P, Smith J, Robinson HP & Livesey FJ (2012). Human cerebral cortex development from pluripotent stem cells to functional excitatory synapses. Nat Neurosci 15, 477–486.

Sigworth, F.J. & Neher, E. (1980). Single Na+ channel currents observed in cultured rat muscle cells. Nature 287, 447 – 44

Sommer, B., Kohler, M., Sprengel, R., and Seeburg, P.H. (1991). RNA editing in brain controls a determinant of ion flow in glutamate-gated channels. Cell 67, 11-19.

Song, B, Sun, G., Herszfeld, D. et al. (2012). Neural differentiation of patient specific iPS cells as a novel approach to study the pathophysiology of multiple sclerosis. Stem Cell Res. 8(2): 259-273.

Song, I & Huganir, R.L. (2002). Regulation of AMPA receptors during synaptic plasticity. Trends Neurosci. 25 (11): 578–88.

Stacpoole, S.R.L., Bilican, B., Webber, D.J., Luzhynskaya, A. & He, X.L. et al. (2011). Derivation of neural precursor cells from human ES cells at 3% O2 is efficient, enhances survival and presents no barrier to regional specification and functional differentiation. Cell Death Differ 18: 1016–1023.

Stiles, J. & Jernigan, T.L. (2010). The Basics of Brain Development. Neuropsychol Rev 20:327–348

Storustovu, S.I. & Ebert, B. (2006). Pharmacological characterization of agonists at δ-containing $GABA_A$ receptors: Functional selectivity for extrasynaptic receptors is dependent on the absence of γ2. J Pharmacol Exp Ther 316, 1351–1359.

Swanson, G.T., Kamboj, S.K., and Cull-Candy, S.G. (1997). Single-channel properties of recombinant AMPA receptors depend on RNA editing, splice variation, and subunit composition. J Neurosci 17, 58-69.

Tajima, Y., Ono, K. & Akaike, N. (1996). Perforated patch-clamp recording in cardiac myocytes using cation-selective ionophore gramicidin. Am J Physiol. 271: 524-32.

Takahashi K, Yamanaka S. (2006). Induction of pluripotent stem cells from mouse embryonic and adult fibroblast cultures by defined factors. Cell 126(4): 663–676.

Talos, D.M., Fishman, R.E., Park, H., Folkerth, R.D., Follett, P.L., Volpe, J.J., & Jensen, F.E. (2006b) Developmental regulation of alpha-amino-3-hydroxy-5-methyl-4-isoxazole-propionic acid receptor subunit expression in forebrain and relationship to regional susceptibility to hypoxic/ischemic injury. II. Human cerebral white matter and cortex. J Comp Neurol 497:61–77.

Tang, X., Kim, J., Zhou, L., Wengert, E., Zhang, L., Wu, Z., Carromeu, C., Muotri, A.R., Marchetto, M.C., Gage, F.H. & Chen, G. (2016). KCC2 rescues functional deficits in human neurons derived from patients with Rett syndrome. Proc Natl Acad Sci. 113(3):751-6.

Tao, R., Li, C., Newburn, E.M., Ye, T., Lipska, B.K., Herman, M.M., Weinberger, D.R., Kleinman, J.E. & Hyde, T.M. (2012).Transcript-Specific Associations of SLC12A5 (KCC2) in Human Prefrontal Cortex with Development, Schizophrenia, and Affective Disorders.J Neurosci. 32(15): 5216-5222.

Ten Bruggencate, G. & Engberg, I. (1971). Iontophoretic studies in Deiter's nucleus of the inhibitory actions of GABA and related amino acids and the interactions of strychnine and picrotoxin. Brain Res, 25, 431-448.

Thompson, S.A.,Wheat, L., Brown, N.A., Wingrove, P.B., Pillai, G.V., Whiting, P.J., Adkins, C.,Woodward, C.H., Smith, A.J., Simpson, P.B., Collins, I. & Wafford, K.A. (2004). Salicylidene salicylhydrazide, a selective inhibitor of β1-containing $GABA_A$ receptors. Br J Pharmacol 142, 97–106.

Trzaskowski B, Latek D, Yuan S, Ghoshdastider U, Debinski A, Filipek S (2012). Action of molecular switches in GPCRs--theoretical and experimental studies. Current Medicinal Chemistry. 19 (8): 1090–109.

Traynelis, S.F., Wollmuth, L.P., McBain, C.J., Menniti, F.S., Vance, K.M., Ogden, K.K., Hansen, K.B., Yuan, H., Myers, S.J., and Dingledine, R. (2010). Glutamate receptor ion channels: structure, regulation, and function. Pharmacol Rev 62, 405-496.

Twelvetrees, A. E., Yuen, E. Y., Arancibia-Carcamo, I. L., MacAskill, A. F., Rostaing, P., Lumb, M. J., Humbert, S., Triller, A., Saudou, F., Yan, Z., and Kittler, J. T. (2010) Delivery of $GABA_A$Rs to synapses is mediated by HAP1-KIF5 and disrupted by mutant huntingtin. Neuron 65, 53–65

Uvarov, P., Ludwig, A., Markkanen, M., Rivera, C. & Airaksinen, M.S. (2006). Upregulation of the neuron-specific K+/Cl- cotransporter expression by transcription factor early growth response 4. J. Neurosci. 26, 13463–13473.

van den Ameele, J., Tiberi, L., Vanderhaeghen, P. & Espuny-Camacho, I. (2014). Thinking out of the dish: what to learn about cortical development using pluripotent stem cells. Trends Neurosci 37, 334–342.

Vandenberg, R.J., French, C.R., Barry, P.H., Shine, J., & Schofield P.R. (1992a). Antagonism of ligand-gated ion channel receptors: two domains of the glycine receptor α subunit form the strychnine-binding site. Proc Natl Acad Sci USA 89: 1765–1769.

Vandenberg, R.J., Handford, C.A., & Schofield, P.R. (1992b). Distinct agonist- and antagonist-binding sites on the glycine receptor. Neuron 9: 491–496.

Von Blankenfeld, G. & & Ketfenmann, H. (1991). Glutamate and GABA receptors in vertebrate glial cells. Mol. Neurobiol. 5: 31-43.

Wafford, K.A., Macaulay, A.J., Fradley, R., O'Meara, G.F., Reynolds, D.S. & Rosahl, T.W. (2004). Differentiating the role of gamma-aminobutyric acid type A ($GABA_A$) receptor subtypes. Biochem Soc Trans 32(3): 553–556.

Wang, D.S., Mangin, J.M., Moonen, G., Rigo, J.M. & Legendre, P. (2006). Mechanisms for picrotoxin block of α2 homomeric glycine receptors. J Biol Chem 281, 3841–3855.

Wang, Q.,Charych, E. I., Pulito,V. L., Lee, J. B., Graziane, N.M.,Crozier, R. A., Revilla-Sanchez, R., Kelly, M. P., Dunlop, A. J., Murdoch, H., Taylor, N., Xie, Y., Pausch, M., Hayashi-Takagi, A., Ishizuka, K., Seshadri, S., Bates, B., Kariya, K., Sawa, A.,Weinberg, R. J.,Moss, S. J., Houslay,M. D., Yan, Z., and Brandon, N. J. (2011) The psychiatric disease risk factors DISC1 and TNIK interact to regulate synapse composition and function. Mol. Psychiatry 16, 1006–1023

Wang, Z., Edwards, J.G., Riley, N., Provance, D.W., Karcher, R., Li, X.D., Davison, I.G., Ikebe, M., Mercer, J.A., Kauer, J.A. & Ehlers, M.D. (October 2008). "Myosin Vb mobilizes recycling endosomes and AMPA receptors for postsynaptic plasticity". Cell. 135 (3): 535–48.

Watanabe, M., Inoue, Y., Sakimura, K., Mishina, M., 1992. Developmental changes in distribution of NMDA receptor channel subunit mRNAs. Neuroreport 3, 1138e1140.

Webb, T.I. & Lynch, J.W. (2007). Molecular pharmacology of the glycine receptor chloride channel. Curr. Pharm. Des. 13, 2350–2367.

Wei, J., Grazianne, N.M., Wang, H., Zhong, P., Wang, Q., Liu, W., Hayashi-Takagi, A., Korth, C., Sawa, A., Brandon, N.J. & Yan, Z. (2014). Regulation of N-methyl-D-aspartate receptors by disrupted-in-schizophrenia-1. Biol Psychiatry. 75 (5):414-424.

Wen, Z., Nguyen, H.N., Guo, Z., Lalli, M.A., Wang, X., Su, Y., Kim, N.S., Yoon, K.J., Shin, J., Zhang, C., Makri, G., Nauen, D., Yu, H., Guzman, E., Chiang, C.H., Yoritomo, N., Kaibuchi, K., Zou, J., Christian, K.M., Cheng, L., Ross, C.A., Margolis, R.L., Chen, G., Kosik, K.S., Song, H. & Ming, G.L. (2014). Synaptic dysregulation in a human iPS cell model of mental disorders. Nature 515, 414–418.

Wernig M, Zhao J-P, Pruszak J et al. (2008). Neurons derived from reprogrammed fibroblasts functionally integrate into the fetal brain and improve symptoms of rats with Parkinson's disease. Proc. Natl Acad. Sci.USA 105(15): 5856–5861

Whitney, N.P., Peng, H., Erdmann, N.B., Tian, C., Monaghan, D.T. & Zheng, J.C. (2008). Calcium-permeable AMPA receptors containing Q/R-unedited GluR2 direct human neural progenitor cell differentiation to neurons. FASEB J 22, 2888–2900.

Wickert, C.S., Fung, S.J., Catts, V.S., Schofield, P.R., Allen, K.M., Moore, L.T., Newell, K.A., Pellen, D., Huang, X.F., Catts, S.V. & Weickert, T.W. (2013). Molecular evidence of N-methyl-D-aspartate receptor hypofunction in schizophrenia. Molecular Psychiatry 18, 1185–1192.

Wright, A. & Vissel, B. (2012).The essential role of AMPA receptor GluR2 subunit RNA editing in the normal and diseased brain. Front Mol Neurosci. 5: 34.
Wu, C. & Sun, D. (2015). GABA receptors in brain development, function, and injury. Metab Brain Dis. 30(2): 367-379.

Wyllie, D.J.A., Livesey, M.R. & Hardingham, G. (2013). Influence of GluN2 subunit identity on NMDA receptor function Neuropharmacology. 74: 4–17.

Xu, J., Du, Y. & Deng, H. (2015).Direct lineage reprogramming: strategies, mechanisms, and applications. Cell Stem Cell 16(2), 119–134.

Yamanaka, S. & Blau, H.M. (2010). Nuclear reprogramming to apluripotent state by three approaches. Nature 465(7299): 704-712.

Yanagi, M., Joho, R.H., Southcott, S.A., Shukla, A.A., Ghose, S. & Tamminga, C.A. (2014). Kv3.1-containing K+ channels are reduced in untreated schizophrenia and normalized with antipsychotic drugs. Molecular Psychiatry 19: 573-579.

Yuen, E. Y., Wei, J., Zhong, P., and Yan, Z. (2012) Disrupted $GABA_AR$ trafficking and synaptic inhibition in a mouse model of Huntington's disease. Neurobiol. Dis. 46, 497–502

Zhang, W., Vogensen, R.A., & Howe, S.B. (2006b) The relationship between agonist potency and AMPA receptor kinetics. Biophys J 91:1336–1346.

Zu T., Liu Y., Bañez-Coronel M., Reid T., Pletnikova O., Lewis J., et al. (2013). RAN proteins and RNA foci from antisense transcripts in C9ORF72 ALS and frontotemporal dementia. Proc. Natl. Acad. Sci. U.S.A. 110, 4968–4978.